Fossil record and new aspects of evolutionary history of Calcium biomineralization and plant waxes in fossil leaves

Disseration

zur

Erlangung des Doktorgrades (Dr. rer. nat.)

der

Mathematisch-Naturwissenschaftichen Fakultät

der Rheinischen Friedrich-Wilhelms-Universität Bonn

Vorgelegt von

Dipl.-Biol. Mahdieh Malekhosseini

aus Bonn

October 2023

Angefertigt mit Genehmigung der Mathematisch-Naturwissenschaftlichen Fakultät der Rheinischen Friedrich-Wilhelms-Universität Bonn

Erstgutachter: Prof. Dr. Jes Rust

Zweitgutachter: Prof. Dr. Thomas Martin

Tag der Promotion: 06.10.23

Erscheinungsjahr: 2023

INDEX

Zusammenfassung

Kapitel 1 In diesem Kapitel wird kurz über die ersten Aufzeichnungen von Calciumoxalat (CaOx)-Abdrücken in der Fossilfundstelle Rott aus dem späten Oligozän berichtet. Ablagerungen von CaOx wurden in verschiedenen Angiospermen von der Fundstätte Rott identifiziert. Einzelheiten der Studie im Vergleich mit dem Verteilungsmuster von CaOx in Bezug auf die vorhandenen Pflanzen und die Entstehung der Untersuchung werden besprochen. Diese Arbeit liefert eine Einführung in die Untersuchung anderer Pflanzengruppen, die im Kapitel 2 ausführlich beschrieben werden.

Kapitel 2 Die Identifizierung von CaOx-Spuren in der Fossilfundstelle Rott regte an, diese Spuren in anderen Pflanzengruppen von primitiven bis zu höheren Pflanzen (rezente und vor allem fossile Exemplare) während geologischer Zeiten zu untersuchen. Die Untersuchung verschiedener Gattungen sowohl an frischen als auch an fossilen Blättern zeigte die große Bedeutung ökologischer Faktoren für den CaOx-Evolutionstrend von Samenfarnen zu modernen Dikotyledonen, wobei in jeder Gruppe Spuren von CaOx mit unterschiedlichen Morphologie-, Größen-, Dichte- und Verteilungsmustern gefunden wurden.

Kapitel 3 Die Beobachtung von CaOx in Form von Kristallen oder Drusen in frischen Blättern und die Identifizierung ihrer übrigbleibenden Hohlräume in Fossilienproben stellen eine besondere Herausforderung dar. In diesem Kapitel werden verschiedene Methoden erläutert, die in der vorliegenden Arbeit zur Identifizierung von CaOx-Kristallen verwendet wurden. Der Vergleich einfacher, aber schneller und genauer Methoden für die untersuchten Biomineralien sowie Vorteile und Schwächen werden diskutiert.

Kapitel 4 Calciumcarbonat ($CaCO_3$)-mineralisation in Form von Cystolithen kommt in 8 Pflanzenfamilien vor, im Gegensatz zu CaOx mit mehr als 250 Familien. Aufgrund ihres relativ einfachen Nachweises, wegen der Lage der Cystolithen unter der Cuticula und ihrer großen Dimension (ca. 100 µm) können sie effektiv in phylogenetischen Studien und der Neuklassifizierung von Pflanzen verwendet werden. Der lichtmikroskopische Nachweis von $CaCO_3$-Cystolithen in einem fossilen Blatt von *Celtis begonioides* aus dem Miozän von Randecker Maar zeigt Ähnlichkeit mit frischen Blättern von *Celtis occidentalis*.

Kapitel 5 Eine weißliche Schicht auf der Epikutikula fossiler Blätter in kohligen Sedimenten ist schon lange bekannt. Vier Exemplare: *Eotrigonobalanus furcinervis* (Oberes Eozän, Leipzig, Deutschland), *Magnolia liblarensis* (Mittleres Miozän, Nochten, Deutschland), *Eotrigonobalanus furcinervis* (Mittleres Eozän, Geiseltal, Deutschland) und *Acer tricuspidatum* (Oberes Oligozän, Norken) wurden näher untersucht. Die Ähnlichkeit der weißlichen Schicht auf den fossilen Blättern mit epikutikulären Wachsschichten auf vielen rezenten Blättern führte zur Untersuchung der chemischen Zusammensetzung der weißen Schichten auf den zuvor erwähnten Exemplaren. Die Analysen zeigten, dass alle fossilen Blätter die typischen aliphatischen Wachsbestandteile wie primäre Alkohole, Fettsäuren und Alkane enthielten. Darüber hinaus zeigte die REM-Untersuchung die 3-D-Struktur des Wachses.

Summary

Chapter 1 First records of calcium oxalate (CaOx) casts in leaves from the Rott fossil site, Late Oligocene, are shortly reported in this chapter. Casts of CaOx in different angiosperms from the Rott site are identified. Details of the study concerning comparision and distribution pattern of CaOx in relation to extant plants and how this study has been performed is discussed. This investigation provided an introduction for the study of other plant groups, which are described in detail in chapter 2.

Chapter 2 Identification of CaOx traces in the Rott fossil site inspirated an investigation of them in other plant groups from primitive to higher plants (extant and fossil plants) over geological times. Investigation of diverse genera in both fresh and fossil leaves revealed the great importance of ecological factors in the evolutionary CaOx trend from seed ferns to modern dicotyledons. Traces of CaOx were found in each group with diverse morphology, size, density and distribution templates.

Chapter 3 Observation of CaOx in form of crystals or druses in fresh leaves and indentification of their casts in fossil samples is always a special challenge. This chapter expoundes different methods that were used in this thesis to identify CaOx crystals. The comparision of simple yet fast and accurate methods for the study of biominerals, their advantages and weakpoints are discussed.

Chapter 4 Calcium carbonate ($CaCO_3$) mineralization in form of cystoliths occurs in 8 plant families in contrast to CaOx with more than 250 families. For this reason and their relatively easy detection due to the location of the cystoliths under the cuticle and their large dimension (i.e.,100 µm), they can be effectively used in phylogenetic studies and reclassification of plants.

The detection of $CaCO_3$ cystoliths in a fossil leaf of *Celtis begonioides* from the Miocene of Randecker Maar with light microscopy showed similarity to fresh leaves of *Celtis occidentalis*.

Chapter 5 Whitish layers on the epicuticle of fossil leaves in coaly sediments are known since a long time. Four specimens: *Eotrigonobalanus furcinervis* (Upper Eocene, Leipzig, Germany), *Magnolia liblarensis* (Middle Miocene, Nochten, Germany), *Eotrigonobalanus furcinervis* (Middle Eocence, Geiseltal, Germany) and *Acer tricuspidatum* (Upper Oligocene, Norken) were examined. The resemblance of the whitish layer on the fossil leaves to the epicuticular wax layers on many extant leaves lead to the examination of the chemical composition of the fossil whitish layers on the before mentioned specimens. The analyses showed that all fossil leaves contained the typical aliphatic wax compounds such as primary alcohols, fatty acids, and alkanes. Furthermore, the SEM examination showed the 3-D structure of the wax.

Abbreviations

Al	Aluminium
BSE	Backscattered electron(s)
C	Carbon
Ca	Calcium
CaOx	Calcium Oxalate
$CaCO_3$	Calcium Carbonate
EDS, EDX	Energy-dispersive X ray spectroscopy
LM	Light-Microscopy
µm	Micrometer
µ-CT	Micro-Computed Tomography
S	Sulphur
Si	Silicon
SEM	Scanning electron microscopy

List of Figures

Chapter 2

FIGURE13. Traces of former CaOx druses in *Ginkgophytopsis delvalii* from the Carboniferous, Upper Silesia, Poland, (Col. Andrzej Gorski, 2021).

FIGURE 14. SEM images of fresh leaves of *Sequoia sempervirens* which show the distribution of CaOx crystals in longitudinal and cross sections.

FIGURE 15. SEM images of CaOx crystal distribution in fresh leaves of *Pinus mugo* und *Welwitschia mirabilis* are illustrated.

FIGURE 16. Fossil leaves of *Walchia*, (coll. Franz, N: 2200), are illustrated.

FIGURE 17. View of possible CaOx traces in veins of fossil leaves (Pliocene, Willershausen) in comparison with incinerated fresh leaves.

FIGURE 18. CaOx traces in remains of the parenchyma of *Betula maximowiczians* (GZG.W.4230, Pliocene, Willershausen) with element mapping is illustrated.

FIGURE19. Fossil and fresh leaf of *Salix* is illustrated.

FIGURE 20. Fossil and fresh leaf of *Quercus* is illustrated.

FIGURE 21. Fossil and fresh leaf of *Quercus* is illustrated.

FIGURE 22. Fossil and fresh leaf of *Parrotia persica* (Pliocene, Willershausen) is illustrated.

FIGURE 23. CaOx crystals and traces of them in fresh and fossil leaves of *Carpinus*.

FIGURE 24. View of the CaOx traces in veins in fossil and fresh leaves of *Acer.*

FIGURE 25. µ-CT images of *Acer*.

FIGURE 26. Image of the CaOx traces in fossil leaves from Rott site, late Oligocene.

FIGURE 27. View of CaOx traces in veins in fossil and fresh leaves of *Acer*

FIGURE 28. CaOx traces and original crystals in *Salix*.

FIGURE 29. CaOx traces and original crystals in fresh (3) and fossil leaf of *Sideroxylon* (1, 2).

FIGURE 30. View of the fossil leaves preserved in glycerin with LM and SEM.

FIGURE 31. Surface of the fossil leaves (PB2021-4-Ls and PB2003-148-Ls) preserved in glycerin with SEM.

FIGURE 32. SEM (SE+BSE image) view of the pyrite in the entire fossil leaf (PB2003-501-Ls, Eckfeld, Middle-Eocene).

FIGURE 33. Amorphous silica beside the granules.

FIGURE 34. Three patterns of casts in fossil leaves of the Oligocene Rott site.

FIGURE 35. Comparison of pollen, bases of trichomes and CaOx occurrences.

FIGURE 36. Occurrence of the CaOx traces in major groups of plants from the Carboniferous to the Neogene.

Chapter 4

FIGURE 1. Distribution pattern of cystoliths in the parenchyma alongside small druses of CaOx and individual CaOx crystals in fresh leaves of *Celtis occidentalis*.

FIGURE 2. View of the dark granules on the surface of the fossil leaf of *Celtis begonioides* (Miocene, Randecker Maar, seemann 15) in comparison with a cystolith in a fresh leaf of *Celtis occidentalis*.

Chapter 5

FIGURE 1. Fossil leaf of *Eotrigonobalanus furcinervis* (Fagaceae), upper Eocene, south of the city Leipzig, Saxony. A whitish layer is preserved on the surface of the fossil leaf.

FIGURE 2. Different fossil leaves of *Magnolia liblarensis* in whitish to brownish color.

FIGURE 3. *Eotrigonobalanus furcinervis*, fossil leaf from the middle Eocene, middle coal of the Geiseltal deposit.

FIGURE 4. *Acer tricuspidatum*, fossil leaf from the late Oligocene, Norken.

FIGURE 5. SEM image of the whitish layer of *Eotrigonobalanus furcinervis* from the upper Eocene south of Leipzig after 600 C° heating.

FIGURE 6. EDX analysis of *Eotrigonobalanus furcinervis* (upper Eocene).

FIGURE 7. Chemical components of the wax (e.g., fatty acids, primary alcohol, sterols, alkanes) of *Eotrigonobalanus furcinervis* (upper Eocene*) which* were measured by GC.

FIGURE 8. Whitish layer of *Magnolia liblarensis* (Magnoliaceae) from the lower-middle Miocene coal, Nochten, Saxony.

FIGURE 9. Chemical components of the wax in *Magnolia liblarensis* (lower-middle Miocene coal, Nochten, Saxony) examined by GC.

FIGURE 10. 3D structure consisting of irregular flake forms in *Eotrigonobalanus furcinervis*, middle Eocene coal (Geiseltal, Germany).

FIGURE 11. Chemical compounds of *Eotrigonobalanus furcinervis*, (middle Eocene coal, Geiseltal, Germany) by GC.

Appendix

FIGURE A3.1. View of different contaminations on fossil leaves.

FIGURE A3.2. Comparison of the preservation of CaOx traces in *Celtis* from different sites. comparison of chemical components in fresh and fossil leaves.

FIGURE A3.3. Comparison of chemical components in fresh and fossil leaves.

List of tables

Table A1.9. List of investigated fossil samples from Carboniferous.

Table A1.10. List of investigated fossil samples from Devonian.

Appendix A2

A2.1. List of the fresh leaves collected in the Botanical Garden, University of Bonn.

Acknowledgments

I would like to give my special thanks to my supervisor, Prof. Dr. Jes Rust, for this opportunity to continue my scientific way and do my PhD in his team, furthermore, he has never withheld his spiritual support, like a caring father, even during his short illness. I wish him all the best.

I give special thanks to Dr. Cornelia Löhne for collecting plant material from the Bonn University Botanic Gardens. I thank Prof. Dr. Maximilian Weigend for his support. I thank all the gardeners too.

I would also like to thank late Dr. Heinz Winterscheid (University of Bonn) for facilitating access to his fossil material from Rott.

Furthermore, I would like give my special thanks to the curators: PD. Dr. Anita Roth-Nebelsick, Dr. Alexander Gehler, Dr. Ludwig Luthardt, Dr. Manuela Aiglstorfer, Dr. Jiří Kvaček and Dr. Thomas Denk for their close cooperation with me to borrow and working in museum. Without their support, it would never have been possible to start and continue this thesis. I wish them the best.

My sincere thanks to Mr. Hans-Jürgen Ensikat, working with him opened a world of experience to my eyes. His calmness, patience, kindness and skills in using tools multiplied the pleasure of working with him. He compassionately taught me whatever art he had in his pocket.

I especially thank Dr. Victoria McCoy for her efforts in correcting the thesis, her constructive points to speed up the process of progressing the thesis and articles. She was always by my side like a caring friend from the time of my master's thesis until now.

I was given the opportunity to meet and learn from PD Dr. Torsten Wappler since my master's thesis and I am grateful for every word that was like a light on my path.

I acknowledge the support of Dr. Alexander Ziegler and Dagmar Wenzel (Institute of Evolutionary Biology and Ecology, University of Bonn) with X-ray and µ-CT images.

I am extremely grateful for any spiritual and scientific support from my dear friends like Dr. med. Hans-Volker Thiel, Teresa Franke, Dr. Bastian Mähler who like my family were by my side in every case.

But I would like too, to thank all the personnel who sincerely helped me in my goals, the secretaries, the laboratory personnel.

My best thanks to my family and my parents for emotional support during my education. Without them I would never have enough motivation to find my way and continue this hard duty. I´am proud of having such a support from my parents. I hope, their existence will always be sustainable.

At the end I will give my thanks to the financial support by DFG. This project was supported by a DFG grant (University of Bonn, DFG Research Unit 2685). The Limits of the Fossil Record: Analytical and Experimental Approaches to Fossilization." I would never find enough peace and time to research without such a great support. I am grateful for this big opportunity.

Chapter 1

Published in Scientific Reports

Title: Traces of calcium oxalate biomineralization in fossil leaves from late Oligocene maar deposits from Germany

Authors: Mahdieh Malekhosseini, Hans-Jürgen Ensikat, Victoria E. McCoy, Torsten Wappler, Maximilian Weigend, Lutz Kunzmann & Jes Rust

Authors contribution: Mahdieh Malekhosseini and Hans-Jürgen Ensikat have been designed the examination and wrote the article. It was supported by the editing of the other authors.

Summary

Calcium oxalate (CaOx) is one of the important bio-minerals in extant plants and plays a major role in plants such as calcium storage and herbivore defense (Nakata, 2003). The occurence of CaOx in 70% of all extant plant species (He, 2014), including algae (Friedmann et al., 1972; Pueschel & West, 2007; Pueschel, 1995), lichens (Jones et al.,1981), fungi (Tait et al., 1999) and vascular plants (Franceschi & Horner, 1980), is examined. CaOx occurs in divers manifestations: druses, crystals and raphide bundles, (Horner & Wagner, 1995; Lersten & Horner, 2000).

In fossil leaves calcium bio-minerals are usually not preserved, but casts ("crystal cavities") have long been known from the cuticles of fossil conifer leaves (Rüffle, 1976). Mentions of the individual crystals in the cuticle of gymnosperms, Late Cretaceous and Cenozoic conifers, exist (Kunzmann, 1999; Kvaček, 2002). In the current thesis fossil angiosperm leaves from the late

Oligocene Rott Fossil Lagerstätte are investigated. For a better understanding of the fossil CaOx distribution pattern plenty of extant leaves were compared with the fossil leaves.

The fossil and fresh samples were examined and documented with different microscopic techniques such as light microscopy (LM), scanning electron microscopy (SEM), and micro-computer tomography (µ-CT).

Well preserved leaves from Rott illustrated traces of former CaOx druses in the residual of the paranchyma. They showed three patterns: empty casts, cavities refilled with organic compounds or with mineral elements which named ghost crystals. Although druses in fresh leaves shows shrinkage and serrated forms, occurrences of CaOx traces mainly identified as granules or spherical forms. It is proposed that the spherical shape of the organic particles results from shrinkage of the casts. Organic material, which has filled the casts, is unlikely to be perfectly stable. It is a highly viscous resin-like material, its surface tension in a moist environment may force it into the spherical shape. The shrinkage also explains why the organic globules easily become detached from the surrounding matter, leaving holes at their positions in the separated fossil samples.

The results show that the casts of CaOx were refilled during fossilization with organic compounds or minerals. Ca, Si, Al, S, and Fe were the main observed mineral components.

The observation of brick-shaped structures in the vascular system in fossil leaves showed similarity in both size and topography of individual CaOx crystals in fresh leaves. The identification of CaOx casts in leaf fossils provides novel insights on the fate of plant bio-minerals during fossilization. It provides an additional aspect of the physiological factors (biotic and abiotic) in the fossilization plants. Thus, improving the accuracy of palaeoecological reconstructions and providing a broader perspective on the evolution of CaOx and its importance in plant ecology across geological time.

Chapter 2

It has not been published

Title: Record of CaOx casts in fossil leaves from basal plants to higher plants from the Devonian to the Quaternary

Examination of fossil samples and microscopic observation was done by Mahdieh Malekhosseini. Modern leaves were prepared to do microscopy by help of Hans-Jürgen Ensikat to recognize type, distribution pattern and density of CaOx in leaves.

The result of this section are three manuscripts:

1. Calcium oxalate in Ginkgophytes through time and its implications for gymnosperm phylogeny

Mahdieh Malekhosseini*, Hans-Jürgen Ensikat, Torsten Wappler, Victoria E. McCoy, and Jes Rust

In review by Communications Biology

2. Stratigraphic and geographic distribution of calcium oxalate druses in fossil leaves of angiosperms and gymnosperms

Mahdieh Malekhosseini*, Hans-Jürgen Ensikat, Victoria E. McCoy, Torsten Wappler and Jes Rust

Submitted to PlosOne

3. Identification of different pattern, type and density of CaOx in extant leaves (gymnosperms and angiosperms)

It is not submitted yet.

2.1 Abstract

Calcium oxalate (CaOx) is one of the most common bio-minerals in extant plants. It plays a major role in a better understanding of plant taphonomy, environmental effects and evolution of calcium minerals in fossil plants. Although CaOx is common in extant leaves of many plant groups, the fossil record of CaOx in fossil leaves is almost completely unknown, due to the imperfect preservation of CaOx bio-minerals and the disintegration of CaOx crystals during fossilization. Recognition of the remains of CaOx in fossil leaves can be challenging.

The record of casts of CaOx in fossil leaves from basal plants, gymnosperms and angiosperms has been established to reconstruct the evolutionary history of CaOx from the Devonian to the Neogene.

The present thesis aims to introduce the different distribution patterns of CaOx traces (individual crystals and druses) in fossil leaves and to compare the substituted or residual chemical components in their casts in fossil leaves from basal to higher plant groups.

In order to achieve this goal, both fossil and modern (for extant groups) leaves of seed ferns, pteridophytes (ferns), gymnosperms (cycadales, ginkgophytales, conifera) and angiosperms have been examined. Fossil samples were borrowed from different sites and ages from natural history museums in Germany. Extant samples were collected in the Botanical Garden, University of Bonn. Light microscopy (LM) and Scanning Electron Microscopy (SEM) were utilized to clarify the distribution of CaOx casts in both fossil and fresh leaves.

The results show that CaOx is almost non-existent in modern ferns. In seed ferns, the casts of former CaOx crystal druses were observed under a carbon layer in a regular distribution pattern with a size of approximately 20 µm. CaOx in cycads and ginkgophytes appeared as aggregated forms or druses in the phloem. Druses in ginkgophyte measured up to 100 µm. Conifera show a different trend: crystals occur as individuals and more or less small size (5-12 µm) on the surface of parenchymatic cells and under the cuticle. In angiosperms CaOx appears commonly and in diverse forms.

In conclusion, the presence of the CaOx as an important chemical factor in plants is reported from primitive seed ferns to the modern gymnosperms and angiosperms. The distributional pattern of CaOx in each major group of plants is different and can be affected by environmental factors and physiological aspects in plants.

Key words: Calcium oxalate; ghost crystals; druses; leaf anatomy; micro-computer tomography; Rott Fossil Lagerstätte; taphonomy.

2.2 Introduction

The most common types of bio-minerals in plants are calcium oxalate (CaOx), calcium carbonate, and silica (Arnott, 1996). CaOx crystals are by far the most prevalent and widespread mineral deposits in higher plants and they have been reported in more than 70% of all plant species (He, 2014); hence, their function and the chemical processes by which they form are widely investigated among certain organisms such as algae (Friedmann et al., 1972; Pueschel & West, 2007; Pueschel, 1995), lichens (Jones et al.,1981), fungi (Tait et al., 1999) and vascular plants (Franceschi & Horner, 1980). In fresh leaves of the bryophyta (Rashid, 1998) and pteridophytes such as ferns, CaOx is rarely observed (Antoons, 2016-2017), while in gymnosperms and angiosperms CaOx appears commonly and takes diverse forms (Lersten & Horner, 2000).

The abundance of CaOx in certain families of dicotyledons within the angiosperms, which take the form of druses, crystals and raphide bundles, have been analysed in many studies (Horner & Wagner, 1995; Lersten & Horner, 2000). In gymnosperms, small CaOx crystals (<10 µm size) occur in most conifers on the surfaces of mesophyll cells and are embedded in the epidermal cell walls (Florin, 1931; Kunzmann, 1999), whereas *Cycad* and *Ginkgo* leaves contain druses with sizes up to 100 µm (Raman & Croom, 1998). Investigation of the formation of CaOx crystals in plants is one of the most important aspects in understanding their evolutionary history and fossilization process. Many studies have described the physiochemical details of CaOx formation (Nakata, 2003; Franceschi & Horner, 1980; Franceschi & Nakata, 2005; Horner & Wagner, 1995). Oxalate synthesis of CaOx is related to ionic balance of elements such as Ca and it seems that CaOx crystals facilitate the ionic balance in plants. In many plants, oxalate is metabolized very slowly or not at all and is considered to be an end product of metabolism. Plant crystal idioblasts may function as a means of removing the oxalate which may otherwise accumulate in toxic quantities (Franceschi & Horner, 1980).

In the process of the CaOx production, endoplasmic reticulum (ER), acidic proteins, cytoskeletal components, and the intravacuolar matrix increased in idioblasts to accelerate synthesis of the CaOx. L-Ascorbic acid and L-galactose are sources for oxalic acid (OxA) and calcium oxalate and plants follow different strategies to utilize them (Keates et al., 2000). Idioblast formation is dependent on the availability of both Ca and oxalate. Under stress conditions, however, crystals may be reabsorbed. When there is more Ca, the size and number of the crystals increase (Khan & Siddiqi, 2014; Mazen, 2004).

In plants, glycolate can be converted to oxalic acid. The oxidation occurs in two steps with glyoxylic acid as an intermediate and glycolic acid oxidase as the enzyme. Glyoxylic acid may be derived from enzymatic cleavage of isocitric acid. Oxaloacetate also can be split to form oxalate and acetate (Li & Franceschi, 1990).

Another significant precursor of oxalate in plants is L-ascorbic acid (Keates et al., 2002). Idioblasts contain the pathway for synthesis of OxA from carbons 1 and 2 of ascorbic asid (AsA). Thus, other than the need for basic carbon and nitrogen substrates, crystal idioblasts are independent of adjoining cells for the critical processes leading to AsA and OxA synthesis and uptake and sequestration of calcium (Kostman et al., 2001), but also are fully capable of producing the OxA needed to complete this important physiological process. These findings are important to our understanding of how crystal idioblasts are able to coordinate calcium uptake with crystal precipitation. Crystal idioblasts operate independently to remove and store excess calcium. Thus, they serve a complex function to the plant that is analogous to that of a tissue or organ, and are thus like a single-celled organ rather than a specialized cell of a more complex organ (Kostman et al., 2001).

The CaOx crystals consist of either the monohydrate whewellite form, or the dihydrate weddellite form and both of these occur in plants (Arnott et al., 1965; Frey-Wyssling, 1981). There are five basic types of calcium oxalate crystals that occur in higher plants: (1) prisms, consisting of simple regular prismatic shapes; (2) druses, which are spherical aggregates of

crystals; (3) styloids, acicular crystals that form singly; (4) raphides, acicular crystals that form in bundles; and (5) crystal sand, small tetrahedral crystals that form in clusters (Franceschi & Horner, 1980).

Many surveys on leaves of extant trees and shrubs revealed different density, features and distribution patterns of CaOx crystals (druses and individual crystals) in the mesophyll and vascular systems (**Figure 1, 2**).

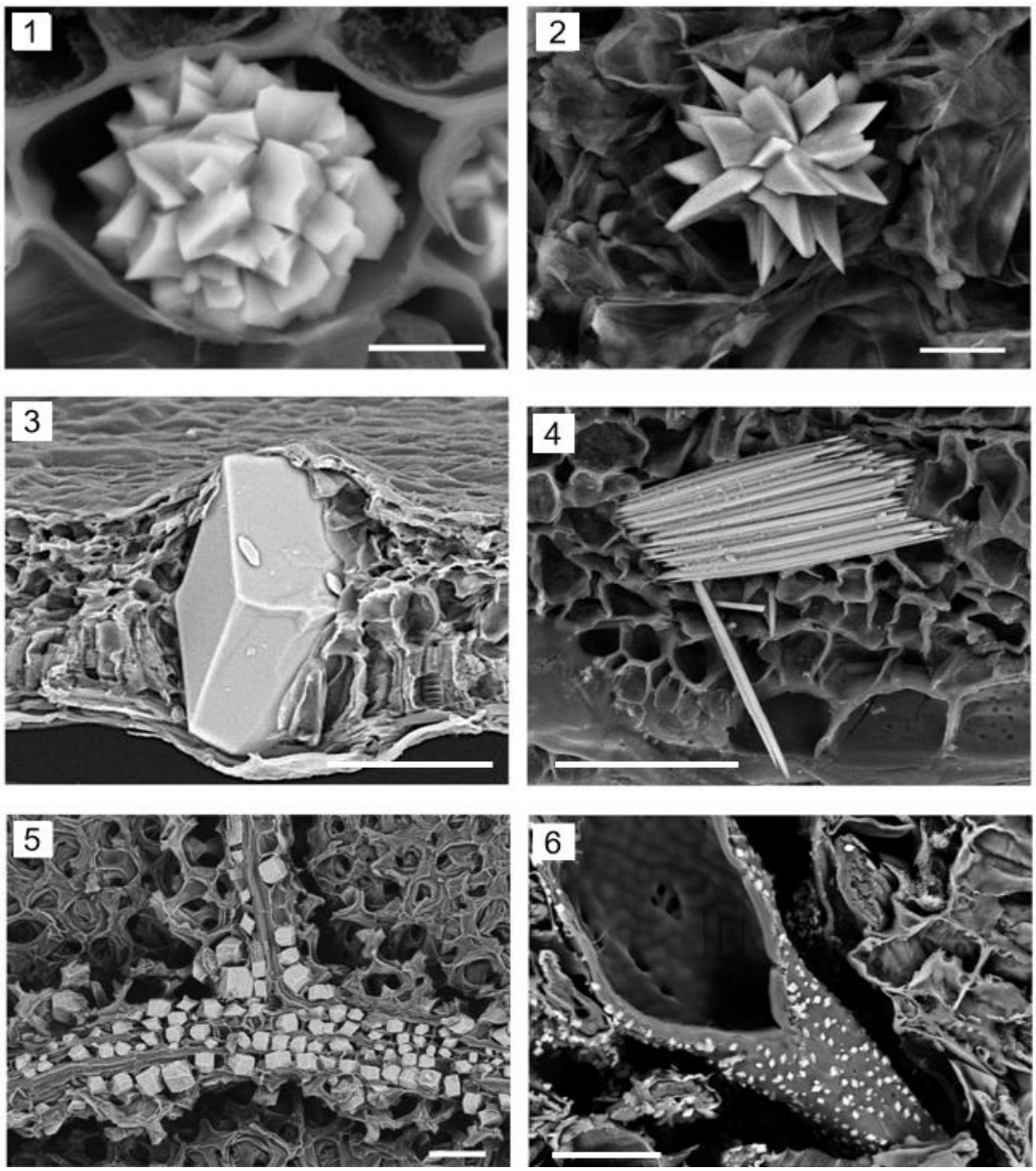

FIGURE 1. Morphology of CaOx druses and crystals in various fresh leaves illustrated by SEM images. 1.1 Compact druse in *Hedera helix* (Araliaceae). 1.2 Druse with emerging sharp-tipped crystals in *Conocarpus erectus* (Combretaceae). 1.3 Large solitary prismatic crystal in *Carpinus kawakamii* (Betulaceae). 1.4 Raphide bundle in

Nannorrhops ritchieana (Arecaceae). 1.5 Small prismatic crystals along veins in *Parrotia persica* (Hamamelidaceae). 1.6 Small crystals on surface of parenchymatic cells in *Araucaria araucana* (Coniferales). Scale bars: 1.1, 1.2 = 10 µm; 1.3, 1.4 = 50 µm; 1.5, 1.6 = 20 µm.

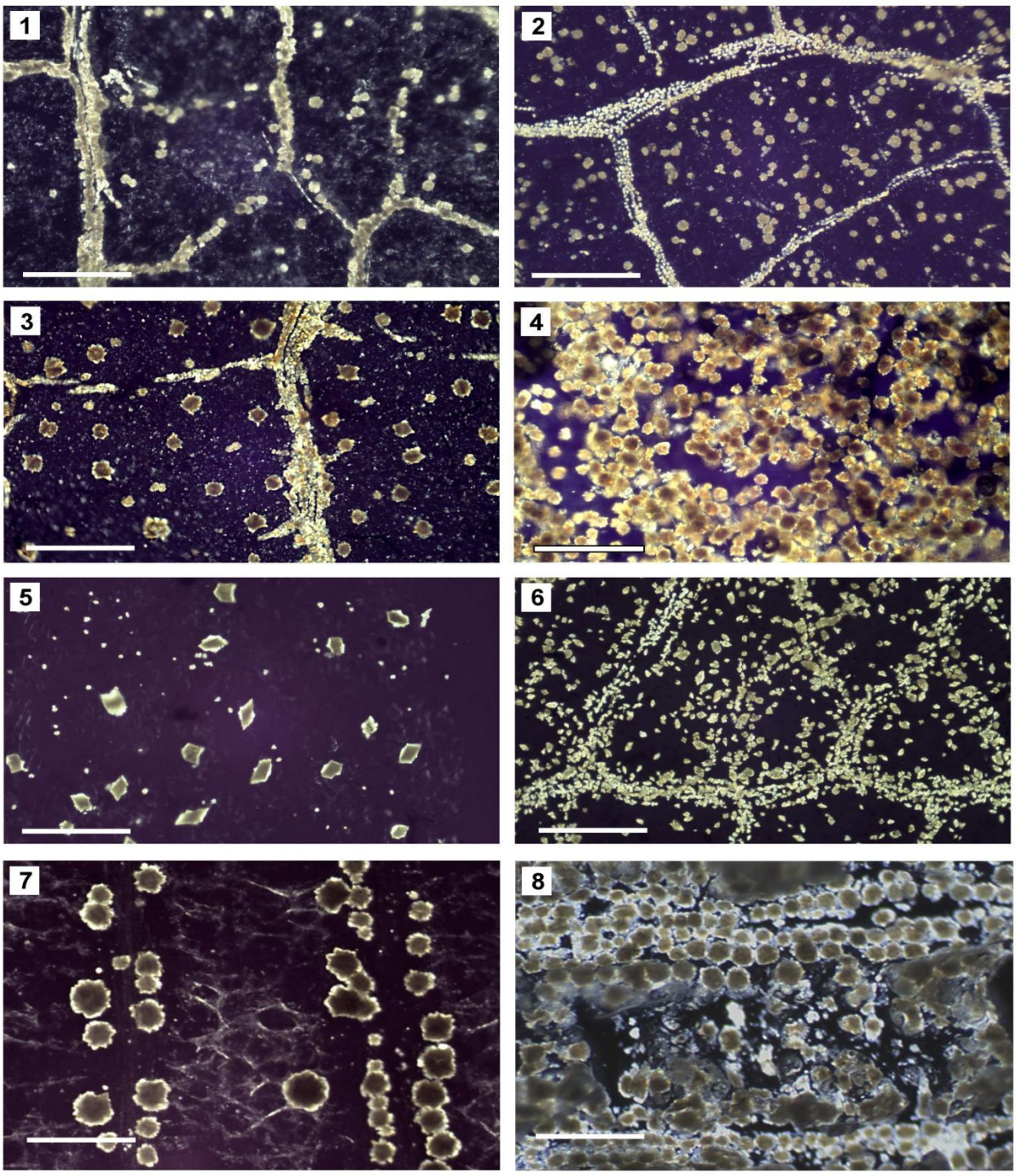

FIGURE 2. Distribution patterns of CaOx druses and crystals in fresh leaves. Polarisation-LM images of incinerated leaves of various tree species, illustrating varying density of druses. CaOx appears bright on dark background. 2.1 *Malus domesticus*. Few druses in parenchyma, veins are covered densely with crystals. 2.2 *Quercus robur*. Areoles with medium density of druses of 20-30 µm size. Veins are covered densely with small

CaOx crystals. 2.3 *Carya ovata*. High density of large druses, up to 60 µm, in areoles. Venation is only partially decorated with small crystals. 2.4 *Camellia japonica* leaf, densely filled with large druses. 2.5 *Carpinus kawakamii*. Very large solitary crystals and few small druses in parenchyma; no CaOx along venation. 2.6 *Agarista populifolia*. Areoles and venation carry numerous individual crystals of medium size, 20-30 µm. 2.7 *Ginkgo biloba*. Very large druses, up to 100 µm, along veins. 2.8 *Encephalartos villosus*. Very large druses along the veins in different layers of the thick leaf overlap each other. Same magnification for all LM images. Scale bars = 200 µm.

CaOx plays a central role in a variety of important functions in plants, including tissue calcium regulation, protection against herbivory, and metal detoxification (Nakata, 2003). Concerning the regulation of Ca in plant cells, idioblasts serve as localized sinks to remove excess calcium from discrete regions of tissue, allowing the surrounding cells to more easily maintain biologically safe intracellular concentrations of calcium (Volk et al., 2001).

A positive correlation between the calcium concentration in the nutrient medium with the production of crystals in the leaves of *Corchorus olitorius* L. and *Malva parviflora* L. has been reported. Actually, heavy metals decreased the number of crystals but CaOx crystals do not play a major role in detoxification (Faheed et al., 2013).

The effect of herbivory on CaOx density has been investigated in many studies. Brenda Molano-Flores (2001) showed that CaOx density in *Sida rhombifolia* increased with herbivory. Despite this, in the desert lily, *Pancratium sickenbergeri*, larvae of *Polytella cliens* (Lepidoptera, Noctuidae, Hadeninae) tend to eat only the leaves that do not include CaOx raphids (Ward, 1997). On the other side, Paiva (2021) stated that CaOx crystals are not an effective defense against herbivory. Especially in vertebrates it seems that raphids play an indirect role against herbivory (Gardner, 1994). In human, some of the poisonous plants, such as fruits of *Caryota* spp. (Arecaceae) and leaf and tubers of several species of Araceae, are known to cause a painful burning sensation on the skin and oral cavity (Ducombs & Paulsen, 2011).

The importance of calcium minerals in fossil plant taphonomy is undeniable. Fossil leaves are an important source of palaeontological information and provide both evolutionary and palaeoecological insights (Nicotra et al., 2011; Chitwood & Sinha, 2016; Moraweck et al., 2019).

In plant fossils, patterns of calcium biominerals are rarely reported because they usually disappear during the process of fossilization. Many factors such as physical and chemical processing during fossilization, the structure of the sediment containing the fossils, and the physiology of the leaves (e. g., thickness of the leaves and position of CaOx minerals in leaves) play a major role in the fossilization of calcium minerals. CaOx druses in fossil leaves can be identified quite well due to their almost globular shape and their distribution pattern.

In the study presented here, traces of CaOx druses in or on fossil leaves from different sites from the Devonian to the Quaternary are investigated. Granular structures in carbonized or mineralized leaf remnants were found in fossils of basal plants, gymnosperms and angiosperms and interpreted as casts of CaOx druses and individual crystals.

Light microscopy and element analyses by scanning electron microscopy revealed varying compositions of the fossils, the fill of the casts, and their surrounding matrix. Identification of the bio-mineral traces is important to help classify or reclassify fossil plants and to better understand taphonomy and diagenetic pathways during fossilization. The identification of former CaOx remains in leaf fossils provides novel insights on the fate of plant bio-minerals during fossilization. More importantly, it provides an additional aspect of the ecophysiology of fossil plants, thus improving the accuracy of palaeoecological reconstructions and can provide a broader perspective on the evolution of CaOx and its role in plant ecology across geological times. Alternative interpretations of the fossil microstructures are discussed, but ruled out.

Identification of fossil leaves can be relatively straightforward based on general morphological features such as size, shape, leaf margin, and details of leaf veins and cuticle micromorphology, but, often, fossil leaf assignments are tentative and may change over time. Additional diagnostic

characters would therefore be highly appreciated to support or refute fossil identifications. One neglected feature common in plant fossils are granular structures observed on leaf fossils, which have not yet received a satisfactory explanation. In the well-preserved leaf fossils from the Rott Fossil Lagerstätte (North Rhine-Westphalia, Germany) and some related fossil sites from the Oligocene of that region, numerous granular structures are found, which have been variously explained by previous authors as algal colonies, pollen grains, trichome bases, or papillose structures of the leaf epidermis (Mörs, 1995; Koenigswald, 1996). Winterscheid & Kvaček (2016) and Moers (1995) interpreted granular structures on fossil leaves as traces of various algae such as *Botryococcus*, *Tetraedron*, and Chrysophyceae, analogous to similar observations in leaf fossils from the Messel fossil site. Krassilov et al. (2005) in their study of 'Late Cretaceous Flora of Southern Negev' present numerous detailed images of fossil leaves which show patterns of granular structures, but these are not discussed in the publication. Generally, no convincing explanation for these rather common granular structures on leaf fossils has been proposed in the literature until now.

Phytolith analysis has important applications in evolutionary and especially archaeological and palaeoecological studies (Strömberg et al., 2018; Piperno, 1989; Piperno, & Pearsall, 1998; Esteban et al., 2017; Strömberg & Song, 2016; Piperno, 2006).

The rich fossil record of silica phytoliths contrasts starkly with the very poor fossil record of original calcium bio-minerals (O'Connell et al., 1983; Genua & Hillson., 1985; Coté, 2009; Anitha & Sandhiya, 2014). This is likely due to the limited chemical stability of both calcium-based bio-minerals. Calcium carbonate (e.g., cystoliths) is soluble even in the weakest acids, including CO_2-saturated water, and is therefore unlikely to survive fossilization (Ogino & Sawada, 1987; Goss & Bogner, 2007).

CaOx itself is less soluble (McComas & Rieman,1942; Hoover & Wijesinha, 1945), but may be gradually oxidized to calcium carbonate during fossilization, which is subsequently lost from the fossil record. Even if calcium bio-minerals survive fossilization itself, they are likely to get

dissolved during fossil extraction or processing by researchers, which is advantageous for the extraction of the much more robust silica phytoliths (Anitha & Sandhiya, 2014).

Calcium bio-minerals themselves are thus usually not preserved in the fossil record, but casts ("crystal cavities") have long been known from the cuticles of fossil conifer leaves (Rüffle, 1976). These casts are interpreted as impressions of CaOx crystals in the leaf epidermis as known from extant conifers (Florin, 1931). These crystal cavities are also used as a minor diagnostic character for conifer taxa such as *Doliostrobus* and *Quasisequoia* (Kunzmann, 1999; Kvaček, Z. 2002). Such crystal cavities have been reported from fossils from the Late Cretaceous (e.g., *Quasiseqoia florinii*, Kunzmann, 1999), Oligocene (*Glyptostrobus europaeus*), Paleogene (e.g., *Doliostrobus taxiformis*) (Kvaček, 2002; Wilde, 1989) and Neogene (e.g., *Cupressospermum saxonicum*) (Mai & Schneider, 1988). The occurrence, distribution (adaxial and abaxial leaf surfaces as well as in the mesophyll) and abundance of crystal cavities varies within fossil-species. It has been proposed that this variability in fossils of *Doliostrobus taxiformis* from the Eocene and Oligocene in Europe can be attributed to palaeoecological factors such as habitat and climate (Kunzmann, 1999; Kvaček, 2002), but no conclusive evidence has been presented for this assumption. Despite the wealth of angiosperm fossils and the prevalence of bio-minerals in their extant representatives, there are as of yet no reports of "crystal cavities" in angiosperm fossils. Thus, an odd contrast between calcium bio-minerals as a common feature of extant angiosperms and the lack of any evidence for these bio-minerals in the fossil record is conspicuous. On the other hand, there are reports of leaf fossils in which obscure granular structures abound. The present study addresses the question of whether these granular structures correspond to calcium-based bio-minerals (CaOx crystals and druses, and calcium carbonate grains), in which case they would most likely be ghost crystals as refill of casts following the distribution pattern of calcium-based bio-minerals in extant taxa. In order to elucidate the identity of the granular structures on fossil leaves, the fine-scale patterns on fossil leaves have been investigated and compared to patterns of CaOx bio-

mineralization of extant plant taxa. Scanning electron microscopy (SEM) and energy dispersive X-ray (EDX) element analysis were used to investigate details of fossil and extant plant materials.

The present work specifically aims at answering the following questions:

(1) Do the granules in fossil leaves correspond in shape and location to CaOx druses in modern leaves? (2) Can alternative explanations for the granular structures, e.g., imprints and/or casts of pollen, peltate trichomes, trichome bases, or stomata, be ruled out? (3) Which chemical and biochemical processes affected the leaves containing CaOx during the fossilization? (4) What micromorphological changes happened during fossilization? (5) Which patterns have developed by fossilization during different periods of time? (6) What are the main inorganic elements in fossil leaves after fossilization? (7) Does the replacement of elements follow a special pattern in different times in the same species?

2.3 Materials

2.3.1 Fossil samples

In the current study a number of leaves from the Devonian to the Quaternary were examined. Fossil material was borrowed from various museums in Germany. Details for each studied specimen, including museum collection, taxonomic identification, museum specimen number and locality information is given in **Appendix 1**.

Obvious granular structures were visible on the surface of many fossil specimens, which were selected for detailed examinations. In addition to the partially damaged specimen surfaces, freshly split charcoal samples were examined, which could be separated from the fossil block with adhesive tape.

2.3.2 Fresh leaves

Fresh leaf samples from extant species were collected from the Botanical Garden, University of Bonn, Germany. Fully developed late-season leaves from adult trees, shrubs and a few aquatic plants were collected in summer and autumn, when CaOx deposits are fully formed. The selection included species or genera closely related to those identified in fossils with granular structures, and additionally some randomly selected deciduous woody species. In total, leaves of more than 24 living species were examined (**Appendix 2**).

2.4 Methods

The fossil and fresh samples were examined and documented with different microscopic techniques such as light microscopy (LM), scanning electron microscopy (SEM), and micro-computer tomography (µ-CT).

2.4.1 LM

A stereomicroscope Leica MZ125 (Leica Microsystems, Wetzlar, Germany) was used for selection of samples and examination at low magnification. Detailed light microscopy (LM) was performed with a standard light microscope (Müller optronic, Erfurt, Germany) with large sample stage. Long distance objectives enabled flexible surface illumination with a LED light source. Both microscopes were used with a Swift SC1803 microscope camera (Swift Optical Instruments, Schertz, Texas, US) with 18-megapixel resolution. A Lumix DMC-G70 photo-camera (Panasonic Corporation, Osaka, Japan) with Lumix macro-objective was used for close-up images.

2.4.2 SEM

Scanning electron microscopy (SEM) was performed with a LEO 1450 SEM (Cambridge Instruments, Cambridge, UK, Nees-Institut, Universität Bonn) and with a Tescan VEGA (Type

4) (Institut für Geowissenschaften). Both were equipped with secondary electron (SE) and backscattered electron (BSE) detectors and an energy dispersive X-ray spectroscopy (EDX) element analysis system with Link ISIS software (www.oxford-instruments.com).

2.4.3 Micro-CT

X-ray images and micro-computer tomography (µ-CT) scans of dry leaves were obtained with a SkyScan 1272 Micro-CT system (Bruker microCT, Kontich, Belgium) in the Institute of Evolutionary Biology and Ecology at the University of Bonn. The images were recorded with a detector of 4,032 × 3,280 pixels with a pixel size of 1 µm. Visualisation of the µ-CT data was performed with ImageJ-Fiji software (https://imagej.net/software/fiji/).

2.5 Specimen preparation

2.5.1 Fossil samples

Fossil specimens were cleaned to remove dust, if necessary, with an air-blower or through careful rinsing with distilled water. For SEM examination, small representative pieces were selected, mounted on a sample holder, and sputter-coated with a thin layer (10 to 15 nm) of palladium. Palladium, in contrast to gold, does not disturb the EDX analyses of relevant elements such as silicon and sulphur, and this thin layer is sufficiently transparent to high-energetic electrons for compositional-contrast BSE imaging.

2.5.2 Fresh leaves

Fresh leaves were examined to investigate the distribution of CaOx druses and crystals in a variety of species. Most leaves are not transparent enough to visualize the crystals directly and need to be subjected to a clearing procedure. We found a very simple procedure, which is particularly useful: pieces of the leaves were simply burnt until the organic matter was largely oxidized, reducing the leaf to a brittle piece of ash. For this purpose, fresh or dry leaves were

incinerated in a temperature-controlled oven (Brennofen Uhlig U15, Efco GmbH, Rohrbach, Germany) at 600 to 650°C. The samples turned white after 5 to 10 min. In many cases, simple burning over a gas burner was also successful and much faster. Usually, the CaOx structures could be easily visualized directly in the ashes using the stereomicroscope or standard LM. If the ash remnants from the epidermal layers were too thick and not transparent enough, the upper and lower halves of the burnt leaf were separated with transparent adhesive tape such as Tesafilm (Tesa SE, Norderstedt, Germany) and each half was attached to a glass slide. Observing the inner side of each half showed the majority of the druses and crystals.

2.5.2.1 Standard preparation of fresh leaves for SEM and µ-CT

Pieces of fresh leaves were fixed in 70% v/v ethanol + 4% v/v formaldehyde in water for at least 20 hrs and dehydrated with ethanol. For freeze-fracturing, ethanol-infiltrated samples were immersed in liquid nitrogen and broken randomly. After unfreezing, all samples were critical-point dried (CPD 020, Balzers Union, Liechtenstein) and mounted on sample holders for SEM or µ-CT.

2.6 Results

First result in this thesis referee to the number of well-preserved leaf fossils from Rott Lagerstätte contained remarkable granular structures. Comparison of their distribution patterns with distribution of CaOx druses in fresh leaves of various plants showed a remarkable similarity, which was the motivation for a detailed survey. Considering that CaOx crystals and druses occur in strongly varying patterns (**Figures 1, 2**), we could identify analogous granular structures with varying properties, depending on fossil species and composition. Remarkably, these casts occurred with varying compositions. CaOx was replaced either by organic material or by various mineral components, or empty cavities were still present (See discussion).

2.6.1 Fossil leaves of basal plants

The basal plants include the Bennettitales and Pteridospermatophyta. The aim of this investigation was to examine whether traces of CaOx exist in basal plant fossils or not.

Bennettitales (also known as cycadeoids) is an extinct order of seed plants that first appeared in the Permian period and became extinct in most areas toward the end of the Cretaceous. Bennettitales were amongst the most common seed plants of the Mesozoic, and had morphologies including shrub and cycad-like forms.

Pteridospermatophyta (also "seed ferns" or "Pteridospermatopsida") is a polyphyletic group of extinct seed-bearing plants (spermatophytes) with fern-like leaves.

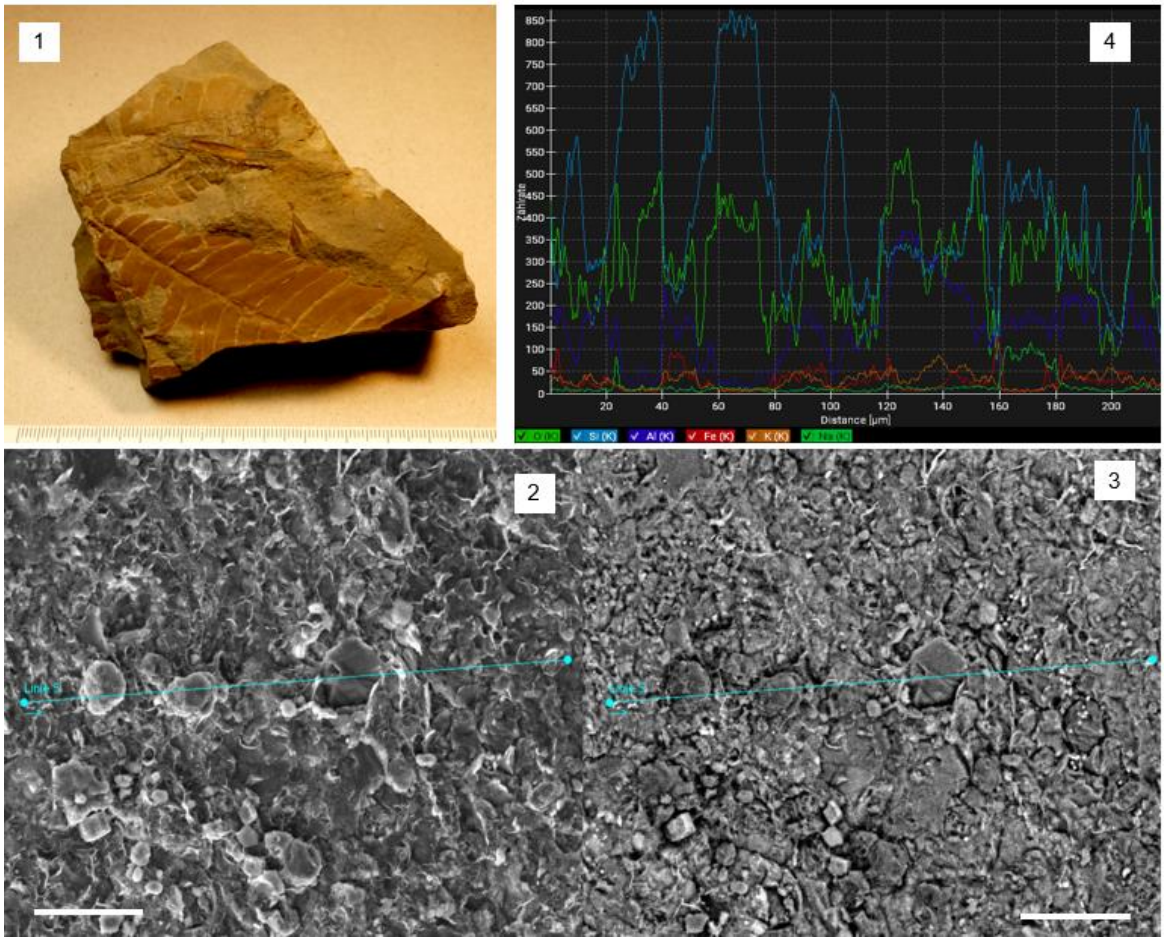

FIGURE 3. Fossil leaf of *Otozamites brevifolius* (Triassic, Rhaetian, Bayreuth, Unternschreez, Germany). 3.1 View of leaflet from *Otozamites brevifolius*. 3.2, 3.3 SE and BSE images which illustrate homogeneous composition in granules and surrounding sediment. 3.4 EDX analysis (line scan for Si, Al, O, K) of granules and matrix. Scale bars: 3.2, 3.3 = 50 µm.

Otozamites brevifolius (Triassic, Rhaetian, Bayreuth, Unternschreez, Germany) is an extinct form genus of leaves which is thought to be related to the Bennettitales. They are known as cycadeoids and the leaves are mostly separated and conserved as pinnae. The leaflet of *Otozamites* has the shape of an elongated triangle with an acute apex. EDX analysis show that the entire leaf is mineralized. Mineral elements such as Si, Al, O, and a little K form the surrounding sediments and also the granular structures. Thus, the granules in this leaf, in contrast with those in many fossil leaves in this study (e.g., *Glossopteris* sp.), can be recognized only by their texture and distribution and not by different constituent elements.

Almost all of the seed fern fossils (Pteridospermatophyta or Pteridospermatopsida) show a carbonized layer except fossil leaves of *Glossopteris* sp. (Permian, Dunedoo, Australia, **Figure 4**). Under the carbon layer regular patches were observed which were mineralized with different compositions. In the following, various example of seed ferns with granular structures from different periods of time are described and interpreted.

Fossil leaves of *Glossopteris* sp. (Permian, Dunedoo, Australia) frequently show granular structures in regions where remains of parenchymatic tissue are preserved (**Figure 4**). With the SEM, round patches of ca. 30 µm diameter were recognised by contrast in color (dark and light grey) and texture (granules show a higher density in comparison with surrounded sediment) (**Figure 4.3**). The EDX reveals the differing mineral compositions of the sediment and the granules. Both contain Si, Al and O, while the granules lack Fe, which is common in the sediment (**Figure 4.5**).

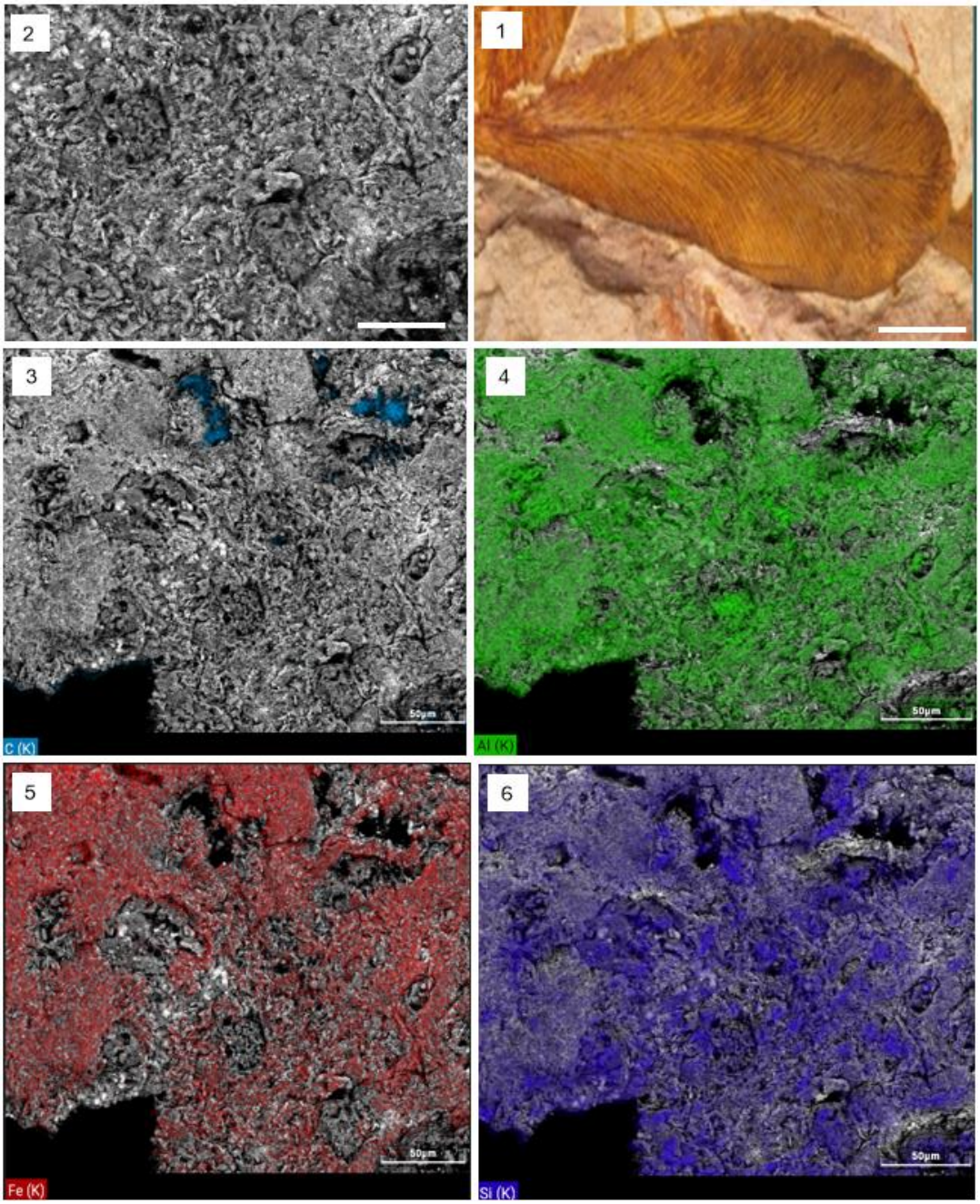

FIGURE 4. Mapping analysis of a fossil leaf of *Glossopteris sp*. (Permian; Dunedoo, Australia). 4.1 View of *Glossopteris* sp. 4.2 Granular structures in a flat fracture surface are recognizable by their texture and slightly different composition. 4.3 Granular structures include the element C (blue). 4.4, 4.6 Sediment and granules made of Al (green) and Si (violet). 4.5 Fe (red) cover the sediment. Scale bars: 4.1 = 1cm; 4.2-4.6 = 50 µm.

Several Carboniferous leaf samples consisted of relatively thick (25-30 µm) carbon layers which easily could be separated from the sediment. SEM images of a fossil leaf of *Paripteris gigantea* (seed ferns, Carboniferous) show under the carbon layer a regular pattern of bright

patches (**Figure 5.2**) which are embedded in the sediment and seem to be arranged along the leaf venation. EDX spectra (**Figure 5.3**) show the composition of granules and sediment. The patches have diameters of 30-50 µm and consist of iron oxide; the sediment consists of Al, Si and O (Si: Al ratio ca. 1:1).

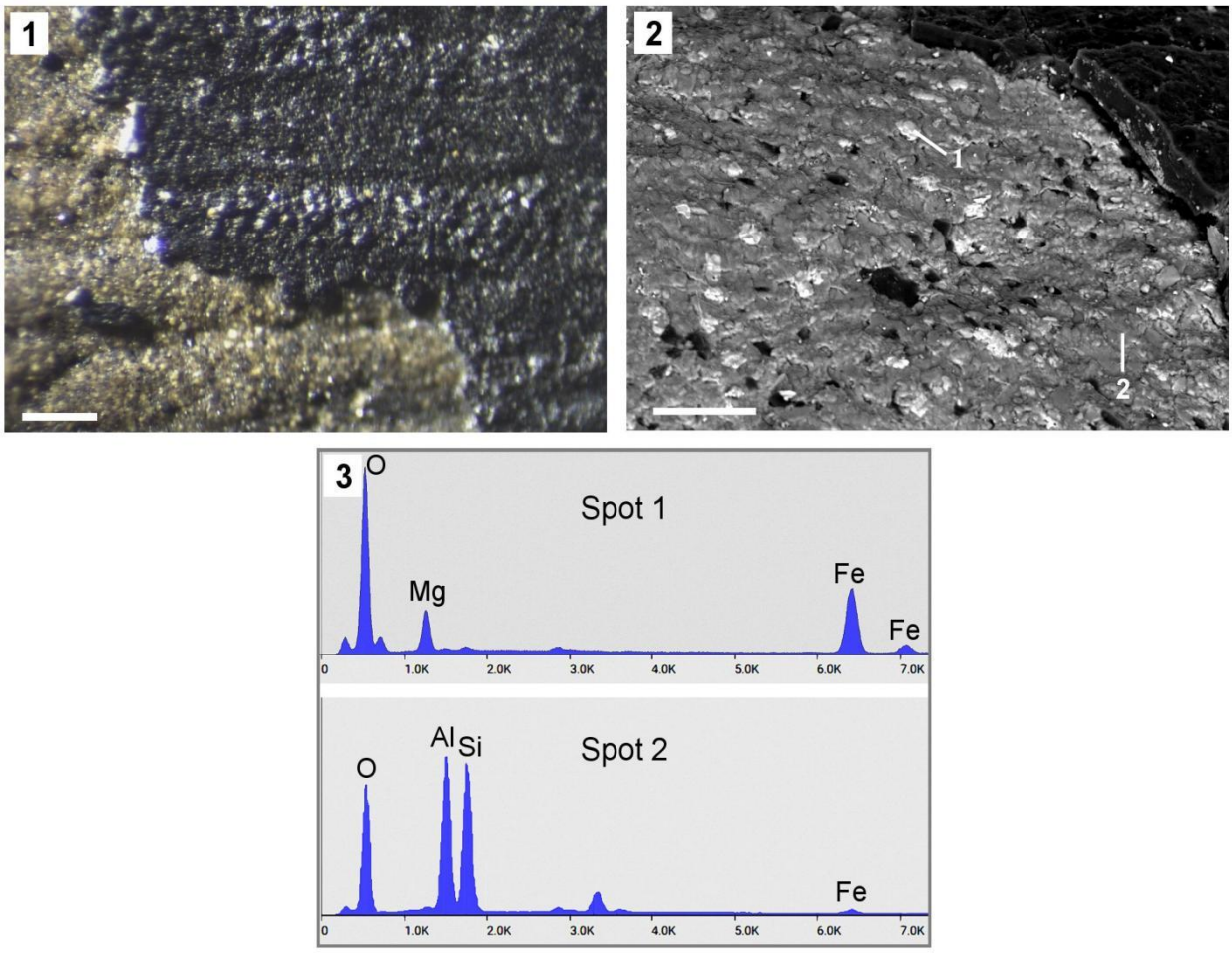

FIGURE 5. Fossil leaf of *Paripteris gigantea* (Carboniferous). 5.1 SEM image of carbon layer (black) and partially removed carbon layer is illustrated. Rough granules parallel of the veins are observed. 5.2 Regular whitish patches under the carbon layer (Spot1, 2). 5.3 EDX spectra show sediment composition. Whitish granules (Spot 1) include of Mg, Fe, and O. Spot 2 (gray, sediment) consists of Si, Al and O. Scale bars: 5.1 = 200 µm; 5.2 = 100 µm.

From a collection of several hundred samples of Late Devonian leaf fossils from Bear Island (Norway) 30 specimens have been selected for a closer examination.

The majority of these samples were assigned to *Archaeopteris roemeriana*, *Cyclostigma kiltorkense*, or *Pseudobornia ursina*.

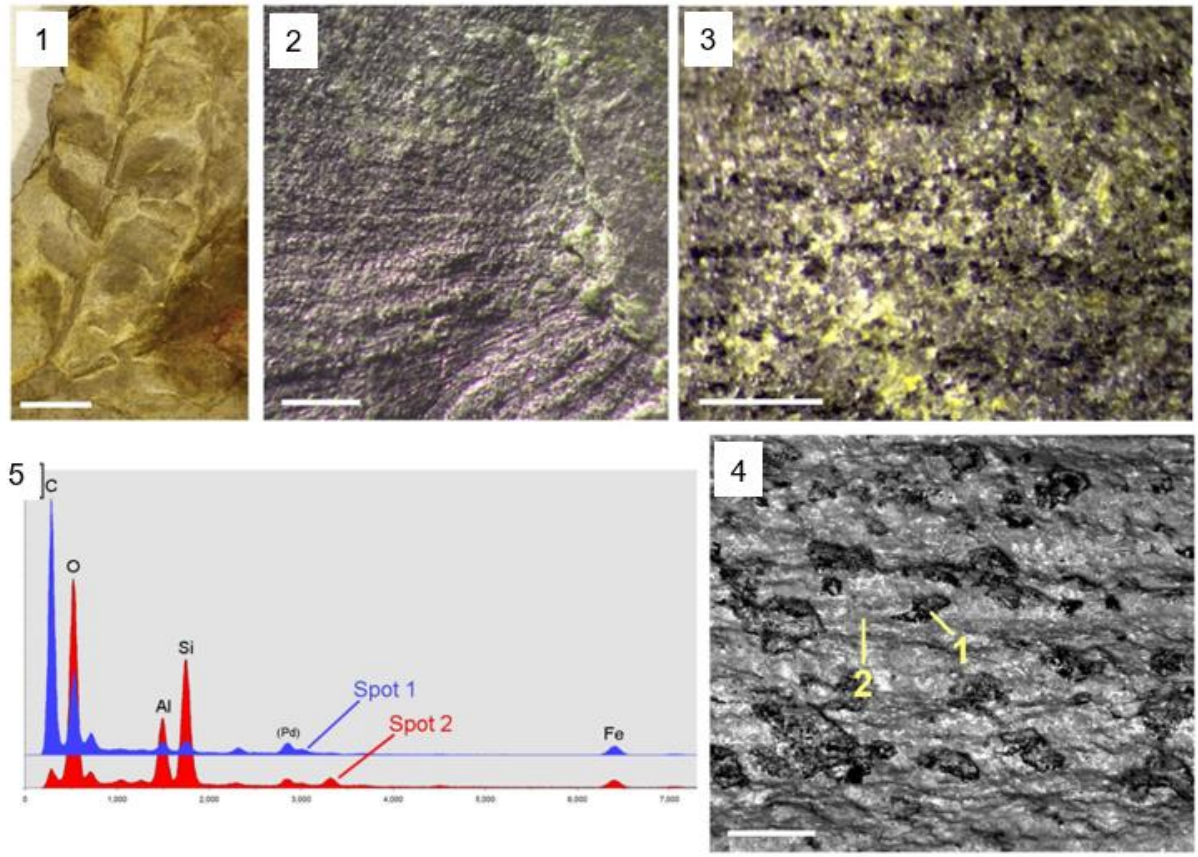

FIGURE 6. Fossil leaf of *Archaeopteris roemeriana*, Devonian, Bear Island, Norway. 6.1 Overview of a stem with leaves. 6.2, 6.3 LM images show rows of dark granules below the removed carbon layer parallel to the venation. 6.4-6.5 SEM compositional contrast (BSE) image of the dark grains and Element analyses. Dark grains consist mainly of carbon (blue spectrum); the red spectrum shows composition of the sediment (oxides of Si, Al, Fe). Scale bars: 6.1 = 10 mm; 6.2 = 1 mm; 6.3 = 400 µm; 6.4 = 100 µm.

The Late Devonian on Bear Island is stratigraphically summarised as Røedvika Formation (e.g., Worsley et al. 2001). This formation is subdivided into three members: Vesalstranda, Kapp Levin and Tunheim members. In contrast Schweitzer (2006) followed a much older subdivision of the Røedvika Formation (Horn & Orvin, 1928). These authors differentiated the formation into the Misery Series, the Barren Series and the Tunheim Series. Only the Misery Series and the Tunheim Series contain macrofloras, which are markedly different from each other

(Schweitzer, 2006). Thus, all Late Devonian plant material investigated in the present study derive from one or the other series of the deposits on Bear Island.

The carbonized leaf remnants of *Archaeopteris roemeriana*, a progymnosperm which is a group of early plants likely ancestral to gymnosperms, show a particularly rough surface structure. In areas where the leaf layer was removed, a pattern of black granules was visible (**Figure 6.2, 6.3**). The size (50-80 µm) and distribution of these patches resembled those of CaOx druses in fresh leaves, particularly those of gymnosperms such as *Ginkgo* or *Encephalartos*. BSE image of the dark grains in **Figures 6.4, 6.5** shows element compounds in dark granules (spot 1) and sediment (spot 2). O, Al and Si allocated high amount in sediment in comparison with granules while C in dark granules showed higher amount.

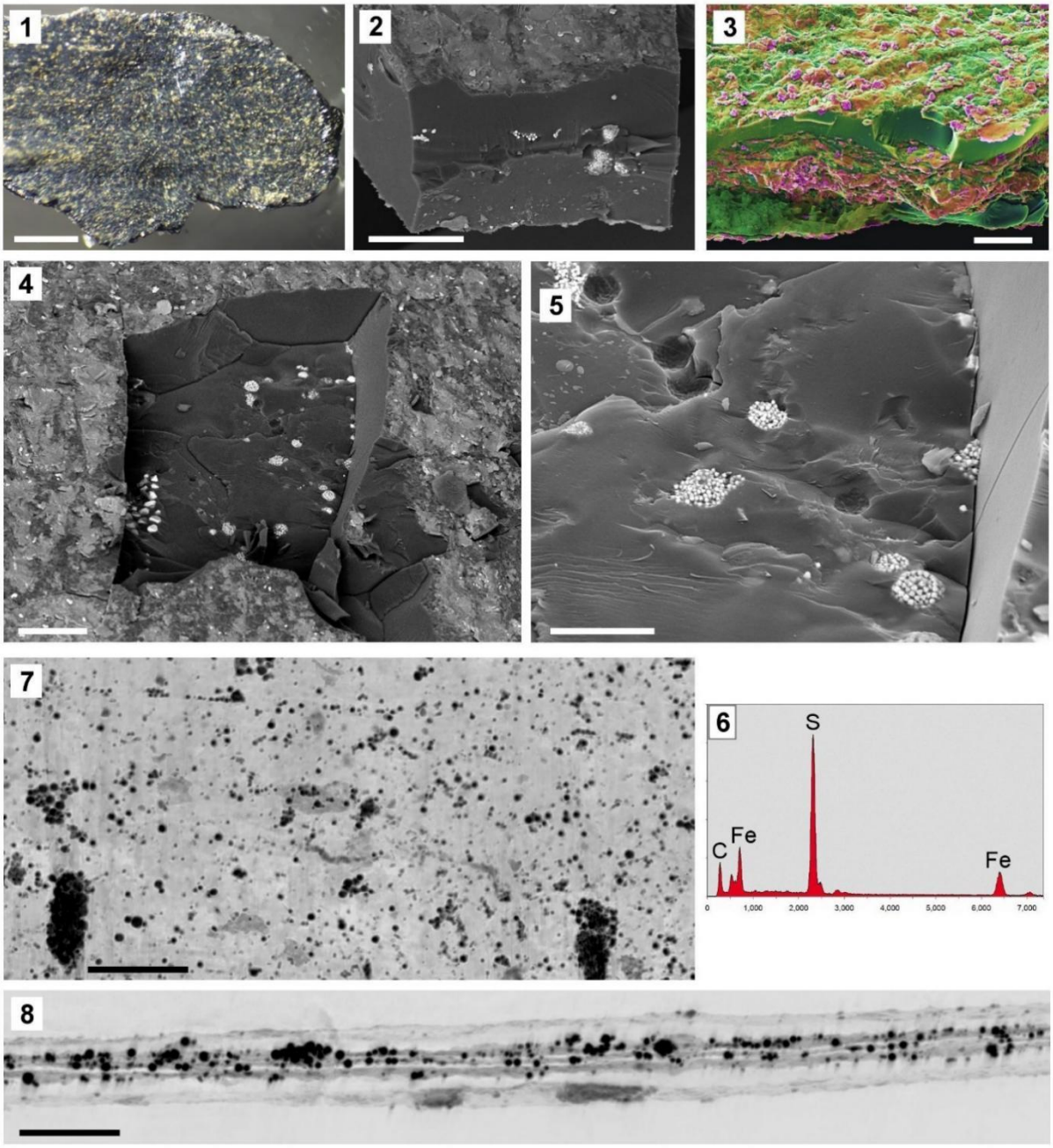

FIGURE 7. Devonian (Bear Island, Norway) leaves assigned to *Cyclostigma kiltorkense* with granular inclusions. Images of a fragment of carbonized leaf. 7.1 Overview by stereo-microscope shows the surface covered with small pyrite particles. 7.2, 7.3 Views on the edge of fragment show mineral inclusions in the middle of the 75 µm thick carbonized layer, either pure pyrite granules (7.2) or mixed with Si-Al oxides (7.3). 7.4, 7.5 Locations where the upper carbon layer is removed; pyrite granules in the middle of the carbon layer are exposed. 7.6 EDX spectrum reveals composition of grains (Fe, S). 7.7, 7.8 µ-CT images of fragment. 7.7 Plan view, entire thickness. 7.8 Reconstructed cross section shows Si-Al-mineral inclusions (gray) and pyrite granules (dark) in the middle of the fragment. The carbon layers appear transparent and almost invisible. Scale bars: 7.1 = 0.5 mm; 7.2-7.4 = 50 µm; 7.5 = 20 µm; 7.7, 7.8 = 200 µm.

Fossil samples assigned to *Cyclostigma kiltorkense*, a lycopsid, consisted of carbonized black leaf remnants on a mineral substrate. Separated fragments of the leaves were covered with small yellow pyrite particles on both sides (**Figure 7.1, 7.3**) which may be casts of the former leaf surface structure. A view onto the edge of the samples shows mineral inclusions in the middle of the 70 to 80 µm thick carbon layer (**Figure 7.2, 7.3**). In some locations, parts of the brittle carbon layer had been broken off, and granular pyrite inclusions were visible in detail (**Figure 7.4, 7.5**). Their shape, size (20-30 µm) and location within the leaf, between the carbonized epidermis layers, are indications that they are casts of former CaOx druses. Micro-CT scans were used to determine the spatial distribution of the mineral inclusions. A plan transmission view (**Figure 7.7**) shows the entire granules. The reconstructed cross section (**Figure 7.8**) shows pyrite granules (black) and Si/Al-minerals (light-gray) in the middle of the fragment. The carbon layer is transparent and almost invisible. The EDS spectrum (**Figure 7.6**) shows the composition (Fe, S) of the granules.

2.6.2 Gymnosperms

The gymnosperms are a group of seed-producing plants that includes conifers, cycads, *Ginkgo*, and gnetophytes. In the following section the distribution of CaOx in fossil and fresh leaves of cycads, *Ginkgo* and conifers are illustrated.

In gymnosperms in contrast with basal plants (e. g. seed ferns and ferns) the occurrence of CaOx and traces of it in fossil leaves show more diversity and better preservation. On the other hand, in comparison with angiosperms, CaOx crystals in extant leaves and traces of them in Cycadophyta, Ginkgophyta and Conifera are similar in preservation.

2.6.2.1 Cycadopsida

In cycads the distribution pattern of CaOx druses shows similarity to the seed ferns (refer to the basal plants, seed ferns, (**Figure 3.6**) and ginkgophytes (**Figures 10-12**). Observation of druses parallel to the veins is a proof of this claim. Differences between cycads and ginkgophytes are found in the type and size of the crystals. In cycads, crystals appear in individual and aggregated forms. In contrast, in ginkgophytes, they are druses. In addition, crystals in cycads are normally smaller than they are in ginkgophytes and in some cycads species they occur only in one side of the veins while in *Ginkgo* they appear around the veins and between them in the vascular system. As it can be seen in **Figures 8** and **9**, diverse distribution patterns occur in cycads. Density and distribution patterns and the formation of druses in different species does not follow the same trend.

The results show that in *Cycas diannanensis,* druses occur almost exclusively on one side of the vascular system (**Figure 8.1**). Almost all of the crystals in *Cycas* appear in druses in which they are aggregated from different individual crystal sizes (**Figure 8.4**). Furthermore, some of the parenchymal cells are filled entirely with one big crystal. In *C. szechuanensis* we observed typical morphology of CaOx crystal aggregates in star form (**Figures 8.5, 8.6**). Their distribution also shows similarities to *Ginkgo biloba*.

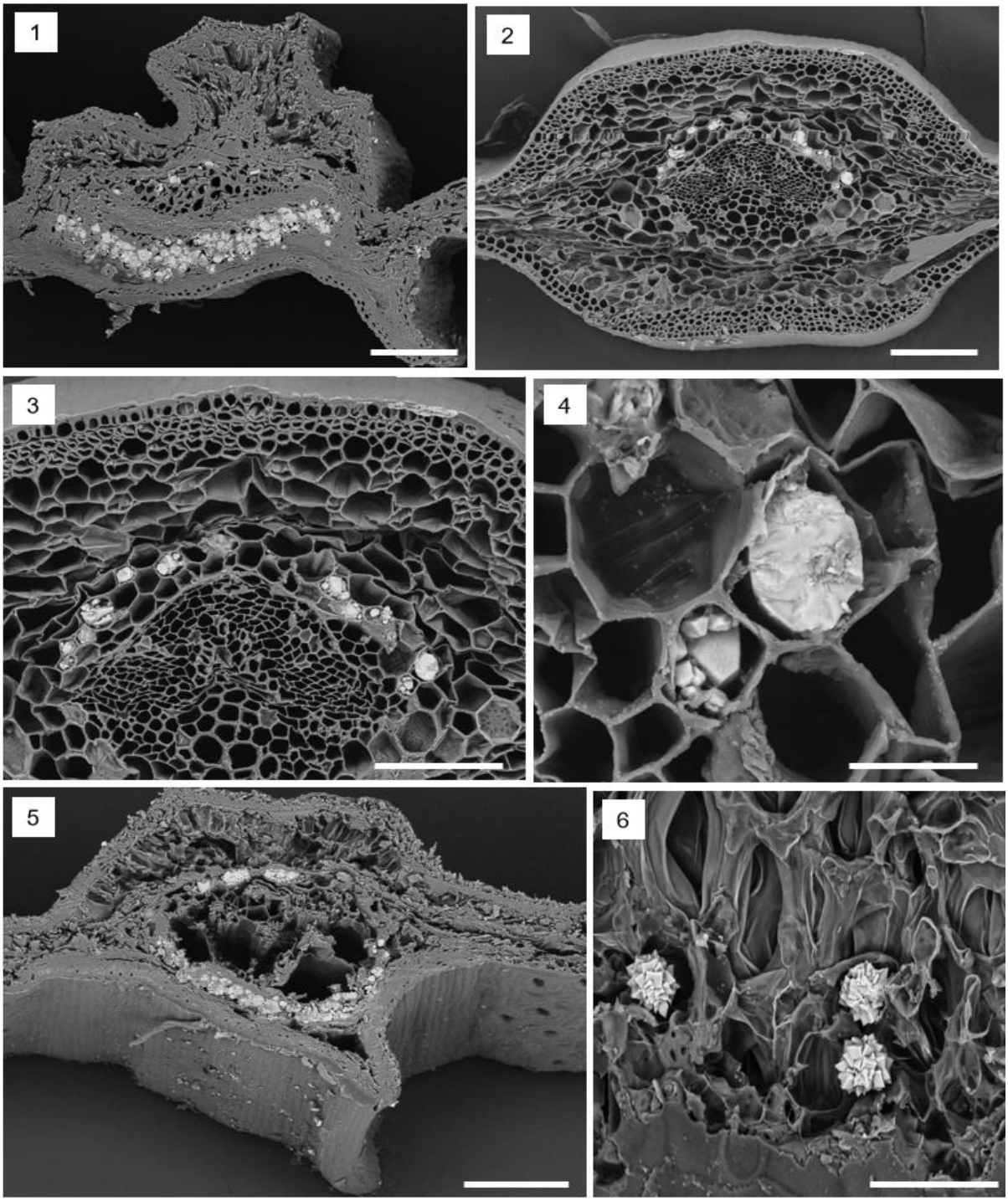

FIGURE 8. Morphology and distribution pattern of CaOx crystals in some extant species of cycadophytes are illustrated. 8.1 Druses in *Cycas diannanensis* observed in a collection of individual crystals. 8.2-8.4 CaOx distribution pattern in *C. rumpii*. CaOx occur mostly in one side of the vein. 8.5, 8.6 illustrates *C. szechuanensis* which druses appear in sharp star forms. Scale bars: 8.1, 8.2, 8.5 = 200 μm; 8.3 = 100 μm; 8.4, 8.6 = 50 μm.

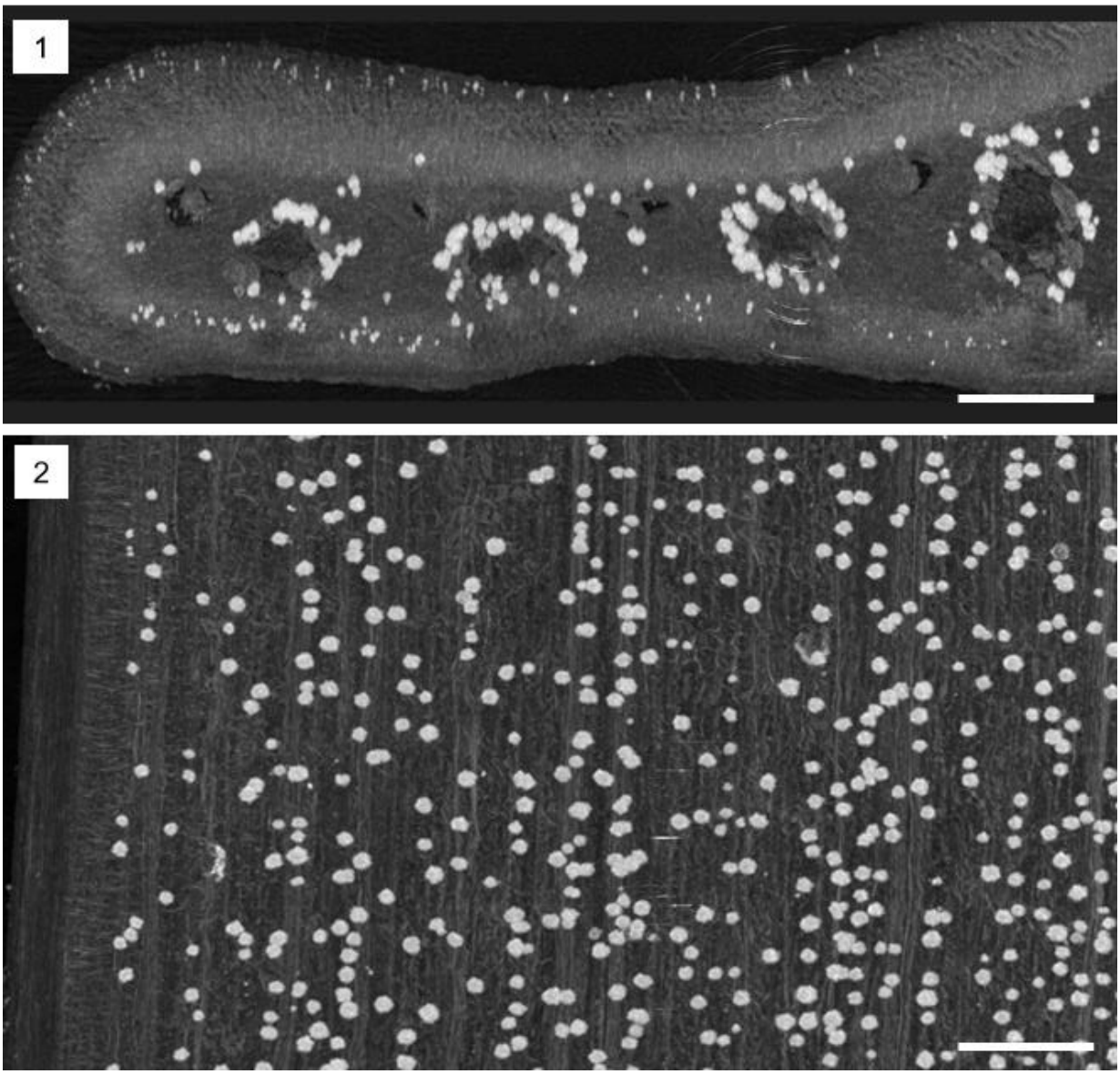

FIGURE 9. µ-CT images of fresh leaf of *Encephalartos lehmannii* illustrate CaOx crystals around the veins. 9.1 Reconstructed cross section shows distribution of CaOx crystals around the veins. 9.2 Plan view of the same region. Occurrence of CaOx crystals parallel to the veins appears similar to the pattern in *Ginkgo biloba*. Scale bar: 400 µm.

SEM images of *Encephalartos lehmanni* showed a similar distribution pattern of CaOx druses in cycads and *Ginkgo biloba:* druses distributed in the phloem and parallel to the vascular system.

2.6.2.2 Ginkgoopsida

Almost all of the fossil samples of the Ginkgoopsida showed at least some granular structures or traces of CaOx druses. Even from the Carboniferous, residues of granular particles are found in carbonized leaf material and are recognizable in fossil leaves with SEM. **Figure 13** shows fine structures of casts refilled with other minerals. The best chances to find traces of former CaOx druses are given in fossil leaves which contain remnants of their parenchymal structures, either carbonized or filled with mineral precipitation, because druses usually occur in the leaf parenchyma, and only rarely in the epidermis. Fossilized remnants of only epidermis or cuticle rarely contain traces of druses. Most useful are freshly exposed fossils, particularly when both sides are available for examination. Among numerous fossil leaf samples which were examined with LM, samples with better chances for CaOx preservation were selected for loan from the institutions or museums. Many fossils consist of coarse-grained sediments, which made a recognition of traces of druses unreliable or impossible.

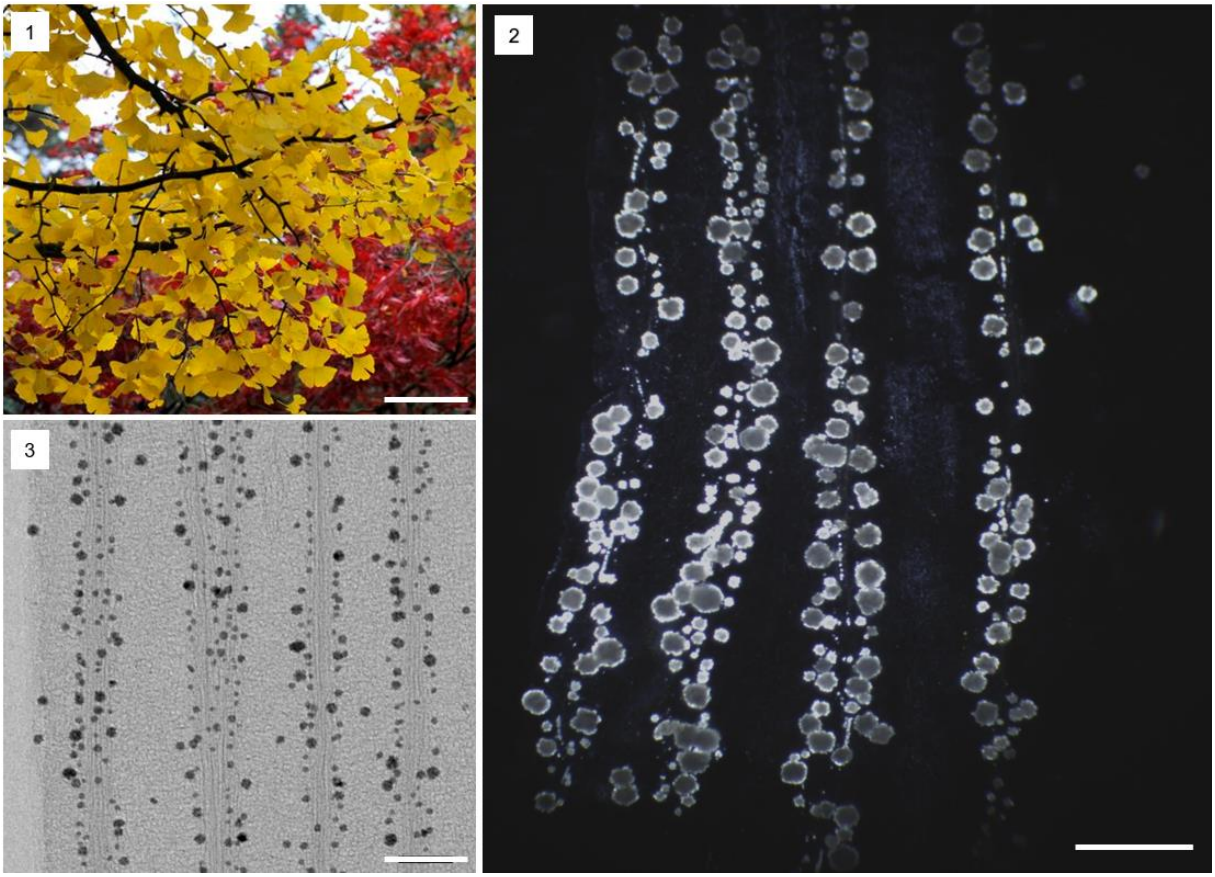

FIGURE 10. View of *Ginkgo biloba* leaf and images of the druse's distribution. 10.1 Close up image of *G. biloba* in front of the Geological Institute, Bonn. 10.2 LM image of CaOx druses from ash of a fresh *Ginkgo* leaf; 10.3 Micro-CT images of CaOx druses, along and between the veins in *G. biloba*. Scale bars: 1 = 30 cm; 10.2, 10.3 = 200 µm.

Figure 10.1 shows a view of *Ginkgo biloba* branches with fresh leaves in front of the Geological Institute, University of Bonn. The leaves are fan-shaped with veins radiating out into the leaf blade, sometimes splitting, but never anastomosing to form a network. Leaves are usually 5–15 cm long. In autumn, the foliage shows saffron yellow as is seen in the image above. In Figure 10.2 druses of CaOx along the veins are illustrated with LM. Diverse size of the druses in range of 3-100 µm in **Figure 10.2** (LM) and **10.3** (Micro-CT image) is observed. In addition, between the veins, individual crystals of CaOx with sizes of 2-5 µm are observable.

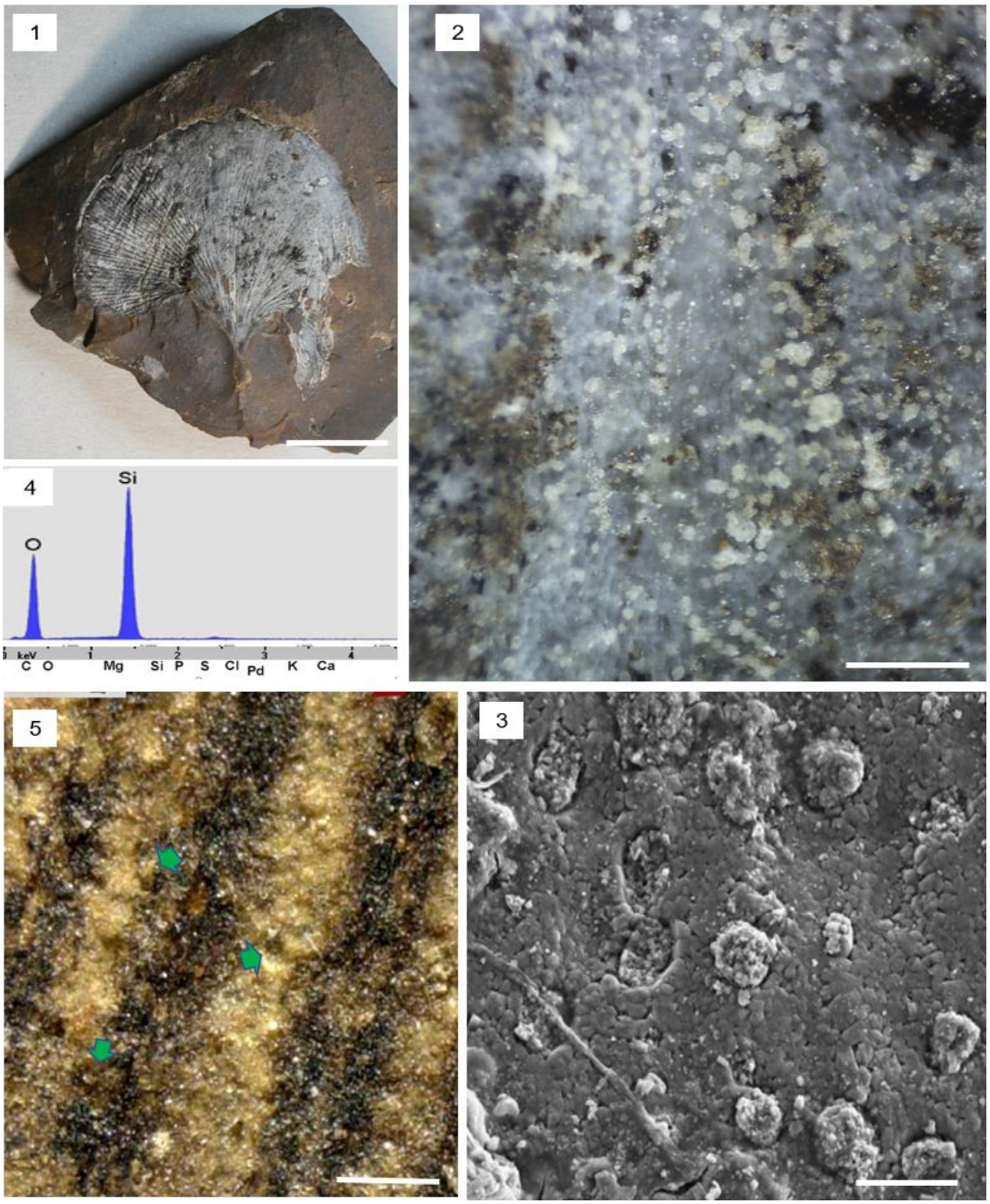

FIGURE 11. Fossil leaves of *Ginkgo adiantoides* from different Lagerstätten from the Cenozoic. 11.1 View of a fossil leaf of *G. adiantoides*, Morton County, USA, Paleocene. 11.2 LM image of CaOx druses shows their distribution under the cuticle layer. 11.3 Detail of the refilled CaOx casts along the veins. 11.4 EDX analysis of the granules shows SiO_2. 2.5 *Ginkgo adiantoides* from Republic NE Washington, Klondike. Veins are observable in dark brown; imprints of druses between and on the veins are marked with green arrows. Scale bars: 11.1 = 10 mm; 11.2, 11.5 = 200 µm; 11.3 = 50 µm.

Fossil leaves of *Ginkgo adiantoides* from different Lagerstätten from the Eocene and Paleocene have been examined with LM and SEM. In both fossil samples casts of former CaOx druses

were observed. In a fossil leaf from the Republic NE Washington, Klondike, dark brown granules which marked with green arrows (**Figure 11.5**) between veins and parallel to them are similar to CaOx druses. In another leaf fossil belong to the late Paleocene, Morton County, USA, white granular structures are observed with LM (**Figure 11.2**). Element analyses with SEM revealed that the white granules and the surrounding white sediment layer consist of silica (**Figure 11.4**). The size of the granules (20-100 µm) and their distribution along the leaf veins indicate that they are refilled casts of CaOx druses, similar to those in extant *Ginkgo biloba* leaves.

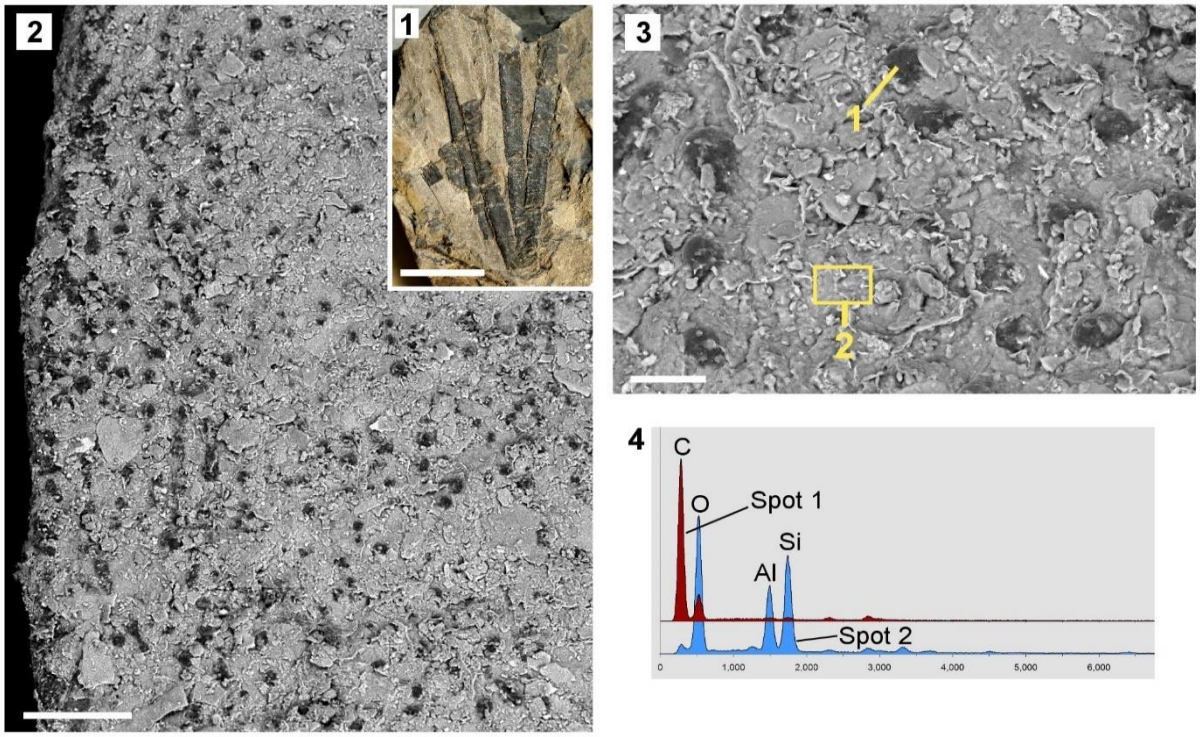

FIGURE 12. Traces of former CaOx druses in fossil leaves of *Baiera* from the Jurassic. 12.1 View of *Baiera canaliculate* from the Jurassic (Cayton Bay b. Scarborough).12.2 Black granules in remain of the parenchyma and parallel to the veins, well preserved.12.3 Close view of the granules and 12.4 EDX analysis show that they made of carbon. Scale bars: 12.1 = 10 µm; 12.2 = 100 µm; 12.3 = 20 µm.

Jurassic

A fossil of *Baiera canaliculata*, Jurassic, Cayton bay, has a typical fan-shaped leaf with deep lobes forming four segments. Under the cuticle (carbon layer), a regular distribution of granules similar to CaOx druses in *G. biloba* (**Figure 10.3**) but smaller (30-60 µm) along the veins were observed **(Figure 12.2).** Veins in *Bairera* in comparison with other ginkgophyte fossils are thinner. EDX analysis show that the granules included carbon (**Figure 12.4**).

Cretaceous

In *Baiera brauniana*, early Cretaceous, Osterwald, Germany, silvery granules lie under the carbonized cuticle layer, observed with LM. Imprints of the druses have been recognized between the veins and on the remaining coal layer of the leaves. They spread in irregular distribution and in different sizes between 20-80 µm along the veins from the petiole to the leaf tip.

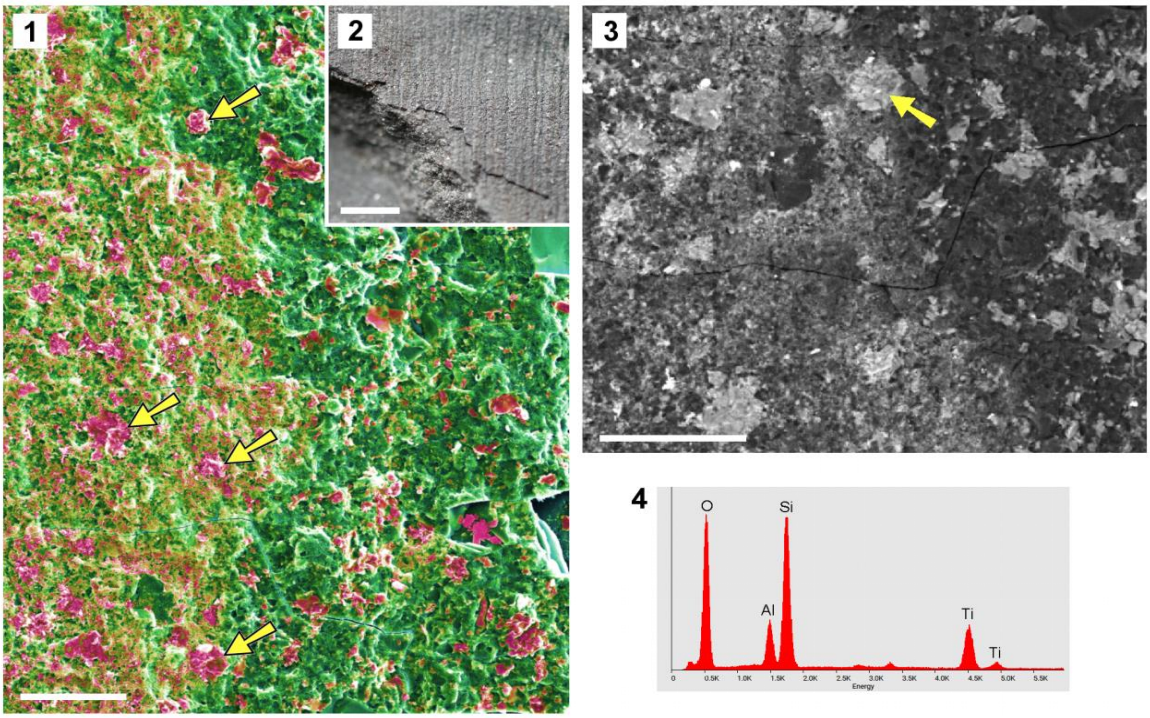

FIGURE13. Traces of former CaOx druses in *Ginkgophytopsis delvalii* from the Carboniferous, Upper Silesia, Poland, (Col. Andrzej Gorski, 2021). 13.1 Combined BSE and SE image of the fossil leaf of *G. delvalii* which is covered by coal. Under the coal along the veins and between them regular granules (red color) are observable.

13.2. Overview photo. 13.3 BSE image of mineralized granular structures embedded in carbonized layer. 13.4 EDX analysis of the granule marked in 13.3, indicating the mineral composition of oxides of Si, Al, with a remarkable content of Ti. Scale bars: 13.1, 13.3 = 100 µm; 13.2 = 1 mm.

Carboniferous

Fossil leaves of *Ginkgophytopsis delvalii* consist of a carbon layer with good preservation of the fine structures (**Figure 13**). Exfoliated flakes of the carbon layer (red color, marked with black arrows) with BSE and SE are illustrated. They show granules with sizes up to 70 µm and distribution patterns which resemble patterns of the CaOx druses in *Ginkgo biloba* (**Figure 10.3**). EDX analyses show that the inclusions consist of carbon **(Figure 13.2**).

2.6.2.3 Conifera

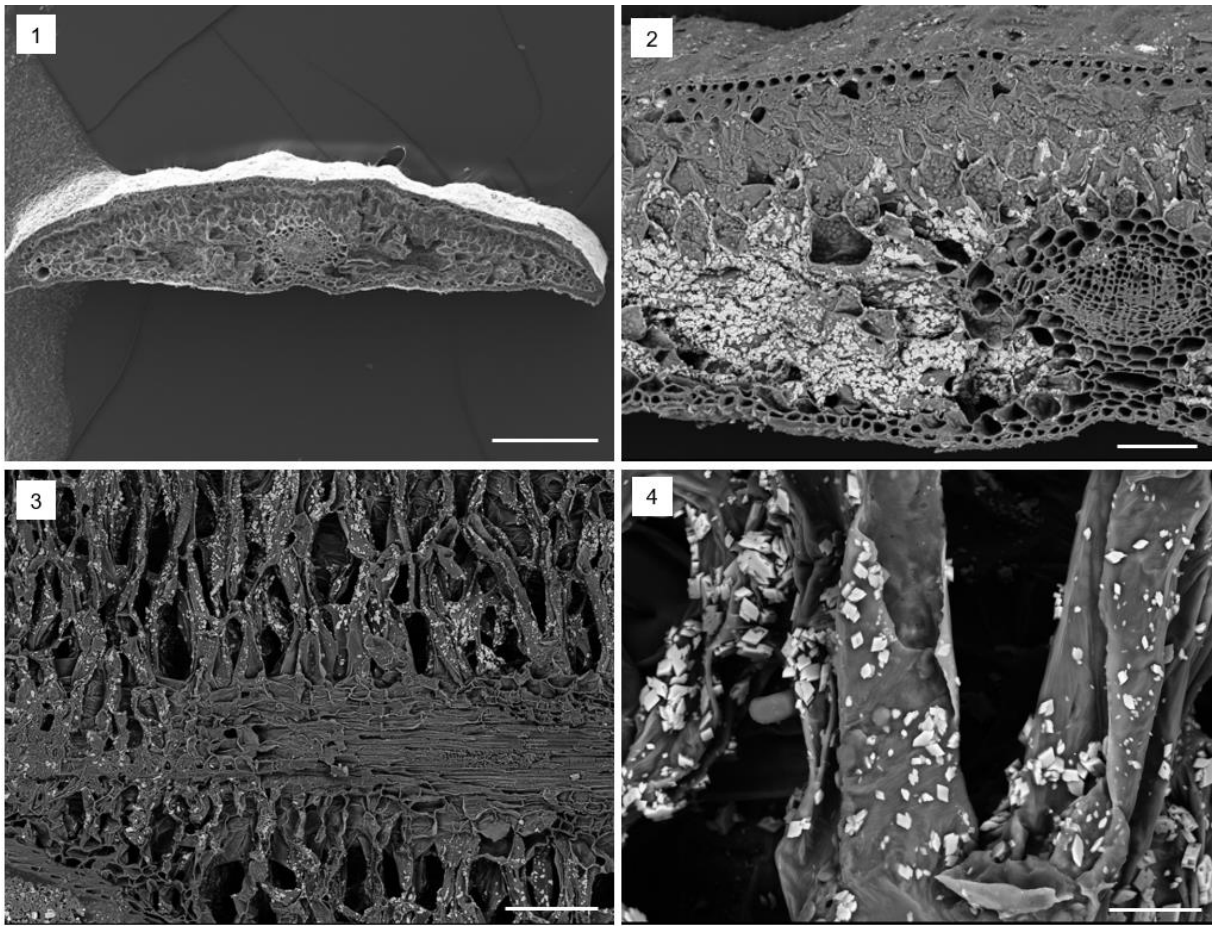

FIGURE 14. SEM images of fresh leaves of *Sequoia sempervirens* which show the distribution of CaOx crystals in cross and longitudinal sections. 14.1 Entire cross-sectional view of *S. sempervirens*. 14.2 Cross section; CaOx druses occur in high density in the aerenchyma. 14.3 Longitudinal section of *S. sempervirens* with CaOx distribution in the aerenchyma. 14.4 Close view of the crystals on surface of parenchymal cells. Scale bars: 14.1 = 500µm; 14.2, 14.3 = 200 µm; 14.4 = 30 µm.

Figure 14 shows transverse and longitudinal sections of a *Sequoia* leaf. In this image, the details of the CaOx crystal distribution are illustrated. **Figure 14.1** illustrates a full view of a *Sequoia* cross section. **14.2** shows crystal occurrences in high density in the aerenchyma. Details in longitudinal sections obviously illustrate the occurrence of crystals on parenchymal cells (**Figures 14.3-4**).

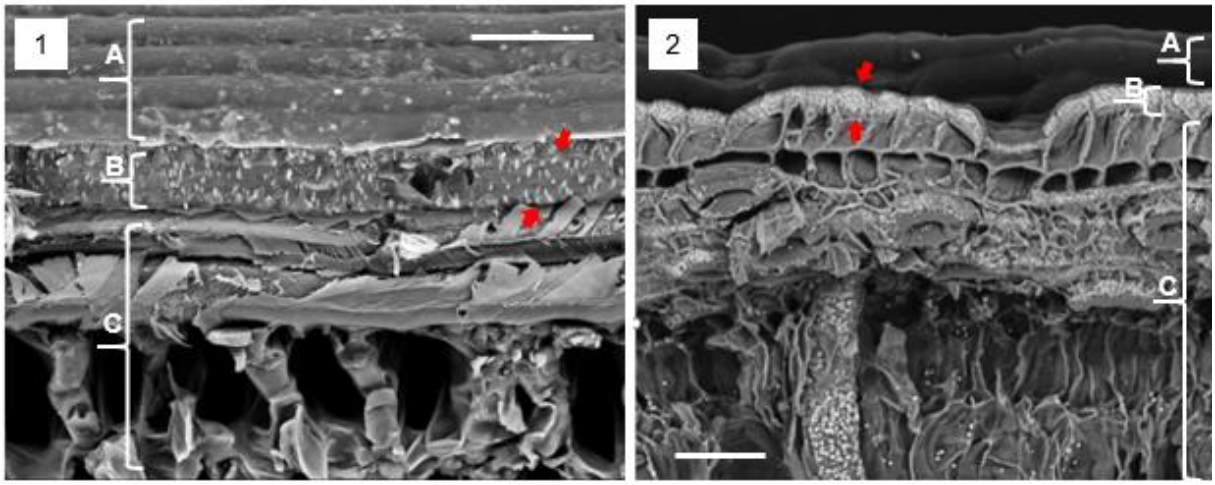

FIGURE 15. SEM images of CaOx crystal distribution in fresh leaves of *Pinus mugo* und *Welwitschia mirabilis* are illustrated. 15.1-2 show cuticle (A), epidermis (B) and parenchymal layer (C) respectively. In both images CaOx crystals are distributed under the cuticle and embedded in the epidermal walls. Scale bars: 15.1, 15.2 = 200 µm.

Another distribution pattern of the CaOx crystals is illustrated in **Figure 15**. In both fresh leaves of *Pinus mugo* und *Welwitschia mirabilis* cuticula, epidermis and parenchymal layer are respectively arranged. Under the cuticle layer individual crystals (bright in the BSE images) are visible and marked with red arrows. Comparison of **Figures 14** and **15** indicate that the pattern

of CaOx distribution is different among conifers. In *Sequoia* (**Figure 14**) crystals occur in the mesophyll, on the chlorenchyma, while in *Pinus* and *Welwitschia* they appear directly under the cuticle layer.

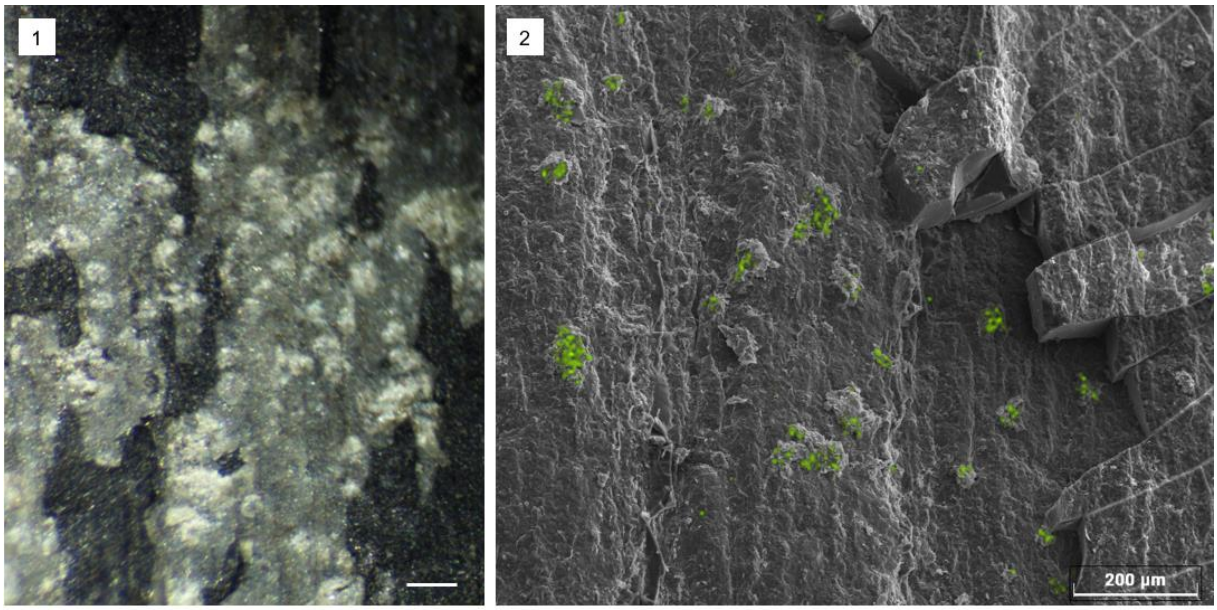

FIGURE 16. Fossil leaves of *Walchia*, (coll. Franz, N: 2200), are illustrated. 16.1 Shows the carbonized cuticle of the leaf in black color and under the cuticle white granular features are visible. 16.2 Detail of the granule's chemical compounds examined with EDX. Green color indicates Ca. Scale bars: 16.1, 16. 2 = 200µm.

In a fossil leaf of the Conifera *Walchia* sp., (Franz, N: 2200, Gerolstein, Permian) traces of CaOx were observed under the carbon layer (cuticle) in granular form. The interesting point is that we expected that casts of CaOx were substituted regularly with organic or mineral elements. However, EDX showed that granules (green color in **Figure 16.2**) were filled with Ca during fossilization. Furthermore, sediments include Si, Al and Mg.

In another fossil leaf of a conifer, *Moriconia cyclotoxon* (Upper Cretaceous), Aachen, Germany, the preservation of CaOx traces was not as good as in *Walchia*. The examination with LM showed that the surface of the leaf is covered with small crystals. The abundance of these small crystals makes the recognition of former CaOx crystals difficult.

2.6.3 Angiosperms

The first examinations of CaOx casts on fossil angiosperm leaves were from the Rott site (late Oligocene, Germany, Malekhosseini et al. 2022). To develop the study further, angiosperms from other ages and sites were examined.

Pliocene (Willershausen, Collection Göttingen)

The structure of the remaining parenchymal tissue in the fossil leaves and traces of CaOx, especially individual crystals in parenchyma, of the Willershausen material was difficult to recognize under the microscope due to the penetration of minerals on the surface of the leaves. This induced a rough, almost sandy appearance on the surface of the fossil leaves.

In **Figure 17.1** and **17.3** two fossil leaves from Fagaceae and Ulmaceae are illustrated, which in comparison to fresh leaves show not very prominent but well-preserved traces of the veins.

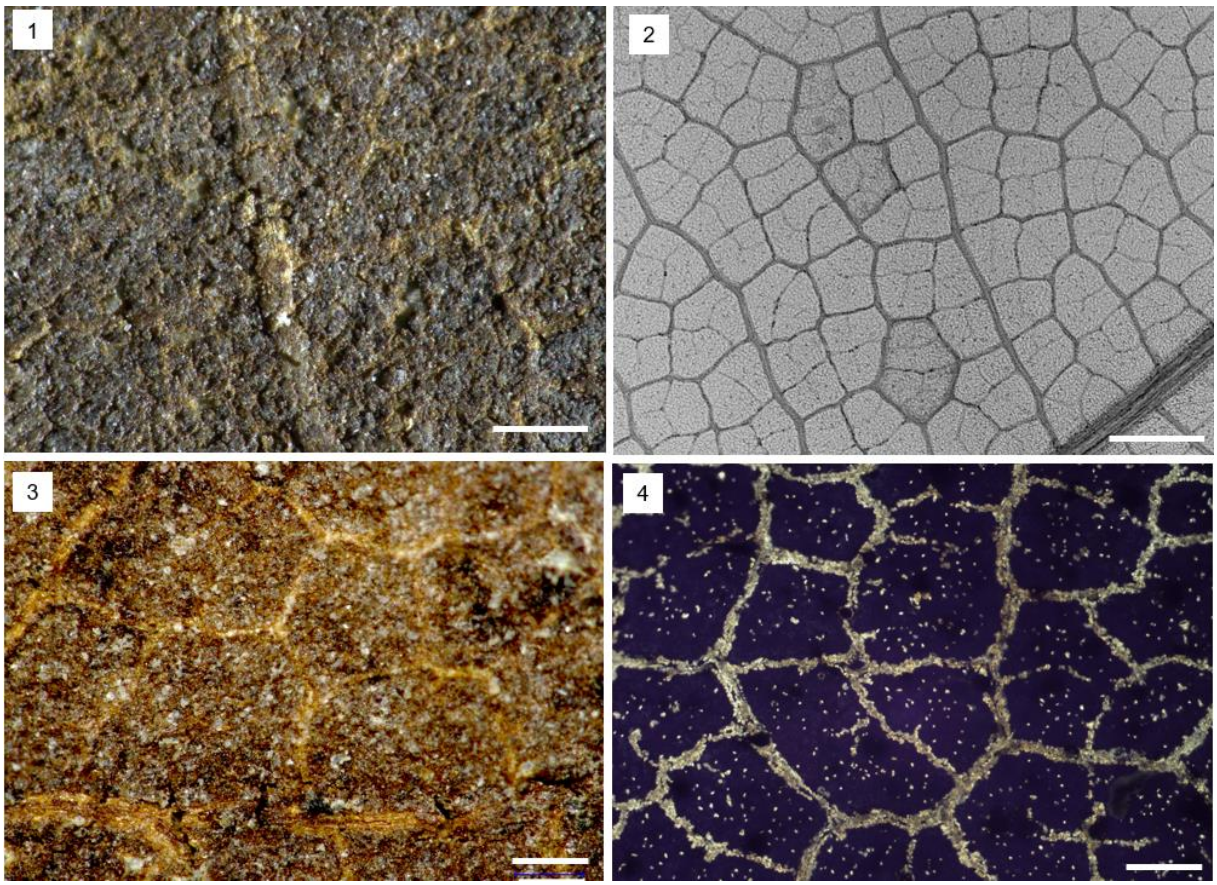

FIGURE 17. View of possible CaOx traces in veins of fossil leaves (Pliocene, Willershausen) in comparison with fresh leaves. 17.1 Fossil Fagaceae (GZG.W.5843, Pliocene, Willershausen). 17.2 X-ray (micro-CT) image of fresh leaf of *Fagus sylvatica*. 17.3 Fossil leaf of *Zelkova ungeri* (GZG.W.3458, Pliocene, Willershausen). 17.4 LM image of incinerated leaf of *Zelkova serrata*. In Figures 17.3-17.4 distribution similarity in CaOx crystals in rest of the parenchyma and fresh leaves parenchyma observed. Trace of the veins in both fossil samples is observable. Scale bars: 17.1, 17.3, 17.4 = 200 µm; 17.2 = 400 µm.

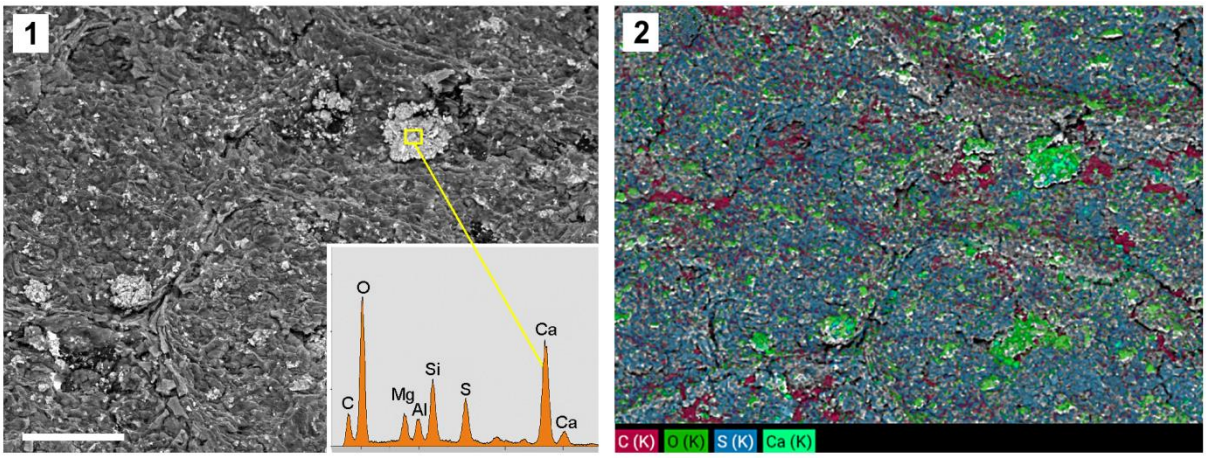

FIGURE 18. Mineralized granular structures in remains of the parenchyma of fossil *Betula maximowiczians* (GZG.W.4230, Pliocene, Willershausen), illustrated with EDS spectrum and element mapping. Granules contain Ca (light green) and other mineral elements (Si, Mg, Al); matrix included C (red) and S (blue) as main components of coal. Scale bar = 100 µm.

In **Figure 18** details of the CaOx traces in fossil leaf of *Betula maximowiczians* (GZG.W.4230, Pliocene, Willershausen) are illustrated. Ca-rich granules appear bright in the BSE image **(Figure 18.1**). EDX analyses show the mineral composition of the granules, whereas the element mapping image shows a high content of sulfur in the coal matrix. The granules are dispersed in a regular trend similar to the fresh leaves of other angiosperms.

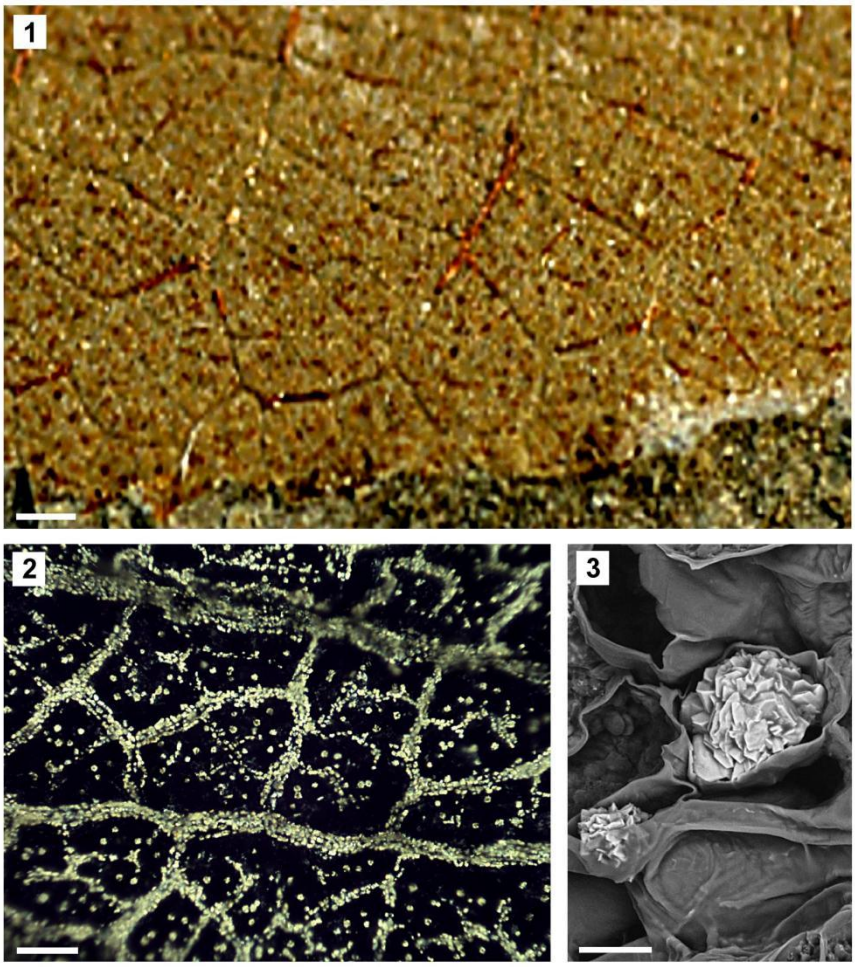

FIGURE 19. Fossil and fresh leaf of *Salix* is illustrated. 19.1 View of *Salix.cf.grandifolia* (Pliocene, Willershausen). 19.2 and 19.3 show individual crystals in veins and druses in cells of parenchyma. Scale bars: 19.1, 19.2 = 100 µm; 19.3 = 30 µm.

Salix was one of the major species in the Pliocene of Willershausen and they show similarities to fresh leaves. Generally, in *Salix,* in comparison with *Quercus,* there is a low amount of CaOx druses in the parenchyma. In addition, some of the species of *Salix* show individual crystals in the parenchyma instead of druses. In the fossil sample dark points, which are traces of CaOx, are visible in cells of the parenchyma.

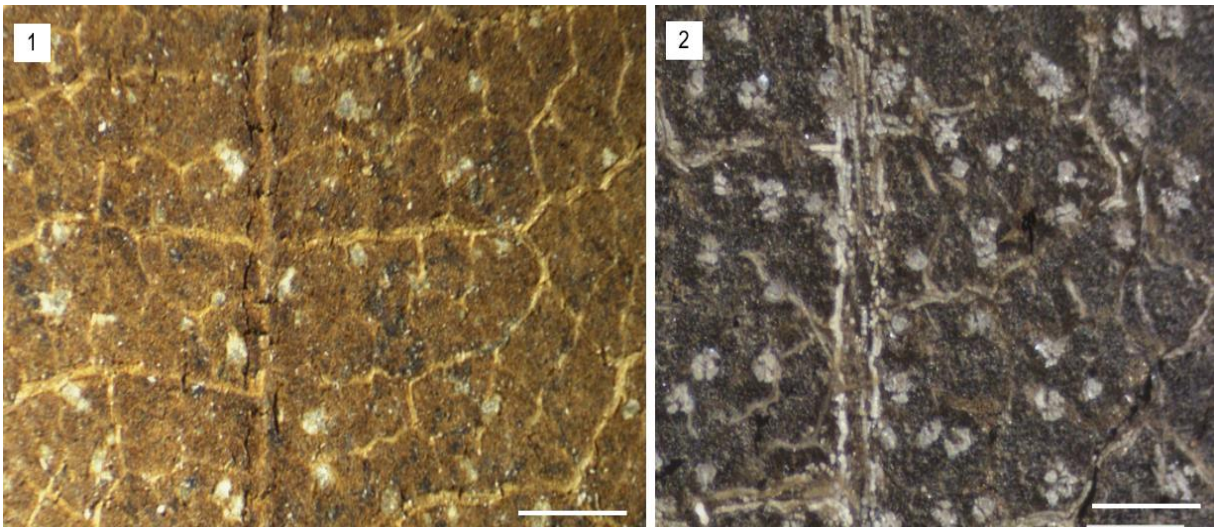

FIGURE 20. Fossil and fresh leaf of *Quercus* is illustrated. 20.1 LM image of CaOx traces (here emoty cast of crystals or druses) in a fossil leaf of *Quercus* (GZG.W. 6943, Pliocene, Willershausen). 20.2 LM image of *Quercus variabilis* (fresh leaf). Scale bars: 20.1, 20.2 = 200 µm.

The LM image shows a similarity in the distribution of CaOx traces in both fresh and fossil leaves of *Quercus*. An estimation of the original distribution and kind of crystals or druses in fossil leaves of *Quercus* species is difficult, due to the vast and diverse distribution patterns of CaOx. In fossil leaves of *Quercus* (GZG.W. 6943, **Figure. 20**) empty casts and dark brown points represent CaOx traces (GZG.W. 14131, **Figure. 21**).

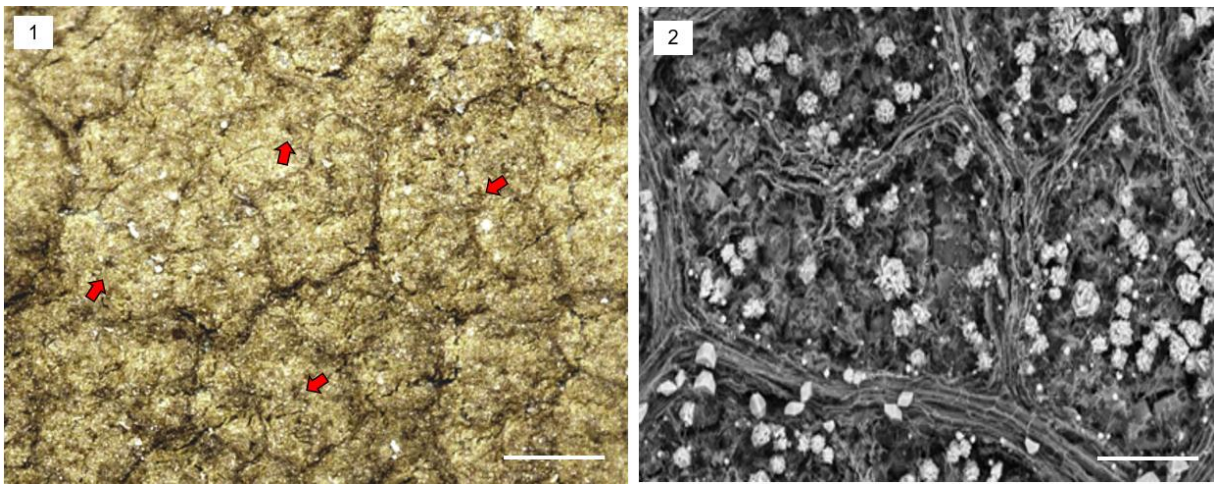

FIGURE 21. Fossil and fresh leaf of *Quercus* is illustrated. 21.1 View of *Quercus* (GZG.W. 14131, Pliocene, Willershausen) with dark brown points, traces of druses in the middle of each parenchymal area are observed. 21.2

SEM image of druses in parenchyma of *Quercus* robur (fresh leaf) are imaged. Scale bars: 21.1 = 200 µm; 21.2 = 50 µm.

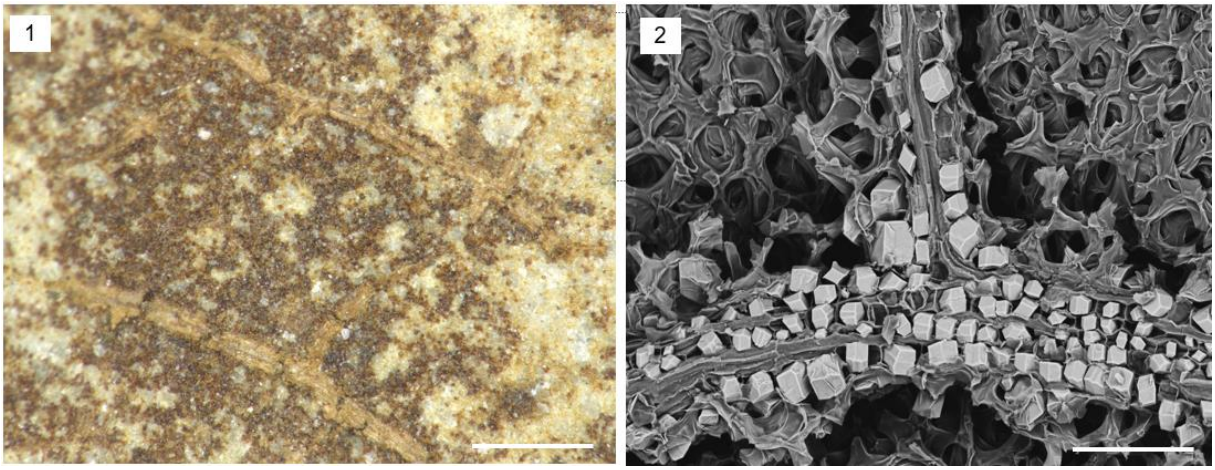

FIGURE 22. Fossil and fresh leaf of *Parrotia persica* (Pliocene, Willershausen) is illustrated. 21.1 Fossil of *Parrotia persica*. 21.2 SEM image of the druses in veins of the fresh leaf. Scale bars: 22.1 = 200 µm; 22.2 = 50 µm.

In members of the Fagaceae (GZG.W.5843, Pliocene, Willershausen) and a fossil leaf of *Zelkova* individual crystals in veins are better preserved than in residual parenchyma due to lignin and tissue of the veins. In *P. persica* imprints of the crystals exist in the form of coffee-colored bricks in the main veins **(Fig. 22.1**).

Miocene, D., Wischgrund near Kostebrau (Collection: Berlin)

As already mentioned in the introduction, the variety of the distribution and size of the CaOx crystals in fresh leaves is outstanding and *Carpinus*, with only a few very huge crystals, is a typical example. As is illustrated in **Figure 23**, crystals of huge size (ca. 80-100 µm) but low quantity are distributed in the parenchyma. Traces of CaOx in a fossil leaf of *Carpinus sp.* (MB.Pb. 1999/1647) were observed in two patterns: a deep line which seems to be an imprint of the big crystals that made it, due to their size and the compaction of the parenchymal layers

during the fossilization process. They are stable in the holding cells and the others are the casts that are seen as triangular structures, which is infilled with other elements.

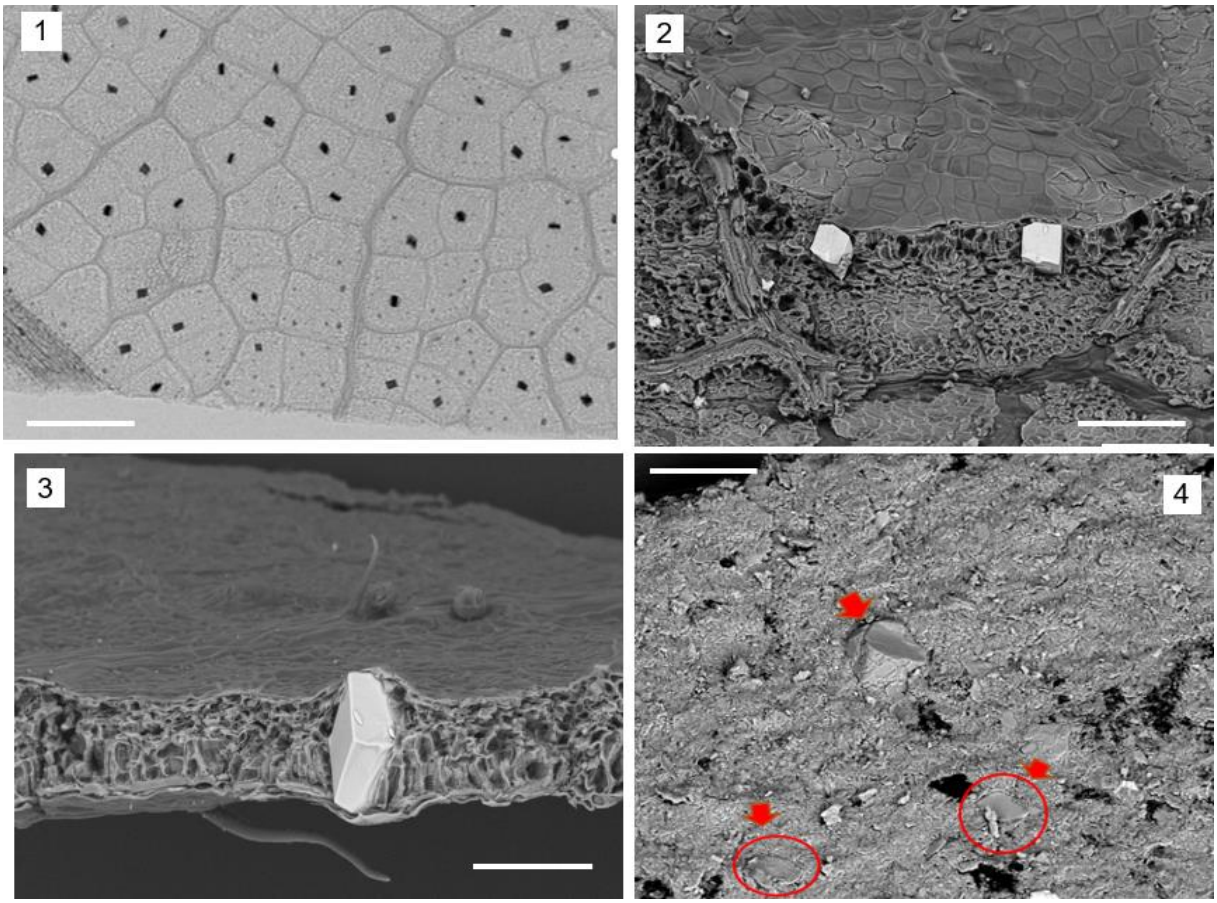

FIGURE 23. CaOx crystals and traces of them in fresh and fossil leaves of *Carpinus*. 23.1 Micro-CT image of an extant leaf of *Carpinus kawakamii*. 23.2 SEM image of *C. kawakamii*, air-dried. 23.3 View of CaOx crystals in entire thickness of the leaf. 23.4 Fossil leaf of *Carpinus sp*. (MB.Pb. 1999/1647). Scale bars: 23.1 = 500 µm; 23.2 = 100 µm; 23.3, 23.4 = 40 µm.

Miocene, Randecker Maar (Collection: Stuttgart)

In the Stuttgart collection, we were only allowed to study the surface of the leaf fossils and it was almost impossible to find out details of the CaOx traces in the remaining parenchyma. Since traces of the small and individual crystals in veins of *Acer* are better preserved than in the rest of the parenchyma, traces of them were observed with LM in dark brown, brick-like forms (**Figure 24.1**). The remarkable aspect about *Acer* and its species is that crystals are so small

and, in some species, they don't exist at all, as illustrated in the µ-CT images (**Figure 25.1, 25.2**). *Acer griseum and Acer palmatum* are illustrated in **Figure 25.1**, **25.2** which show almost no crystals. This finding indicates that in a fossil leaf of *Acer sp*. preserved crystals in veins are almost invisible. This presumably depends on the preservation situation.

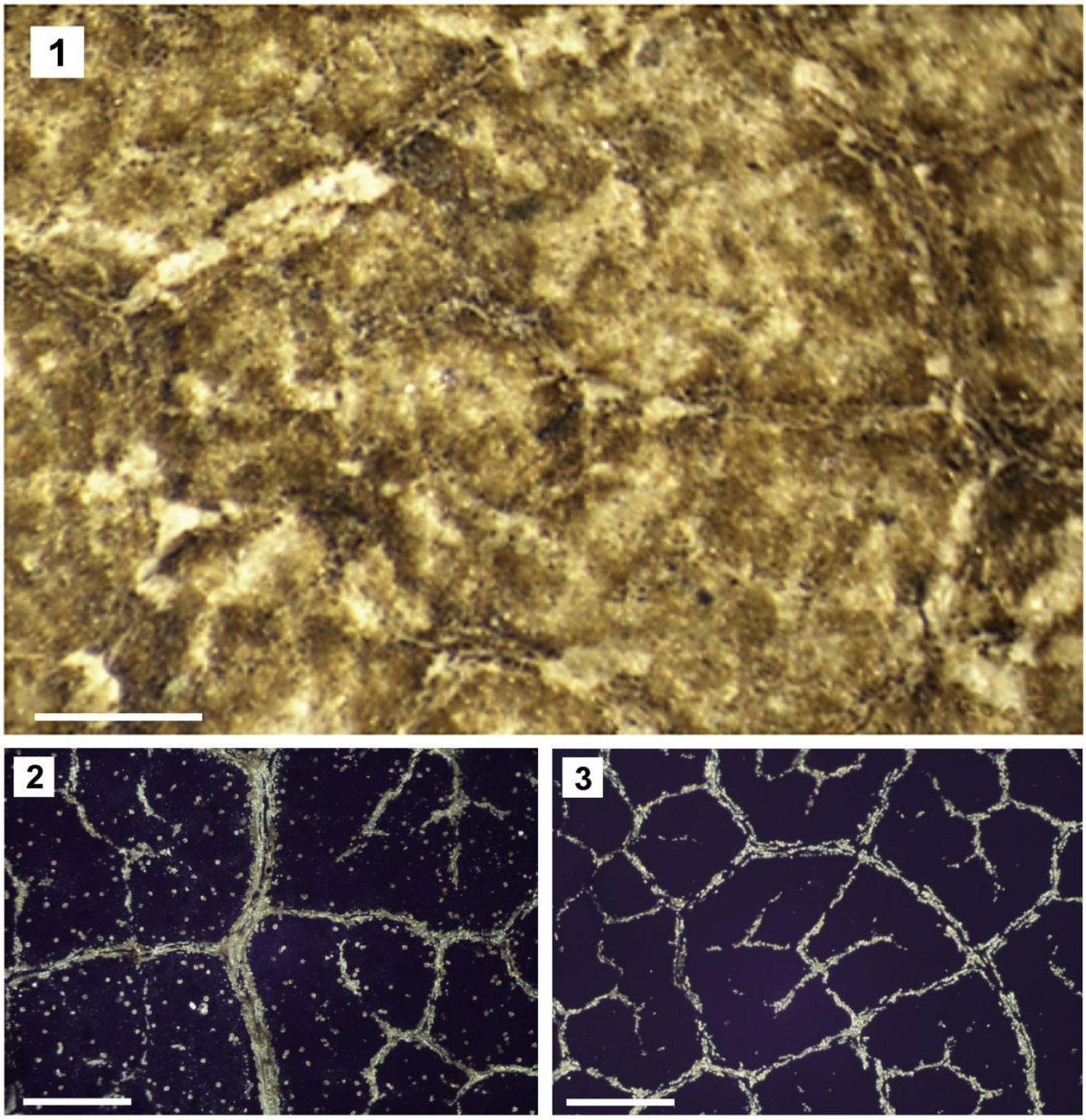

FIGURE 24. View of the CaOx traces in veins in fossil and fresh leaves of *Acer* with LM. 24.1 Fossil leaf of *Acer sp*. Öhingen, Germany. 24.2 Illustration of CaOx crystals in veins and parenchyma, ash of *Acer tataricum* with a few druses in parenchyma. 24.3 Ash of *Acer carpinifolium* with small crystals in veins. Scale bars: 24.1- 24.3 = 500 µm.

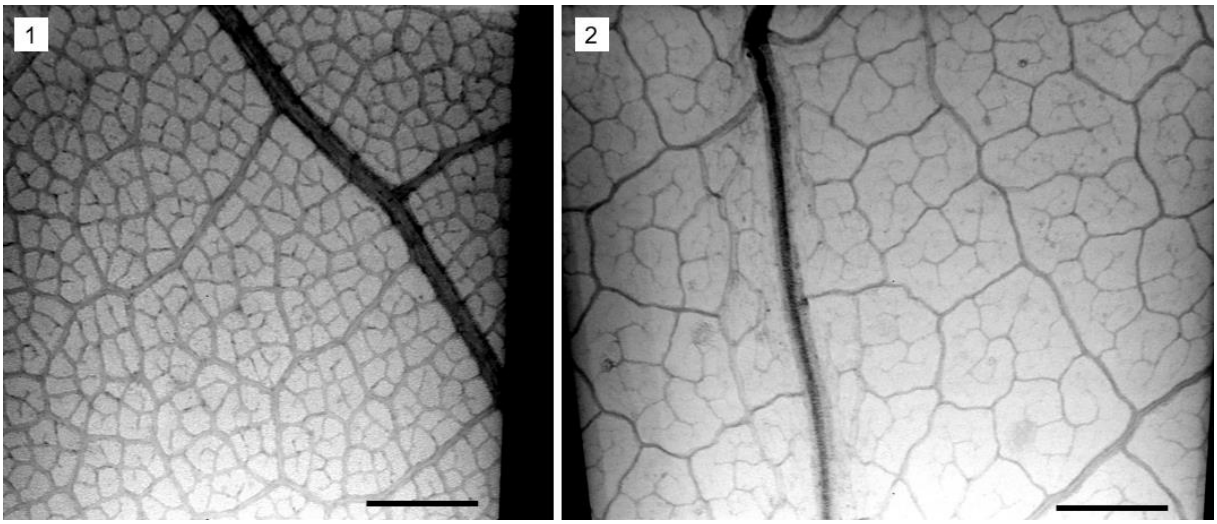

FIGURE 25. µ-CT images of fresh *Acer* leaves. 25.1 *Acer griseum*, 25.2 *Acer pelmatum*. Scale bars 25.1, 25.2 = 200 µm.

Late Oligocene, Rott Lagerstätte (Collection: Bonn)

The first observation of granular structures on leaves and sediments with a stereomicroscope was in material from the late Oligocene of Lagerstätte Rott, Germany. Because of the type of the sediments, and the very small size of the constituent particles, a surface view of the fossil leaves itself presented the traces. The structures appeared as globular or lobed particles with a maximum diameter of 25-70 µm. Most striking were globules, spherical structures of yellow or brown color with a smooth surface. Several samples contain black structures of irregular or angular shape. Many more samples may have had such granular structures, but they were not sufficiently well preserved for further investigations, or the granules were too small for a reliable identification. Some examples of poorly preserved fossils, where a recognition of the granules is difficult, are presented in **Appendix 3**.

The fossil samples derive mostly from diatomite (German term ‚Polierschiefer ‘), a bright material rich in silica skeletons of algae, or laminated bituminous shale (leafy coal bed) (Winterscheid, et al., 2018), a dark brown organic material. Many leaf remnants were very thin as most of the organic material has been lost during fossilization; others consisted of thicker

dark-brown layers being coalified remains called compressions (Winterscheid, et al., 2018). While the old surfaces of the fossils were severely damaged, freshly cleaved planes of some leaf coal samples show their structures in detail. Some specimens show a distinct pattern of empty cavities with diameters up to 50 µm, which resembled the distribution of CaOx druses in fresh leaves. Even small cavities of less than 10 µm are clearly visible.

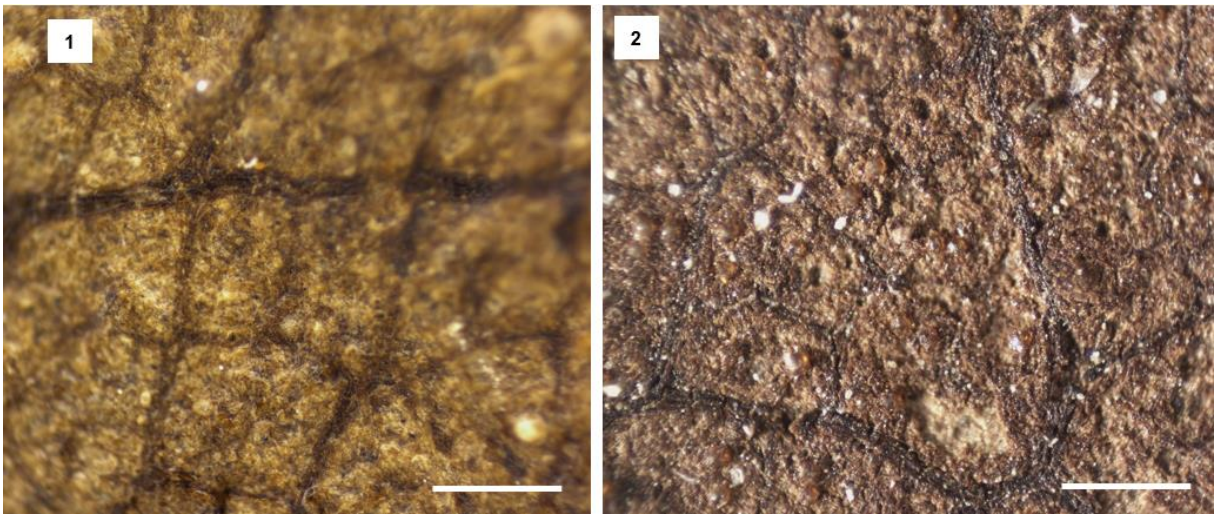

FIGURE 26. Image of the CaOx traces in fossil leaves from Rott site, late Oligocene. 26.1 *Acer* (Ro-4.4). 26.2 *Laurus primigenia* (Ro-82.1). Scale bars: 200 µm.

In *Acer*, as in other *Acer* species from other sites, traces of CaOx in the remains of the parenchyma could not be observed (**Figure 26.1**). Just in veins traces of them specially in some of the fossil pieces named as a Magnoliposida were observable (**Figure 27.1**). In fresh leaves of *Acer griseum,* CaOx individual crystals in comparison with Magnoliopsida were observed (**Figure 27.2**). In contrast, in *Laurus primigenia* (Ro-82.1) traces of CaOx are manifested in parenchyma and veins.

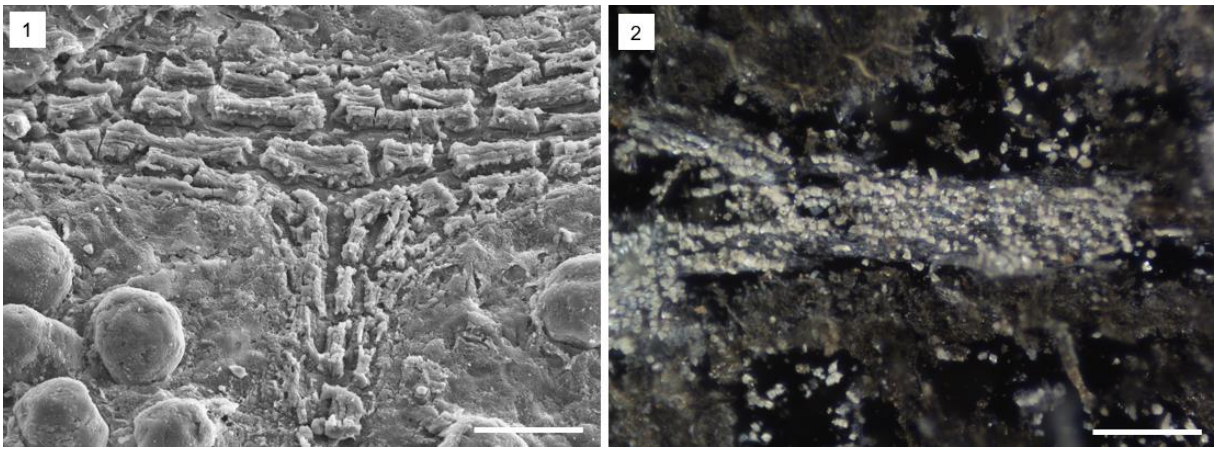

FIGURE 27. View of CaOx traces in veins in fossil and fresh leaves of *Acer*. 27.1 SEM image of fossil leaf of *Acer sp*. Öhingen, Germany. 27.2 Illustration of CaOx crystals in veins and parenchyma; LM image of ash of *Acer sempervirens*. Scale bars: 27.1 = 30 µm; 27.2 = 100 µm.

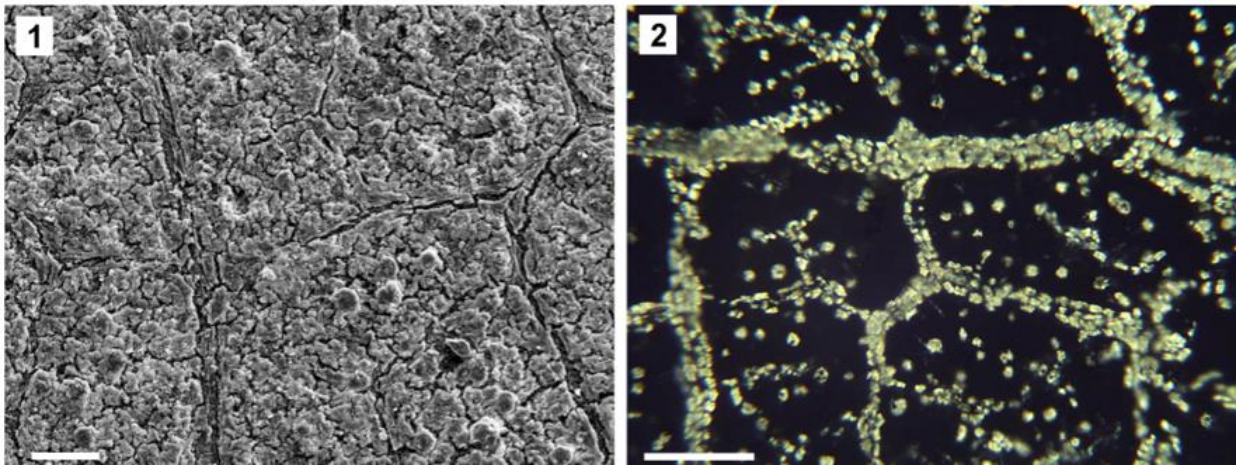

FIGURE 28. CaOx traces and original crystals in *Salix*. 28.1 Fossil leaf of *Salix integra* (Ro-97.3). 28.2 Crystals in a leaf of the extant *Salix gracilistyla.* Scale bars: 100 µm.

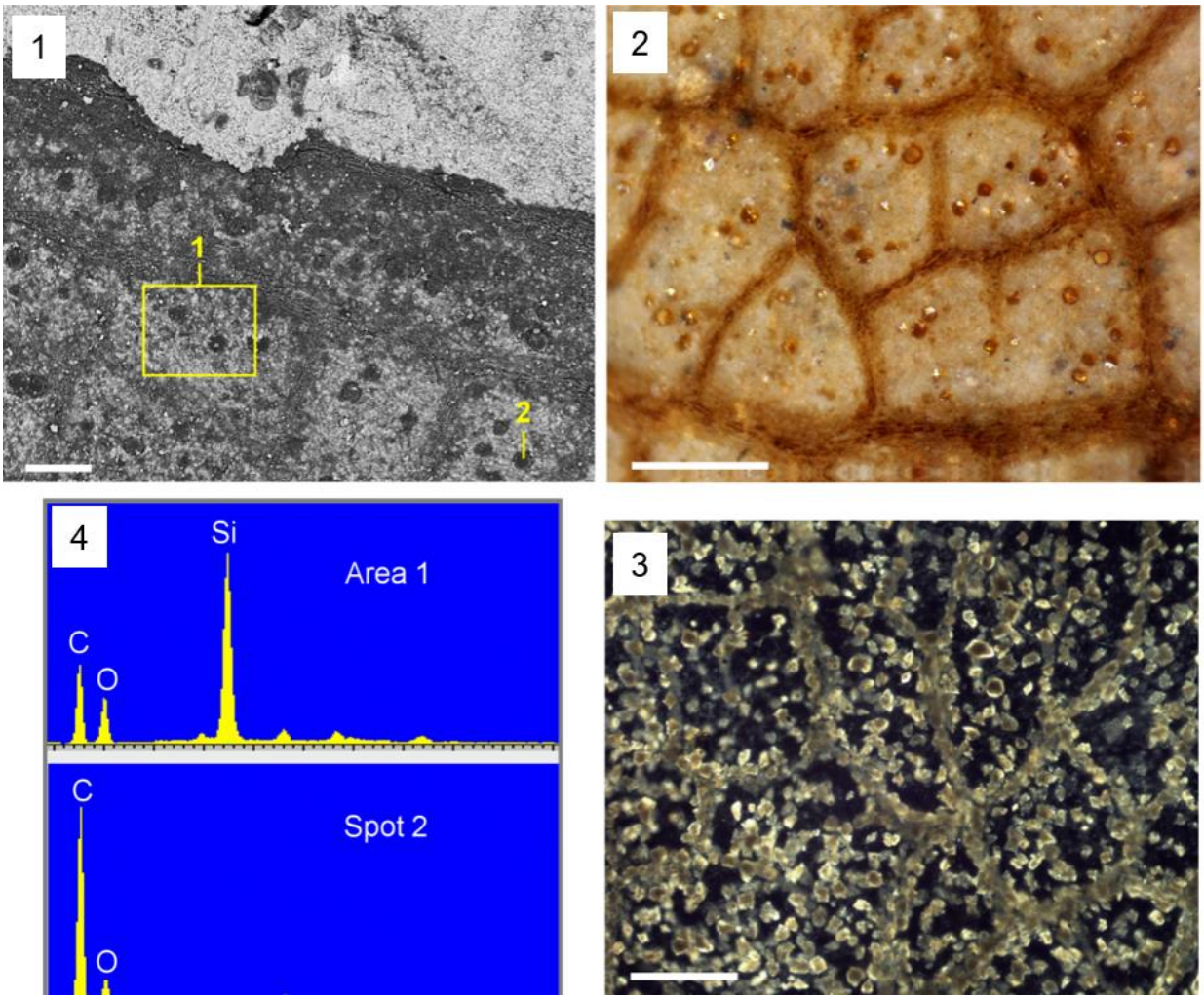

FIGURE 29. CaOx traces and original crystals in fresh (29.3) and fossil leaf of *Sideroxylon* (29.1, 29.2). 29.1 SEM image, 29.2 LM image of *Sideroxylon salicites* (Ro-59). 29.3 LM image of CaOx crystals in incinerated leaf of *Sideroxylon reclinatum*. 29.4 EDS spectra from mineralized leaf and from granule. Sediment is composed of Si (Area 1), while the granules are made of C (Spot 2). Scale bars: 29.1- 29.3 = 100 µm.

In *Salix* and *Sideroxlyon*, individual crystals are present in the veins. As is illustrated in **Figure 28, 29** traces of them are visible as granules in the remains of the parenchyma. During fossilization and compression of the hyper-parenchymal layer and tissues surrounded the crystals, they became unstable in cells and are moved towards the centers. In this case they have been observed in the parenchyma while they originally belonged to the veins. EDX analyses located in **Figure 29.2** showed that the sediment is composed of Si (Area 1), while the granules are made of C (Spot 2).

Eckfeld, Middle-Eocene (Coll. Mainz)

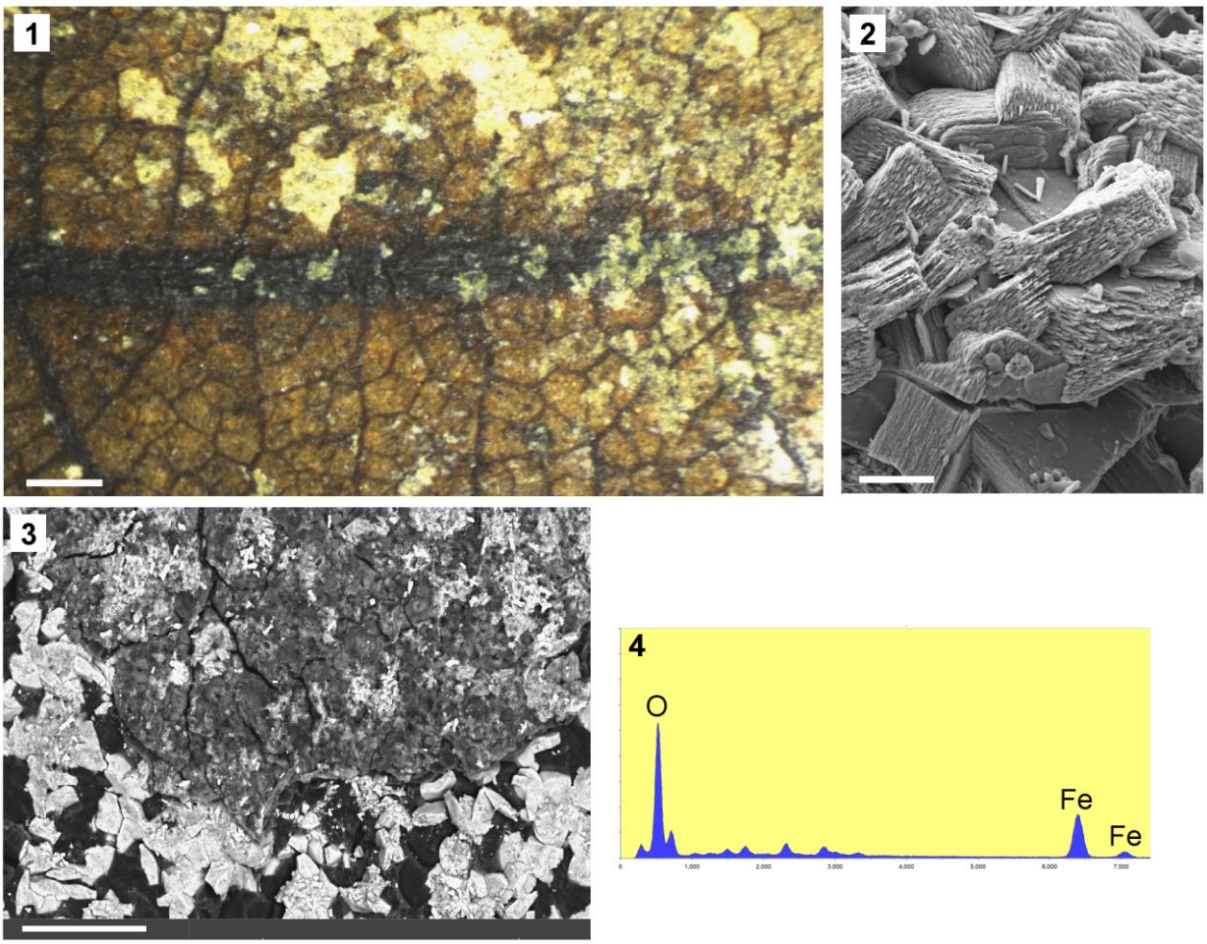

FIGURE 30. View of the fossil leaves preserved in glycerin with LM and SEM. 30.1, 30.3 Illustrations of contamination of the leaf (PB2021-4LS, Eckfeld, Middle-Eocene) with iron oxide made by LM and SEM respectively. 30.2 Detail of the iron oxide crystals. 30.4 EDS spectrum of crystals in 30.2. Scale bars: 30.1 = 300 µm; 30.2 = 30 µm; 30.3 = 100 µm.

Fossil leaves from the middle Eocene of Eckfeld are preserved in glycerol, which limit the potential avenues of investigation. Recognition of the CaOx traces was difficult due to patches of iron oxide coating the surface of the leaf (**Figure 30**). Furthermore, the fossil leaves of Eckfeld are not systematically identified, so that there was no background for a comparison of the distribution pattern of CaOx with modern plants. In order to examine the fossil leaves, a small piece of the surface was cleaned with water and a soft brush. The result showed two

patterns of CaOx cast distribution as imaged in **Figure 31** and **32**: regular distribution of the pyrite-rich granules under the cuticle layer in fossils number PB2021-4-Ls and PB2003-148-Ls (**Figure 31**); in contrast, fractured samples of another fossil leaf (PB 2021-5-LS) show that they were distributed entirely throughout the leaf (**Figure 32**). EDX analyses reveal the composition of the granules (Fe, S) and the surrounding matrix (Si, Al, O).

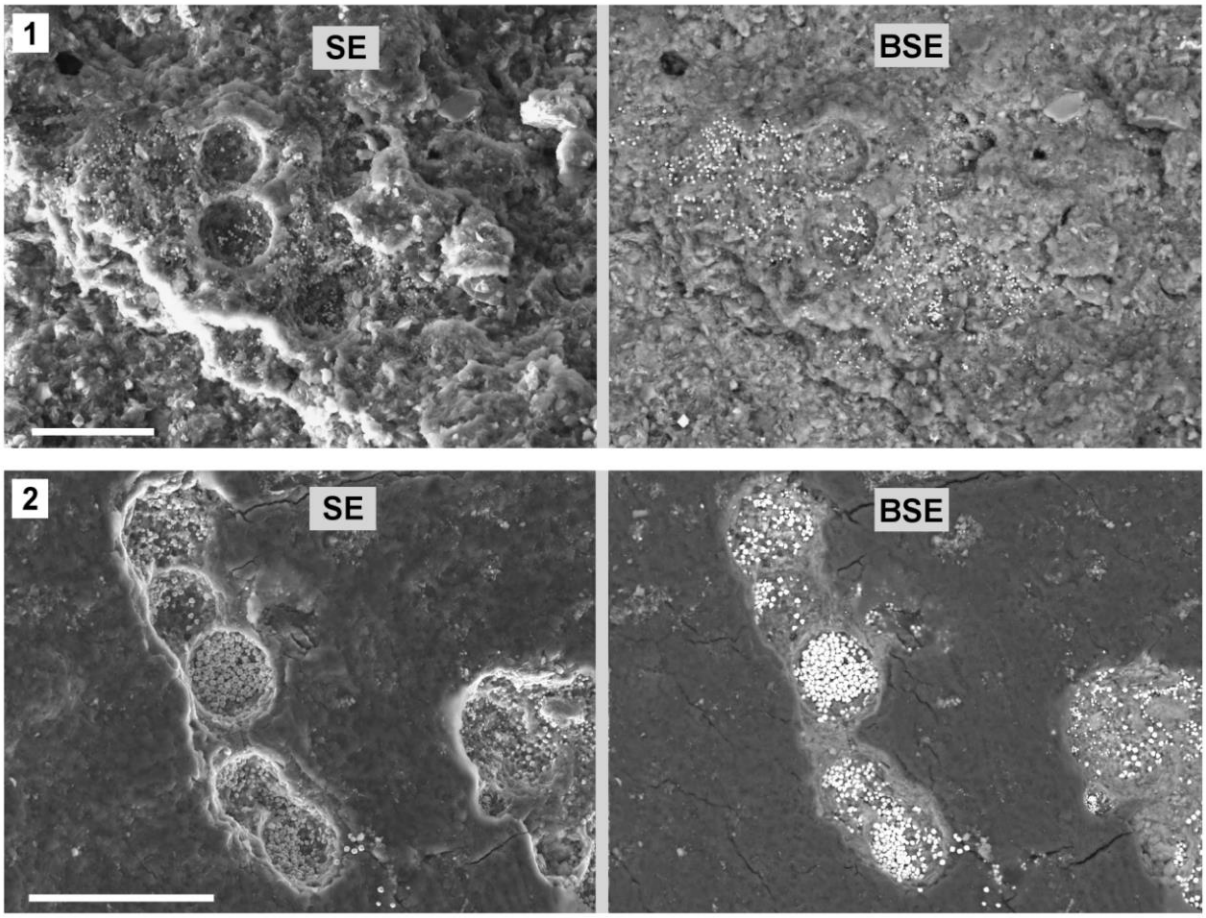

FIGURE 31. Surface of the fossil leaves (PB2021-4-Ls and PB2003-148-Ls) preserved in glycerin with SEM. 31.1, 31.2 Images of pyrite in probable casts of CaOx druses. Scale bars: 31.1 = 50 µm; 31.2 = 100 µm.

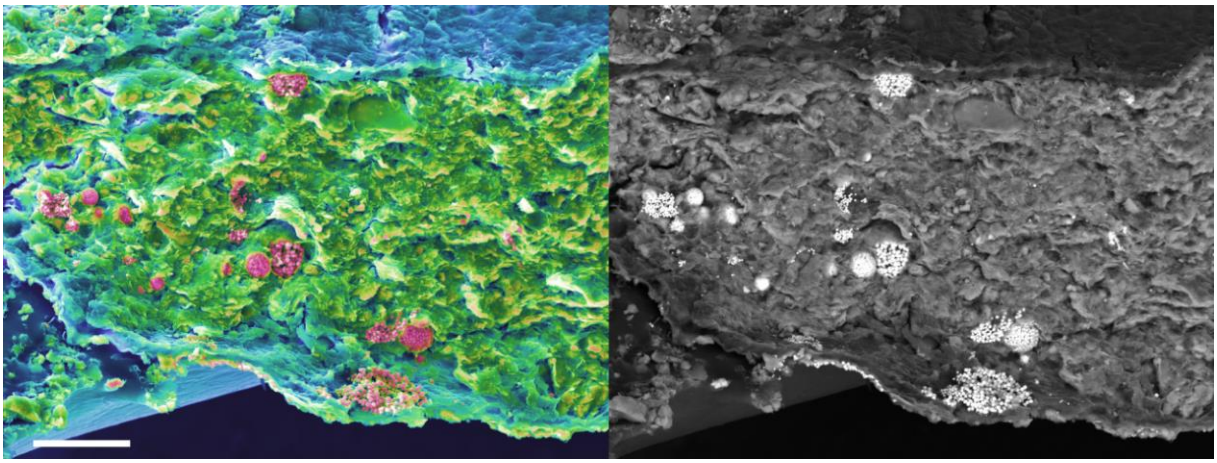

FIGURE 32. SEM (combined SE+BSE image) view of the pyrite granules in cross fracture of the entire fossil leaf (PB2003-501-Ls, Eckfeld, Middle-Eocene). Under a carbon layer (blue color in left and dark color in right image) the entire leaves show casts of probable CaOx druses refilled with pyrite. Scale bars = 30 µm.

2.7 Discussion

This study involves describing the distribution and micromorphology of CaOx traces and their elemental composition in remnants of the parenchyma in fossil leaves.

All of the details of the processes of CaOx fossilization are still not fully understood, but the scenario provided herein is helpful to figure out this process during geological times and different fossil sites (Malekhosseini et al., 2022). As is common across most fossilization processes, fossilization of CaOx in leaves starts with terrestrial or freshwater plant material sinking into the anoxic depths of the former maar lakes, which are then preserved in different kinds of sediment. During fossilization, some of the organic material is decomposed and any remnants are compressed. The vascular system, because of lignified and cutinized peripheral cell walls and the presence of biominerals such as CaOx crystals, is more likely to be preserved than parenchymal layers in leaves. The many observations of crystal imprints in veins of fossil leaves of various taxa, such as *Acer*, *Parrotia* and Magnoliopsida, and from various fossil sites supports this statement (see **Figures 22, 24, 27** in this chapter).

Preparation of fresh leaves to observe CaOx showed that the crystals are not stable due to the damage of surrounding parenchymal tissues. For this reason, the preservation of any original

CaOx crystals through the fossilization process is not expected. Furthermore, CaOx crystals are eventually decomposed or dissolved during fossilization (Malekhosseini et al., 2022). If the sediments are already lithified and sufficiently hardened, the disappearance of the druses and crystals will leave cavities which – depending on sediment and local conditions - will be refilled with organic or inorganic material. The results above show this replacement in various taxa such as *Otozamites* and *Glossopteris* sp. (see **Figure 3, 4** in this chapter). Thus, the constituent elements in the refilled casts of crystals or druses could be completely different than the surrounding sediments. The processes by which this replacement occurs are still not clear. In *Glossopteris* sp., granules were lacking iron, while the surrounding sediment had abundant iron. The replacement process and the reason why in some fossil samples the casts are subtly filled with relatively pure elements can be due to the difference in time of the discharge or dissolution of calcium oxalate and its gradual replacement by other elements during diagenesis.

Deposition of very fine materials such as amorphous silica may form precise replicas of the former CaOx crystals. In **Figure 33** amorphous silica beside the empty casts are observed and they were one of the major mineral elements in CaOx traces in the fossils examined in the present study.

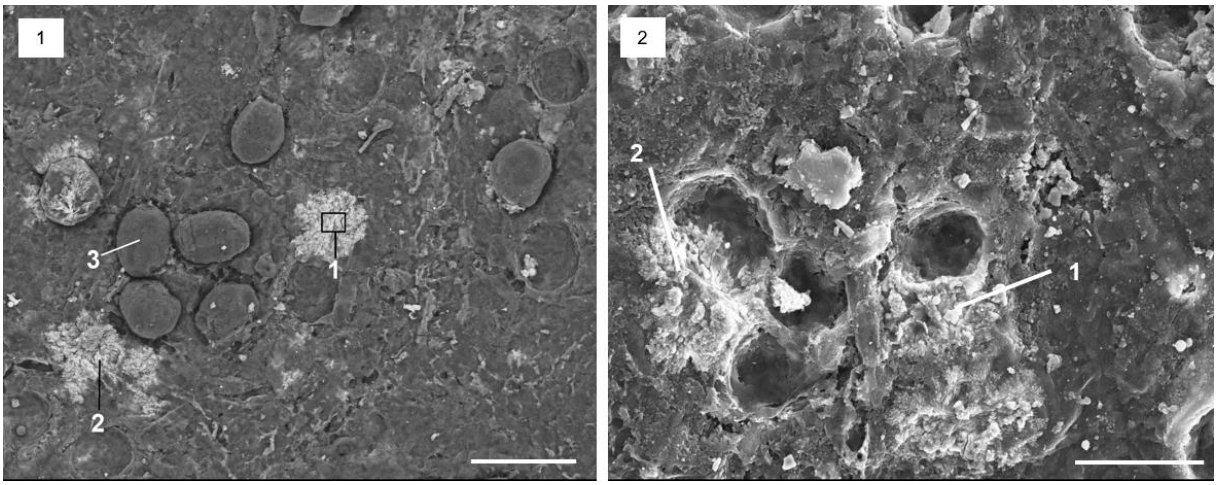

FIGURE 33. Amorphous silica beside the granules. 33.1 Amorphous silica (marked with number 1, 2) beside the granules which are composed of carbon (marked with 3) is imaged. 33.2 Other refilled traces of CaOx with silica (silica marked with 1, 2). Scale bars: 33.1, 33.2 = 60 µm.

Traces of CaOx show three main patterns: empty casts with imprints of the shrunk crystals; casts filled with organic compounds, mostly carbon; casts totally or partially infilled with mineral elements.

In the Oligocene fossil deposit Rott, Germany, due to exceptional preservation, empty casts with imprints of serrated druses or completely spherical forms were significantly more common in comparison with other sites. Figure 34 illustrates the before-mentioned three patterns. Fossil leaf of *Quercus*, Rott 59_9, as seen in **Figure 34.1**, exhibits many casts with imprints of serrated forms that show similarities to the pattern of CaOx druses in extant species of *Quercus*. Different sizes of granules which are infilled with carbon are observed in *Sideroxylon*, Rott 2_2 (**Figure 34.2**). The third pattern is seen in *Nymphaea*, Rott 13_3. Elements: C, O, K, Si, Fe and S were measured by EDX in granules and their surrounding sediment (black color, **Figure 34.3-5**).

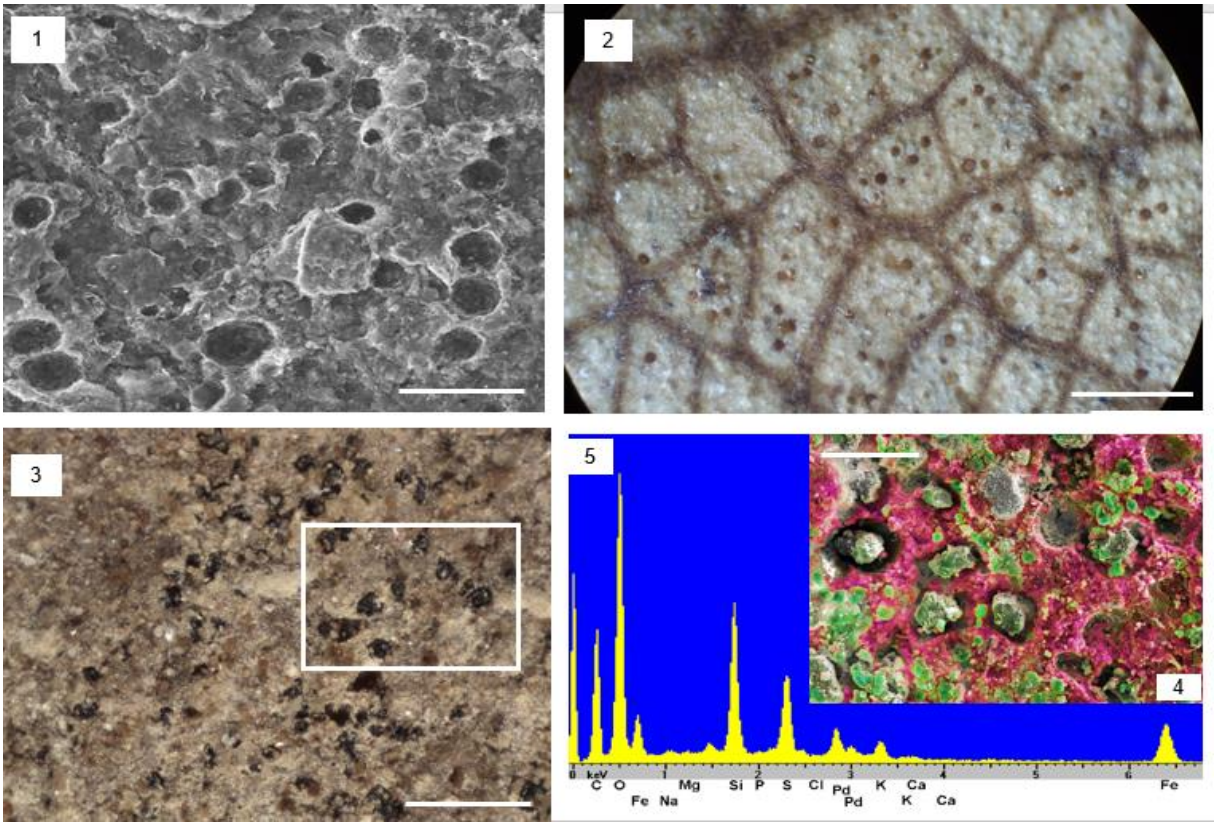

FIGURE 34. Three patterns of casts in fossil leaves of the Oligocene Rott site. 34.1 *Quercus*, Rott 59_9, with empty cast of CaOx. 34.2 Different size of the casts refiled with carbon in *Sideroxylon*, Rott 2_2. 34.3 LM image of *Nymphaea*, Rott 13_3, illustrate granules with a closer view of them (inside the white square) with SEM and BSE image (34.4). In combination with an EDX analysis it can be shown that they consist of different minerals containing Fe, S, Si, Al, K, and organic material and the surrounding sediment with an additional fraction of Si and Al (34.5). Scale bars: 34.1= 20 µm, 34.2 = 200 µm; 34.3 = 100 µm; 34.4 = 20 µm.

Although druses in fresh leaves show shrinkage and serrated forms, occurrences of CaOx traces in fossils are mainly identified as granules or spherical forms, which leaves open questions.

It is proposed that the spherical shape of the organic particles results from shrinkage of the casts. Organic material, which has filled the voids, is unlikely to be perfectly stable. It may slowly lose its form and start to shrink; as it is a highly viscous resin-like material, its surface tension in a moist environment may force it into the spherical shape. The shrinkage also explains why the organic globules easily become detached from the surrounding material, leaving holes at their positions in the separated fossil samples. Further shrinkage and dissolution of the organic inclusions leaves voids which may be finally filled by inorganic minerals from the environment, resulting in the black ferruginous particles or in the calcium sulfate shells observed around some of the organic globules or other mineral elements around the granules (see **Figure 34**).

The identity of the granules has previously been interpreted as pollen, algal colonies, trichome bases or ‘subcrustations, preserving epidermal structures’(Koenigswald, 1996). The study of Krassilow et al. (2005) on ‘Late Cretaceous Flora of Southern Negev’ includes a wealth of excellent images of fossils; many of them show patterns of granules which resemble the granules here studied, but the authors do not provide an explanation for the structures.

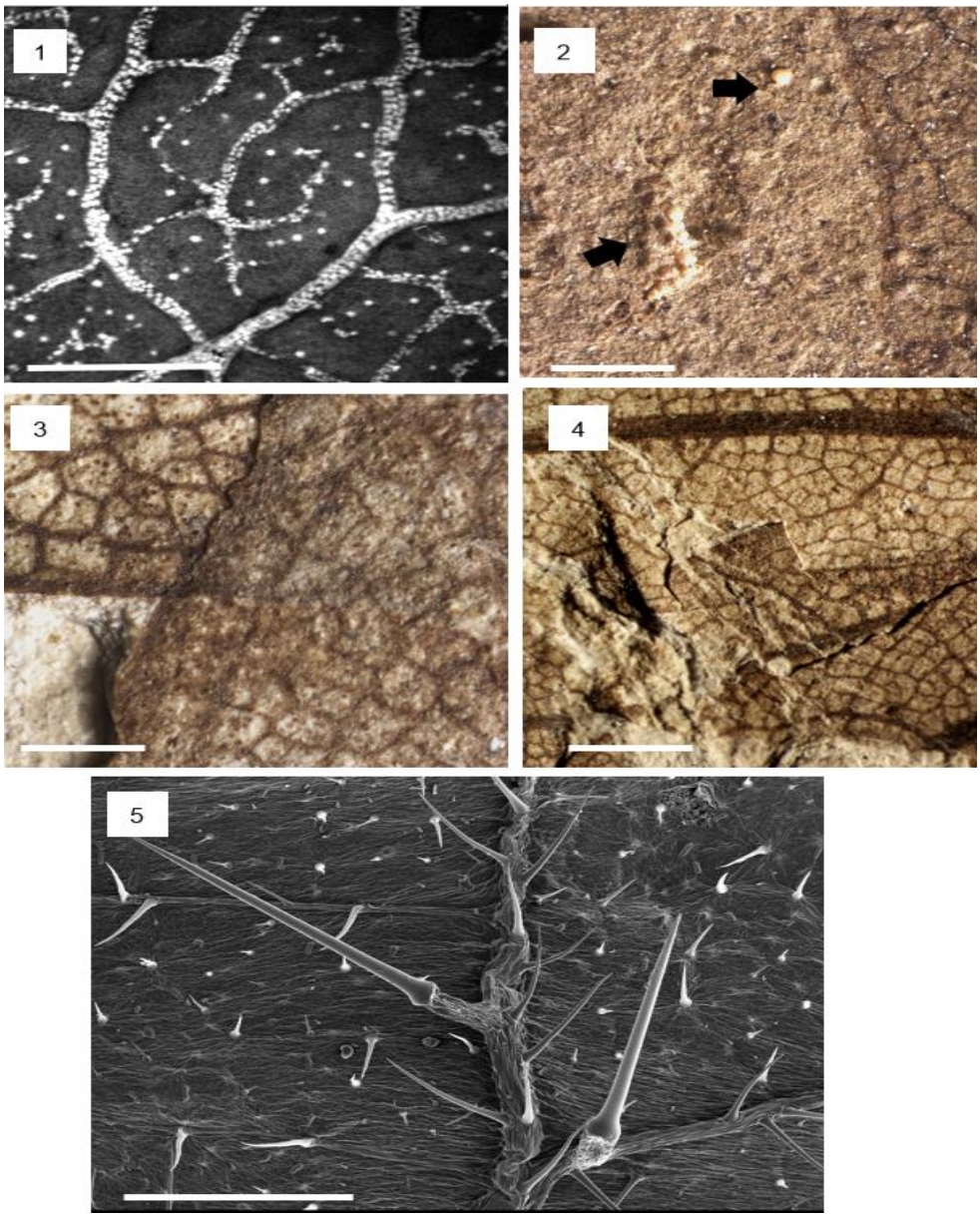

FIGURE 35. Comparison of pollen, bases of trichomes and CaOx occurrences. 35.1 Pol-LM image of CaOx crystals in an extant leaf of *Sideroxylon*. 35.2 Possible pollen occurrence (black arrows) next to a fossil *Acer* leaf, Rott_105 with LM. 35.3 Close-up view of CaOx traces in *Sideroxylon* fossil leaves (LM image). 35.4 multiple layers of *Sideroxylon* fossil leaves with traces of CaOx (LM image). 35.5. SEM image of a fresh leaf of *Urtica diotica*, showing trichomes and their bases on the cuticule. Scale bars: 35.1-35.4 = 300µm; 35.5 = 400 µm.

Further investigations with the help of a fluorescent microscope did not track them either in multiple layers of *Sideroxylon,* Rott_2, or in other sites studied. Yellow granules next to a leaf of *Acer*, Rott_105, are probably pollen, but these and similar traces don't show occurrence trends like those of CaOx traces. In other words, pollen grains exhibit very small size

distributions, have sculptures on the exine and occur in irregular distributions. Imprints of the druses on multiple layers a *Sideroxylon* leaf (**Figure 35.4**) as well as CaOx traces another fossil leaf of *Sideroxylon* that are very similar to the patterns of CaOx occurrence in extant *Sideroxylon* leaves (**Figure 35.3**, **Figure 35.1**) rebut the pollen interpretation for these granules. In addition, as clarified in the results, druses or crystals appear in different layers of the parenchymal tissue and beside or inside of the vascular system, while the bases of trichomes mostly occur on the epidermis of plants (**Figure 35.5**) which refutes the possibility of them being well-preserved in fossils, and especially in those fossil leaves (e.g., from the Rott fossil site) that are lacking a preserved cuticle.

The evolutionary history of the origin and formation of CaOx in basal plants up to the advanced groups is still an unresolved question. Although the present thesis revealed many aspects of CaOx fossilization in different plant groups, the necessity for further investigations in this field remains.

Our results did not include any evidence of CaOx in modern ferns, although there are reports of CaOx present in modern ferns and lycophytes (Kohl, 1889; Poirault, 1893). In seed ferns, we observed CaOx traces under the carbon layer in a regular distribution pattern with a size of ca. 20 µm. CaOx in cycads and ginkgophytes appear in aggregated forms or druses in the phloem. Druses in ginkgophytes measure up to 100 µm. Conifera show a different trend, crystals occuring as individuals, and with a small size (5-12 µm), under the cuticle.

Beyond superficial resemblances between cycads and palms, there are essential differences between them. Cycads are gymnosperms, while palms are classified as angiosperms (monocotyledons). Furthermore, the distribution pattern and form of CaOx show major differences between them. CaOx crystals commonly occur in monocotyledon plant cells (Dahlgren et al., 1985) in styloid forms (Esau, 1977). Raphides are a common type in palms, which has been reported in various parts of the plant by Micheels (1891) in *Ptychosperma*

alexandrae and a species of *Caryota*, while in cycads they have been mainly observed in the vascular system of the leaves and stems (see results).

As explained in Malekhosseini et al, (2022), in well preserved fossil leaves, casts of CaOx have been filled with organic or inorganic components which have been referred to as crystal ghosts (Bommanavar et al., 2020). The homogeneous distribution of granules and the absence of iron in a fossil leaf of *Glossopteris* sp. and granules composed of carbon compounds in Baiera brauniana is a confirmation of this assertion and could well interpret the presence of basic granular structures in seed ferns. The occurrence of the regular pattern of granules in other seed ferns demonstrate similar results to *Glossopteris* sp. and cycads. Observations of the granules similar to the CaOx druses in *G. biloba* (extant) in fossil leaves of *Baiera canaliculata* (Jurassic, Cayton bay) and *Baiera brauniana* (Lower Cretaceous, Osterwald, Germany) under the carbon layer reveals this similarity of the distribution of former CaOx druses in veins.

An overview of the main groups of plants from the basal Pteridospermatophyta, seed ferns, to the more highly developed angiosperm dicotyledons, is illustrated in **Figure 36**. It depicts the evolutionary relationship between different groups of plants in addition to the special features and the size of CaOx structures in their groups. As discussed above and explained in the results, the similarity in the distribution pattern of the casts parallel to the veins between seed ferns and cycads was observed; differences between gymnosperms were primarily in the diverse sizes and density of casts. Angiosperms continued to develop these trends due to more complexity between the environmental factors and physiological requirements of the plants so that all sizes, shapes, and distributions of CaOx were identified in this group.

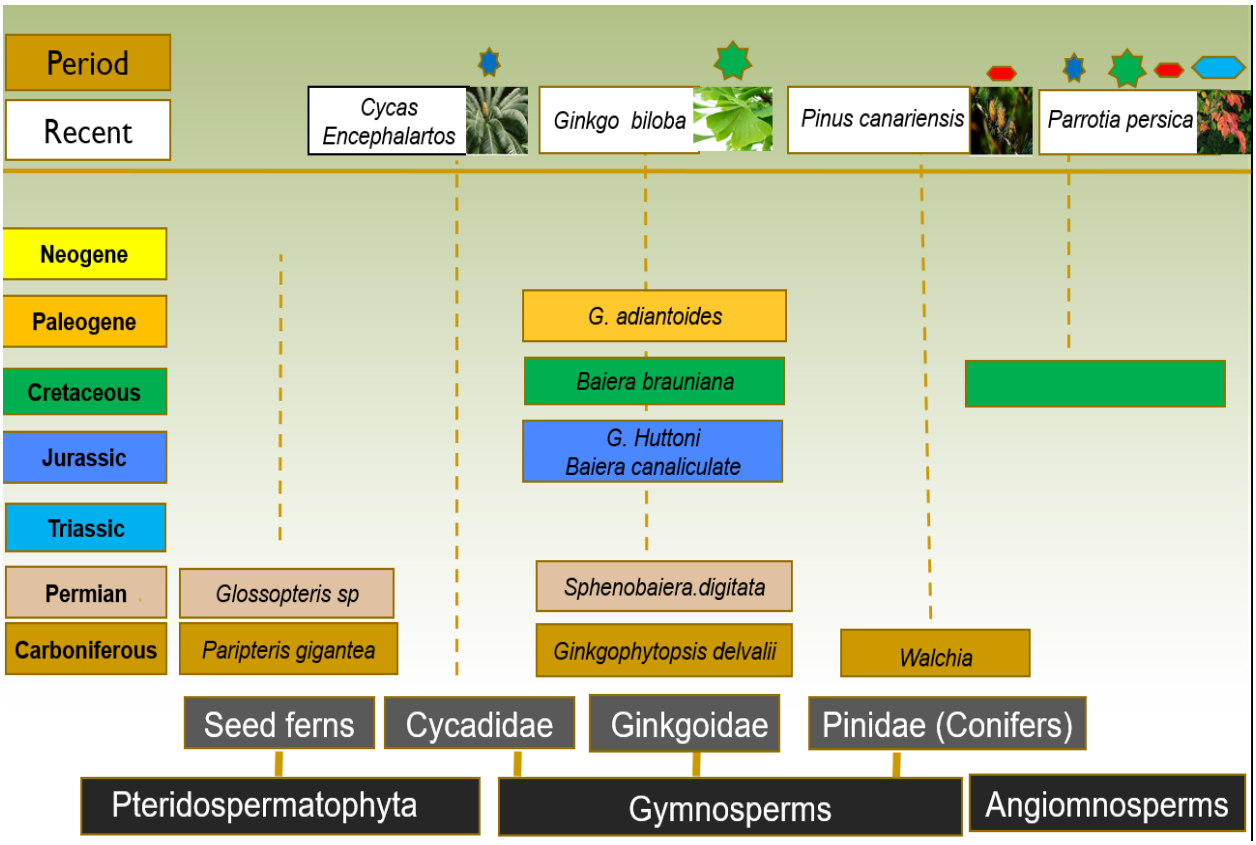

FIGURE 36. Occurrence of the CaOx traces in major groups of plants from the Carboniferous to the Neogene. Big druses (green star) were observed in Ginkgoales, while small druses (blue star) appear in Cycadales; Conifera show small crystals (red crystal) while all CaOx features and size variety are found in angiosperms.

2.8 Conclusions

Currently, the interpretation of fossil biomineral casts and imprints is mostly limited by our rudimentary knowledge of biomineralization in extant plants. A comprehensive database of current biomineralization patterns, investigation of physiological aspects (effective factors in quantity of Ca absorption and production of CaOx etc.) and ecological factors (e.g. insect interaction) in plants is highly desirable to progress in the near future.

The current study:

- Provides a valuable tool for paleobotany, profoundly improving fossil taxonomic assignments and thus greatly improving our understanding of both plant evolution and paleoecology.

- Improves our understanding of micromorphological structures of fossil leaves and the processes taking place during fossilization.

- Provides a basis for the study of the evolution of plant biomineralization across a range of different lineages.

- Provides an additional set of characters for improving taxonomic assignments of fossil leaves, if they are appropriately preserved.

- Confirms the presence of CaOx as an important factor, especially concerning herbivory, in plants.

- Confirms the importance of CaOx as an essential biomineral in main groups of plants from basal seed ferns to modern gymnosperms and angiosperms with presenting a wide range of diverse distribution pattern and size of CaOx in each group that depends mainly on environmental factors that change over periods of time and preservation localities.

Chapter 3

Published in Journal of Microscopy

Title: Visualization of calcium oxalate crystal macropatterns in plant leaves using an improved fast preparation method.

Authors: Hans-Jürgen Ensikat, Mahdieh Malekhosseini, Jes Rust, Maximilian Weigend

Authors contribution: Main of the part has been done by Hans-Jürgen Ensikat. All of the authors helped to design the study and wrote the manuscript.

Summary

The observation of biominerals in plants especially Calcium oxalate (CaOx) in each form (individual or aggregated crystals) are striking to the identification of plant species in extant and fossil leaves.

Some of the crystals and druses (crystal aggregates) are visible under the light microscope, but ideally a polarizing microscope is used, to identify and investigate the morphological details. Examination with a scanning electron microscope (SEM) is also almost required. Although there are many investigations concerning visualization of minerals and microscopy, there is no accurate method quick enough to identify crystals in extant plants or casts of them (in the present case, casts of CaOx) in fossil leaves.

In the current study a refined fast preparation method to visualize CaOx crystals is described and advantages and disadvantages are discussed. Leaf samples were incinerated at > 600°C

until all organic material was oxidized and the ashed remnants of the leaf were examined under a polarizing microscope after immersion in oil. This is a rapid method and overcomes many shortcomings of other methods, such as chemical clearing, and provides the visualization of the entire CaOx in extant leaves. Burning eliminates all organic components such as cellulose which would cause a disturbing background signal and the usage of oil immersion provides a good transparency to observe minerals. Further aspects for CaOx investigations by micro-CT and scanning electron microscopy are discussed in the paper. Thus, the burnt CaOx crystals are clearly visible whereas other ash components appear invisible in the polarizing microscope. With this simple preparation method, the investigation of CaOx distribution patterns in leaves may not only become favorable for amateur microscopists, for botanists they are a key for the understanding of the functions of CaOx, which are still in parts enigmatic and a matter of speculations.

It is argued that this method of incineration provides a valuable complementary tool for the study of leaf biomineralization, with the particular benefits: simple and easy and it is applicable to most of the plant tissues and specially leaves.

A comprehensive picture of CaOx in leaves can then be obtained by the complementary use of leaf clearing, SEM and micro-CT, leading to a genuine, three-dimensional picture and permitting even the identification of the element composition of the biominerals present. In view of these promising insights, it is believed that the increased ease of visualization, e.g., by the incineration method will provide a tool for the study of CaOx and other biominerals to accelerate investigation and functional aspects in physiological studies and mechanisms of CaOx deposition in leaf tissue.

Chapter 4

It has not yet published

Title: Calcium carbonate mineralization and traces of cystoliths in a fossil leaf of *Celtis occidentalis*, Middle Miocene, Randecker Maar, Germany

This chapter is a small part of Ca-mineralization refering to the identification of cystoliths, which was done in the laboratory of the Nees Institute, University of Bonn, by Mahdieh Malekhosseini and Hans-Jürgen Ensikat. This part has not been published yet and opens a new window to find an evolutionary trend of calcium carbonat in fossil leaves of angiosperms.

4.1 Abstract

In addition to calcium oxalate, calcium carbonate also plays a major role in the biomineralization of plants. Calcium carbonate biominerals in leaves are referred to as cystoliths. Cystoliths are an outgrowths of the epidermal cell wall consisting of calcium carbonate and silica. They occur in only eight specific families and, in contrast to calcium oxalate crystals, they are not present in the majority of plants.

In the current study, only one well-preserved example of a fossil leaf with preserved cystoliths, a fossil identified as *Celtis begonioides* from the Miocene Randecker Maar fossil site, has been found. In order to interpret this specimen and confirm the preserved granules are remnants of calcium carbonate cystoliths, fresh and fossil leaves of *Celtis* were compared. An ashed extant *Celtis occidentalis* leaf was examined with a light microscope using both normal light and a polarization filter. In the parenchyma, large cystoliths were observed alongside CaOx druses. The cystoliths were about five times larger in diameter (i.e.100 µm) than the CaOx druses. Furthermore, CaOx crystals occurred at a high density in the veins of *C. occidentalis*. The surface of the leaf fossil *Celtis begonioides* (Miocene, Randecker Maar, seemann 15) was examined with light microscopy (LM), and showed large, dark granules interpreted as the remains of cystoliths. Under SEM, more details were apparent, and the cystolith granules in the fossils showed similar distribution patterns and size ranges to those of cystoliths in the fresh leaves of *Celtis*. In general, the current study demonstrates the preservation of traces of cystoliths in a fossil leaf. Future studies of the stratigraphic and taxonomic distribution of cystoliths in fossil leaves will contribute to a better understanding of the evolutionary process of mineralization in fossil leaves containing cystoliths.

Key words: cystoliths; fossil leaves; biomineralization.

4.2 Introduction

Biological calcium deposition is common in plants. It is long been known that insoluble calcium salts in form of carbonate, sulfate, and oxalate occur in a wide variety of plants (Solereder, 1908). Of these, calcium oxalate and calcium carbonate are the most commonly deposited calcium salts (Arnott & Pautard, 1970; He et al., 2014). Calcium carbonate is frequently formed in algae or aquatic plants, and is generally deposited on the outer surfaces of the plant or in the intercellular spaces in the plant tissues (Borowitzka, 1984). $CaCO_3$ biomineralization is a widespread defensive phenomenon, and has been observed in the stem and cell walls of trichomes in many genera (Hopewell et al., 2021; Ensikat & Weigend, 2021). In land plants, the most common form of calcium carbonate deposition is cystoliths (Arnott, 1980).

Cystoliths are ergastic inclusion bodies consisting of amorphous calcium carbonate. They are spindle shaped bodies and form at the tip of the peg and grow in lithocyst wall, which consists of cellulose microfibris associated with pectins and other polysaccharides (Ajello, 1941; Pireyre, 1961; Frey-Wyssling, 1976). Lithocysts are cytoplasmically similar to other cells and the main differences are their dense mitochondria and specialized golgi system which allow them to transfer more Ca and produceg cystoliths (Watt et al., 1987).

Ca and calcium carbonate are main components of cystoliths, and silica is a minor component (Gal et al., 2012). Silicon has been observed in some sheath layers of the cystoliths (Arnott, 2018; Wendy et al., 1987). Occurrence of the Si in cystoliths in contrast with lithocysts in different genera of the same family follows different trends. Many surveys reported the mineral composition of leaf idioblasts (Gal et al., 2010). In the Cecropiaceae family, in all six genera, idioblasts usually occur as trichomes or enlarged epidermal cells. Si accumulated in them, in contrast to the idioblasts of other genera of the Urticales, which mostly possess cystoliths containing abundant Ca and Si.

The horizontally elongate, mineralized structures of Poikilospermum, reported formerly as “cystoliths” also contain mainly Si and little Ca. The six genera of Cecropiaceae share a

common characteristic in accumulating abundant Si in idioblasts of the leaf epidermis, while lacking cystoliths composed of abundant Ca and Si (Setoguchi et al., 1993). Cystoliths have been observed in certain families: Urticaceae, Ulmaceae, Moraceae, Cucurbitaceae and Acanthaceae (Ajello, 1941; Scott, 1946; Arnott, 1980). Cystoliths were found in abundance on both sides of the leaves (Siti Maisara et al., 2021), stem tissue and wood; these were oriented in two different directions in leaves while in stems they show only one orientation (Tripp & Fekadu, 2014). They are present in the form of papillate, hair-like lithocysts and swollen veinlets or swollen tracheids in many species of *Ficus* (Badron et al., 2014).

Since cystoliths occur in various organs and tissues, they are important in comparative anatomy and systematics of the plants. They are a useful feature to define families, genera and species. Recognition of the cystolith cells in the epidermis and parenchyma cortex of *Justicia gendarussa*, a traditional medicine in Peninsular Malaysia, differentiate this species from other species in the family of Acanthaceae or the *Acanthus* family (Zakaria et al., 2020; Patil & Patil, 2011). Observation of the cystoliths as anatomical characters in *Ficus religiosa* separated it from other studied species and it was introduced as a medicine species (Sethuramani et al., 2021). The presence of cystoliths in some genera of Moraceae, such as *Broussonetia*, *Chlorophora*, *Conocephalus*, *Ficus* and *Morus* emphasis the importance of them in plant taxonomy (Akinlabi & Oladipo, 2021). Furthermore, they have been observed in many genera of Acanthaceae (Tripp, 2014) and Urticaceae during their later flowering and seed setting stages (Watt et al., 1978). Other examples include *Cannabis*, Cannabaceae, which produce leaf and flower cystoliths (Dayanandan & Kaufman, 1976). The occurrence of cystoliths consisting of calcium carbonate in the lithocysts is one of the most prominent characters of Acanthaceae and is valuable for the recognition of some genera in this family (Miao-Ling Lin et al., 2004). In the leaves and sepals of *Justicia*, the lithocysts occurred frequently in the epidermis (LL Kuo-Huang &TB Yen, 1996). In the fossil leaves, cystoliths are important in the recognition of the genus. In a fossil Fig-tree from the Miocene of southwestern China, the occurrence of the

veinlet gland delicate role of the cystoliths in recognition of the genera (Huang Kuo-Huang & Yen, 1996; Huang et al., 2018).

In view of the physiological aspect, presence of cystoliths helps explain the adaptation of plants to the ambient ecological conditions (Naji et al., 2022). The role of cystoliths in plant physiology and photosynthesis has been addressed by Pierantoni in, 2000. In some species of *Ficus*, cystoliths affect the quantity of the light absorption by chlorophyll. It seems that they optimize the photosynthesis process by reducing the light waste and channeling it into the center of the leaf, where a low light regime exists. In this way, plants benefit from the mineral scattering.

In the current study we observed, large, dark granules which mostly distributed alongside the veins on the surface of a fossil leaf of *Celtis begonioides*. The preservation, size, position of the cystoliths in *Celtis* were examined and illustrated. Future studies aim to continue the investigation of more fossil species containing cystoliths for a better understanding of the evolutionary process of the cystolith development through geologic time

4.3 Materials and methods

A Leica MZ125 (Leica Microsystems, Wetzlar, Germany) stereomicroscope was used to recognize the granular structures on the surface of the fossil leaves. For higher magnifications, a light microscop (LM) with long distance objectives, which allows for surface illumination, was used (Müller optronic, Erfurt, Germany). Both microscopes were used with a Swift SC1803 microscope camera (Swift Optical Instruments, Schertz, Texas, US) with 18-megapixel resolution. A Lumix DMC-G70 photo-camera (Panasonic Corporation, Osaka, Japan) with Lumix macro-objective was used for close-up images.

Scanning electron microscopy was performed with a Tescan VEGA (Type 4) (Institute of Geosciences, Department of Palaeontology, University of Bonn). The SEM is equipped with

secondary electron (SE) and backscattered electron (BSE) detectors and energy-dispersive X-ray spectrometers (EDS) for element analysis. The Tescan SEM has low-vacuum capability.

4.4 Results

On the cuticule layer of the fossil leaf, *Celtis begonioides* (Miocene, Randecker Maar, seemann 15), dark brown granules were observed under LM, and compared to the occurrence of cystoliths in fresh leaves of *Celtis occidentalis*. Figure 1 illustrates different views of cystoliths and crystals under the cuticule layer in a fresh leaf of *Celtis occidentalis.* In this species, the cystoliths are several times larger than the calcium oxalate druses, which are clusters of CaOx crystals, in the parenchyma. In addition, individual crystals of calcium oxalate were observed in the veins of *C. occidentalis*. In the SEM image the $CaCO_3$ is red-colored under the cuticular layer (**Figure 2**).

In **Figure 2.2** and **2.3** LM images of the cuticule layer in a fossil leaf are illustrated. Cystoliths are distributed alongside the veins and reach a size of 80µm in diameter. The SEM shows more details of the fossil leaf *Celtis begonioides,* which exhibits cystoliths with 40-80 µm in diameter (**Figure 2**).

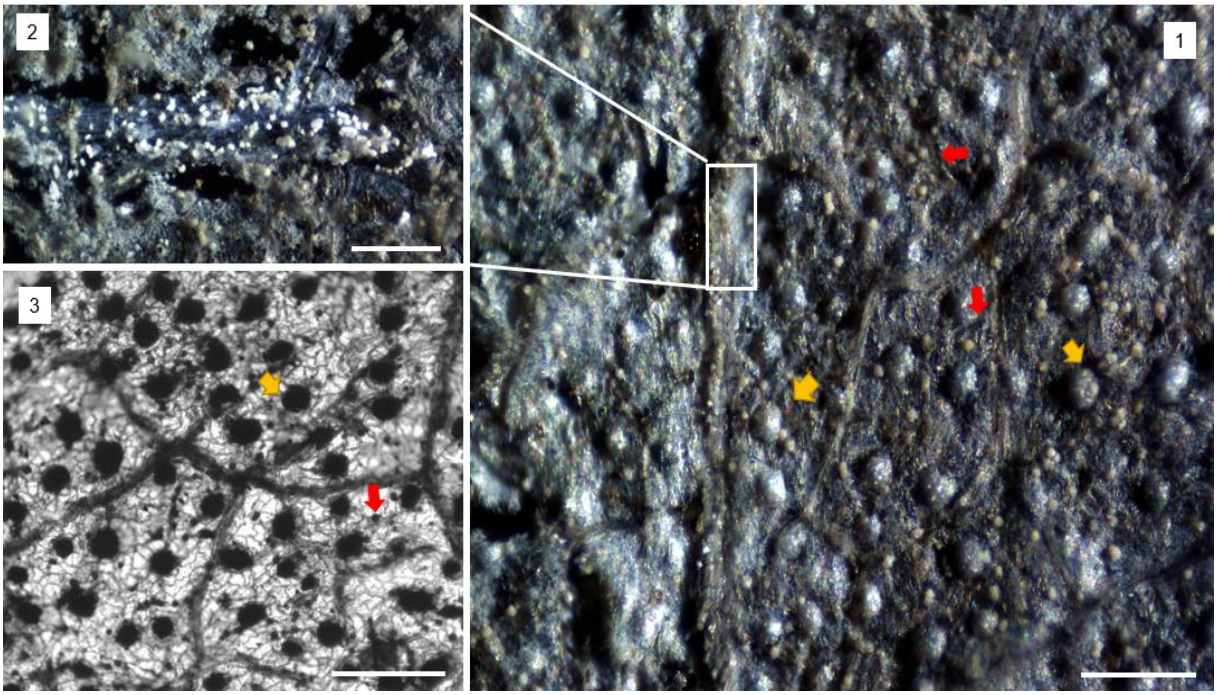

FIGURE 1. Distribution pattern of cystoliths in the parenchyma alongside small druses of CaOx and individual CaOx crystals in fresh leaves of *Celtis occidentalis*. 1.1 LM image of ash of *Celtis occidentalis* showing large granular structures, cystoliths, that have been marked with yellow arrows. Small druses of CaOx occur among the cystoliths and are marked with red arrows. 1.2 Close-up view of the vein illustrating individual crystals of CaOx. 1.3 Transmission LM image of *Celtis occidentalis*, shows another view of the cystoliths (yellow arrow) alongside the small druses of CaOx (red allow). Scale bars:1.1, 1.3 = 200 µm, 1.2 = 100 µm.

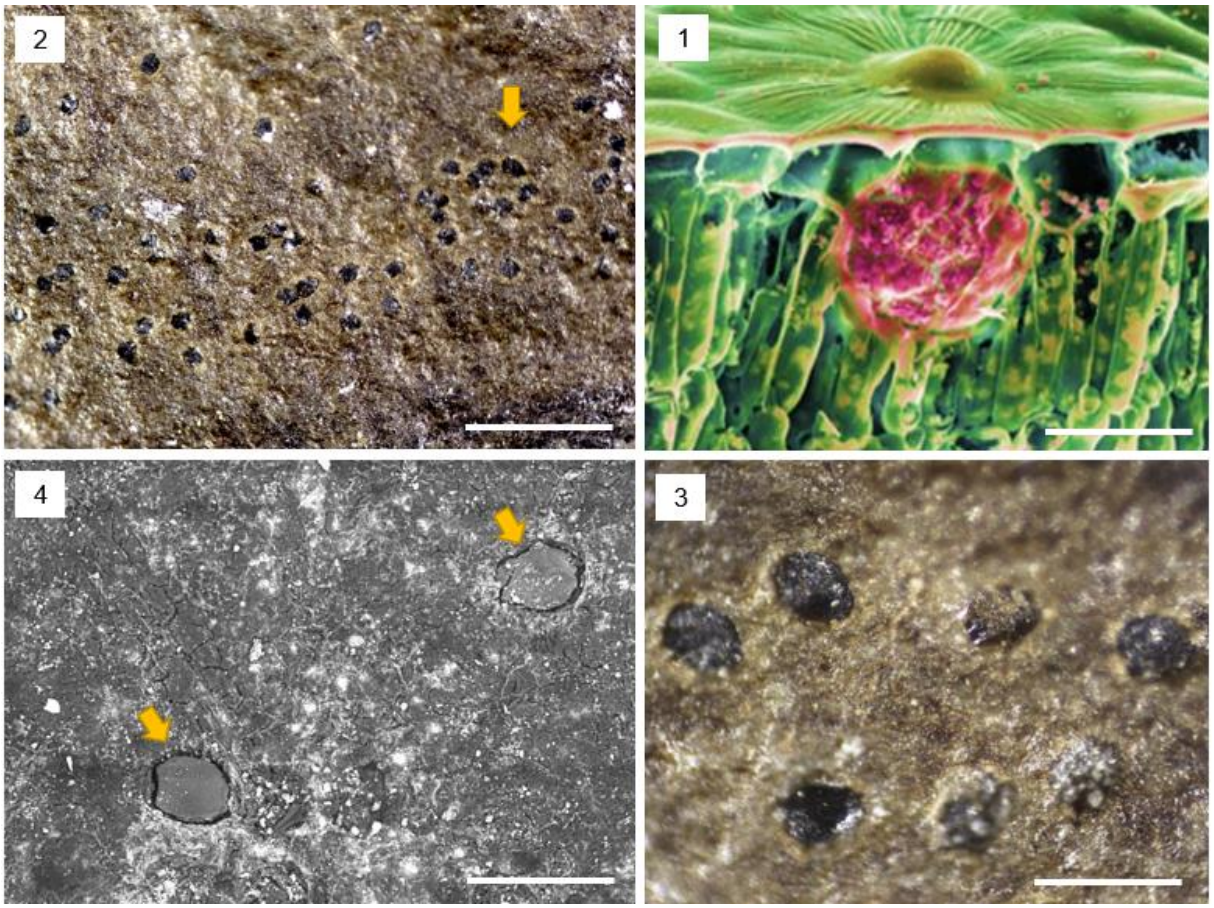

FIGURE 2. View of the dark granules on the surface of the fossil leaf of *Celtis begonioides* (Miocene, Randecker Maar, Seemann 15) in comparison with a cystolith in a fresh leaf of *Celtis occidentalis*. 2.1 View of a cystolith under the epidermis in a fresh leaf of *Celtis occidentalis*, red color is $CaCO_3$. 2.2 LM image of the fossil surface cystoliths (dark granules). 2.3 Close-up view of the cystoliths in the fossil leaf with LM. 2.4 SEM image of the cystoliths (yellow arrows) in the fossil leaf. Scale bars: 2.1 = 50 µm; 2.2 = 500 µm; 2.3, 2.4 = 100 µm.

4.5 Discussion

Cystoliths (cavity stones) are made of silica and calcium carbonate (Setoguchi et al. 1989). They are an important feature for the identification of different species. Cystoliths are described in eight plant families of plants including several dicotyledonous families: *Acanthaceae* (*Asterids*, *Lamiales*), *Boraginaceae* (*Asterids*, *Boraginales*), *Cannabaceae* (*Rosids*, *Rosales*), *Cucurbitaceae* (*Rosids*, *Cucurbitales*), *Moraceae* (*Rosids*, *Rosales*), *Opiliaceae* (*Rosids*,

Santales), *Ulmaceae* (*Rosids, Rosales*) and *Urticaceae* (*Rosids, Rosales*) (Solereder, 1908b; Linsbauer 1921; Metcalfe and Chalk, 1950).

These families that produce cystoliths do not form a monophyletic group. The most important aspects of cystolith production among vascular plants are anatomy, systematics, and ecology, as well as biogeochemistry due to their importance as a source of Ca and Si.

In the present study, cystoliths were observed under the cuticular layer of a fossil leaf of *Celtis begonioides* (Miocene, Randecker Maar, seemann 15). They occur as large, dark granules which are not distributed along the veins. Cystolith distribution in the fossil leaf shows a similar pattern to cystolith distribution in the extant leaves of *Celtis occidentalis* (Cannabaceae). Figures 1 and 2 in this chapter illustrate this similarity. A fresh leaf of *C. occidentalis* also contains CaOx in small size in addition to the much larger cystoliths in parenchyma. The identification of CaOx traces in *Celtis begonioides* (Miocene, Randecker Maar, seemann 15) was impossible, because of the preservation conditions and the small size of the druses.

Cystoliths in the *Acanthaceae* are primarily long, with either pointed or bulbous ends. In *Urticaceae* they are tapered (Watt et al., 1987). They have been found in the Moraceae family with round to pear shapes (Gal et al., 2012) and in *Cannabaceae* they have a teardrop-shape and have been found in the base of trichomes (Dayanandan & Kaufman, 1976).

Gal et al. (2012) studied the internal structure of cystoliths from *Morus alba* L. and *Ficus microcarpa* L.f. While cystoliths show layering, the layers are more abundant and thinner in both species than in *Barleria repens*. Sugimura and Nitta (2007) also showed fine, thin layers in *M. alba* cystoliths as did Watt et al. (1987) in *Pilea cadierei.*

Furthermore, different types of calcium carbonate precipitations are deposited on plant outer surface, in the intercellular spaces in the stem, or in the cell walls and lumen of trichomes in many genera (Hopewell et al., 2021; Ensikat & Weigend, 2021). In some publications, these deposits are also referred to as cystoliths, in a broader sense.

The amount of Ca and Si in cystoliths have been reported for various species. In land plants the most common form of calcium carbonate deposition is cystoliths (Arnott, 1980).

The presence of cystoliths in *Celtis ehrenbergiana* and *Celtis occidentalis* was described by Fernández Honaine (2018). This comparison shows a significant difference among *Celtis* species, so that phytolith association of *C. ehrenbergiana* is dominated by cystoliths (88%) and silicified epidermal cells (18%), while in *C. occidentalis* cystoliths reached 44% and silicified hairs 37%. In the present study, casts of cystoliths in a fossil leaf of *Celtis begonioides* did not have any remaining CaOx, but were infilled with C compounds and Si. C and Si show a similar trend in comparison with the fresh leaf of *C. occidentalis* in Fernández Honaine (2018) study.

4.6 Conclusions

Cystoliths as biomineralization markers are important to recognize different species in certain plant families such as Urticaceae, Ulmaceae, Moraceae, Cucurbitaceae and Acanthaceae. They are considered to be a key element for the classification of species in modern and of these mentioned families, and are therefore likely equally important for the classification of fossil species.

Future studies should focus on the distribution patterns of cystoliths in fossil leaves and try to determine whether or not the trend of calcium carbonate mineralization in certain species has changed over time.

4.7 Perspectives

1. Comparison of the distribution pattern of cystoliths in identified fossil and fresh leaves.
2. Investigation of the influence of physiological factors (e.g. thickness of the leaf, darkness and lightness) on the density of cystoliths.

Is there any correlation between the density of the cystoliths and photosynthesis?

Chapter 5

Titele: Decoding the whitish layer on fossil leaves in brown coal from the Eocene, Miocene and Oligocene, Germany.

All of the examinations and microscopy work has been done by Mahdieh Malekhosseini and Hans-Jürgen Ensikat.

This chapter has not been published yet. All of the material was prepared by Dr. Lutz Kunzmann, Senckenberg Naturhistorische Sammlungen Dresden, Museum für Mineralogie und Geologie, and the chemical analyses have been done by help from Prof. Dr. Lukas Schreiber and his team in the Department of Ecophysiology, IZMB, University of Bonn.

5.1 Abstract

Observation of the whitish layer on fossil leaves in coal opens a new window to understand fossil leaves. To date, our knowledge concerning the chemical composition of the whitish cuticular layer is poor. In the current study, four specimens were examined: *Eotrigonobalanus furcinervis (*upper Eocene), *Magnolia liblarensis (*middle Miocene), *Eotrigonobalanus furcinervis* (middle Eocence) and *Acer tricuspidatum* (late Oligocene, Norken). Since the leaves of many plants today show a similar white outer waxy layer which resembles the white layer of the fossils, we concluded that this layer could be wax. We analyzed the whitish layers (on the cuticule) and chloroform extracts of the coal under the cuticle to determine whether any wax-specific compounds occur. Two quick tests, dissolving in chloroform and heating to 70 C°, were carried out to understand the nature of whitish layer. The topography and composition of the wax were illustrated using scanning electron microscopy (SEM) and gas chromatography (GC) respectively. The results showed that wax components occurred in all fossil leaf specimens. In one of the specimens, *Eotrigonobalanus furcinervis,* mineral elements (Al, Si) were observed and wax components measured. After heating at 600 C°, flake-like structures were observed. The percentage of the primary alcohols in *E. furcinervis (*upper Eocene) (soluble in cold chloroform) was higher than in other fossil specimens. In *Magnolia liblarensis*, a tubular structure of the whitish wax layer was observed.

Primary alcohols made up the largest component of the whitish layer. Primary alcohols, fatty acids and esters respectively made up high percentages among the wax components in the third fossil sample, *Eotrigonobalanus* (middle Eocence) The 3-D structure of the wax in the cuticule layer was observed with SEM and showed irregular forms. In the fourth sample, *Acer tricuspidatum,* long-chain fatty acids were not detected and primary alcohols were rare.

In summary, it can be well acknowledged that the white cuticular layer in fossil specimens consists of wax. The presence of a high percentage of aliphatic wax compounds, such as those measured in *Magnolia liblarensis (*middle Miocene), are responsible for building 3-dimensional

crystals on the leaf surfaces, whereas other components make mostly disordered wax films such as observed in *Eotrigonobalanus*. Further investigation is necessary to understand the controls on the specific color of the cuticule layers of the fossils, and whether the color was consistent throughout fossilization of changed due to oxidation processes during fossilization.

5.2 Introduction

Wax provides a waterproofing effect, and plants secrete wax as a way to control evaporation, to reflect ultraviolet light, for self-cleaning, and to protect against pathogens (Rahman et al., 2021; Borodich et al., 2010; Barthlott & Neinhuis, 1997). Many plants secrete wax on and in the cuticle layer. Wax is an organic compound consisting of long aliphatic alkyl (C_nH_{2n+1}) chains (Baker & Gaskin, 1978). They are lipophilic, insoluble in water, but soluble in organic and nonpolar solvents such as chloroform and hexane (Bewick, 1993). Waxes include higher alkanes and lipids, typically with melting points above 40 °C. Natural waxes may contain unsaturated bonds and include various functional groups such as fatty acids, primary and secondary alcohols, ketones, aldehydes and fatty acid esters (6 Lim & Lee, 2017). Synthetic waxes often consist of homologous series of long-chain aliphatic hydrocarbons (alkanes or paraffins) that lack functional groups (Ivengar & Schlenk, 1969).

Epicuticular waxes cover the outer surface of the plant cuticle, and take the form of a whitish film or bloom on leaves, fruits and other plant organs (Trivedi et al., 2019). Epicuticular waxes are predominantly made of straight-chain aliphatic hydrocarbons that may be saturated or unsaturated and contain a variety of functional groups. Chemical compounds of waxes, their morphotypes and the morphology of the epicuticular surface are useful tools to differentiate species in modern plants (Eglinton et al., 1962; Dyson& Herbin, 1968; Mimura, et al., 1998, Barthlott et al. 2017). In Table 1 some examples of wax occurrences in plants are given (Ensikat et al., 2006).

Epicuticular waxes show a high variety of 3D morphotypes which can be verified by X-ray powder diffraction (XRD), electron diffraction (ED) and nuclear magnetic resonance (NMR) techniques: platelets, rods, and tubules. Recrystallization of plant waxes led to a better understanding of the correlation between wax morphotypes and chemistry and is a suitable method for studying the self-assembly process of crystal development in plant waxes (Ensikat et al., 2006; Koch & Barthlott, 2006; Meusel & Barthlott, 2000).

Table 1. Some examples of the wax types in different species of the fresh leaves.

Species	Wax type	Melting Point	Major components
Aquilegia canadensis L.	Nonacosanol tubules	76–79 ◦C	sec. alcohol C29
Aristolochia tomentosa Sims	Transversaly ridged rodlets	75–76 ◦C	ketones
Benincasa hispida Thunb.	Longitudinal ridged rodlets	170–180 ◦C	triterpenol-acetates
Brassica oleracea L.	Dendritic rodlets	65–67 ◦C	ketones C29, alkanes C29
Chelidonium majus L.	Nonacosanol tubules	72–73 ◦C	sec. alcohol C29
Chrysanthemum segetum L.	Coiled rodlets	64–73 ◦C	beta-diketone C31
Convallaria majalis L.	Platelets		prim. alcohol C26, C28, aldehydes,
Crassula ovata Mill.	Crust		

Waxes, especially long-chain alkanes and fatty acids, are useful biomarkers and are important tools for the reconstruction of past vegetation and paleo-environments (Marynowski et al., 2007; Zech et al., 2012; Liu et al., 2022).

The preservation of unaltered biomarkers among fossils and sediments is outstanding (Simoneit, 1986). For example, Marynowski et al. (2007) reported the occurrences of ferruginol derivatives (6,7-dehydroferruginol, sugiol,11,14-dioxopisiferic acid) and other polar diterpenoids, as well as their diagenetic products, in a conifer wood *Protopodocarpoxylon* from the Middle Jurassic of Poland. In Miocene leaves from the Clarkia Lake, Idaho, USA, the

distribution of n-alkane and n-alkanol homologues play a major role in differing fossil genera. N-alkanes were observed in *Platanus*, while n-alkanols have been observed in *Quercus* (Lockheart, et al., 2000).

In fossil leaves of conifers from the Eocene (Saxony, Germany) the terpenoid composition (e.g ferruginol, 6,7-dehydroferruginol, hydroxyferruginols, sugiol) is similar to that of related modern species such as *Taxodium balticum* (Otto, & Simoneit, 2001).

In the present study we investigated a whitish layer on fossil leaves from the Upper and Middle Eocene, Middle Miocene and Late Oligocene. Fossil leaves exist in different layers of the sediment and they look whitish and brownish in color. Since wax in many fresh leaves appears as a white layer on the cuticle, called epicuticular wax, we investigated the possibility that the whitish layer on the fossil leaves represented preserved wax. Thus, the current study addresses the following questions: 1) What are the whitish and brownish layers on the fossil leaves? 2) Are the different colors caused by varying oxidative processes? 3) If the whitish layer is wax, which chemical compounds are measurable? 4) Are there any differences between fresh and fossil leaves of *Magnolia*?

5.3 Materials and methods

Four fossil leaves with whitish coatings from different deposits and time periods were examined in this study. In Fig 1-4 they are illustrated.

1. Fossil leaf of *Eotrigonobalanus*; from the middle Eocene middle coal of the Geiseltal deposit, Saxony.
2. Fossil leaf of *Eotrigonobalanus furcinervis* (Fagaceae), upper Eocene Coal, Leipzig Bay. 3rd lignite seam complex, Bruckdorf Member, Borna Formation, Priabonian (late Eocene), appr. 36-35 Ma, opencast mine Schleenhain, south of the city Leipzig, Saxony.

3. Fossil leaf of *Magnolia liblarensis* (Magnoliaceae), 2nd seam complex, Welzow Member, Brieske Formation, Langhian (lower-middle Miocene), appr. 16-15 Ma, opencast mine Nochten, Saxony.
4. Fossil leaf of *Acer tricuspidatum* , from the late Oligocene, Norken.

FIGURE 1. Fossil leaf of *Eotrigonobalanus furcinervis* (Fagaceae), upper Eocene, south of the city Leipzig, Saxony. A whitish layer is preserved on the surface of the fossil leaf.

FIGURE 2. Different fossil leaves of Magnolia liblarensis in whitish to brownish color. *L*ower-middle Miocene coal, Nochten, Saxony.

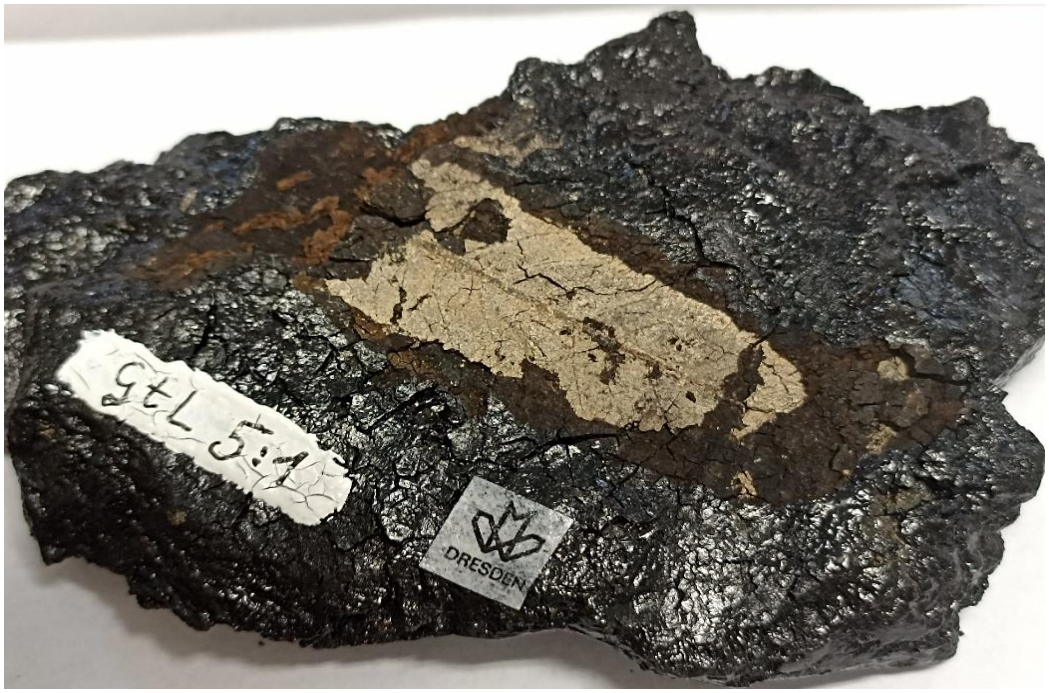

FIGURE 3. *Eotrigonobalanus furcinervis*, fossil leaf from the middle Eocene, middle coal of the Geiseltal deposit. A whitish layer is preserved on the surface of the leaf.

FIGURE 4. *Acer tricuspidatum*, fossil leaf from the late Oligocene, Norken. A whitish layer is preserved on the surface of the leaf.

Tests and analyses:

- Melting point: Heating to ca 60-70 C °

The melting point of wax is approximately 60 C°. To find out if the whitish layer shows characteristics of wax or not, we put a small piece of each fossil leaf on a heater with a temperature of 70 C ° for 2-3 min.

- Solubility in organic liquids: Dissolve in chloroform

Since chloroform is one of the solvents of wax, fragments of the samples were detached from the fossil piece and either left untreated or extracted with chloroform (10 min in boiling CHCl3). Both treated and untreated specimens were examined by SEM and therefore sputter-coated with a thin layer (ca. 15 nm) of palladium.

- Gas Chromatography (GC)

To identify the chemical compounds of the supposed fossil wax, gas chromatography (GC) was employed. One cm^2 of the leaf cuticle was prepared for the GC.

- Preparation of the sample

In order to measure the epicuticle wax compounds, we tried to make a pure sample of the whitish layer. Some iron powder was sprinkled over the fossil leaf and pulled on the epicuticular layer with the help of the toothpick wrapped well with cotton. The iron powder with adherent wax was collected with the help of a magnet and labeled for the GC analysis.

To determine the composition of the chemical components for all of the material the same protocol has been executed. In a first experiment, potential waxes were extracted by applying five times 1 ml of chloroform on the samples since no typical wax monomers could be removed. Then the second experimental procedure was performed. A piece of 1 cm^2 of the white (waxy) side was scratched out of the sample and was extracted in 5 ml chloroform overnight on the roll bank. 20 µg of tetracosane (alkane C24) was added to the sample prior incubation. 1µl of the sample was analyzed by on-column injection. Typical wax monomers (fatty acids and alkanes) could be identified. Again, a piece of 1 cm^2 of the potential waxy side and the non-waxy side

was scratched out (as potentially negative control) and extracted in hot chloroform (60 C°) over night. Prior to incubation in the heating block, the samples were piqued with 20 µg of the internal standard tetracosane. Again 1 µl of the samples were analyzed by column injection. This process was repeated for all the fossil samples.

5.4 Results

The results of the melting point analysis show that the white layer is wax. This whitish layer disappeared during heating and boiling in chloroform. In addition, chemical components of wax (e.g., fatty acids, primary alcohol, sterols, alkanes) were measured in all samples of the fossil specimens.

The wax layer in a fossil leaf of *Eotrigonobalanus furcinervis* (Fagaceae), upper Eocene coal, did not show any regular 3D structure. Instead, regular sculpture in the form of flakes was observed after heating the fossil leaf up to 600 C° **(Figure 5**). In the third specimen, *Eotrigonobalanus furcinervis,* middle Eocene coal, the 3D structure of the wax, which had an irregular flake form, was observed (**Figure 10**). In contrast to the two other fossil specimens a very distinct 3D structure consisting of coiled tubes was apparent in *Magnolia liblarensis* (Magnoliaceae) (**Figure 8**).

EDX of the incinerated sample of *Eotrigonobalanus furcinervis* from the upper Eocene south of Leipzig shows that the remaining whitish layer was made of mineral elements (Si, Al, O). Details of the EDX analyses are shown in **Figure 6**.

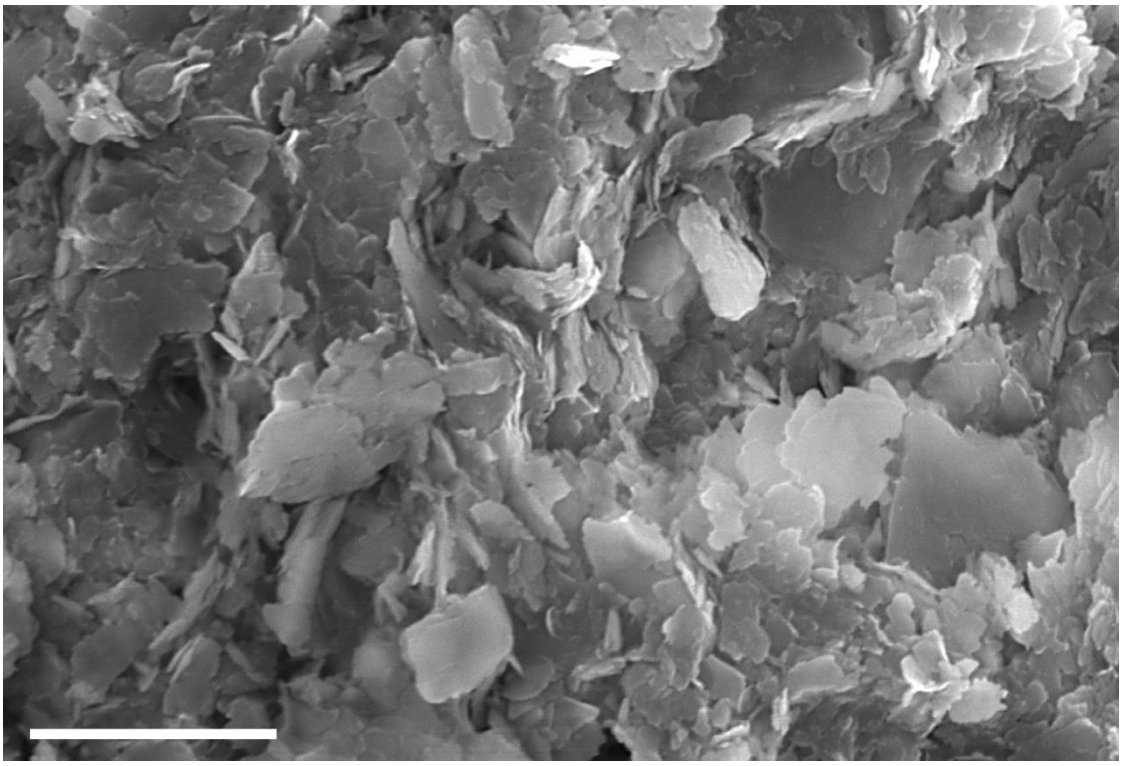

FIGURE 5. SEM image of the whitish layer of *Eotrigonobalanus furcinervis* from the upper Eocene south of Leipzig after 600 C° heating. 3D structure of irregular platelet form is observable. Scale bar = 5 µm.

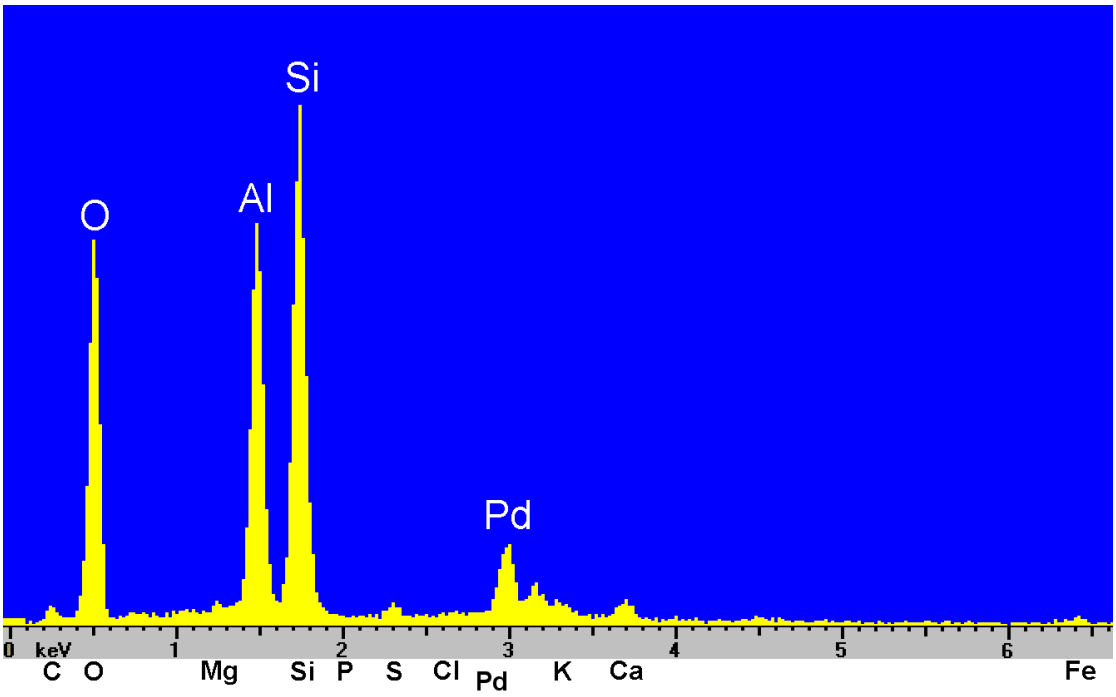

FIGURE 6. EDX analysis of *Eotrigonobalanus furcinervis (*upper Eocene). Spectrum from crystalline structures which are illustrated in FIGURE 5, indicating oxides of Si and Al.

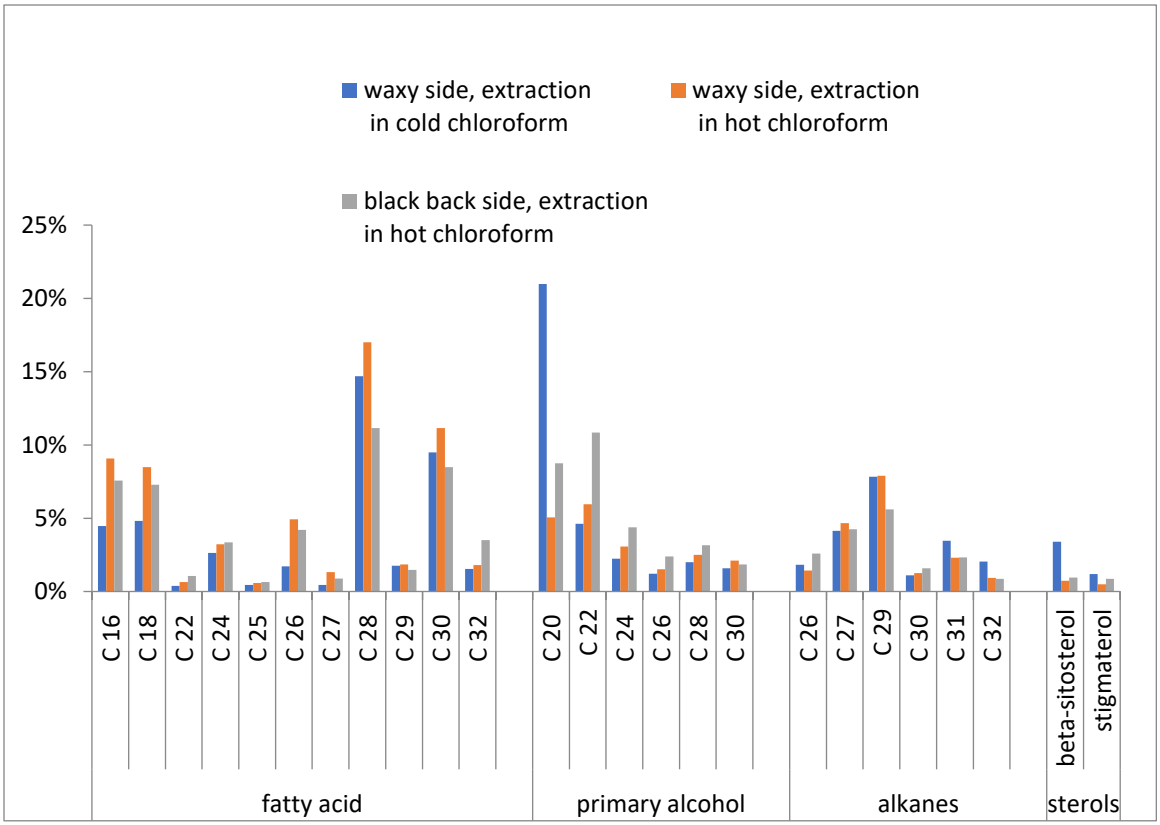

FIGURE 7. Chemical components of the wax (e.g. fatty acids, primary alcohol, sterols, alkanes) of *Eotrigonobalanus furcinervis* (upper Eocene*) which* were measured by GC.

GC analysis of *Eotrigonobalanus furcinervis* (upper Eocene), in both waxy and not waxy sides, show chemical components of the wax (**Figure 7**). Fatty acids, primary alcohol, alkanes and sterols (beta-sitosterol, stigmasterol) with details of the long-chain aliphatic hydrocarbons are illustrated in Figure 7. In this figure, fatty acids with chains of C16, C18, C 22, C24, C25, C27, C28, C29, C30, C32 in both waxy and in non- waxy sides of the fossil leaf are observed. Primary alcohols with C20, C22, C24, C26, C26 and C28 and alkanes including C26, C27, C29, C30, C31 and C32 were indicated.

C28, C30 and C32 were higher in extraction of the waxy side in hot chloroform than in cold chloroform. In the not waxy side (no whitish layer) C16, C18, C24, C28, C30 show lower amounts in comparison with the waxy side that were dissolved in hot chloroform.

Primary alcohols did not show much difference between the waxy side in both hot and cold chloroform, and only the C20 primary alcohol shows higher percentage in cold chloroform. Alkanes (C27 and C29) in the waxy side extracted in cold chloroform were higher than in the not waxy side. Beta-sitosterol extracted in cold chloroform also was higher than in the not-waxy side.

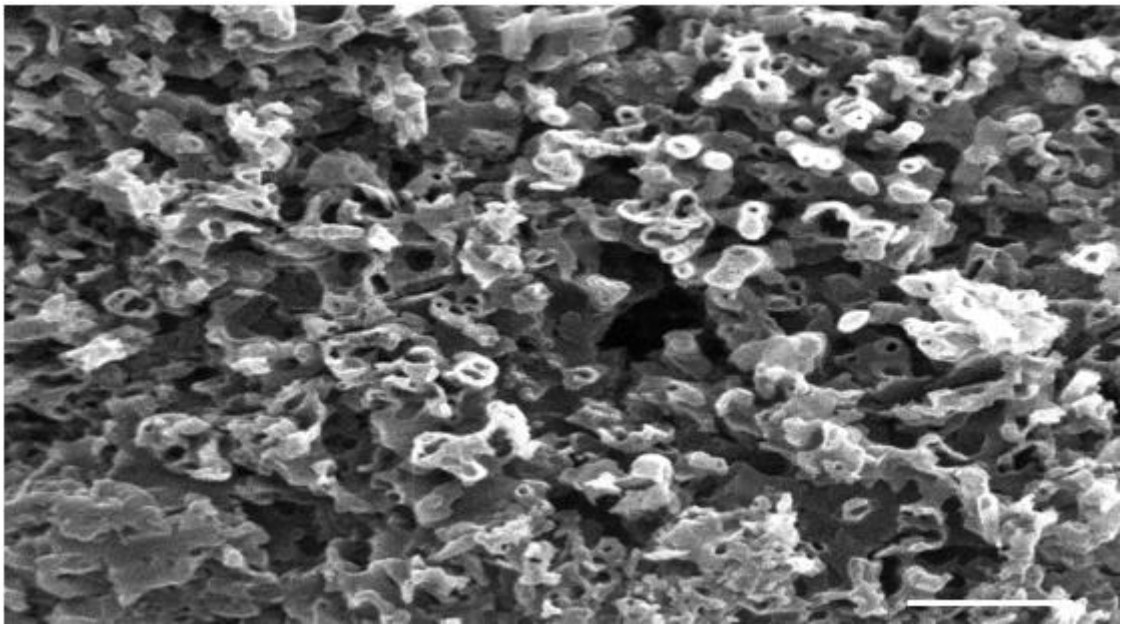

FIGURE 8. Whitish layer of *Magnolia liblarensis* (Magnoliaceae) from the *l*ower-middle Miocene coal, Nochten, Saxony. 3D structure of the wax in form of coiled tubes is apparent. Scale bar = 5µm.

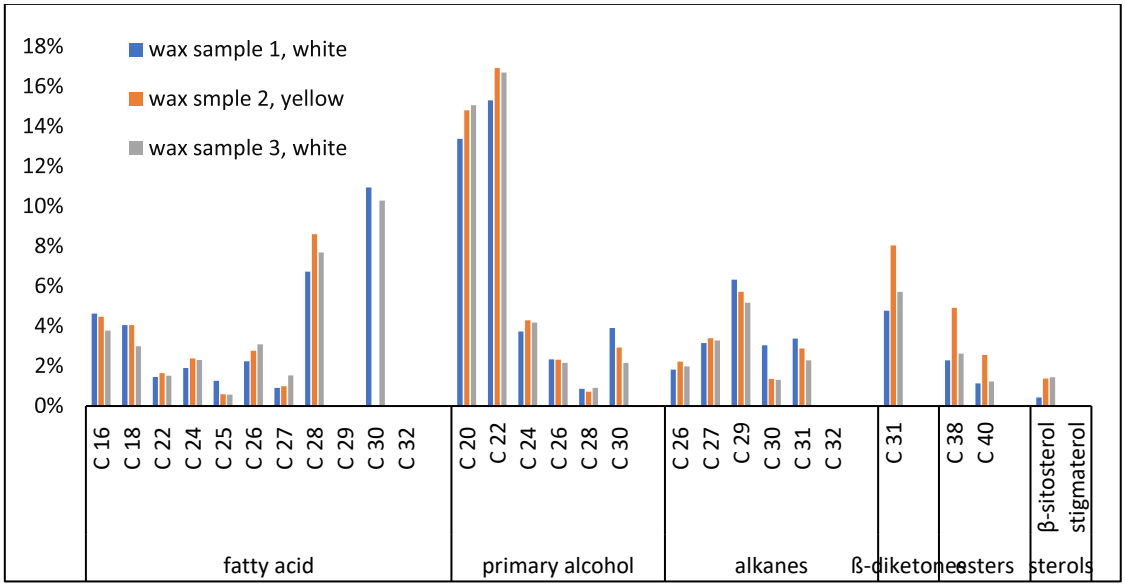

FIGURE 9. Chemical components of the wax in *Magnolia liblarensis* (lower-middle Miocene coal, Nochten, Saxony) examined by GC. Three samples of the same fossil specimen in white and yellow examined with GC and details of the components are summarized.

We prepared 3 samples of the wax on the leaf surface of different *Magnolia liblarensis* specimens (lower-middle Miocene coal, Nochten, Saxony) which show different colors like white, yellow and brown, to see if there are differences in their chemical components. Our results showed that there is no difference between yellow and white color of the wax samples in *Magnolia liblarensis*. C29 and C32 fatty acid chains did not exist in these specimens. Primary alcohols occur in almost the same quantity in whitish and yellowish specimens. Alkanes C26, C27, C29, C30, C31, except C32, were measured in all specimens. Beta-diketones, C31, was identified with GC in whitish and yellowish specimens. Esters and sterols were measured in all specimens.

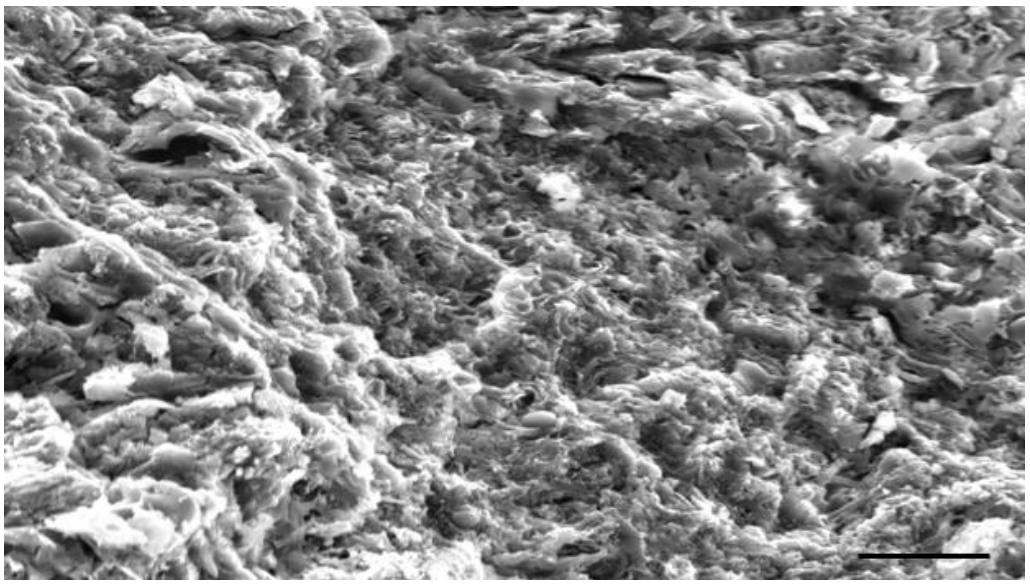

FIGURE 10. Morphology of irregular flake forms in *Eotrigonobalanus furcinervis*, middle Eocene coal (Geiseltal, Germany).

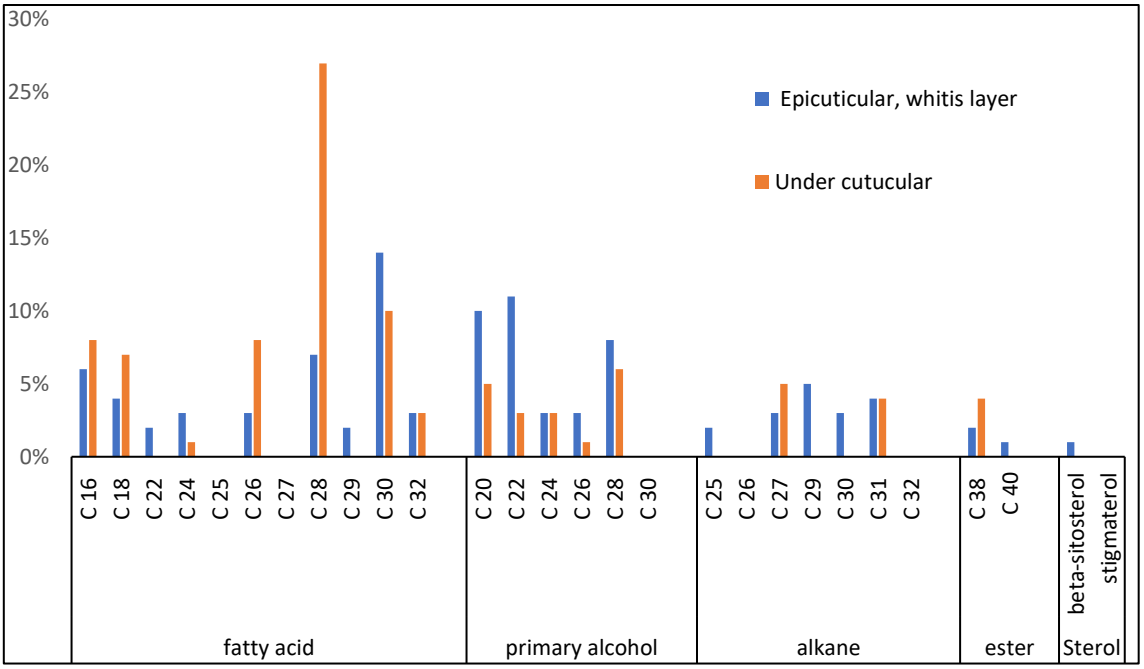

FIGURE11. Chemical compounds of *Eotrigonobalanus furcinervis*, (middle Eocene coal, Geiseltal, Germany) by GC.

In Figure 10, fatty acids with chains of C16, C18, C 22, C24, C25, C27, C28, C29, C30, and C32 on both waxy and non-waxy sides of the fossil leaf are illustrated.

Primary alcohols with C20, C22, C24, C26, C26 and C28 and alkanes including C26, C27, C29, C30, C31 and C32 are measured. C30 and C32 in primary alcohols and alkanes were not observed.

In comparison with *Eotrigonobalanus furcinervis* from the upper Eocene the middle Eocene material clearly contain smaller amounts of esters. Sterols in both the waxy and non-waxy side did not occur in a significant amount.

Two samples of fossil leaves of *Acer tricuspidatum* showed varying compositions of the white layers. The isolates gained with the iron powder method contained aliphatic wax compounds, mainly alkanes, and C16 and C18 fatty acids in Sample 2, but also a high content of a triterpenoid and sterols particularly in Sample 1 (**Table 1**). Long-chain fatty acids were not detected and primary alcohols only rarely.

Table 2 Comparison of the chemical wax components in 2 pieces of *Acer tricuspidatum*, Late Oligocene, Norken.

Acer tricuspidatum Sample 1		*Acer tricuspidatum* Sample 2
	%	%
C16 acid	3,18	19,47
C 18 acid	3,18	13,90
	6,36	33,38
C 18 primary alcohol	1,09	3,82
C 29 primary alcohol	3,78	
C24-2-OH	0,90	
C23 alkane	1,13	0,81
C26 alkane	3,81	3,12
C28 alkane	5,31	5,70
C29 alkane	5,01	20,50
C 30 alkane	4,95	1,26
C 31 alkane	4,86	9,13
C 32 alkane	5,42	7,08
C 34 alkane	2,36	
C 35 alkane	1,86	1,44
	34,71	49,04
triterpenoid hederagenin	32,41	10,38
Stigmasterol	2,65	
beta-Sitosterol	15,09	3,38
	50,15	13,76
sum	100,00	100,00

5.5 Discussion

Comparative characterization of the wax in fresh leaves demonstrates that there is a widespread pattern of chemical compounds in plants, but these characters can change in fossil leaves during fossilization. Factors such as, for example, time, depth of embedding, elements in the sediment and diagenetic processes all can affect the wax. Investigation of extant Ginkgo biloba and fossil leaves of *Eretmophyllum andegavense*, a ginkgoalean plant of Cenomanian age, demonstrates that in *Ginkgo biloba* n-alkanes, alkylphenols, alpha-tocopherol and n-acids respectively are the main stable wax constituents (Tu et al., 2003). Cranwell (1981) showed that the stability of free lipids shows the following trend with increasing depth in the sediment: n-alkanes > alkan-2-ones > sterols > n-alkanoic acids > n- alkanols > n-alkenoic acids, which coincides with the results of *Ginkgo biloba*.

In the current study the examination of *Eotrigonobalanus furcinervis* specimens from two different sites and times show different results which make it clear that the composition of chemical wax components changes over time. A comparison of the preserved epicuticular wax lipids in *E. furcinervis* (upper Eocene) with *E. furcinervis* (middle Eocene) present all fatty acids in both the whitish and under the whitish layer of the fossil leaves, while in *E. furcinervis* from the middle Eocene C25 and C27 were not observed. Additionally, C28 in the subcuticular layer was higher than in the epicuticular one. In contrast, in the subcuticular layer C22 and C29 were not observed.

Low quantities of the primary alcohols and alkanes in *E. furcinervis (*middle Eocene) in comparison with *E. furcinervis (upper Eocene) r*eveals the reason for the absence of regular and salient 3D crystal structures of the wax on the surface of the leaves. Although microscopic images did not show any crystalline 3D structure in the fossil leaves belonging to the upper Eocene, the presence of fatty acids indicated the occurrence of wax in both layers. Furthermore, under the whitish layer we measured all of the wax chemical compounds, which indicates that certain components are able to move under the cuticle.

In the extant *Magnolia grandiflora* L. wax is present as a smooth layer. These results are in line with research on *M. grandiflora* which has been conducted by Gülz et al. (1992). They reported that the abaxial epidermis of *M. grandiflora* has no crystalloids or sculptures. The epidermis includes a continuous wax layer on the surface and the abaxial epidermis also shows a continuous wax layer but with little irregular granular sculptures. In contrast, in our investigations, the topography of the wax in M. liblarensis was shown to have tubular sculptures with a regular distribution pattern in the whitish layer on the cuticle. Those findings on modem leaf tissues and wax indicates that certain components of wax including platelets, tubules, films and rodlets can be affected by environmental factors during fossilization.

5.6 Conclusions

Observations on the whitish layer on the fossil leaves belonging to the Eocene, Miocene and Oligocene raise the question what kind of processes (oxidation, development of pigments, etc.) occurred. Since the cuticle of many extant plants presents a waxy whitish layer, the probability of the presence of wax in the fossil samples was estimated. GC analyses of *Eotrigonobalanus furcinervis (*upper Eocene and middle Eocene) indicated that the whitish layer on the fossil leaves is made of wax and that there is a difference in the quantity and type of the fatty acids which are a chemical component of the wax. This shows that chemical components can change over time in the same species. Furthermore, components of the wax measured in the epicuticular layer and under the cuticle demonstrate that fatty acids were able to move between these layers of the fossil leaves. Despite the low amount of fatty acids, a 3D structure was detected in *Eotrigonobalanus furcinervis (*middle Eocene). Probably, a lack of a clear 3D structure in the same species from the upper Eocene is due to remaining fatty acids under the cuticle layer. A specific 3D structure on the epicuticular layer of Miocene *Magnolia liblarensis* was observed. The epicuticular wax on fossil leaves is an impressive illustration for the durability of small-molecular organic compounds over millions of years. The comparison with waxes on living

plants may provide information about the stability of the diverse wax constituents, their decay processes, and their mobility in the soil over paleontological times.

Chapter 6

Gerneral discussion and conclusion

The identification of minerals and biomarkers in plant fossils have always been useful indicators for ecological studies and the recognition of factors affecting the fossilization and the evolution of mineralization during geological periods. Meanwhile, the role of calcium biominerals such as calcium oxalate (CaOx), calcium carbonate ($CaCO_3$) and compounds that form wax has always been bold.

There are plenty of studies, mainly on extant plants, on these bio-minerals and wax-forming compounds (Baker & Gaskin, 1978; Bewick, 1993) as well as the types of Ca-biominerals such as crystals of CaOx (Franceschi & Horner, 1980) and cystoliths (Setoguchi et al. 1989; Solereder, 1908b; Linsbauer 1921; Metcalfe and Chalk, 1950), location of Ca-biominerals (Florin, 1931; Kunzmann, 1999), effective genes in producing and control of Ca-biominerals, in plants such as algae (Friedmann et al., 1972; Pueschel & West, 2007; Pueschel, 1995), lichens (Jones et al.,1981), fungi (Tait et al., 1999) and vascular plants (Franceschi & Horner, 1980) and how they are formed (Nakata, 2003; Franceschi & Horner, 1980; Franceschi & Nakata, 2005).

Therefore, it may seem that our knowledge of Ca-biominerals is sufficient, but there was no investigation of the fossil record of CaOx crystals, except well preserved individual crystals of conifers in amber (Sadowski & Kunzmann, 2022). Concerning cystoliths (cavity stones) in fossil leaves due to their big size and position under the cuticle the identification of them is easier than it is in CaOx. In the current study one well preserved sample with casts of cystoliths in a fossil leaf of *Celtis begonioides* (Miocene, Randecker Maar, seemann 15) has been

recorded. The cystolith distribution in the fossil leaf shows a similar pattern to the cystolith distribution in extant leaves of *Celtis occidentalis* (Cannabaceae).

All of the details of the processes of CaOx fossilization are still not fully understood, but in this thesis a scenario is helpful to figure out this process over geological times and different fossil sites (Malekhosseini et al., 2022). The present study involves a description of the distribution and micromorphology of Ca-biomineral traces and their elemental composition in remnants of the parenchyma of fossil leaves which are named “ghost crystals”.

The record of casts of CaOx in fossil leaves from basal plants (seed ferns) to the higher plats, gymnosperms and angiosperms has been established to reconstruct the evolutionary history of CaOx from the Devonian to the Neogene.

Wax as a protection of the plants cuticle against biotic factors (avoiding water loss, defense against pathogens with anti-adhesive effects, protection against UV radiation) and abiotic stresses (control of mechanical damage, wind, heavy rain, self-cleaning) are important. What multiplies the importance of wax in paleontology studies is the presence of their chemical compounds that make them an effective help for the identification of fossil plants and predicting the ecological effect to form sculptures of wax.

Comparative characterization of the wax in fresh and fossil leaves demonstrates that factors such as time, depth of embedding, elements in the sediment and diagenetic processes all can affect the occurrence of wax. A comparison of the preserved epicuticular wax lipids in *Eotrigonobalanus furcinervis* (upper Eocene) with *E. furcinervis* (middle Eocene) present all fatty acids in both the whitish and under the whitish layer of the fossil leaves, while in *Eotrigonobalanus furcinervis* from the middle Eocene C25 and C27 were not observed. Additionally, C28 in the subcuticular layer was higher than in the epicuticular one. In contrast, in the subcuticular layer C22 and C29 were not observed.

The comparison with waxes on living plants may provide information about the stability of the diverse wax constituents, their decay processes, and their mobility in the soil over geological times.

References

1. Arnott, H. J. (1966). Studies of calcification in plants. In Calcified Tissues 1965 Springer, Berlin, Heidelberg. 152-157.

2.Anitha, R., & Sandhiya, T. (2014). Occurrence of calcium oxalate crystals in the leaves of medicinal plants. *IJP*, 1(6), 389-393.

3.Arnott, H. J., Pautard, F. G. E., & Steinfink, H. (1965). Structure of calcium oxalate monohydrate. *Nature*, 208(5016), 1197-1198.

4.Anthoons, B. (2017). Distribution of calcium oxalate crystals in ferns and lycophytes. Master of Science Thesis, Ghent University. Faculty of Sciences. Ghent, Netherlands.

5.Arnott, H. J., & Pautard, F. G. (1970). Calcification in plants. In *Biological calcification: Cellular and molecular aspects*, 375-446.

6.Arnott, H. J. (1980). Carbonates in higher plants. *Mechanisms of Biomineralization in Animals and Plants.*, 211-218.

7.Ajello, L. (1941). Cytology and cellular interrelations of cystolith formation in *Ficus elastica*. *American Journal of Botany*, 589-594.

8.Arnott, H. J. (1982). Three systems of biomineralization in plants with comments on the associated organic matrix. In *Biological mineralization and demineralization*. 199-218.

9.Akinlabi, A. A., & Oladipo, O. T. (2021). Venation studies of some species in the genus Ficus Linn. in Southwestern Nigeria. *Notulae Scientia Biologicae*, 13(2), 10760-10760.

10.Badron, U. H., Talip, N., Mohamad, A. L., Affenddi, A. E. A., & Juhari, A. A. A. (2014). Studies on leaf venation in selected taxa of the genus *Ficus* L.(Moraceae) in peninsular Malaysia. *Tropical life sciences research*, 25(2), 111.

11.Baker, E. A., & Gaskin, R. E. (1987). Composition of leaf epicuticular waxes of Pteridium subspecies. *Phytochemistry*, 26(10), 2847-2848.

12.Barthlott, W., & Neinhuis, C. (1997). Purity of the sacred lotus, or escape from contamination in biological surfaces. *Planta*, 202, 1-8.

13.Bewick, T. A., Shilling, D. G., & Querns, R. (1993). Evaluation of epicuticular wax removal from whole leaves with chloroform. *Weed Technology*, 7(3), 706-716.

14.Borodich, F. M., Gorb, E. V., & Gorb, S. N. (2010). Fracture behaviour of plant epicuticular wax crystals and its role in preventing insect attachment: a theoretical approach. *Applied Physics A*, 100, 63-71.

15.Bommanavar, S., Hosmani, J., Togoo, R. A., Baeshen, H. A., Raj, A. T., Patil, S., ... & Birkhed, D. (2020). Role of matrix vesicles and crystal ghosts in bio-mineralization. *Journal of Bone and Mineral Metabolism*, 38, 759-764.

16.Borowitzka, M. A. (1984). Calcification in aquatic plants. *Plant, Cell & Environment*, *7*(6), 457-466.

Chitwood, D. H., & Sinha, N. R. (2016). Evolutionary and environmental forces sculpting leaf development. *Current Biology*, 26(7), R297-R306.

17.Böttcher, R., Kern, A. K., Eder, J., & Schoch, R. R. (2013). The Randeck Maar: Palaeoenvironment and habitat differentiation of a Miocene lacustrine system. *Palaeogeography Palaeoclimatology Palaeoecology*, 392, 426-453.

18.Cranwell, P. A. (1981). Diagenesis of free and bound lipids in terrestrial detritus deposited in a lacustrine sediment. *Organic Geochemistry*, *3*(3), 79-89.

19.Coté, G. G. (2009). Diversity and distribution of idioblasts producing calcium oxalate crystals in Dieffenbachia seguine (Araceae). *American Journal of Botany*, 96(7), 1245-1254.

20.Dahlgren, R. M., Clifford, H. T., & Yeo, P. F. (1984). The families of the monocotyledons: Structure, evolution, and taxonomy. Springer Science & Business Media.

21.Dyson, W. G., & Herbin, G. A. (1968). Studies on plant cuticular waxes-IV: leaf wax alkanes as a taxonomic discriminant for cypresses grown in Kenya. *Phytochemistry*, *7*(8), 1334-1344.

22.Dayanandan, P., & Kaufman, P. B. (1976). Trichomes of *Cannabis sativa* L.(Cannabaceae). *American Journal of Botany*, 63(5), 578-591.

23.Esau, K. (1977). Anatomy of seed plants. John Wiley & Sons. *Inc.*, *Nero York*, 44-88.

24.Esteban, I., De Vynck, J. C., Singels, E., Vlok, J., Marean, C. W., Cowling, R. M., ... & Albert, R. M. (2017). Modern soil phytolith assemblages used as proxies for Paleoscape reconstruction on the south coast of South Africa. *Quaternary International*, 434, 160-179.

25.Eglinton, G., Gonzalez, A. G., Hamilton, R. J., & Raphael, R. A. (1962). Hydrocarbon constituents of the wax coatings of plant leaves: a taxonomic survey. *Phytochemistry*, 1(2), 89-102.

26.Ensikat, H. J., Boese, M., Mader, W., Barthlott, W., & Koch, K. (2006). Crystallinity of plant epicuticular waxes: electron and X-ray diffraction studies. *Chemistry and Physics of lipids*, 144(1), 45-59.

27.Ensikat, H. J., & Weigend, M. (2021). Distribution of Biominerals and Mineral-Organic Composites in Plant Trichomes. *Frontiers in Bioengineering and Biotechnology*, 1101.

28.Florin, R. (1931). Untersuchungen zur Stammesgeschichte der Coniferales und Cordiatales: T. 1, Morphologie und Epidermisstruktur der Assimilationsorgane bei den rezenten Koniferen (Doctoral dissertation, Almqvist & Wiksell).

29.Faheed, F., Mazen, A., & Elmohsen, S. A. (2013). Physiological and ultrastructural studies on calcium oxalate crystal formation in some plants. *Turkish Journal of Botany*, 37(1), 139-152.

30.Frey-Wyssling, A. (1981). Crystallography of the two hydrates of crystalline calcium oxalate in plants. *American Journal of Botany*, 68(1), 130-141.

31.Fikáček, M., Schmied, H., Prokop, J., & Sinica, A. G. (2010). Fossil hydrophilid beetles (Coleoptera: Hydrophilidae) of the Late Oligocene Rott Formation (Germany). *Acta Geologica Sinica*, 84(4), 732.

32.Florin, R. (1931). Untersuchungen zur Stammesgeschichte der Coniferales und Cordaitales. I. Morphologie und Epidermisstruktur des Assimilationsorgane bei den regenten Koniferen. *K. Svenska Vetensk. Acad. Handl.*, 10, 1-588.

33.Franceschi, V. R., & Horner, H. T. (1980). Calcium oxalate crystals in plants. *The Botanical Review*, 46(4), 361-427.

34.Franceschi, V. R., & Nakata, P. A. (2005). Calcium oxalate in plants: formation and function. *Annu. Rev. Plant Biol.*, *56*, 41-71.

35.Fernández Honaine, M., De Rito, M., & Osterrieth, M. (2018). Análisis de los silicofitolitos presentes en especies de las familias Cannabaceae, Moraceae y Urticaceae del SE bonaerense y estudio comparativo de los cistolitos. *Boletín de la Sociedad Argentina de Botánica*, *53*(2), 1-10.

36.Friedmann, E. I., Roth, W. C., Turner, J. B., & McEwen, R. S. (1972). Calcium oxalate crystals in the aragonite-producing green alga Penicillus and related genera. *Science*, 177(4052), 891-893.

37.Gardner, D. G. (1994). Injury to the oral mucous membranes caused by the common houseplant, Dieffenbachia: a review. *Oral surgery, oral medicine, oral pathology*, 78(5), 631-633.

38.Genua, J. M., & Hillson, C. J. (1985). The occurrence, type and location of calcium oxalate crystals in the leaves of fourteen species of Araceae. *Annals of Botany*, 56(3), 351-361.

39.Goss, S. L., Lemons, K. A., Kerstetter, J. E., & Bogner, R. H. (2007). Determination of calcium salt solubility with changes in pH and PCO2, simulating varying gastrointestinal environments. *Journal of Pharmacy and Pharmacology*, 59(11), 1485-1492.

40.Gülz, P. G., Müller, E., Schmitz, K., Marner, F. J., & Güth, S. (1992). Chemical composition and surface structures of epicuticular leaf waxes of Ginkgo biloba, Magnolia grandiflora and Liriodendron tulipifera. *Zeitschrift für Naturforschung C*, 47(7-8), 516-526.

41.Gal, A., Hirsch, A., Siegel, S., Li, C., Aichmayer, B., Politi, Y., ... & Addadi, L. (2012). Plant cystoliths: a complex functional biocomposite of four distinct silica and amorphous calcium carbonate phases. *Chemistry–A European Journal*, 18(33), 10262-10270.

42.Gal, A., Weiner, S., & Addadi, L. (2010). The stabilizing effect of silicate on biogenic and synthetic amorphous calcium carbonate. *Journal of the American Chemical Society*, 132(38), 13208-13211.

43.He, H., Veneklaas, E. J., Kuo, J., & Lambers, H. (2014). Physiological and ecological significance of biomineralization in plants. *Trends in plant science*, 19(3), 166-174.

44.Hoover, A. A., & Wijesinha, G. S. (1945). Influence of pH and salts on the solubility of calcium oxalate. *Nature*, 155(3943), 638-638.

45.Horn, G., & Orvin, A. K. (1928). Geology of Bear Island: with special reference to the coal deposits, and with an account of the history of the island.

46.Horner, H. T., & Wagner, B. L. (2020). Calcium oxalate formation in higher plants. In *Calcium oxalate in biological systems*, 53-72. CRC press.

47.Huang, J., Su, T., Jia, L. B., Spicer, T., & Zhou, Z. K. (2018). A fossil fig from the Miocene of southwestern China: Indication of persistent deep time karst vegetation. *Review of Palaeobotany and Palynology*, 258, 133-145.

48.Hopewell, T., Selvi, F., Ensikat, H. J., & Weigend, M. (2021). Trichome biomineralization and soil chemistry in Brassicaceae from Mediterranean ultramafic and calcareous soils. *Plants*, 10(2), 377.

49.Jones, D., Wilson, M. J., & McHardy, W. J. (1981). Lichen weathering of rock-forming minerals: application of scanning electron microscopy and microprobe analysis. *Journal of Microscopy*, 124(1), 95-104.

50.Kolibáč, J., Adroit, B., Gröning, E., Brauckmann, C., & Wappler, T. (2016). First record of the family Trogossitidae (Insecta, Coleoptera) in the Late Pliocene deposits of Willershausen (Germany). PalZ, 90, 681-689.

51.Kaiser, F. W. E. (1897). Geologische Darstellung des Nordabfalles des Siebengebirges,10. Universitäts-Buchdruckerei von G. Georgi.

52.Koenigswald, W. (2007). 29. Mammalian faunas from the interglacial periods in Central Europe and their stratigraphic correlation. In Developments in Quaternary Sciences, 7, 445-454). Elsevier.

53.Kuo-Huang, L. L., & Yen, T. B. (1996). The Development of Lithocysts in the Leaves and Sepals of *Justicia procumbens* L. *Taiwania-Taipei*, 41, 17-26.

54.Koch, K., Dommisse, A., & Barthlott, W. (2006). Chemistry and crystal growth of plant wax tubules of lotus (Nelumbo n ucifera) and nasturtium (Tropaeolum m ajus) leaves on technical substrates. *Crystal growth & design*, *6*(11), 2571-2578.

55.Keates, S. E., Tarlyn, N. M., Loewus, F. A., & Franceschi, V. R. (2000). L-Ascorbic acid and L-galactose are sources for oxalic acid and calcium oxalate in Pistia stratiotes. *Phytochemistry*, 53(4), 433-440.

56.Khan, A. S., & Siddiqi, R. (2014). Environmental factors affect calcium oxalate crystals formation in Tradescantia pallida (Commelinaceae). *Pakistan Journal of Botany*, 46(2), 477-482.

57.Kostman, T. A., Tarlyn, N. M., Loewus, F. A., & Franceschi, V. R. (2001). Biosynthesis of L-ascorbic acid and conversion of carbons 1 and 2 of L-ascorbic acid to oxalic acid occurs within individual calcium oxalate crystal idioblasts. *Plant Physiology*, 125(2), 634-640.

58.Kunzmann, L. Koniferen der Oberkreide und ihre Relikte im Tertiär Europas. *Abhandlungen des Staatlichen Museums für Mineralogie und Geologie Dresden*, 45, 3–191 (1999).

59.Keates, S. E., Tarlyn, N. M., Loewus, F. A., & Franceschi, V. R. (2000). L-Ascorbic acid and L-galactose are sources for oxalic acid and calcium oxalate in Pistia stratiotes. *Phytochemistry*, 53(4), 433-440.

60.Koenigswald, W. V., Mörs, T., Mosbrugger, V., & Koenigswald, W. V. (1996). Rott im Überblick. *Fossillagerstätte Rott bei Hennef im Siebengebirge. Das Leben an einem subtropischen See vor*, 25, 105-109.

61.Krassilov, V. A., Lewy, Z., Nevo, E., & Silantieva, N. (2005). Late Cretaceous (Turonian) Flora of southern Negev, Israel. Pensoft.

62.Krassilov, V., Lewy, Z., Nevo, E. & Silantieva, N. *Late Cretaceous (Turonian) flora of Southern Negev, Israel* (Pensoft Publishers, Sofia, Bulgaria, 2005).

63.Kvaček, Z. (2002). Novelties on Doliostrobus (Doliostrobaceae), an extinct conifer genus of the European Palaeogene. *Časopis Národního Muzea*, 171, 131-175.

64.Kohl, F. G. (1889). Anatomisch-physiologische Untersuchung der Kalksalze und Kieselsäure in der Pflanze: Ein Beitrag zur Kenntnis der Mineralstoffe im lebenden Pflanzenkörper. Éditeur non identifié.

65.Liu, J., Zhao, J., He, D., Huang, X., Jiang, C., Yan, H., ... & An, Z. (2022). Effects of plant types on terrestrial leaf wax long-chain n-alkane biomarkers: Implications and paleoapplications. *Earth-Science Reviews*, 104248.

66.Linsbauer, K. (1921). Uber die kalkfreien Zystolithen der Acanthaceen. *Berichte der Deutschen Botanischen Gesellschaft*, *39*, 41-49.

67.Lim, J., Hwang, H. S., & Lee, S. (2017). Oil-structuring characterization of natural waxes in canola oil oleogels: Rheological, thermal, and oxidative properties. *Applied Biological Chemistry*, 60, 17-22.

68.Lockheart, M. J., van Bergen, P. F., & Evershed, R. P. (2000). Chemotaxonomic classification of fossil leaves from the Miocene Clarkia Lake deposit, Idaho, USA based on n-alkyl lipid distributions and principal component analyses. *Organic Geochemistry*, 31(11), 1223-1246.

69.Iyengar, B. T. R., & Schlenk, H. (1969). Melting points of synthetic wax esters. *Lipids*, 4(1), 28-30.

70.Li, X. X., & Franceschi, V. R. (1990). Distribution of peroxisomes and glycolate metabolism in relation to calcium oxalate formation in Lemna minor L. *European journal of cell biology*, 51(1), 9-16.

71.Le Coz, C. J., Ducombs, G., & Paulsen, E. (2011). Plants and plant products. *Contact dermatitis*, 873-925.

72.Lersten, N. R., & Horner, H. T. (2000). Calcium oxalate crystal types and trends in their distribution patterns in leaves of Prunus (Rosaceae: Prunoideae). *Plant Systematics and Evolution*, 224(1), 83-96.

73.Maisarah, S., Mahayuddin, A. M., & Fadzilah, H. (2021). Assessing bone marrow involvement in diffuse large B-cell lymphoma with 18F-FDG PET/CT: A preliminary experience at Hospital Pulau Pinang. *The Medical Journal of Malaysia*, *76*(5), 665-671.

74.Metcalfe, C. R., & Chalk, L. (1950). Anatomy of the Dicotyledons: leaves, stem, and wood, in relation to taxonomy,. *Science*, 112(2914), 541-542

75. Lin, M. L., Tsair-Bor Yen, T. B., & Kuo-Huang, L. L. (2004). Formation of Calcium Carbonate Deposition in the Cotyledons during the Germination of *Justicia procumbens* L. (Acanthaceae) Seeds. *Taiwania*, 49(4): 250-262.

76.Mimura, M. R., Salatino, M. L., Salatino, A., & Baumgratz, J. F. (1998). Alkanes from foliar epicuticular waxes of Huberia species: taxonomic implications. *Biochemical Systematics and Ecology*, 26(5), 581-588.

77.Meusel, I., Neinhuis, C., Markstädter, C., & Barthlott, W. (2000). Chemical composition and recrystallization of epicuticular waxes: coiled rodlets and tubules. *Plant Biology*, *2*(4), 462-470.

78.Marynowski, L., Otto, A., Zatoń, M., Philippe, M., & Simoneit, B. R. (2007). Biomolecules preserved in ca. 168-million-year-old fossil conifer wood. *Naturwissenschaften*, 94, 228-236.

79.Micheels, H. (1891). De la preÂsence de raphides dans l'embryon de certains palmiers. *Bulletins de l'AcadeÂmie Royale des Sciences, des Lettres et des Beaux Arts de Belgique, seÂr*, 3(22), 11.

80.Malekhosseini, M., Ensikat, H. J., McCoy, V. E., Wappler, T., Weigend, M., Kunzmann, L., & Rust, J. (2022). Traces of calcium oxalate biomineralization in fossil leaves from late Oligocene maar deposits from Germany. *Scientific Reports*, 12(1), 15959.

81.Mazen, A. M., Zhang, D., & Franceschi, V. R. (2004). Calcium oxalate formation in Lemna minor: physiological and ultrastructural aspects of high-capacity calcium sequestration. *New phytologist*, 435-448.

82.Molano-Flores, B. (2001). Herbivory and calcium concentrations affect calcium oxalate crystal formation in leaves of Sida (Malvaceae). *Annals of Botany*, 88(3), 387-391.

83.Moraweck, K., Grein, M., Konrad, W., Kvaček, J., Kova-Eder, J., Neinhuis, C., ... & Kunzmann, L. (2019). Leaf traits of long-ranging Paleogene species and their relationship with depositional facies, climate and atmospheric CO2 level. *Palaeontographica,* Abteilung B, 93-172.

84.Meischner, D., & Paul, J. (1982). Die pliozäne Fossilfundstätte Naturdenkmal Tongrube Willershausen. Mitteilungen des Arbeitskreises für Paläobotanik und Palynologie, 1982.

85.Meischner, D. (2000). Der pliozäne Teich von Willershausen am Harz. *Europäische Fossillagerstätten*, 223-228.

86.Meischner, D., Paul, J., Pelzer, G., & Riegel, W. (1982). «Wallensen, Wealden, Willershausen, Westersteine». Arbeitskreis für Paläobotanik und Palynologie, 11.-13.3. 1982, Dassel-Exkursion B.

87.Mörs, T. (1996). Die Säugetiere der oberoligozänen Fossillagerstätte Rott bei Bonn (Rheinland) The mammals of the upper Oligocene fossillagerstätte Rott near Bonn (Rhineland). *Decheniana (Bonn)*, *149*, 205-232.

88..Mörs, T. (1995). Die Sedimentationsgeschichte der Fossillagerstätte Rott und-ihre Alterseinstufung anhand neuer Säugetierfunde- (Oberoligozän, Rheinland).

89.Mai, D. H., & Schneider, W. (1988). Uber eine altertumliche Konifere im Jungtertiar und deren Bedeutung fur Braunkohlen-und Bernsteinbildung. *Feddes Repertorium*.

90.McComas Jr, W. H., & Rieman III, W. (1942). The effect of pH on the solubility of calcium oxalate. *Journal of the American Chemical Society*, 64(12), 2948-2949.

91.Nicotra, A. B., Leigh, A., Boyce, C. K., Jones, C. S., Niklas, K. J., Royer, D. L., & Tsukaya, H. (2011). The evolution and functional significance of leaf shape in the angiosperms. *Functional Plant Biology*, 38(7), 535-552.

92.Naji, H., Soheili, F., Panahi, P., Hatamnia, A. A., Woodward, S., & Abdul-Hamid, H. (2022). Leaf Microstructure and Adaptation Relationships in Ten Woody Species from the Semi-Arid Forests. *Iranian Journal of Forest*.

93.Nakata, P. A. (2003). Advances in our understanding of calcium oxalate crystal formation and function in plants. *Plant Science*, 164(6), 901-909.

94.O'Connell, A. M., Malajczuk, N., & Gailitis, V. (1983). Occurrence of calcium oxalate in karri (Eucalyptus diversicolor F. Muell.) forest ecosystems of south western Australia. *Oecologia*, 56(2), 239-244.

95.Otto, A., & Simoneit, B. R. (2001). Chemosystematics and diagenesis of terpenoids in fossil conifer species and sediment from the Eocene Zeitz formation, Saxony, Germany. *Geochimica et Cosmochimica Acta*, 65(20), 3505-3527.

96.Ogino, T., Suzuki, T., & Sawada, K. (1987). The formation and transformation mechanism of calcium carbonate in water. *Geochimica et Cosmochimica Acta*, 51(10), 2757-2767.

97.Pireyre N. (1961). Contributions to the morphological, histological and physiological study of cystoliths. *Reviews of Cytology and Plant Biology*, 23, 93–320.

98.Frey-Wyssling, A. (1976). The plant cell wall. In: Encyclopedia of Plant Anatomy. Band III / 4. Ed.: Gebr. Borntraeger, Berlin, Germany.

99.Patil, A. M., & Patil, D. A. (2011). Occurrence and significance of cystoliths in Acanthaceae. *Current Botany*, *2*(4).

100.Paul, J., & Meischner, D. (1991, September). Very early diagenetic dolomite as a preservative of perfect organic fossils. In *Dolomieu Conference of Carbonate Platforms and Dolomitization, Ortisei/St. Ulrich, Val Gardena/Grödental, The Dolomites, Italy* (pp. 16-21).

101.Pierantoni, M., Paudel, I., Rephael, B., Tenne, R., Brumfeld, V., Slomka, S., ... & Klein, T. (2020). Cystoliths in Ficus leaves: increasing carbon fixation in saturating light by light scattering off a mineral substrate. *bioRxiv*, 2020-04.

102.Piperno, D. R. (2006). *Phytoliths: a comprehensive guide for archaeologists and paleoecologists*. Rowman Altamira.

102.Paiva, É. A. S. (2021). Do calcium oxalate crystals protect against herbivory? *The Science of Nature*, 108(3), 1-7.

103.Poirault, G. (1893). L'oxalate de calcium chez les Cryptogrames vasculaires. *Le Journal de Botanique*, *7*, 72-75.

104.Pueschel, C. M., & West, J. A. (2007). Calcium oxalate crystals in the marine red alga Spyridia filamentosa (Ceramiales; Rhodophyta). *Phycologia*, 46(5), 565-571.

105.Pueschel, C. M. (1995). Calcium oxalate crystals in the red alga Antithamnion kylinii (Ceramiales): cytoplasmic and limited to indeterminate axes. *Protoplasma*, 189, 73-80.

106.Piperno, D. R. (1989). The occurrence of phytoliths in the reproductive structures of selected tropical angiosperms and their significance in tropical paleoecology, paleoethnobotany and systematics. *Review of Palaeobotany and Palynology*, 61(1-2), 147-173.

107.Piperno, D. R., & Pearsall, D. M. (1998). The silica bodies of tropical American grasses: morphology, taxonomy, and implications for grass systematics and fossil phytolith identification. *Smithsonian contributions to Botany*.

108.Rasser, M. W., Bechly, G., Böttcher, R., Ebner, M., Heizmann, E. P. J., Höltke, O., ... & Ziegler, R. (2013). The Randeck Maar: Palaeoenvironment and habitat differentiation of a Miocene lacustrine system. *Palaeogeography, Palaeoclimatology, Palaeoecology*, *392*, 426-453.

109.Rahman, T., Shao, M., Pahari, S., Venglat, P., Soolanayakanahally, R., Qiu, X., ... & Tanino, K. (2021). Dissecting the roles of cuticular wax in plant resistance to shoot dehydration and low-temperature stress in Arabidopsis. *International Journal of Molecular Sciences*, 22(4), 1554.

110.Raman, A., & Croom Jr, E. M. (1998). The anatomical features of powdered Ginkgo biloba L. leaf as observed by light microscopy. *Journal of Medicinal Food*, 1(2), 89-95.

111.Rashid, A. (1998). An introduction to bryophyta: diversity, development and differentiation. *Vikas Publishing House*, 29-35.

112.Rüffle, L. (1976). Myricaceae, Leguminosae, Icacinaceae, Sterculiaceae, Nymphaeaceae, Monocotyledones, Coniferae. Eozäne Floren des Geiseltales. *Abh. Zentr. Geol. Inst. Paläont. Abh*, 26, 199-238.

113.Solereder, H. (1908). *Systematic anatomy of the dicotyledons: a handbook for laboratories of pure and applied Botany* (Vol. 2). Clarendon Press, Scott, Oxford.

114.Sadowski, E. M., Schmidt, A. R., & Kunzmann, L. (2022). The hyperdiverse conifer flora of the Baltic amber forest. *Palaeontographica Abteilung B*, 1-148.

115.Solereder H. 1908b. Systematic anatomy of the Dicotyledons: A handbook for laboratories of pure and applied botany 2. Translated from the original 1899 edition by L.A. Boodle and F.E. Fritsch and revised by D.H. Scott. Clarendon Press, Oxford.

116.Sugimura, Y., & Nitta, I. (2007). Cytological changes during cell wall sac formation in mulberry idioblasts. *Protoplasma*, 231, 123-125.

117.Setoguchi, H., Okazaki, M., & Suga, S. (1989). Calcification in higher plants with special reference to cystoliths. *Origin, evolution, and modern aspects of biomineralization in plants and animals*, 409-418.

118.Sethuramani, A., Soundariya, R., & Dharani, V. (2021). Morpho-Playnological study on *Ficus religiosa* L. Leaves. *Journal of Pharmacognosy and Phytochemistry*, 10(2), 1358-1365.

119.Setoguchi, H., Tobe, H., Ohba, H., & Okazaki, M. (1993). Silicon-accumulating idioblasts in leaves of Cecropiaceae (Urticales). *Journal of Plant Research*, 106(4), 327-335.

120.Scott, F. M. (1946). Cystoliths and plasmodesmata in Beloperone, Ficus, and Boehmeria. *Botanical Gazette*, 107(3), 372-378.

121.Simoneit, B. R. (1986). Characterization of organic constituents in aerosols in relation to their rigin and transport: a review. *International Journal of Environmental Analytical Chemistry*, 23(3), 207-237.

122.Schweitzer, H. J. (2006). Die Oberdevon-Flora der Bäreninsel-5. Gesamtübersicht. *Palaeontographica Abteilung B*, 1-191.

123.Strömberg, C. A., Dunn, R. E., Crifò, C., & Harris, E. B. (2018). Phytoliths in paleoecology: analytical considerations, current use, and future directions. Methods in paleoecology: Reconstructing Cenozoic terrestrial environments and ecological communities, 235-287.

124.Strömberg, C. A., Di Stilio, V. S., & Song, Z. (2016). Functions of phytoliths in vascular plants: an evolutionary perspective. *Functional Ecology*, 30(8), 1286-1297.

125.Tu, T. T. N., Derenne, S., Largeau, C., Mariotti, A., & Bocherens, H. (2003). Comparison of leaf lipids from a fossil ginkgoalean plant and its extant counterpart at two degradation stages: diagenetic and chemotaxonomic implications. *Review of Palaeobotany and Palynology*, 124(1-2), 63-78.

126.Trivedi, P., Nguyen, N., Hykkerud, A. L., Häggman, H., Martinussen, I., Jaakola, L., & Karppinen, K. (2019). Developmental and environmental regulation of cuticular wax biosynthesis in fleshy fruits. *Frontiers in Plant Science*, 10, 431.

127.Tripp, E. A., & Fekadu, M. (2014). Comparative leaf and stem anatomy in selected species of Ruellieae (Acanthaceae) representative of all major lineages. *Kew Bulletin*, 69(4), 1-8.

128.Tait, K., Sayer, J. A., Gharieb, M. M., & Gadd, G. M. (1999). Fungal production of calcium oxalate in leaf litter microcosms. *Soil Biology and Biochemistry*, 31(8), 1189-1192.

129.Volk, G. M., Lynch-Holm, V. J., Kostman, T. A., Goss, L. J., & Franceschi, V. R. (2002). The role of druse and raphide calcium oxalate crystals in tissue calcium regulation in Pistia stratiotes leaves. *Plant Biology*, 4(01), 34-45.

130.Wappler, T., & Engel, M. S. (2003). The middle Eocene bee faunas of Eckfeld and Messel, Germany (Hymenoptera: Apoidea). *Journal of Paleontology*, *77*(5), 908-921.

131.Wappler, T., & Andersen, N. M. O. (2004). Fossil water striders from the Middle Eocene fossil sites of Eckfeld and Messel, Germany (Hemiptera, Gerromorpha). *Paläontologische Zeitschrift*, *78*, 41-52.

132.Wappler, T., & Heiss, E. (2006). Flatbugs from Paleogene limnic sediments. II. Eckfeld maar (Heteroptera: Aradidae). *Mainzer Naturwissenschaftliches Archiv*, *44*, 53-60.

133.Watt, W. M., Morrell, C. K., Smith, D. L., & Steer, M. W. (1987). Cystolith development and structure in Pilea cadierei (Urticaceae). *Annals of Botany*, 60(1), 71-84.

134.Walters, Wendy L. & Griffiths, C. L. (1987). Patterns of distribution, abundance and shell utilization amongst hermit crabs, Diogenes brevirostris. *African Zoology*, 22(4), 269-277.

135.Ward, D., Spiegel, M., & Saltz, D. (1997). Gazelle herbivory and interpopulation differences in calcium oxalate content of leaves of a desert lily. *Journal of Chemical Ecology*, 23(2), 333-346.

136.Worslex, D., Agdestein, T., Gjelberg, J. G., Kirkemo, K., Mørk, A., Nilsson, I., ... & Stemmerik, L. (2001). The geological evolution of Biørnøya, Arctic Norway: implications for the Barents Shelf. *Norwegian Journal of Geology/Norsk Geologisk Forening*, 81(3).

137.Wilde, V. (1989). Untersuchungen zur Systematik der Blattreste aus dem-Mitteleozän der Grube Messel bei Darmstadt (Hessen, Bundesrepublik Deutschland).

138.Winterscheid, H., & Kvaček, Z. (2016). Revision der Flora aus den oberoligozänen Seeablagerungen der Grube „Stößchen "bei Linz am Rhein (Rheinland-Pfalz, Deutschland). Palaeontographica, Abteilung B, 111-151.

139.Weyland, H. (1943). Beiträge zur Kenntnis der Rheinischen Tertiärflora: VI. Vierte Ergänzungen und Berichtigungen zur Flora der Blätterkohle und des Polierschiefers von Rott im Siebengebirge. *Palaeontographica Abteilung B*, 94-136.

140.Weyland, H. (1948). Beiträge zur Kenntnis der Rheinischen Tertiärflora. VII. Fünfte Ergänzungen und Berichtigungen zur Flora der Blätterkohle und des Polierschiefers von Rott im Siebengebirge. *Palaeontographica Abteilung B*, 113-188.

141.Zech, M., Rass, S., Buggle, B., Löscher, M., & Zöller, L. (2012). Reconstruction of the late Quaternary paleoenvironments of the Nussloch loess paleosol sequence, Germany, using n-alkane biomarkers. *Quaternary Research*, 78(2), 226-235.

142.Zakaria, S. M., Amiri, C. N. A. C., Talip, N., Latiff, A., Juhari, A. A. A., Shahari, R., & Rahman, M. R. A. (2020). The variation of cystoliths and its taxonomic significance in Acanthaceae of Peninsular Malaysia. *Malaysian Applied Biology*, 49(5), 25-31.

scientific reports

Check for updates

OPEN

Traces of calcium oxalate biomineralization in fossil leaves from late Oligocene maar deposits from Germany

Mahdieh Malekhosseini[1]✉, Hans-Jürgen Ensikat[2], Victoria E. McCoy[3], Torsten Wappler[4], Maximilian Weigend[2], Lutz Kunzmann[5] & Jes Rust[1]

Calcium oxalate (CaOx) is one of the most common bio-mineral in extant plants and is believed to serve a variety of functions such as calcium storage and herbivore defense. However, traces of CaOx crystals have rarely been identified in fossil plants, and they are primarily known from fossil gymnosperms, where empty cavities of former CaOx crystals or ghost crystals have been reported from leaf cuticles of some Late Cretaceous and Cenozoic conifers. Here we investigate fossil angiosperm leaves from the late Oligocene Rott Fossil Lagerstätte and report ghost crystals of various shapes, sizes and topology (distribution patterns), and cavities. These micromorphological structures of fossil leaves are compared to CaOx deposits in leaves of extant plants: globular structures in fossil leaves resemble CaOx druses (crystal aggregates) in fresh leaves in size and distribution; and angular or brick-shaped structures in the vascular system of fossil leaves closely resemble prismatic CaOx crystals in the vascular system of extant leaves in both size and topology. Chemically, CaOx druses have survived fossilization as cavities only, and were replaced by organic matter and ghost minerals containing Ca, Si, Al, S, and Fe. The identification of former CaOx remains in leaf fossils provides novel insights on the fate of plant bio-minerals during fossilization. More importantly, it provides an additional aspect of the ecophysiology of fossil plants thus improving the accuracy of palaeoecological reconstructions and can provide a broader perspective on the evolution of CaOx and their rule in plant ecology across geological timescales. Alternative interpretations of the fossil microstructures are discussed but ruled out.

Fossil leaves are an important source of palaeontological information and provide both evolutionary and palaeoecological insights[1–3]. Interpretation of fossil leaves can be relatively straightforward based on broad morphological features such as size, shape, leaf margin, and details of leaf veins and cuticle micromorphology, but often, fossil leaf assignments are tentative and may change over time. Additional diagnostic characters would therefore be highly welcome to support or refute fossil identifications. One neglected feature common in plant fossils are granular structures observed on leaf fossils, which have not yet received a satisfactory explanation. In the well-preserved leaf fossils from the Rott Fossil Lagerstätte (North Rhine-Westfalia, Germany) and some related fossil sites from the Oligocene of that region, numerous granular structures are found, which have been variously explained by previous authors as algal colonies, pollen grains, trichome bases, or papillose structures of the leaf epidermis[4,5]. Winterscheid and Kvaček[6,7] and Moers[4] interpreted granular structures on fossil leaves as traces of various algae such as *Botryococcus*, *Tetraedron*, and Chrysophyceae, analogous to similar observations in leaf fossils from the Messel fossil site. Krassilov et al.[8] in their study of 'Late Cretaceous Flora of Southern Negev' present numerous detailed images of fossil leaves which show patterns of granular structures, but these are not discussed in the publication. Generally, no convincing explanation for these rather common granular structures on leaf fossils has been proposed in the literature until now.

[1]Palaeontology Section, Institute of Geosciences, Rheinische Friedrich-Wilhelms Universität Bonn, Nussalle 8, 53115 Bonn, Germany. [2]Nees-Institut für Biodiversität der Pflanzen der Universität Bonn, Meckenheimer Allee 170, 53115 Bonn, Germany. [3]Department of Geosciences, University of Wisconsin-Milwaukee, 3209 N. Maryland Avenue, Milwaukee, WI 53211, USA. [4]Hessisches Landesmuseum Darmstadt, Friedensplatz 1, 64283 Darmstadt, Germany. [5]Senckenberg Naturhistorische Sammlungen Dresden, Königsbrücker Landstraße 159, 01109 Dresden, Germany. ✉email: s6mhmale@uni-bonn.de

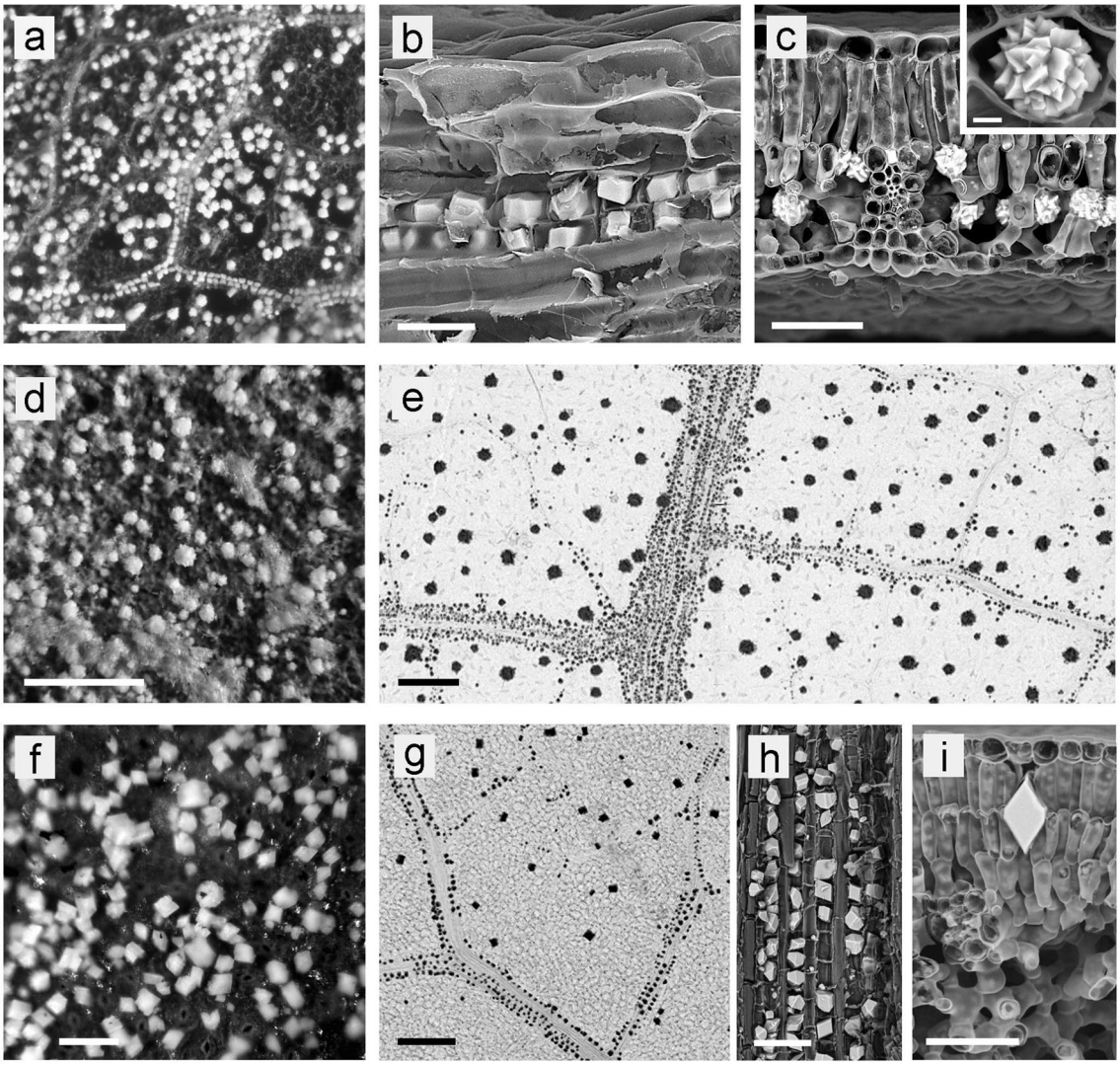

Figure 1. CaOx crystals and druses in leaves of extant plants. (**a**,**d**,**f**) LM images of the ash of carefully incinerated leaves show their distribution in a planar view. (**b**,**c**,**h**,**i**) SEM images of freeze-fractured leaves show crystal and druse morphology in detail. (**e**,**g**) Micro-CT images of CP-dried leaves. (**a**–**c**) *Quercus robur*; high density of druses (15–25 µm) in the areoles and prismatic crystals along the veins. (**d**) *Hedera helix*; leaf densely filled with druses of varying size. (**e**) *Juglans regia*; large druses (50–70 µm) in areoles, and small druses along veins. (**f**) *Prunus laurocerasus*; high density of prismatic crystals (20–30 µm) everywhere. (**g**–**i**) *Parrotia persica;* numerous small crystals along veins and larger crystals in areoles. Scale bars: (**a**,**d**,**e**,**g**) = 200 µm; (**b**) = 20 µm; (**c**,**h**,**i**) = 50 µm; (**f**) = 100 µm; inset in (**c**) = 5 µm.

Many extant plants contain biominerals in various forms, such as mineralized cell walls or mineral particles embedded in tissues[9,10]. The most common forms of plant biominerals are silica bodies (phytoliths)[11], calcium carbonate (cystoliths)[12] and various forms of calcium oxalate: individual crystals, druses (crystal aggregates), or raphide bundles[13,14]. Silica biominerals—phytoliths—have been widely studied[15] and often survive fossilization independent of the surrounding plant tissue, making up microfossil assemblages in their own right[16]. Phytolith analysis therefore has important applications in evolutionary and—especially—archaeological and palaeoecological studies[16–22]. However, the phytolith fossil record is strongly biased towards grasses[16,19]. Calcium carbonate and CaOx are extremely widespread in the plant kingdom and CaOx especially may be found in almost any plant organ or tissue, often specifically in plant groups where silica biomineralization plays a minor role[23–25]. Figure 1 shows a few examples of the variability of the distribution patterns of CaOx druses and crystals in leaves of extant plants, such as *Quercus robur* and *Juglans regia*.

The rich fossil record of silica phytoliths contrasts starkly with the very poor fossil record of calcium biominerals. Despite their ubiquity and importance in extant plants calcium biominerals have rarely been reported from the fossil record[26–29]. This is likely due to the limited chemical stability of both calcium-based biominerals. Calcium carbonate (e.g., cystoliths) is soluble even in the weakest acids, including CO_2-saturated water, and is therefore unlikely to survive fossilization[30,31]. CaOx itself is less soluble[32,33], but may be gradually oxidized to calcium carbonate during fossilization, which is subsequently lost from the fossil record. Even if calcium

biominerals survive fossilization itself, they are likely to be dissolved during fossilization, which is designed for the extraction of the much more robust silica phytoliths[29].

Calcium biominerals themselves are thus usually not preserved in the fossil record, but casts ("crystal cavities") have long been known from the cuticles of fossil conifer leaves[34]. These casts are interpreted as impressions of CaOx crystals in the leaf epidermis as known from extant conifers[35]. These crystal cavities are also used as a minor diagnostic character for conifer taxa such as *Doliostrobus* and *Quasisequoia*[36,37]. Such crystal cavities have been reported from fossils from the Late Cretaceous (e.g., *Quasiseqoia florinii*)[36], Oligocene (*Glyptostrobus europaeus*)[6], Paleogene (e.g., *Doliostrobus taxiformis*)[37,38] and Neogene (e.g., *Cupressospermum saxonicum*)[39]. The occurrence, distribution (adaxial and abaxial leaf surfaces as well as in the mesophyll) and abundance of crystal cavities varies within fossil-species. It has been proposed that this variability in fossils of *Doliostrobus taxiformis* from the Eocene and Oligocene in Europe can be attributed to palaeoecological factors such as habitat and climate[36,37], but no conclusive evidence has been presented for this assumption. Despite the wealth of angiosperm fossils and the prevalence of bio-minerals in their extant representatives, we are not aware of any reports of "crystal cavities" in angiosperm fossils. We thus observe an odd contrast between calcium biominerals as a common feature of extant angiosperms and the lack of any evidence for these biominerals in the fossil record. On the other hand, there are reports of leaf fossils in which obscure granular structures abound. The present study addresses the question of whether these granular structures correspond to calcium-based biominerals (CaOx crystals and druses, and calcium carbonate grains) or most likely to ghost crystals following the calcium-based biominerals in extant taxa. According to[40] [page 761] the term crystal ghosts is original defined as a globular assembly of numerous needle-shaped mineral crystals that are organic. In the case presented in the current article, we have CaOx crystals or druses, which left a crystal cavity after they disappeared (e.g. by dissolution) and then were refilled by sediments or organic or mineral crystals (the ghosts).

We therefore re-examine fossil angiosperm leaves from Rott for a better characterization and convincing interpretation of the granular structures. The Rott fossil site is located near Bonn, south of Hennef (Sieg) in the Rhein-Sieg Kreis, North-Rhine-Westfalia, Germany. It is a limnic sedimentary deposit from a freshwater maar lake, famous for its diverse and exceptionally well-preserved plant and animal fossils in the leafy coal beds, diatomite and silica slates of the Rott Formation[5,41,42]. Therefore, it is acknowledged as a fossil lagerstätte[42]. The Rott Formation is dated to Mammal Paleogene zone MP30, which is assigned to the Chattian, uppermost Oligocene (appr. 23 to 24 ma)[4].

In order to elucidate the identity of the granular structures on fossil leaves, we investigate the fine-scale patterns on fossil leaves and compare them to patterns of CaOx biomineralization of extant plant taxa. Scanning electron microscopy (SEM) and energy dispersive X-ray (EDX) element analyses are used to investigate details of fossil and extant plant materials. Our study specifically aims at answering the following questions:

(1) Do these granules in fossil leaves correspond in shape and location to CaOx druses in modern leaves? (2) Can alternative explanations for the granular structures, e.g., imprints and/or casts of pollen, peltate trichomes, trichome bases, or stomata, be ruled out? (3) Which chemical and biochemical processes affected the leaves containing CaOx during the fossilization? (4) What micromorphological changes happened during fossilization?

Materials and methods

In the current study, 1120 fossil leaf specimens of the Rott fossil site were examined with a stereomicroscope. All samples are from the collection of the late Heinrich Winterscheid, which is kept in the Goldfuß Museum in the Institute of Geosciences, University of Bonn, Germany. The taxonomic assignments of the fossils derive from the works of H. Weyland between 1934 and 1948[4]. Obvious granular structures were visible on the surface of 64 specimens, which were subject of further detailed examinations. In addition to the partially damaged and contaminated specimen surfaces, we examined freshly split charcoal samples, which could be separated from the fossil block with adhesive tape.

Fresh leaf samples from extant species were collected from the Bonn University Botanic Gardens, Germany. The following species appear in this study: *Carya ovata* (accession 14964, Herbarium T. Jossberger 2406); *Ginkgo biloba* (accession 1894, T. Jossberger 183); *Hedera helix* (accession 8757); *Juglans regia ssp. regia* (accession 9662, T. Jossberger 2418); *Nelumbo nucifera* ssp. *nucifera* (accession 1074, T. Jossberger 2155); *Nymphaea lotus* (accession 41078); *Parrotia persica* (accession 12241, T. Jossberger 534); *Prunus laurocerasus* (accession 34457); *Quercus robur* (accession 1887); *Quercus variabilis* (accession 35458); *Salix miyabeana* (accession 35019, T. Jossberger 2474); *Sideroxylon reclinatum* (accession 34392). Fully developed late-season leaves from adult trees, shrubs and a few aquatic plants were collected in summer and autumn, when CaOx deposits are fully formed (S1). The selection included species or genera closely related to those identified in fossils with granular structures, and additionally some randomly selected deciduous woody species. In total, leaves of more than 50 living species were examined (see Supplementary Table online).

Microscopy. A stereomicroscope Leica MZ125 (Leica Microsystems, Wetzlar, Germany) was used for selection of samples and examination at low magnification. Detailed light microscopy (LM) was performed with a standard light microscope (Müller optronic, Erfurt, Germany) with large sample stage. Long distance objectives enabled flexible surface illumination with a LED light source. Both microscopes were used with a Swift SC1803 microscope camera (Swift Optical Instruments, Schertz, Texas, US) with 18-megapixel resolution. A Lumix DMC-G70 photo-camera (Panasonic Corporation, Osaka, Japan) with Lumix macro-objective was used for close-up images.

Scanning electron microscopy (SEM) was performed with a LEO 1450 SEM (Cambridge Instruments, Cambridge, UK), equipped with secondary electron (SE) and backscattered electron (BSE) detectors and an EDX element analysis system with Link ISIS software (www.oxford-instruments.com). X-ray images and micro-computer

tomography (µ-CT) scans of dry leaves were obtained with a SkyScan 1272 Micro-CT system (Bruker microCT, Kontich, Belgium) in the Institute of Evolutionary Biology and Ecology at the University of Bonn. The images were recorded with a detector of 4032 × 3280 pixels with a pixel size of 1 µm. Visualisation of the µ-CT data was performed with ImageJ-Fiji software (https://imagej.net/software/fiji/).

Specimen preparation. Fossil samples were cleaned to remove dust, if necessary, with an air-blower or through careful rinsing with distilled water. For SEM examination, small representative pieces were selected, mounted on a sample holder, and sputter-coated with a thin layer (10–15 nm) of palladium. Palladium, in contrast to gold, does not disturb the EDX analyses of relevant elements such as silicon and sulphur, and this thin layer is sufficiently transparent for high-energetic electrons necessary for compositional-contrast BSE imaging.

Fresh leaves were examined to investigate the total amount and distribution of CaOx druses and crystals in a variety of species. Most leaves are not transparent enough to visualize the crystals directly and need to be subjected to a clearing procedure. We found a very simple procedure particularly useful: pieces of the leaves were simply burnt until the organic matter was largely oxidized, reducing the leaf to a brittle piece of ash. For this purpose, fresh or dry leaves were incinerated in a temperature-controlled oven (Brennofen Uhlig U15, Efco GmbH, Rohrbach, Germany) at 600–650 °C. The samples turned white after 5–10 min. In many cases, simple burning over a gas burner was also successful and much faster. Usually, the CaOx structures could be easily visualized directly in the ashes using the stereomicroscope or standard LM. If the ash remnants from the epidermal layers were too thick and not transparent enough, we separated the upper and lower halves of the burnt leaf with transparent adhesive tape such as Tesafilm (Tesa SE, Norderstedt, Germany) and attached each half to a glass slide. Observing the inner side of each half showed the majority of the druses and crystals.

Standard preparation of fresh leaves for SEM and µ-CT: Pieces of fresh leaves were fixed in 70% v/v ethanol + 4% v/v formaldehyde in water for at least 20 h and dehydrated with ethanol. For freeze-fracturing, ethanol-infiltrated samples were immersed in liquid nitrogen and broken randomly. After unfreezing, all samples were critical-point dried (CPD 020, Balzers Union, Liechtenstein) and mounted on sample holders for SEM or µ-CT.

Plant collection statements. All plant samples collected in this study were taken from species cultivated in the Botanical Garden, University of Bonn. This sample collection complies with relevant institutional, national, and international guidelines and legislation.

Results

Fossil leaves. A first examination with a stereomicroscope showed at least 64 samples with obvious granular structures in a total of 1,120 fossil leaf specimens. (Figs. 2a,c, 3a–f). The structures appeared as globular or lobed particles with maximum diameters of 25–70 µm. Most striking were globules, spherical structures of yellow or brown colour with a smooth surface. Several samples contained black structures of irregular or angular shape. Many more samples may have had such granular structures, but they were not sufficiently well preserved for further investigation, or the granules were too small for reliable identification. Some examples of poorly preserved fossils, where recognition of the granules is difficult, are presented in Supplementary Figure S1 online.

Our fossil samples were mostly from diatomite (German term ‚Polierschiefer'), a bright material rich in silica skeletons of algae, or laminated bituminous shale (leafy coal bed)[42], a dark brown organic material. Many leaf remnants were very thin as most of the organic material has been lost during fossilization; others consisted of thicker dark-brown layers being coalified remains called compressions[42]. While the old surfaces of the fossils were severely contaminated and damaged, freshly cleaved planes of some leaf coal samples showed their structures in detail. Some specimens showed a distinct pattern of empty cavities with diameters up to 50 µm, which resembled the distribution of CaOx druses in fresh leaves (Table 1). Even small cavities of less than 10 µm were clearly visible.

CaOx in fresh leaves. We examined numerous fresh leaves from extant species searching for a correlation of the granular structures in the fossils with structures in living plants. Most of the extant leaves of trees and perennial shrubs contained CaOx druses (crystal aggregates) and individual crystals of varying sizes and distribution densities; Fig. 1 illustrates some of the patterns. Druses have a spherical shape (not elongated) and may be compact with a serrated surface, or with emerging sharp crystal tips. Small individual crystals are often found along veins; solitary crystals in the mesophyll can reach sizes up to 100 µm.

Appropriate methods for determining the density of druses are required for a detailed correlation. Light microscopic (LM) examination of the ash of burnt leaf pieces is particularly useful and allows even small crystals clearly imaged. X-ray imaging and µ-CT are effective techniques for assessing the druses and crystals without any preparation artefacts (Fig. 1e,h).

The size and distribution of the larger druses of various species match the sizes and distribution patterns observed for the fossil granules (see Supplementary Table S1 online). Typically, e.g., in *Quercus* leaves, globular CaOx druses (crystal aggregates) occur preferentially in the areoles whereas CaOx crystals (single or twinned prismatic crystals) are associated with the leaf veins (Fig. 1a–c). Other species contain in areoles and veins only druses (e.g., *Hedera helix*, Fig. 1d; *Juglans regia*, Fig. 1e) or only crystals (*Parrotia persica,* Fig. 1g–i), thus details of the crystal type, size, and morphology are quite variable (Table 2; Supplementary Table S1 online). Quite large druses with diameters of 40–80 µm were found in some *Quercus* species and in Juglandaceae (*Juglans regia, Carya ovata*)—genera which have been reported from the Rott fossil flora—and in *Ginkgo biloba* (Table 2).

Morphology of the granular structures in fossil leaves in leafy coal beds and diatomites. Under a binocular microscope, globular particles and venation patterns were clearly visible on many of the selected fos-

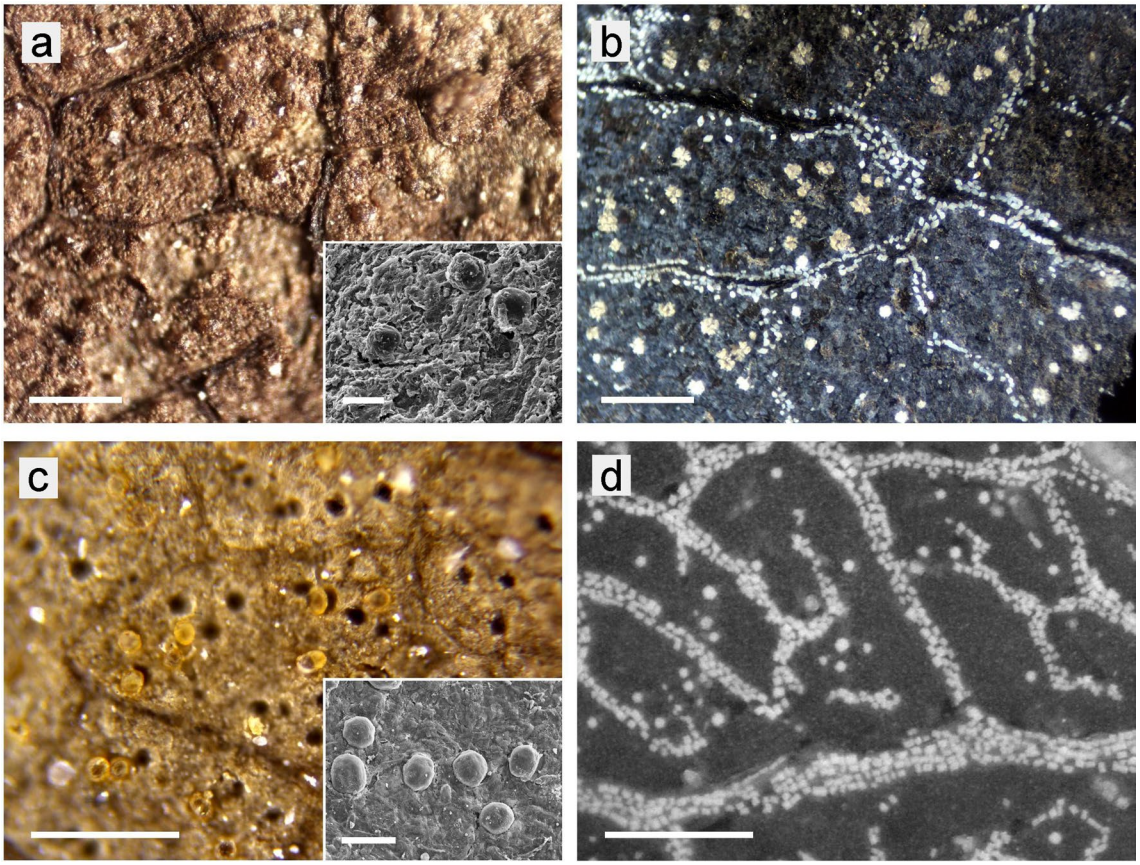

Figure 2. Globular structures in fossil leaves in comparison with CaOx druses of fresh leaves. LM images; surface illumination, 10 × objective. (**a**) Fossil sample Ro-90_1 (*Quercus neriifolia*) with large brown globules; the inserted SEM image shows globules in detail. (**b**) druses of various size and small crystals in a burnt leaf of *Quercus variabilis*. (**c**) Fossil sample Ro-100_5 (*Salix longa*) with yellow transparent globules and many empty cavities, which remained when globules were pulled out during splitting the fossil. (**d**) Druses and crystals in a burnt leaf of *Salix miyabeana*. Scale bars: (**a**–**d**) = 200 µm; insets (**a**,**c**) = 40 µm.

sil leaf samples. The sizes of the particles, typically 20–40 µm, match well the sizes of CaOx druses in leaves of extant species, as demonstrated in Fig. 2 with the fossil samples Ro-90_1 (assigned to *Quercus neriifolia*) and Ro-100_5 (*Salix longa*) (Fig. 2a,c) in comparison with leaves from extant *Quercus* and *Salix* species (Fig. 2b,d). However, sizes of up to 100 µm were found for globules in other fossil samples, as well as for CaOx druses of certain extant species (Table 2).

Figure 3 shows various distinctive patterns of granular structures in Rott fossils that are apparent in LM and SEM images. Yellow-to-brown globules in areoles between brown leaf veins (Fig. 3a) are clearly visible contrasting in colour against white background of diatomitic sediment in fossil no. 'Ro-2.2' ('*Sideroxylon salicites*'). Compositional contrast (BSE) SEM image (Fig. 3b) shows fragmented granules embedded in sediment, indicating they differ in chemical compositions. Dark appearance of granules in the SEM image indicates they are organic material, whereas background sediment is a mix of organic and mineral (bright) components.

In several leafy coal bed-based samples like 'Ro-110.6' ('Magnoliopsida'), brown globules, which were on brown organic background between dark brown veins, were more difficult to recognise and distinguish from background by LM due to low colour contrast. Lateral illumination made them more easily visible because most of the globules projected above the level of surrounding leaf area. Globules and a corresponding number of cavities were present in cleaved samples. In 'Ro-110.6' (Fig. 3c) globules were evenly dispersed across leaf surface, as often observed in fresh leaves. Brick-like structures in veins appear similar to CaOx crystal patterns along the veins of fresh leaves (Fig. 3d). Sizes of the globular structures may be either variable, as in 'Ro-2.2' (Fig. 3a), or nearly uniform. Both variable and uniform sizes were also found as common patterns in CaOx druses in fresh plant leaves; e.g., in *Hedera helix*.

Black serrated particles on a mineral background occur on the whole surface of a large leaf on specimen 'Ro-13.3' ('*Nymphaea nymphaeoides*') (Fig. 3e,f) and also on some other specimens [Ro-106.1 ('*Nyssa rottensis*', Ro-58.5 ('*Zizyphus zizyphoides*')]. The size and shape of the serrated granules resemble CaOx druses which are found in many fresh leaves. Smaller yellow globules between the black granules are difficult to recognise under the LM due to low contrast and also by SEM due to the heterogeneous structure of the surrounding area.

Freshly cleaved areas of the leafy coal bed sample 'Ro-59.9' (Fig. 3g,h) showed numerous empty cavities which resembled CaOx druses of fresh leaves in size and distribution. The polygonal shape corresponds to the angular

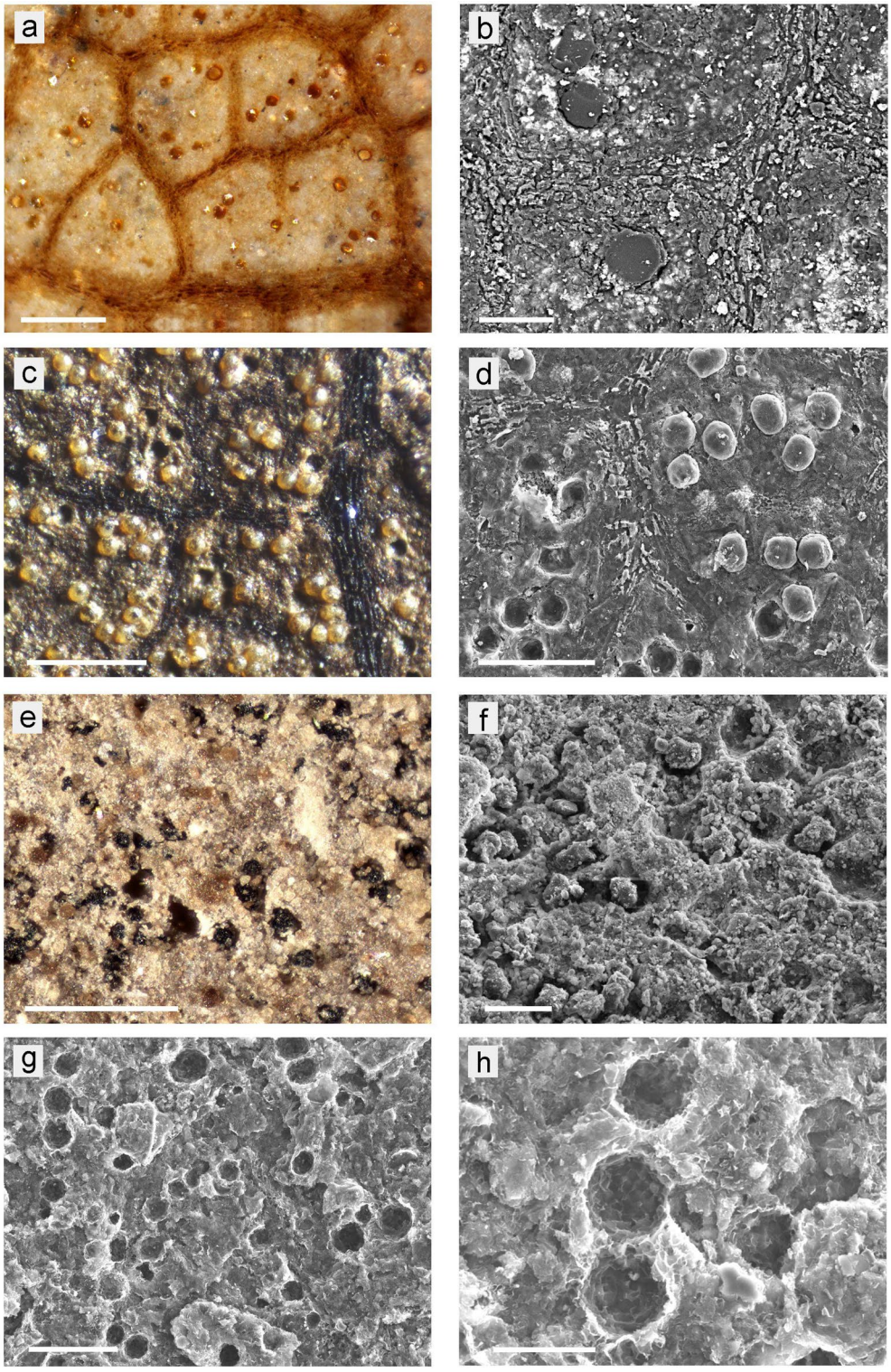

Figure 3. Granular structures in various leaf fossil samples. (**a**,**c**,**e**) LM images; surface illumination, 10 × objective; (**b**,**d**,**f**,**g**,**h**) SEM images. (**a**,**b**) Sample 'Ro-2.2' ('*Sideroxylon salicites*'); the LM image (**a**) shows leaf veins and yellow to brown globules of varying sizes embedded in a bright mineral sediment matrix; in the compositional contrast (BSE) SEM image (**b**), the fragmented globules appear dark, indicating organic material; minerals appear bright. (**c**,**d**) Sample 'Ro-110.6' ('Magnoliopsida'); globules (not fragmented) and holes indicate weak adhesion to the surrounding sediment. Brick-like structures in leaf veins resemble crystals in fresh leaves. (**e**,**f**) Sample 'Ro-13.3' ('*Nymphaea nymphaeoides*'); LM image shows black serrated particles and (difficult to see) smaller yellow globules. The SEM images shows empty space around granules, perhaps a result of shrinkage. (**g**,**h**) Freshly cleaved area of the leaf coal sample Ro-59.9; numerous empty cavities of various size, up to 30 µm, are distributed evenly. The detail image (**h**) illustrates the angular shape of the cavities which resemble casts of CaOx druses. Scale bars: (**a**,**c**,**e**) = 200 µm; (**b**,**f**,**g**) = 50 µm; (**d**) = 100 µm; (**h**) = 20 µm.

Fossil sample	Selected fossil samples with traces of CaOx druses				
	Assignment	Type of traces	Size (µm)	Composition	References
Ro-90.1	*Quercus neriifolia*	Globules, brown	40–50	Organic	Figure 2
Ro-100.5	*Salix longa*	Globules, yellow	30–35	Organic	Figure 2
Ro-2.2	*Sideroxylon salicites*	Globules, brown	30–40	Organic	Figures 3, 4
Ro-110.6	*Magnoliopsida*	Globules, yellow	ca. 30	Organic	Figures 3, 4
Ro-13.3	*Nymphaea nymphaeoides*	Globules, yellow	20–25	Organic	Figures 3, 5
		Granules, black	45–55	Mineral + org	
Ro-59.9	*n.n*	Empty cavities	15–25		Figures 3, 6
Ro-58.5	*Zizyphus zizyphoides*	Granules, black	40–50	Mineral	Figure 7
		Globules, yellow	90–100	Organic	
Ro-4.4	*Acer integrilobum*	Globules (pollen?)	ca. 60		Figure 7
Ro-2.2	(2nd leaf fragment)	Angular particles, black	12–20	Mineral	Figure 7
Ro-101.6	*Zizyphus paradisiaca*	Granules, black	75–80	Mineral	Suppl. Fig. S1

Table 1. List of selected fossil samples with granular structures (traces of CaOx druses).

Species	Characterization of CaOx in fresh leaves					
	CaOx in areoles			CaOx along veins		
	Type	Size (µm)	Abundance	Type	Size (µm)	Abundance
Carya ovata	Druses	35–50	4	Druses	10–20	5
Ginkgo biloba	Large druses	60–100	2	Druses	60–100	4
Hedera helix	Druses	25	5	Druses	10	3
Juglans regia	Druses	20–55	4	Druses	10	4
Nelumbo nucifera	Druses	25–30	3	n. d.		
Nymphaea lotus	Small crystals	2–3	2	None		
Parrotia persica	Crystals	40–75	2	Crystals	10	3
Prunus laurocerasus	Crystals	25–30	5	Crystals	15–20	2
Quercus robur	Druses	15–20	5	Crystals	10–15	4
Quercus variabilis	Druses (large/small)	45; 20	4	Crystals	15–20	4
Salix miyabeana	druses	15–20	3	Crystals	7–10	4
Sideroxylon reclinatum	crystals	20–25	3	Crystals	20	2

Table 2. Distribution pattern, size and abundance of calcium oxalate (CaOx) crystals and druses in leaves of extant species presented in this study. Abundance of the CaOx bodies is indicated with numbers. 1 = occasional or not clearly apparent; 2 = few; 3 = regular but not many; 4 = many; 5 = densely.

surface of druses, whereas the smooth surface of the organic globules (Fig. 3c,d) seems to be caused by their shrinkage. The variation in size, up to 30 µm, is remarkable and corresponds to extant druses. On such clean specimens, cavities of less than 10 µm diameter can be clearly recognised.

Compositional analyses of granules in leaf fossils. EDX element analyses of selected fossil samples were conducted with an SEM (Figs. 4, 5). In the mineral-based sample 'Ro-2.2' ('*Sideroxylon salicites*') (Fig. 4a–c) the globules appear dark in the BSE image (Spot 1), whereas mineral ghost inclusions in the leaf and the mineral background appear bright. EDX spectra show that the globules are organic and contain mainly carbon (C) with a little oxygen (O) and sulphur (S). The mineral background consists of silica (SiO_2). Calcium was not found.

The globules in the brown-coal based sample 'Ro-110.6' ('Magnoliopsida') (Fig. 4d–f) consisted of organic material, composed mainly of C with a little O and S, but they were accompanied by calcium sulphate (Ca, S, O), which surrounded many of the organic globules like a shell with a serrated surface. Small amounts of silicon (Si) and iron (Fe) occurred in the background brown-coal material.

The mineral sample 'Ro-13.3' ('*Nymphaea nymphaeoides*') (Figs. 3e–f, 5) had serrated black granules, marginally smaller than the corresponding cavities in the sediment, and smaller yellow-to-brown spherical globules. The red colour in Fig. 5a indicates a high Si content in the surrounding sediment; the BSE image (Fig. 5b) illustrates the opal-like structure consisting of fine spherical silica particles. EDX spectra (Fig. 5c) revealed that the small globules (Spot 2) were organic material (mainly composed of C), the black granules (Spot 1) contained mainly C, O, Fe, and S, and the mineral background was silica (Si, O). The small spherical organic globules are difficult to recognize between other organic structures, but they are also visible in LM as distinct structures (see Fig. 3e).

Other samples: Globules with a size of 30–70 µm were the most obvious type and relatively abundant. Some samples had much smaller globules with less characteristic shape (e.g., Ro-110.27), but their size and density

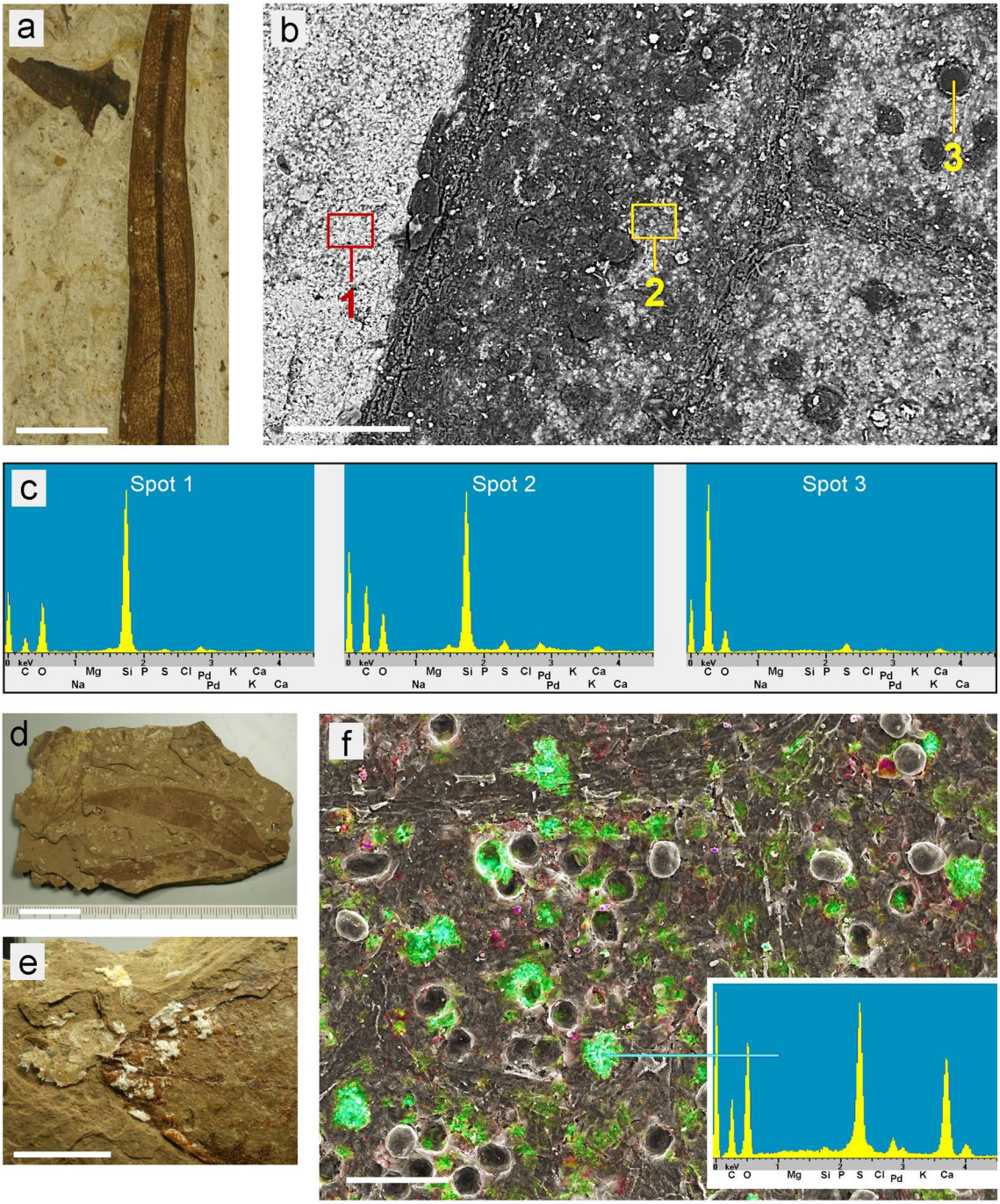

Figure 4. Analyses of samples with globules. (**a**–**c**) 'Ro-2.2' ('*Sideroxylon salicites*'). (**a**) Overview photo of the brown leaf embedded in white mineral. (**b**) Compositional contrast (BSE) SEM image showing organic leaf material dark, background mineral (left part) bright, and ghost mineral inclusions in the leaf area (bright). The fractured globules (e.g., Spot 3) appear dark, indicating organic material. (**c**) EDX spectra show the composition of background sediment (Spot 1; mainly Si and O), the leaf area 'Spot 2' (Si, C, O, and traces of S and Al), and globules (Spot 3; mainly C with little O and S). (**d**–**f**) 'Ro-110.6' ('Magnoliopsida'). (**d**,**e**) Overview photos showing the leaf embedded in coal. (**f**) Combined SEM topographic contrast and element-mapping image showing Ca in green and Si in red; organic structures are in grey scales. The EDX spectrum in the box shows the co-localization of Ca, S, and O as calcium sulphate ($CaSO_4$). Globules are organic (C and little O). Many cavities contain a shell of $CaSO_4$ which had surrounded the globules which have been torn out of the coal matrix. Calcium sulphate occurred also on other parts of the sample in form of gypsum deposits (**e**). Scale bars: (**a**,**e**) = 5 mm; (**b**,**f**) = 100 µm; (**d**) = 20 mm.

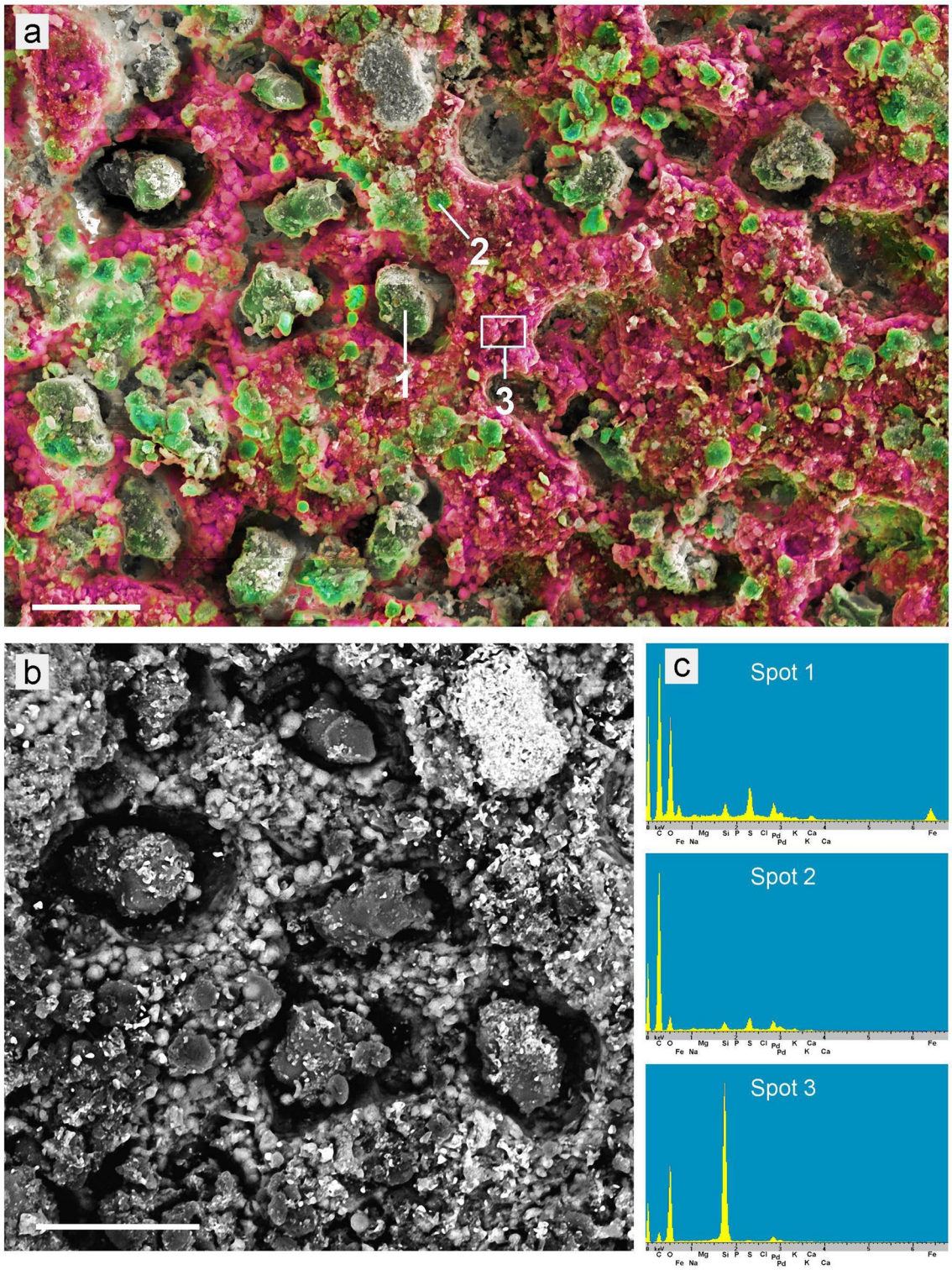

Figure 5. Element distribution in the fossil sample 'Ro-13.3' ('*Nymphaea nymphaeoides*'). (**a**) Combined SEM topographic contrast and element-mapping image showing Si in red and C in green colours. Small globules of organic material (e.g., Spot 2) are difficult to recognise between other organic particles. (**b**) Detailed BSE image of a section of (**a**) illustrating the grainy opal-like structure of the background sediment. (**c**) EDX spectra show the composition of black granules (Spot 1: C, O, Fe, S), small globules (Spot 2: mainly C), and background sediment (Spot 3: Si, O). Scale bars: (**a**,**b**) = 40 µm.

are in accordance with similar patterns of CaOx druses in certain fresh leaves such as *Prunus laurocerasus, Sideroxylon reclinatum* (Table 2).

The analyses demonstrate that the granular structures in the leaf fossils do not currently consist of calcium oxalate. This is the result of the decomposition of the original biomineral, leaving behind cavities which subsequently filled with organic or inorganic material. These ghost minerals roughly replicating the shape of original biomineral. Spherical globules were found to be purely organic, whereas serrated globules contained minerals; Fe and S were usually found in black particles.

Discussion

The present study illustrates the distribution, micromorphology and elemental composition of granular structures in fossil leaves and compares them to those of CaOx druses and crystals in extant leaves. We provide a brief review of a possible fossilization scenario of the leaves that could lead to the formation of the brownish granular structures in fossil leaves (Fig. 6). Leaves of terrestrial plants and freshwater plants sank into the anoxic depths of a maar lake and were preserved in different sediments. During fossilization, parts of the organic material decomposed; any remnants are compressed. Vasculature with its lignified cellular walls, cutinized peripheral walls and mineral inclusions is more likely to be preserved. During fossilization, CaOx will eventually decompose or dissolve. If the sediments are already consolidated and sufficiently hardened, then the disappearance of the druses and crystals will leave cavities which—depending on local conditions—will be filled either with organic or inorganic ghost minerals. Deposition of very fine material such as amorphous silica may form replicas which resemble the former CaOx crystals (ghost crystals, see Fig. 5). In an inorganic mineralogical system these replicas would be called pseudomorphs.

The mostly spherical shape of the globules requires an explanation, since CaOx crystals even in druses are usually polygonal and very angular structures. We propose that the spherical shape of the organic globules results from shrinkage of the casts. Organic material, which has filled the voids, is unlikely to be perfectly stable. It may lose material and shrink, and, as it is a highly viscous resin-like material, its surface tension in the wet environment may force it into the spherical shape. The shrinkage also explains why the organic globules easily become detached from the surrounding sediment, leaving spherical cavities at their positions in the separated fossil samples. Further shrinkage and dissolution of the organic inclusions leaves voids which may be finally filled by inorganic ghost minerals from the environment, resulting in the black ferruginous particles or in the calcium sulphate shell observed around some of the organic globules.

Granular structures like the ones here studied have been previously reported from fossil plants and have been variously interpreted as pollen(clumps), algal colonies, trichomes and trichome bases[5], or 'subcrustations, preserving epidermal structures'[8]. The study of Krassilov et al.[8] on the 'Late Cretaceous Flora of Southern Negev' includes a wealth of excellent images of fossils; many of them show patterns of granules which resemble the granules here studied, but the authors do not provide an explanation for the structures.

The globular structures in our samples were mostly found within the boundaries of the leaf fossils, but occasionally also in the surrounding sediment (Fig. 7a,b). The latter might indicate an extraneous origin—e.g., the presence of pollen—rather than an integral component of the leaf such as CaOx crystals. However, we propose that CaOx druses in decomposing plant remains can be partly dislocated, e.g., by water movement. Druses in leaves occur in different conditions; some are enclosed by massive cell walls whereas others are almost free and only weakly connected to cellular structures (Fig. 7g). The weakly connected druses may easily become dislocated from tissue during decomposition[43]. Thus, their traces might be found outside the leaves in the sediment. Pollen and algae may be found in fossil samples, and the fossilized plants from Rott have been described as 'rich in pollen'[4,44,45]. A detailed study of the distribution of the granular structures shows that in many of our samples, such as Ro-2.2 ('*Sideroxylon*') (Fig. 7c–e), the distribution of granules is highly regular. This indicates that the structures were an integral part of the leaf, since pollen would be expected to be randomly distributed on and around the leaf. Two large leaves of one type in Fig. 7c,d show a similar distribution of globules to each other, whereas a different type of leaf on the same specimen (Fig. 7c,e) has both a different type of fossil particles (smaller, black) and a different distribution. No globules were found in the mineral sediment surrounding the leaves of this specimen, clearly indicating that the granular structures are part of the fossils proper and also that both size and distribution may be characteristic for the two different types of leaf here preserved. Various leaf structures, such as peltate trichomes, trichome bases, or calcium carbonate cystoliths, may also cause visible traces in fossilized leaves. However, extant relative plants of most of the assumed fossil-species from Rott bear very few peltate trichomes on their leaves and no cystoliths. The distribution pattern of trichomes—if present—on leaves differs clearly from the distribution of the granules in fossils: most trichomes are located on the abaxial leaf side on the veins; trichomes on the adaxial side usually occur singly in the areoles between veins, but not in such a high density.

Of course, a careful and critical examination of the fossils is generally necessary to avoid misinterpretations. Some indications are helpful to identify granular structures as traces of former druses: their spherical shape, their occurrence in the remnants of the parenchym, and the regular distribution within the leaf, which resembles that of druses in fresh leaves. In case of the Rott Fossil Lagerstätte it seems to be very unlikely that the cavities filled with granules are originated by soft-tissue remains such as paltate trichomes or pollen clumps. If such structures are preserved as impressions in fine-grained sediments like leafy coal beds any additional micromorphological structures should be visible, e.g., pollen clumps: individual grains of pollen clumps, wall structure and aperture of pollen grains; cell structure, bases and glands of peltate trichomes. None of these features have been recognized by our observations.

Fossilization conditions in the former 'Rott Lake' were major factors for the decomposition of the organic plant material and the formation of fine-grained or amorphous inorganic deposits in the sediments including

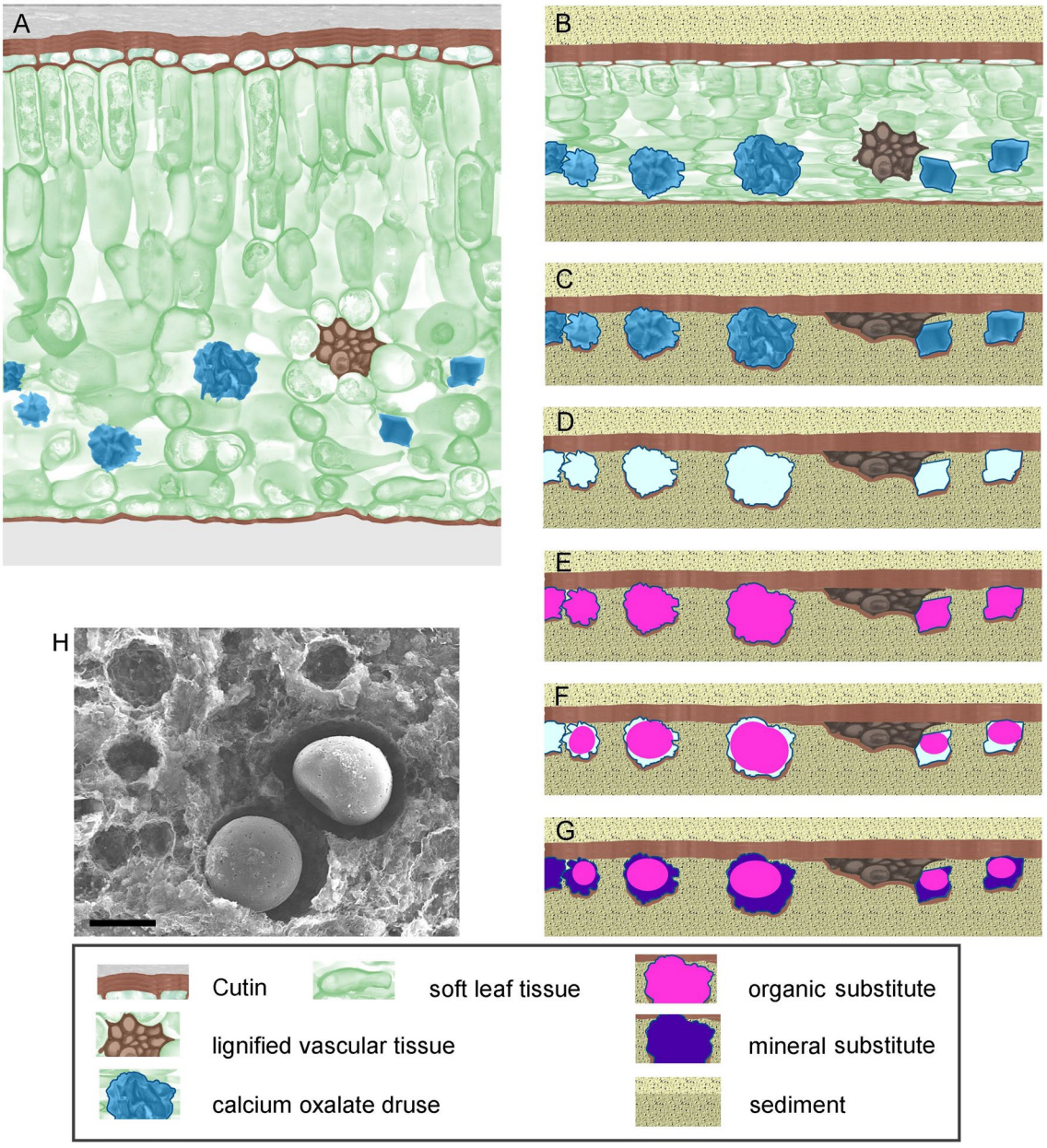

Figure 6. Model of the fossilization processes that lead to the formation of globular and serrate replications of CaOx crystals and druses. (**A**) Distribution of CaOx and other structures in a fresh leaf. (**B**–**G**) Fossilization steps. (**B**) Covering with sediment; compression, loss of water; (**C**) Decomposition of soft organic tissue material; (**D**) Dissolution of CaOx forms voids; (**E**) Voids are filled with organic matter, perhaps cutin components; (**F**,**G**) partial shrinkage of organic material forms globules due to surface tension; new voids formed by shrinkage are filled with ghost mineral components. (**H**) SEM image of a freshly cleaved plane of leaf coal sample Ro-59.9 (see Fig. 3g–h). Larger cavities contain shrunken remnants of organic material, whereas smaller cavities are empty. Scale bar = 20 µm.

the elements Si, Al, Fe, S, and sulphate ions[4]. Anaerobic conditions, indicated by the presence of pyrite, may have inhibited the oxidation of calcium oxalate to carbonate, thereby facilitating preservation.

The presence of calcium oxalate druses or crystals and their distribution patterns as well as their fossil traces may be utilized as additional useful micromorphological features for the identification of fossil plant taxa in the future, if more records are available and if these records can be unambiguously related to extant taxa. Pattern, shapes and sizes of CaOx traces could be particularly helpful if leaf cuticles are not preserved. Angiosperms show a great variability of biomineralization patterns including CaOx, particularly dicotyledons contain almost all forms of CaOx druses and crystals. Some families of monocotyledons (e.g., Araceae, Arecaceae) contain CaOx raphide bundles, others such as Poaceae (grasses) are usually mineralized with silica but not with CaOx. In Gymnosperms, CaOx occurs in different forms: Conifers usually contain small crystals (< 10 µm) on the surfaces

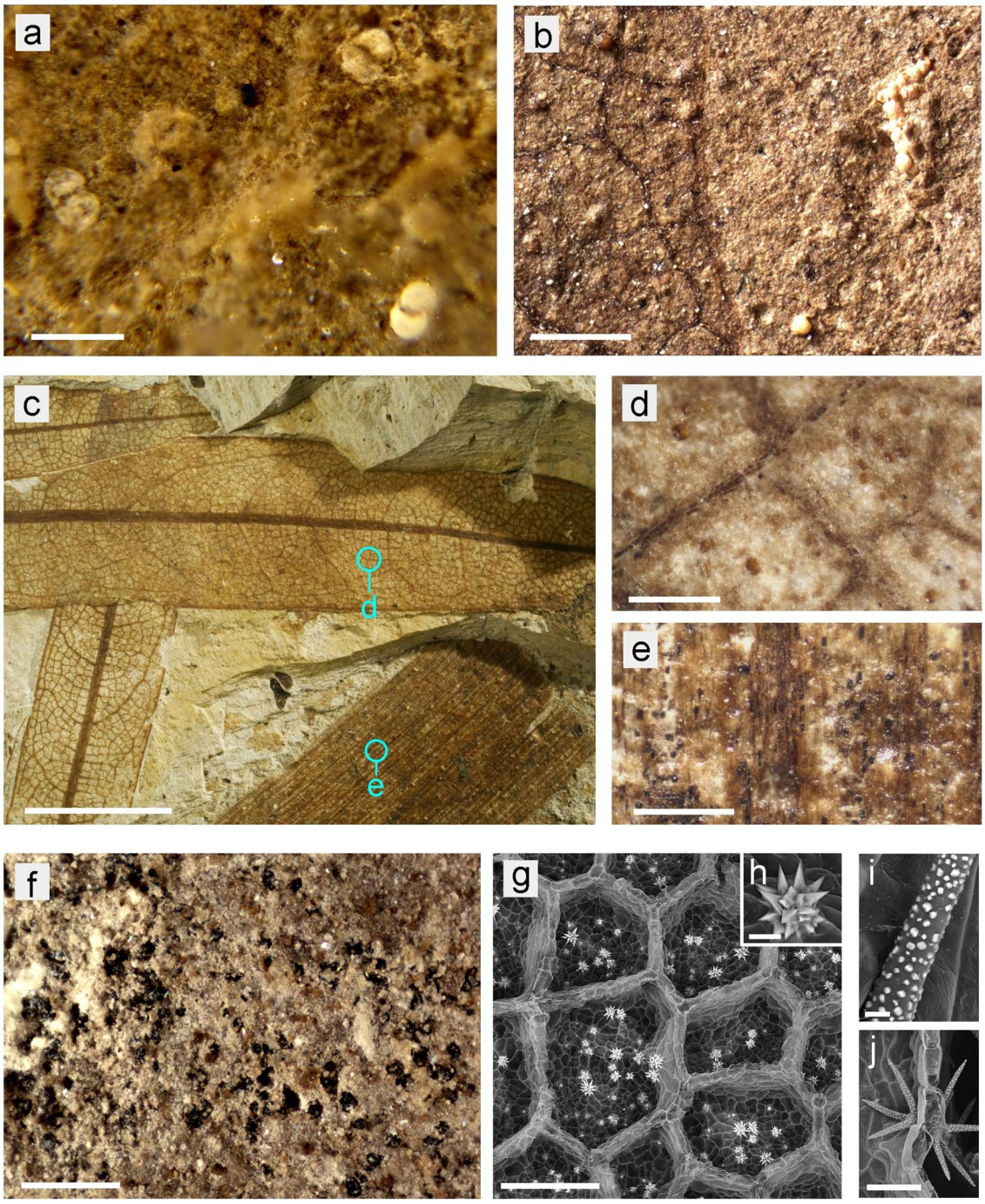

Figure 7. Topics for Discussion: (**a**–**e**) Differentiation between traces of druses and pollen. LM image of Sample Ro-58.5 ('*Zizyphus zizyphoides*') with pollen-like structures randomly distributed. Their shape resemble conifer pollen. (b) Sample Ro-4.4 ('*Acer integrilobum*'); the globules of ca. 100 µm diameter, distributed on (left side) and beside (right side) leaf area may be pollen. (**c**–**e**) Sample Ro-2.2 ('*Sideroxylon*') with different leaves. The larger ones contain globules of different size (**d**), the other one small black particles (**e**), no globules were found in the mineral sediment. Such patterns cannot originate from pollen. (**f**–**j**) Uncertainty in the identification of leaf fossils. (**f**) LM image of sample Ro-13.3, which has been assigned to '*Nymphaea nymphaeoides*', shows black granules. (**g**–**h**) SEM images of a fresh leaf of *Nelumbo nucifera* (Lotus) show CaOx druses in similar distribution and size as sample Ro-13.3; inset (**h**) shows a single druse in detail. (**i**,**j**) SEM images of mesophyll cells in a fresh leaf of *Nymphaea lotus*, carrying only small CaOx crystals (< 5 µm) (**i**) on the surface of sclereid cells (**j**). Scale bars: (**a**) = 100 µm; (**b**) = 500 µm; (**c**) = 5 mm; (**d**,**e**,**f**,**g**) = 200 µm; (**h**,**i**) = 10 µm; (**j**) = 100 µm.

of mesophyll cells, whereas Ginkgo and Cycadeae usually contain druses of 30–80 µm diameter[46]. Sporophytes rarely contain CaOx; small crystals have been found in few fern species[47].

Unfortunately, there is still a striking scarcity of literature on calcium oxalate crystals in the leaves of extant plant taxa also reported from the fossil record. The absence of detailed data on biomineral occurrence, sizes and topology renders an interpretation of fossil patterns a challenging exercise.

Particularly for the fossil leaves from Rott, the future utilization of CaOx traces in fossil leaves may provide a valuable set of additional characters for the species- or genus-level identification of appropriately preserved leaf material. Identification of fossil leaves is particularly difficult or impossible if only leaf fragments or leaves without cuticles are preserved. Many early taxonomic assignments of leaf fossils from Rott such as the works of H. Weyland between 1934 and 1948 have been shown to be partially unreliable due to poor preservation[5] and several revisions of have been made in the recent years[6,7,48].

Our comparisons of fossil samples with extant plants showed inconsistences in several cases. The shapes and distribution patterns of granules in fossil leaves assigned to *Sideroxylon salicites* were different from those of CaOx druses in extant *Sideroxylon* leaves, casting serious doubt on the fossil identification. However, the fossil flora of Rott is currently under taxonomic revision and justification or adjustment of the determination is expected. Similarly, fossil leaf fragments designated as *Nymphaea nymphaeoides* (Nr. Ro-13.3) (Fig. 7f) contained numerous globular inclusions whereas recent *Nymphaea* leaves (Fig. 7i,j) contain only minute CaOx crystals and lack druses. Extant Lotus (*Nelumbo nucifera*, Fig. 7g,h) however, which has similar leaves and ecology, contains druses in similar distribution and size as the globules in the fossil sample named *Nymphaea*. Fossils of both genera of water plant—*Nymphaea* and *Nelumbo*—have been reported from the Rott fossil site[49,50], but the data in the present study indicate that at least some *Nymphaea*-fossils might be better placed in *Nelumbo*.

The venation patterns of fossil leaves are an important characteristic for identification of species. If our observations that the brick-like structures in the venation largely result from the traces of former CaOx crystals are validated in future studies, it will be an important step to a more precise interpretation of the fossil record of plants. Based on ongoing research, we will be able to add data from other fossil sites of different stratigraphic positions which will demonstrate similar granular structures in fossils of some gymnosperms (e.g., *Ginkgo*, leaves without trichomes) and other dicotyledonous taxa.

In conclusion, the identification of cavities and imprints in fossil leaves as former CaOx crystals and druses has considerable consequences:

- It improves our understanding of micromorphological structures of fossil leaves and the processes taking place during fossilization.
- It may provide a basis for a study of the evolution of plant biomineralization across a range of different lineages.
- It could provide an additional set of characters for improving taxonomic assignments of fossil leaves if appropriately preserved.
- It may become a useful additional aspect of leave trait analyses.

Currently, our interpretation of biominerals in fossil plants is severely limited by our rudimentary knowledge of biomineralization in living plants. A comprehensive database of current biomineralization patterns would be highly desirable to get progress in this topic. It promises to be a valuable tool in palaeobotany and greatly improve our understanding of both plant evolution and palaeoecology.

Data availability

The data that support the findings of this study are based on microscopic images which are archived in the Microscopy/SEM facilities of the Institute of Geosciences and the Nees Institute, Bonn. Images are available on request from the corresponding author M. Malekhosseini and from co-author Prof. Dr. M. Weigend.

Received: 8 December 2021; Accepted: 9 September 2022
Published online: 24 September 2022

References

1. Nicotra, A. B. *et al.* The evolution and functional significance of leaf shape in the angiosperms. *Funct. Plant Biol.* **38**, 535–552 (2011).
2. Chitwood, D. H. & Sinha, N. R. Evolutionary and environmental forces sculpting leaf development. *Curr. Biol.* **26**, 297–306 (2016).
3. Moraweck, K. *et al.* Leaf traits of long-ranging Paleogene species and their relationship with depositional facies, climate and atmospheric CO_2 level. *Palaeontographica (B)* **298**, 93–172 (2019).
4. Mörs, T. Die Sedimentationsgeschichte der Fossillagerstätte Rott und ihre Alterseinstufung anhand neuer Säugetierfunde (Oberoligozän, Rheinland). *Cour. Forsch. Inst. Senckenberg* **187**, 1–129 (1995).
5. Koenigswald, W. (ed.) *Fossillagerstätte Rott bei Hennef am Siebengebirge: Das Leben an einem subtropischen See vor 25 Millionen Jahren* (Rheinlandia, 1996).
6. Winterscheid, H. & Kvaček, Z. Revision der Flora aus den oberoligozänen Seeablagerungen von Orsberg bei Unkel am Rhein (Rheinland-Pfalz). *Palaeontographica (B)* **291**, 1–83 (2014).
7. Winterscheid, H. & Kvacek, Z. Revision der Flora aus den oberoligozänen Seeablagerungen der Grube „Stößchen" bei Linz am Rhein (Rheinland-Pfalz, Deutschland). *Palaeontographica (B)* **294**, 111–151 (2016).
8. Krassilov, V., Lewy, Z., Nevo, E. & Silantieva, N. *Late Cretaceous (Turonian) flora of Southern Negev, Israel* (Pensoft Publishers, 2005).
9. He, H., Veneklaas, E. J., Kuo, J. & Lambers, H. Physiological and ecological significance of biomineralization in plants. *Trends Plant Sci.* **19**, 166–174 (2014).
10. Pierantoni, M. *et al.* Mineral deposits in *Ficus* leaves: Morphologies and locations in relation to function. *Plant Phys.* **176**, 1751–1763 (2018).
11. Currie, H. A. & Perry, C. C. Silica in plants: Biological, biochemical and chemical studies. *Ann. Bot.* **100**, 1383–1389 (2007).

12. Gal, A. *et al.* Plant cystoliths: A complex functional biocomposite of four distinct silica and amorphous calcium carbonate phases. *Chem. Eur. J.* **18**, 10262–10270 (2012).
13. Webb, M. A. Cell-mediated crystallization of calcium oxalate in plants. *Plant Cell* **11**, 751–761 (1999).
14. Franceschi, V. R. & Nakata, P. A. Calcium oxalate in plants: Formation and function. *Annu. Rev. Plant Biol.* **56**, 41–71 (2005).
15. Prychid, C. J., Rudall, P. J. & Gregory, M. Systematics and biology of silica bodies in monocotyledons. *Bot. Rev.* **69**, 377–440 (2004).
16. Strömberg, C. A. E., Dunn, R. E., Crifo, C. & Harris, E. B. Phytoliths in paleoecology: Analytical considerations, current use, and future directions. In *Methods in Paleoecology Vertebrate Paleobiology and Paleoanthropology* (eds Croft, D. *et al.*) 235–288 (Springer, 2018).
17. Rovner, I. Potential of opal phytoliths for use in paleoecological reconstruction. *Quat. Res.* **1**, 343–359 (1971).
18. Piperno, D. R. The occurrence of phytoliths in the reproductive structures of selected tropical angiosperms and their significance in tropical paleoecology, paleoethnobotany and systematics. *Rev. Paleobot. Palynol.* **61**, 147–173 (1989).
19. Piperno, D. R. & Pearsall, D. M. The silica bodies of tropical american grasses: Morphology, taxonomy, and implications for grass systematics and fossil phytolith identification. *Smithson. Contrib. Bot.* **85**, 1–40 (1998).
20. Esteban, I. *et al.* Modern soil phytolith assemblages used as proxies for Paleoscape reconstruction on the south coast of South Africa. *Quart. Int.* **434**, 160–179 (2017).
21. Strömberg, C. A. E., Di Stilio, V. S., Song, Z. & De Gabriel, J. Functions of phytoliths in vascular plants: An evolutionary perspective. *Funct. Ecol.* **30**, 1286–1297 (2016).
22. Piperno, D. R. *Phytoliths. A Comprehensive Guide for Archaeologists and Paleoecologists.* Lanham, New York, Toronto, Oxford: AltaMira Press (Rowman & Littlefield), 2006.
23. Franceschi, V. R. & Horner, H. T. Calcium oxalate crystals in plants. *Bot. Rev.* **46**, 361–427 (1980).
24. Horner, H. T. & Wagner, B. L. 1995 Calcium oxalate formation in higher plants. In *Calcium Oxalate in Biological Systems* (ed. Khan, S.) (CRC Press, 1995).
25. Lersten, N. R. & Horner, H. T. Calcium oxalate crystal types and trends in their distribution patterns in leaves of *Prunus* (Rosaceae: Prunoideae). *Plant Syst. Evol.* **224**, 83–96 (2000).
26. O'Connell, A. M., Malajczuk, N. & Gailitis, V. Occurrence of calcium oxalate in Karri (*Eucalyptus diversicolor* F. Muell.) forest ecosystems of South Western Australia. *Oecologia (Berlin)* **56**, 239–244 (1983).
27. Genua, J. M. & Hillson, C. J. The occurrence, type and location of calcium oxalate crystals in the leaves of fourteen species of Araceae. *Ann. Bot.* **56**, 351–361 (1985).
28. Cote, G. G. Diversity and distribution of idioblasts producing calcium oxalate crystals in *Dieffenbachia seguine* (Araceae). *Am. J. Bot.* **96**, 1245–1254 (2009).
29. Anitha, R. & Sandhiya, T. Occurrence of calcium oxalate crystals in the leaves of medicinal plants. *IJP* **1**, 389–393 (2014).
30. Ogino, T., Suzuki, T. & Sawada, K. The formation and transformation mechanism of calcium carbonate in water. *Geochim. Cosmochim. Acta* **51**, 2757–2767 (1987).
31. Goss, S. L., Lemons, K. A., Kerstetter, J. E. & Bogner, R. H. Determination of calcium salt solubility with changes in pH and pCO^2, simulating varying gastrointestinal environments. *JPP* **59**, 1485–1492 (2007).
32. McComas, W. H. & Rieman, W. The effect of pH on the solubility of calcium oxalate. *J. Am. Chem. Soc.* **64**, 2948–2949 (1942).
33. Hoover, A. A. & Wijesinha, G. S. Influence of pH and salts on the solubility of calcium oxalate. *Nature* **155**, 638 (1945).
34. Rüffle, L. Myricaceae, Leguminosae, Icacinaceae, Sterculiaceae, Nymphaeaceae, Monocotyledones, Coniferae. Abhandlungen des Zentralen Geologischen Instituts. *Paläontologische Abhandlungen* **26**, 337–438 (1976).
35. Florin, R. *Untersuchungen zur Stammesgeschichte der Coniferales und Cordaitales.* Erster Teil: Morphologie und Epidermisstruktur der Assimilationsorgane bei den rezenten Koniferen. 588 pp. (Almquist & Wiksells Boktryckeri-A.-B., 1931).
36. Kunzmann, L. Koniferen der Oberkreide und ihre Relikte im Tertiär Europas. *Abhandlungen des Staatlichen Museums für Mineralogie und Geologie Dresden* **45**, 3–191 (1999).
37. Kvaček, Z. Novelties on Doliostrobus (Doliostrobaceae), an extinct conifer genus of the European Palaeogene. *Časopis Národního muzea, Řada přirodovedná* **171**, 47–62 (2002).
38. Wilde, V. Untersuchungen zur Systematik der Blattreste aus dem Mitteleozän der Grube Messel bei Darmstadt (Hessen, Bundesrepublik Deutschland). *Cour. Forschungsinst. Senck.* **115**, 1–213 (1990).
39. Mai, D. H. & Schneider, W. Über eine altertümliche Konifere im Jungtertiär und deren Bedeutung für Braunkohlen- und Bernsteinforschung. *Feddes Repertorium* **99**, 101–112 (1988).
40. Bommanavar, S. *et al.* Role of matrix vesicles and crystal ghosts in bio-mineralization. *J. Bone Miner. Metab.* **38**, 759–764 (2020).
41. Gee, C. T. & Sander, P. M. 25 Millionen Jahre alte Pflanzenfossilien aus Rott bei Hennef: Die Odyssee der historischen Sammlung Statz und ihre Rückkehr ins Rheinland. In *Fundgeschichten, Archäologie in Nordrhein-Westfalen (Exhibition catalog to the Landesausstellung NRW 2010)* (eds Otten, T. *et al.*) 30–32 (Verlag Philipp von Zabern, 2010).
42. Winterscheid, H., Kvacek, Z., Vana, J. & Ignatov, M. S. Systematic-taxonomic revision of the flora from the late Oligocene Fossillagerstätte Rott near Bonn (Germany). Part 1: Introduction; Bryidae, Polypodiidae, and Pinidae. *Palaeontographica (B)* **297**, 103–141 (2018).
43. Ensikat, H. J. & Weigend, M. EDX and Raman spectroscopy reveal the unexpected complexity of plant biomineralisation. *Microsc. Anal.* **45**, 20–23 (2019).
44. von der Brelie, G., Hager, H. & Weiler, H. Pollenflora und Phytoplankton in den Kölner Schichten sowie deren Lithostratigraphie im Siegburger Graben. *Fortschr. Geol. Rheinld. u. Westf.* **29**, 21–58 (1981).
45. Schäfer, A., Utescher, T. & Mörs, T. Stratigraphy of the Cenozoic Lower Rhine Basin, northwestern Germany. *Newsl. Stratigr.* **40**, 73–110 (2004).
46. Duarte, M. R., Souza, D. C. & Costa, R. E. Comparative microscopic characters of *Ginkgo biloba* L. from South America and Asia. *Lat. Am. J. Pharm.* **32**, 1118–1123 (2013).
47. Anthoons, B. *Distribution of Calcium Oxalate Crystals in Ferns and Lycophytes.* Master of Science Thesis, Ghent University. Faculty of Sciences. Ghent, Netherlands (2017).
48. Winterscheid, H. Oligozäne und untermiozäne Floren in der Umgebung des Siebengebirges. Teil 1 – Textband. *Documenta Naturae* **158**, 1–297 (2006).
49. Gee, C. T. & Winship Taylor, D. Aquatic macrophytes from the upper Oligocene fossillagerstätte of Rott (Rhineland, Germany). Part II: A new fossil leaf species of *Nymphaea* (subgenus Lotos), *N. elisabethae* Gee et David W. Taylor sp. nov.. *Palaeontographica (B)* **295**, 33–43 (2016).
50. Taylor, D. W., Gee, C. T., & Winterscheid, H. Origination of the Sacred lotus family: Preliminary Phylogenetic Placement of the Nelumbonaceae, with New Nelumbolike Leaves from the Late Oligocene Fossillagerstätte of Rott near Bonn, Germany. in *10th European Palaeobotany – Palynology Conference Program & Abstracts*, pp. 245 (2018).

Acknowledgements

We give special thanks to Dr. Cornelia Löhne for collecting plant material from the Bonn University Botanic Gardens. We would also like to thank late Dr. Heinz Winterscheid (University of Bonn) for facilitating access to his fossil material from Rott. We acknowledge the support of Dr. Alexander Ziegler and Dagmar Wenzel (Institute of Evolutionary Biology and Ecology, University of Bonn) with X-ray and μ-CT images. This project was

supported by a DFG grant (University of Bonn, DFG Research Unit 2685). This is contribution no. 49 of the DFG Research Unit 2685, "The Limits of the Fossil Record: Analytical and Experimental Approaches to Fossilization."

Author contributions

J.R. and M.W. led the project management. M.M. and H.J.E. carried out microscopy and laboratory work and analysis of the data. V.E.M., T.W., J.R. and L.K. helped with their expertise in palaeontology; M.W. with his expertise in botany and plant systematics. All authors contributed to writing of the manuscript.

Funding

Open Access funding enabled and organized by Projekt DEAL.

Competing interests

The authors declare no competing interests.

Additional information

Supplementary Information The online version contains supplementary material available at https://doi.org/10.1038/s41598-022-20144-4.

Correspondence and requests for materials should be addressed to M.M.

Reprints and permissions information is available at www.nature.com/reprints.

Publisher's note Springer Nature remains neutral with regard to jurisdictional claims in published maps and institutional affiliations.

Received: 31 January 2023 | Revised: 5 April 2023 | Accepted: 12 April 2023

DOI: 10.1111/jmi.13187

Journal of Microscopy RMS

TECHNICAL NOTE

Visualisation of calcium oxalate crystal macropatterns in plant leaves using an improved fast preparation method

Hans-Jürgen Ensikat[1] | **Mahdieh Malekhosseini**[2] | **Jes Rust**[2] | **Maximilian Weigend**[1]

[1]Nees-Institut für Biodiversität der Pflanzen der Universität Bonn, Bonn, Germany

[2]Institute of Geosciences, Rheinische Friedrich-Wilhelms Universität Bonn, Bonn, Germany

Correspondence
Mahdieh Malekhosseini, Institute of Geosciences, Rheinische Friedrich-Wilhelms Universität Bonn, Nussalle 8, 53115, Bonn, Germany.
Email: m.malekhosseini.UniBonn@gmail.com

Funding information
DFG, Grant/Award Number: 396637283

Abstract

Leaves of the majority of plants contain calcium oxalate (CaOx) crystals or druses which often occur in spectacular distribution patterns. Numerous studies on CaOx in plant tissues across many different plant groups have been published, since it can be visualised readily under a light microscope (LM). However, there is surprisingly limited knowledge on the actual, precise distribution of CaOx in the leaves of quite ordinary plants such as common native and exotic trees. Traditional sample preparation for the documentation of the distribution of CaOx crystals in a given sample – including overall distribution – requires time-consuming clearing procedures. Here we present a refined fast preparation method to visualise the overall CaOx complement in a sample: The plant material is ashed and the ash viewed under the polarising microscope. This is a rapid method which overcomes many shortcomings of other methods and permits the visualisation of the entire CaOx content in most leaf samples. Pros and cons in comparison with the conventional clearing technique are discussed. Further aspects for CaOx investigations by micro-CT and scanning electron microscopy are discussed.

KEYWORDS

CaOx druses, clearing, incineration, microanalysis, polarising microscope

1 | INTRODUCTION

Calcium oxalate (CaOx) crystals and druses (crystal aggregates) are very striking, but still quite enigmatic structures in higher plants. They are visible under the light microscope, ideally the polarising microscope, but for an investigation of the morphological details a scanning electron microscope (SEM) is usually required.[1–4] Apart from the shape and size of the individual CaOx crystals and clusters, they also show characteristic distribution patterns in plant tissues (Figures 1 and 2).

The majority of trees and woody plants, including common forest and garden trees, as well as many other plants, form CaOx deposits in their leaves, which show tremendous diversity in morphology and distribution.[1] However, the physiological or ecological roles of CaOx deposits are still subject to speculation.[5,6] It has been argued that they play a role in herbivore deterrence, but this is difficult to validate experimentally.[7] Alternatively, the localisation and shape of the CaOx druses has been demonstrated to play a role in light harvest with a measurable effect on photosynthesis.[8–10] Apart from these functional

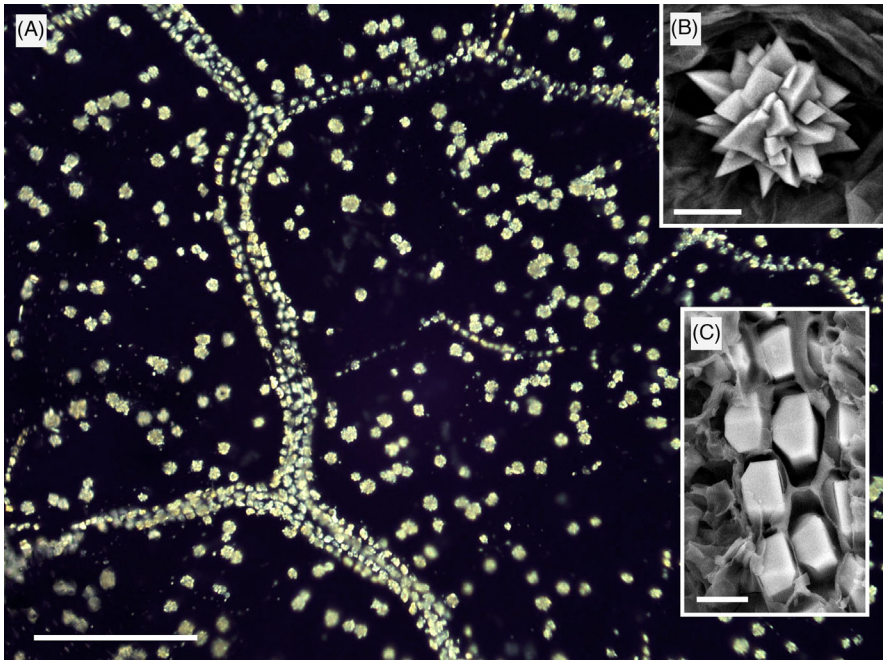

FIGURE 1 Distribution of CaOx crystals and druses in a *Quercus mongolica* leaf. Polarisation light microscopy (Pol-LM) image of the ash of an incinerated leaf sample. Small individual prismatic crystals are associated with veins; larger druses are distributed randomly in the parenchyma. Insets show SEM images of a druse (B) and crystals (C). Scale bars: (A) = 200 μm; (B, C) = 10 μm.

interpretations, it has also been convincingly argued that CaOx crystals are often simply inert deposits of excess Ca.[11]

The uncertainty regarding functionality may be part of the reason, why there are relatively few critical studies providing an overview on CaOx distribution patterns in plant tissues. Larger studies were performed mainly by a limited number of botanists specialised on biomineralisation and often focused on certain plant groups only.[1]

CaOx crystals in leaves can be visualised well in transparent samples, either by light microscopy (LM; Figure 2A) or by microcomputed tomography (micro-CT) with X-rays (Figure 2B). Scanning electron microscopy (SEM) as a surface-imaging technique is able to visualise the CaOx in great detail on exposed layers and is additionally able to provide EDX element analyses (Figure 2C). Remnants of CaOx crystals may also be visible in the ash of incinerated leaves (Figure 2D).

The most established preparation technique for LM examinations uses clearing of the leaves with bleach, such as sodium hypochlorite, and immersion in xylene or a different mounting medium to provide transparency for polarisation microscopy (Pol-LM) (Figure 2A).[3,12] If samples are too thick and transparency cannot be achieved, then leaves may have to be dissected or cleaved. A complication arises from the fact that cellulose is not effectively cleared which may then interfere with the visualisation of CaOx.

In our recent study of patterns of granular structures in fossil leaves, resembling CaOx druses in related fresh leaves, we identified the necessity to get a reference image database for better comparison of structures in fossil and fresh leaves.[13] Thus, we tried to improve on existing methods. We had previously often used incineration as a quick test to look for biomineral structures in plants: simply, we incinerated the sample and examined the ash with a stereo microscope, and we found that cystoliths, CaOx druses and mineralised trichomes usually were clearly visible within amorphous ash remnants from cell walls. It is not new that biomineral structures such as silica phytoliths and CaOx crystals withstand incineration and can be analysed in ash samples.[14,15] Controlled incineration leads to carbonisation of the leaf sample which retains its basic shape and structure and the biominerals are preserved in their original shape and location. We initially examined incinerated leaf samples under a LM with surface illumination. Ashed leaves that remained too intransparent were separated into an upper and lower part with the help of adhesive tape, so that the inside (mesophyll) of the leaf could be viewed (Figure 2D).[13] However, the results were not entirely satisfactory and further improvements were necessary for satisfying results. These were obtained by viewing and imaging ashed leaves under the polarising microscope. Here we present some of these results in comparison with those of the established clearing methods, and we discuss advantages and disadvantages of both techniques. Additional examinations and analyses with microcomputer tomography (micro-CT) and SEM will be mentioned, providing complementary information

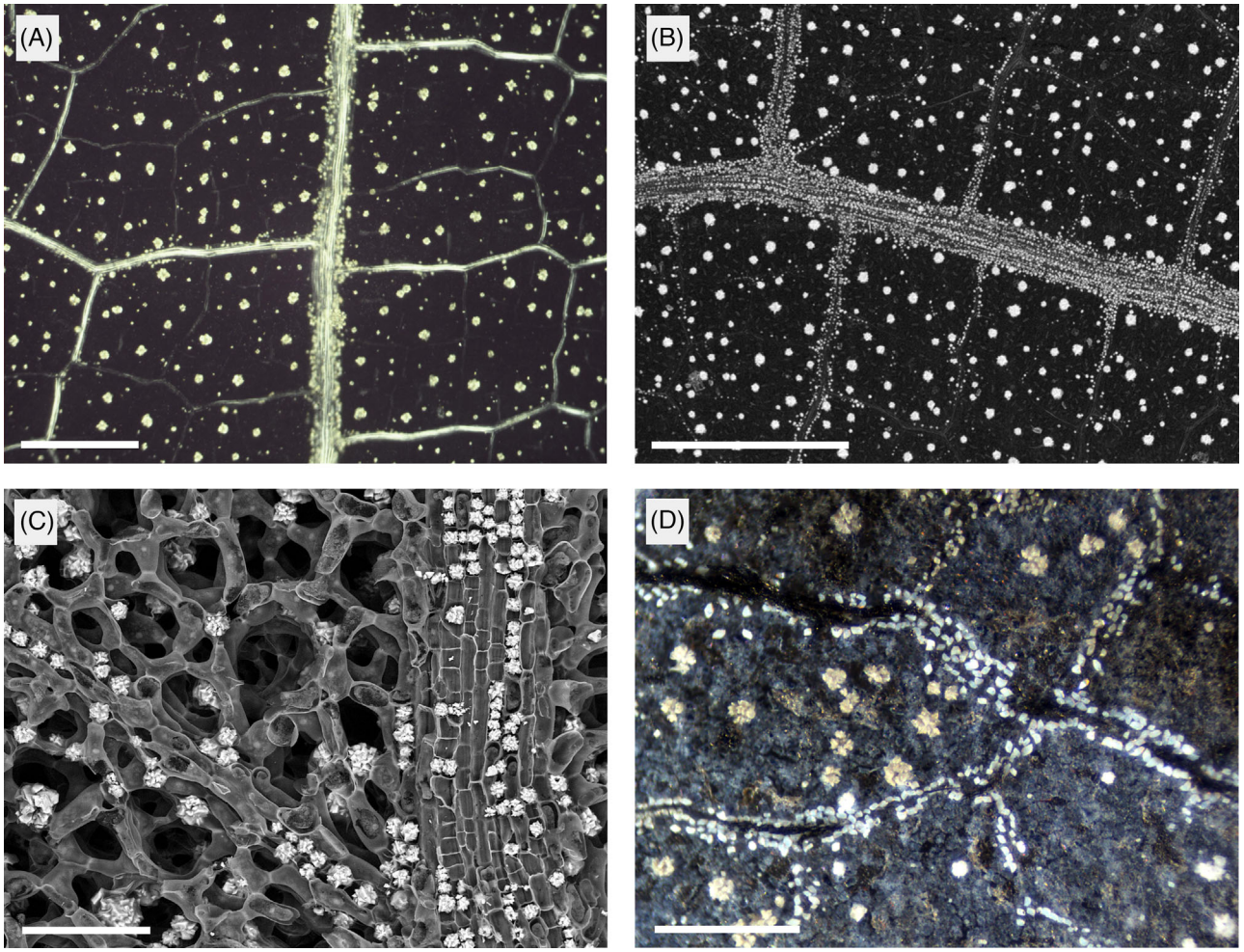

FIGURE 2 Examples of CaOx macropatterns visualised by traditional methods: (A) Pol-LM image of chemically cleared leaf of *Juglans regia*. CaOx crystals and cellulosic cell walls appear bright. (B) Micro-CT image of a dried *Juglans regia* leaf; reconstructed planar view showing entire content of CaOx crystals. Large druses in the aerenchyma and small druses along veins appear bright. (C) SEM image of the inner face of a split leaf of *Hedera helix*; critical point-dried. Small CaOx druses are associated with veins; larger druses are randomly distributed in aerenchyma. (D) Large druses and small crystals in a split piece of an incinerated leaf of *Quercus variabilis*. LM image with epi-illumination. Scale bars: (A, B) = 500 μm; (C) = 100 μm; (D) = 200 μm.

on localisation and composition of biomineral structures in leaves.

2 | MATERIAL AND METHODS

2.1 | Plant material

The new preparation method was successfully used for leaf samples from numerous trees and shrubs from the Botanical Gardens, University of Bonn, and from other locations. Fresh, fully developed leaves of different ages as well as air-dried leaves were prepared successfully. The following species appear in this study: *Banksia serrata* (accession 00664); *Carpinus kawakamii* (accession 34895); *Ceanothus spinosus* (accession 34717); *Hedera helix* (accession 8757); *Juglans regia* (accession 9662); *Lindera angustifolia* (accession 11686); *Musa basjoo* (accession 18095); *Parrotia persica* (accession 12241); *Pterocarya rhoifolia* (accession 39872); *Quercus mongolica* (accession 13312); *Quercus robur* (accession 1425); *Quercus variabilis* (accession 35458).

2.2 | Microscopy equipment

Light microscopy (LM) was carried out with a standard microscope (Müller Optronic, Erfurt, Germany) with an additional polarisation filter attachment. Scanning electron microscopy (SEM) was performed with a LEO 1450 SEM (Cambridge Instruments, Cambridge, UK), and a Tescan Vega 4 SEM (Tescan GmbH; www.tescan.com),

both equipped with secondary electron (SE) and backscattered electron (BSE) detectors and EDX element analysis systems. X-ray images and microcomputed tomography (micro-CT) scans of dry leaves were obtained with a SkyScan 1272 Micro-CT system (Bruker microCT, Kontich, Belgium) in the Institute of Evolutionary Biology and Ecology at the University of Bonn.

2.3 | Specimen preparation methods

2.3.1 | Standard preparation of fresh leaves for SEM and micro-CT

Pieces of fresh leaves were fixed in 70% v/v ethanol + 4% v/v formaldehyde in water for at least 20 h and dehydrated with ethanol. For freeze-fracturing, ethanol-infiltrated samples were immersed in liquid nitrogen and broken randomly. After unfreezing, all samples were critical point-dried (CPD 020, Balzers Union, Liechtenstein) and mounted on sample holders for SEM or micro-CT. SEM samples were sputter-coated with an approximately 10 nm thin layer of palladium.

2.3.2 | Leaf clearing with sodium hypochlorite-based household bleach

Fresh leaf samples were immersed in boiling ethanol for 30 sec in order to dissolve epicuticular wax and improve permeability of the cuticle, followed by immersion in distilled water for 1 h. Then samples were transferred to household bleach (DanKlorix, www.colgate.com; 2.8% NaClO) until they appeared colourless, usually 2 to 12 h, depending on leaf permeability. Then the samples were rinsed with water, followed by dehydration with ethanol and acetone. After immersion in xylene or immersion oil, the samples were ready for Pol-LM.

2.3.3 | Ashing

Pieces of fresh or dry leaves were heated to approximately 600°C to 750°C until all organic components were oxidised and the remains were almost white. We used two incineration methods: either a temperature-controlled oven (Brennofen Uhlig U15, Efco GmbH, Rohrbach, Germany). Leaf pieces were placed between glass slides, with a spacer that ensured entrance of air (Figure 3A–C). At 600°C–650°C, the oxidation was accomplished after 5 to 15 min. Much faster was incineration in a gas flame: leaf samples were placed between two nickel meshes (screen printing meshes 'Rotamesh'; kindly provided by the printing company Frintrup, Bonn, Germany), and burnt in a low-intensity gas flame at red heat for 2 to 3 min (Figure 3D–F). The remaining piece of ash is quite fragile. For polarisation-LM, the ash piece was immersed in a thin layer of immersion oil on a microscopy glass slide, or an embedding medium with higher viscosity. A drop of the liquid was dispersed on the glass slide over ca. 4 cm^2, and the ash piece was dropped into it. A coverslip was omitted to avoid fragmentation of the fragile specimens.

3 | RESULTS

We used the incineration method successfully for leaves of more than 100 species, mostly mature leaves of dicotyledonous trees and shrubs. In most cases, the remaining piece of ash was quite fragile, but stable enough to withstand the immersion in oil without heavy disaggregation. The ash consisted of amorphous calcium compounds as remnants of cell walls, sometimes silica, and the compact incinerated remnants of druses and crystals, which retained their original shape. Under the polarisation-LM between crossed pol filters, amorphous ash and silica appeared almost invisible (dark) whereas the incinerated CaOx druses and crystals appeared bright. Any other structures, such as residual carbon remnants and even air bubbles were invisible, so that the CaOx remnants could be seen with excellent contrast and without interference from any other structures. The method reached its technical limitations when the ashed samples became intransparent as a result of melting processes, for example, in presence of phosphates, or when the ashed tissue was so thin and fragile, that it disaggregated during immersion in oil.

The incineration in the oven took approximately 20 min. At ca. 400°C the samples became black; at 600°C to 650°C it took usually 10 to 15 min until the samples became white and all carbon was oxidised. Some samples rich in Si or P (e.g., Moraceae, Urticaceae leaves) required up to 20 min at 700°C to turning white. The enclosure between glass slides prevented ignition of the samples so that the oxidation proceeded under controlled conditions. It was found useful to interrupt the heating after reaching ca. 450°C and verify that the sample does not stick to the glass slide, so that the ash finally could be transferred easily into the immersion oil. Burning in a gas flame takes usually 2–3 min for complete oxidation and the overall results were similar to the results of oven heating. The risk of fragmentation during immersion in oil was a slightly increased, so that visualisation of large areas proofed to be problematic. The entire preparation took no more than 5 min from cutting the leaf to the visualisation under the microscope. On the other hand, the bleaching procedure took between 3 and 10 h if the leaves had been

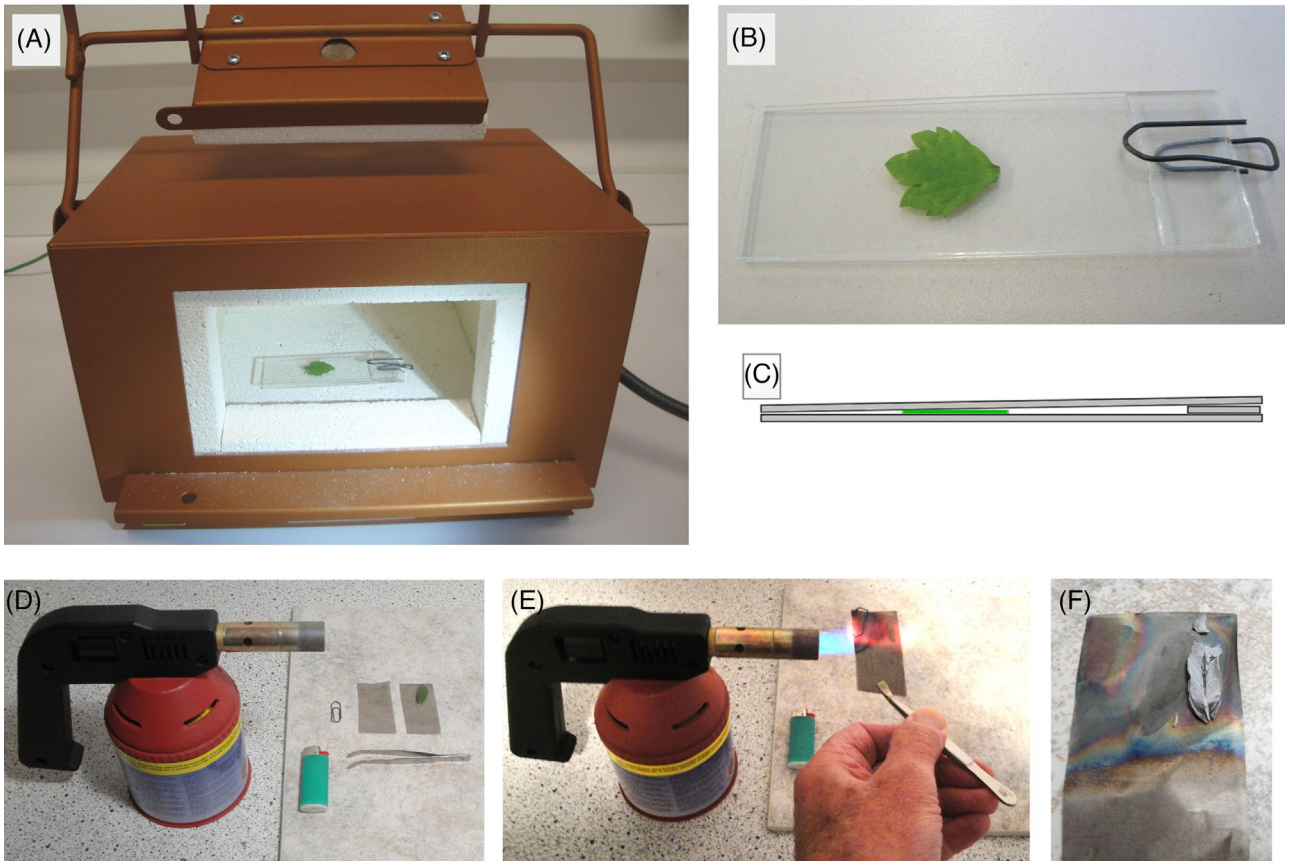

FIGURE 3 Equipment for two incineration methods. (A–C) Incineration in temperature-controlled furnace. (B, C) Fresh or dry leaf pieces are placed between glass slides; a glass spacer ensures access of air. (D–F) Incineration in a gas flame. A leaf piece is placed between two nickel (or steel) meshes and heated to red heat for 2–3 min. Incineration is completed when the ash piece is white (F).

pretreated with hot ethanol in order to dissolve wax layers; longer without previous pretreatment. After washing in water, dehydration, and immersion in xylol or immersion oil, the samples were transparent and CaOx crystals and druses were clearly visible in the Pol-LM. The cleared specimens were stable, and the positions of the CaOx particles and leaf veins could be visualised precisely. In stereoscopic viewing, their spatial distribution was clearly visible. Figure 4A–D shows a comparison of *Quercus* and *Parrotia* leaves prepared by ashing and by clearing. The low magnification images of *Quercus* (4× objective) show the leaf vasculature and numerous druses in the areoles. Small CaOx crystals are present in the bundle sheaths and can be seen clearly at higher magnification (10× objective; Figure 4C and D). In the incinerated samples (Figure 4A and C) only the CaOx appears bright, so that the individual particles can be seen clearly. Stereoscopic views revealed that the height positions of the particles were still preserved in sufficiently stable ash pieces. In the cleared sample (Figure 4B and D), the crystals and also the cell wall structures of the veins appear bright, so that the crystals in the bundle sheaths are obscured and only partly visible. Pol-LM images with crossed polarisers show only polarisation-active structures. Amorphous ash, silica, and carbon remnants remained invisible (dark), but they became visible in brightfield imaging mode, simply by removing one polarising filter. Figure 4E and F shows the same area of an incinerated *Pterocarya* leaf in both modes: Pol-LM shows numerous druses in the parenchyma and few small crystals along a vein. The corresponding brightfield image shows the druses, but also the pattern of medium and small veins with remnants of amorphous ash and traces of carbon. Only larger veins are decorated with CaOx crystals.

Both preparation methods, clearing and ashing, have advantages and shortcomings and should be seen as complementary techniques. The ashing method had been developed as a quick test, but has the potential to help in generating excellent images, not least by eliminating the organic background signal. The clearing method gives best structural preservation and stable specimens, which can be used subsequently, for example, for SEM examinations and analyses. Thick leaf tissue may result in technical limitations for both methods, but to different extent. Incinerated samples have a higher transparency than cleared ones, so that thicker leaves can be examined. Figure 5A shows a

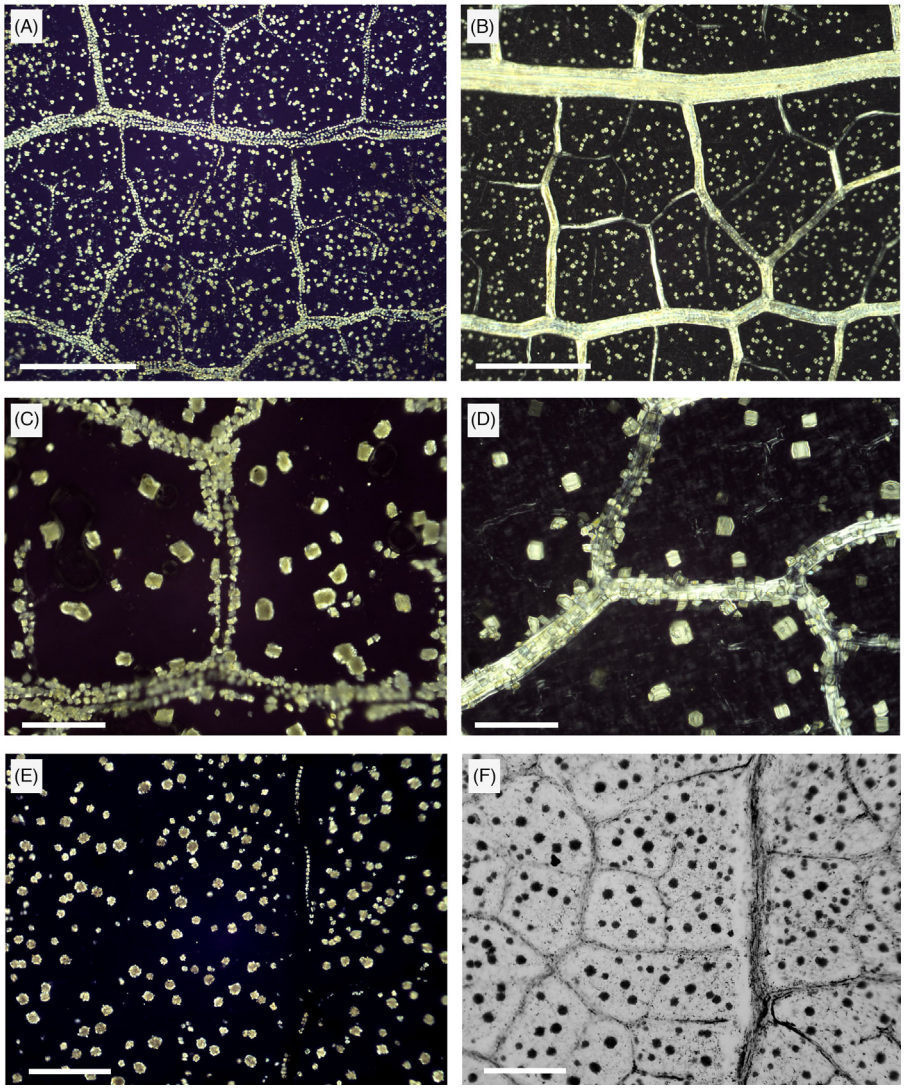

FIGURE 4 Comparison of incinerated and chemically cleared leaf samples. (A, B) *Quercus mongolica* leaf at low magnification (4× objective) showing venation network. (A) Pol-LM image of incinerated leaf shows druses randomly distributed in parenchyma, small crystals along veins. (B) Pol-LM image of cleared leaf. Druses in parenchyma and cellulose-rich veins appear bright; small CaOx crystals along veins are obscured and only partly visible. (C, D) *Parrotia persica* leaf at higher magnification (10×). (C) Pol-LM image of incinerated leaf shows individual crystals, partially out of focus due to different height. (D) Pol-LM image of cleared leaf. Crystals in parenchyma are clearly visible; smaller crystals along veins are obscured by cellulosic cell wall structures. (E, F) Incinerated leaf of *Pterocarya rhoifolia* leaf, same area in polarisation (E) and brightfield (F) imaging mode. CaOx druses are visible in both images. Network of small veins is visible only in brightfield. Only few small crystals decorate medium-size vein. Scale bars: (A, B) = 500 μm; (C–F) = 200 μm.

Pol-LM image of the ash of a *Ceanothus* leaf with a strong background signal. On the other hand, leaves, which produce too little ash, may be unsuitable for ashing, because the remnants disintegrate or collapse (Figure 5B).

In many young leaves with low cellulose content, the background signal in Pol-LM of chemically cleared samples may be negligible, so that perfect images are possible. However, several different cellulose structures can be present, for example, at stomata or trichomes, and may cause misinterpretations (Figure 5C). In some cases, we observed a chemical preparation artefact during clearing. Clouds of small crystals occurred irregularly in some samples, most likely CaOx, but possibly calcium carbonate, which were never observed in incinerated samples (*Juglans regia;* Figure 5D). By contrast, incineration caused sometimes alterations in samples with a high content of alkali (K, Na) salts and Si or phosphate, which form melting compounds (*Banksia serrata;* Figure 5E). This may be avoided by a pretreatment, which removes these soluble components, for example, fixation in formaldehyde.

As demonstrated above, the two-dimensional distribution of CaOx crystals and druses in plant leaves and their morphology can be studied successfully by light microscopy, particularly Pol-LM. For a more

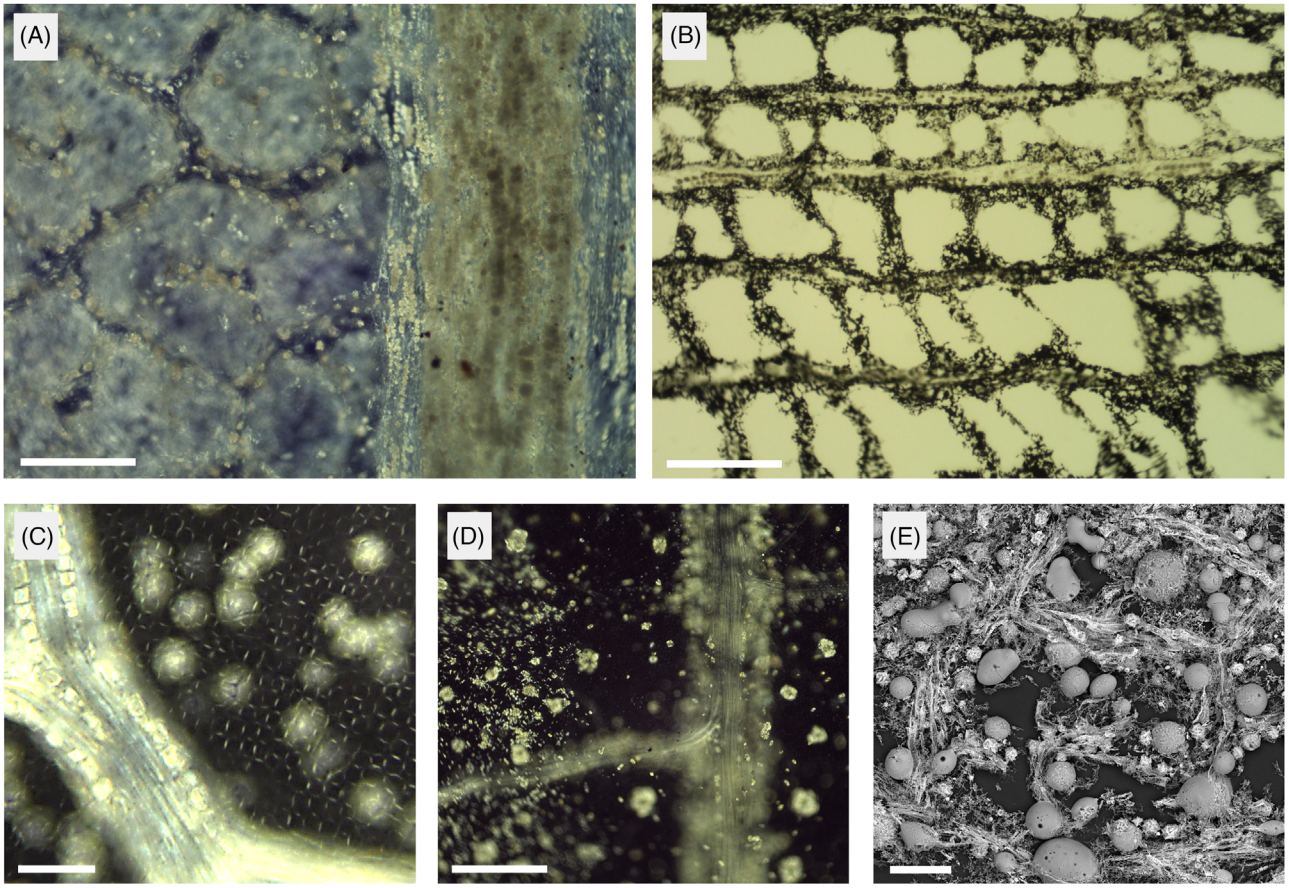

FIGURE 5 Limitations and preparation artefacts of incineration and clearing. (A) *Ceanothus spinosus*; sample too thick and opaque. Ash of incinerated leaf generates bright background in Pol-LM image; druses are hardly visible. (B) *Musa basjoo*; sample produces too little ash and therefore loses structural integrity; brightfield-LM image. (C) *Quercus mongolica*; Pol-LM image of cleared leaf with focus on epidermis shows fine cellulose cell wall structures of stomata, which could be misinterpreted as CaOx raphides. (D) *Juglans regia*; Pol-LM of a cleared leaf with irregular precipitations of small crystals across the sample. (E) *Banksia serrata*; SEM image of incinerated leaf with molten ash particles rich in Si, K and Na. Scale bars: (A, B, D) = 200 μm; (C, E) = 50 μm.

comprehensive understanding, additional microscopic techniques such as SEM and micro-CT are required. SEM, with its high resolution and depth of field, reveals minute details and provides impressive images from sample surfaces. EDX element analyses are a valuable feature for the chemical identification of biominerals. Druse-like structures are not always CaOx; Silica, calcium carbonate, calcium sulphate and other salts may display similar morphology. Raman spectroscopy can discriminate between different anions such as carbonate, oxalate or phosphate. Micro-CT is additionally valuable for the determination of the 3-D distribution of biominerals, but it has limitations. The resolution is sufficient for CaOx particles of 10 μm or more, but we could not visualise biominerals of smaller dimensions, such as those found, for example, in conifers. Micro-CT is applicable for correlative studies of chemically cleared Pol-LM samples, after suitable preparation including CP drying.

4 | DISCUSSION

The present article compares different methods to visualise CaOx crystals especially in leaf tissue – traditional bleaching and clearing for Pol-LM, SEM, incineration and micro-CT. Neither of these approaches provides a magical bullet for the specific task – each has its advantages and drawbacks. From the point of view of simply obtaining a comprehensive overview over the CaOx in a leaf sample, the incineration method described here has the clear advantage of providing an unobstructed view of the crystals in their original shape and largely their original position. The crystals are not obscured by organic matter (esp. cellulose) under polarised light and can therefore be imaged precisely. This advantage is particularly striking in the extensive biomineralisation associated with, for example, leaf veins – which may be completely obscured by sclerenchymatic and xylem cells in cleared samples. The

TABLE 1 A Comparison of the advantages and limitations of the incineration and clearing methods for viewing CaOx in leaves (more advantageous method bold type).

	Incineration	Clearing
Sample preparation time	**5 (burner) to 20 (furnace) min**	Several hours
Background signal	**Minimal**	Often strong (e.g. cellulose)
Visualisation with Pol-LM	**Optimal**	Interference by e.g. cellulose
Transparency of sample	**Very high**	Variable
Artefacts	Possibly minor dislocation of crystals and shrinking of sample	**Few if any**
Sample stability	Low (thin and/or young leaves disintegrate)	**High**
Sample size	Small; larger samples may disintegrate	**Larger; good for obtaining overview**
Alternative analyses with sample	Histological detail lost	**Histological detail preserved**

incineration method is highly suitable for mature leaves of normal thickness, including those that are too thick for clearing to provide satisfactory results. Both cleared and incinerated leaves can be used for subsequent SEM-studies with compositional contrast using the backscattered electrons signal (BSE), or EDX for identification of the element composition. Another major advantage of the incineration method are the very short sample preparation times, which permit the screening of larger sample numbers (without the generation of chemical waste) in a relatively short time span for comparative studies.

However, the incineration method also has certain disadvantages: It cannot be used for thin and fragile leaf tissue, as incineration of those samples yields fragile ash fragments without sufficient stability for subsequent mounting and investigation. These are, on the other hand, the type of samples most suited for the clearing method. Also, since the organic material is reduced to ash, a certain degree of shrinkage and dislocation of the crystals is inevitable with the incineration method. As the images and Table 1 show, the differences may be negligible in most material but need to be kept in mind for critical comparative studies.

In the LM view the three-dimensional arrangement of crystals in the leaf tissue is only represented as a two-dimensional image. This shows precisely, for example, the differential distribution of crystal druses in the intercostal area versus tiny crystals along the leaf veins. A stereo-microscopic view provides an impression of the three-dimensional location of the crystals, but it is difficult to illustrate it sufficiently by LM micrographs. The traditional method of sectioning can be used for this purpose, but leads to notoriously unpredictable results especially in heavily mineralised leaves, including the laceration of sections and crystal dislocation by the microtome blade. Alternatively, micro-CT can be used for this purpose and the images shown in Figure 6 beautifully demonstrate how the precise location of CaOx in the leaf tissue can be visualised with this technique.

5 | CONCLUSION

The addition of another tool for our study of plant biomineralisation presented here should be greatly helpful for deepening our understanding of this – to date surprisingly poorly documented and understood – phenomenon. Recent studies have been able to provide some unexpected insights into the range of functions that biominerals may play in plant tissues, adding to the widely accepted role in herbivore defence. The demonstration of the light-scattering mechanism, for example, in *Ficus* leaves, is an example.[10,16] To the best of our knowledge, no explanation has so far been provided for the peculiar patterns of thick layers of crystals along the leaf veins, or the differentiation in CaOx deposits in the intercostal areas versus those along the leaf veins. However, in recent years, a large number of studies has started to elucidate the physiological role of CaOx in more detail, demonstrating a complex role in carbon dioxide storage and associations with drought and other abiotic stressors. This indicates that far from being an inert mineral deposit, CaOx plays an active role in both the carbon and calcium cycles.[17,18]

We therefore argue that incineration provides a valuable complementary tool for the study of leaf biomineralisation, with the particular benefit of being widely applicable to most leaf tissues and permitting the rapid screening of multiple samples. A comprehensive picture of CaOx in leaves can then be obtained by the complementary use of leaf clearing, SEM and micro-CT, leading to a genuine, three-dimensional picture and permitting even the identification of the element composition of the biominerals present. In view of these promising insights, we believe that the increased ease of visualisation, for example, by the

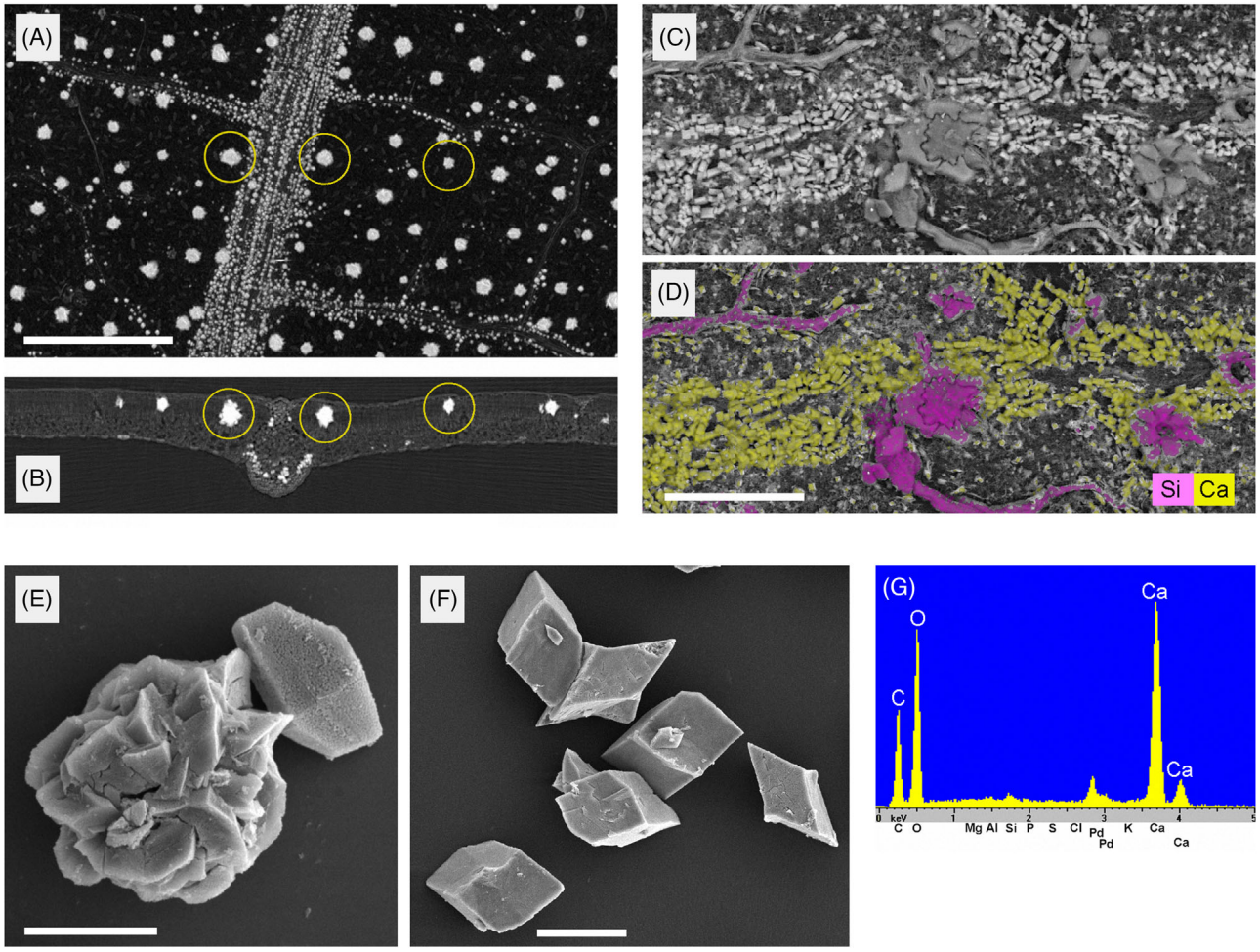

FIGURE 6 Prospects for correlative microscopic studies of CaOx macropatterns. (A, B) Micro-CT images of *Juglans regia*. Micro-CT is even applicable for chemically cleared samples for correlative studies. Planar view (A) and reconstructed cross section (B) provide spatial distribution. Identical druses are encircled in both views. (C, D, G) SEM images of *Lindera angustifolia* demonstrate capability of high-resolution imaging and element analyses; applicable for both, incinerated and cleared samples. (C) BSE image (compositional contrast), showing contents of heavier elements (Ca) brighter than lighter elements (Si, C). (D) Element mapping image showing Ca in yellow and Si in magenta. (E, F) Druses and crystals isolated from ashed leaves of *Quercus robur* (E) and *Carpinus kawakamii* (F). (G) Element spectrum of an incinerated CaOx crystal. Scale bars: (A, B) = 500 μm; (C, D) = 100 μm; (E) = 10 μm; (F) = 50 μm.

incineration method described in detail here, will provide a tool for the study of CaOx and other biominerals, opening the field to functional and physiological studies elucidating both the causes and mechanisms of CaOx deposition in leaf tissue.

ACKNOWLEDGEMENTS

This project was supported by a DFG grant (University of Bonn, DFG Research Unit 2685) with project number: 396637283.

Open access funding enabled and organized by Projekt DEAL.

ORCID

Mahdieh Malekhosseini https://orcid.org/0000-0002-3847-918X

REFERENCES

1. Franceschi, V. R., & Nakata, P. A. (2005). Calcium oxalate in plants: formation and function. *Annual Review of Plant Biology*, *56*, 41–71.
2. Lersten, N. R., & Horner, H. T. (2006). Crystal macropattern development in *Prunus serotina* (Rosaceae, Prunoideae) leaves. *Annals of Botany*, *97*(5), 723–729.
3. Zhang, J., Lu, H., & Huang, L. (2014). Calciphytoliths (calcium oxalate crystals) analysis for the identification of decayed tea plants (*Camellia sinensis* L.). *Scientific Reports*, *4*, 6703.
4. Cuéllar-Cruz, M., Pérez, K. S., Mendoza, M. E., & Moreno, A. (2020). Biocrystals in plants: A short review on biomineralization processes and the role of phototropins into the uptake of calcium. *Crystals*, *10*, 591.
5. Franceschi, V. R., & Horner, H. T. (1980). Calcium oxalate crystals in plants. *The Botanical Review*, *46*(4), 361–427.
6. Karabourniotis, G., Horner, H. T., Bresta, P., Nikolopoulos, D., & Liakopoulos, G. (2020). New insights into the functions of

carbon–calcium inclusions in plants. *New Phytologist*, *228*(3), 845–854.
7. Paiva, É. A. S. (2021). Do calcium oxalate crystals protect against herbivory? *The Science of Nature*, *108*, 24.
8. Kuo-Huang, L. L., Ku, M. S. B., & Franceschi, V. R. (2007). Correlations between calcium oxalate crystals and photosynthetic activities in palisade cells of shade-adapted *Peperomia glabella*. *Botanical Studies*, *48*, 155–164.
9. Horner, H. T. (2012). Peperomia leaf cell wall interface between the multiple hypodermis and crystal-containing photosynthetic layer displays unusual pit fields. *Annals of Botany*, *109*(7), 1307–1315.
10. Pierantoni, M., Tenne, R., Brumfeld, V., Kiss, V., Oron, D., Addadi, L., & Weiner, S. (2017). Plants and light manipulation: The integrated mineral system in okra leaves. *Advanced Science*, *4*(5), 1600416.
11. Webb, M. A. (1999). Cell-mediated crystallization of calcium oxalate in plants. *The Plant Cell*, *11*(4), 751–761.
12. Horner, H. T., Samain, M.-S., Wagner, S. T., & Wanke, S. (2015). Towards uncovering evolution of lineage-specific calcium oxalate crystal patterns in Piperales. *Botany*, *93*(3), 159–169.
13. Malekhosseini, M., Ensikat, H.-J., Mccoy, V. E., Wappler, T., Weigend, M., Kunzmann, L., & Rust, J. (2022). Traces of calcium oxalate biomineralization in fossil leaves from late Oligocene maar deposits from Germany. *Scientific Reports*, *12*, 15959.
14. Morgan-Edel, K. D., Boston, P. J., Spilde, M. N., & Reynolds, R. E. (2015). Phytoliths (plant-derived mineral bodies) as geobiological and climatic indicators in arid environments. *New Mexico Geology*, *37*(1), 3–20.
15. Canti, M. G., & Brochier, J. É. (2017). Plant ash. In: Nicosia, C., & Stoops, G. (Eds.), *Archaeological soil and sediment micromorphology* (pp. 147–154). Chichester, UK: John Wiley & Sons Ltd.
16. Pierantoni, M., Tenne, R., Rephael, B., Brumfeld, V., Van Casteren, A., Kupczik, K., Oron, D., Addadi, L., & Weiner, S. (2018). Mineral deposits in *Ficus* leaves: Morphologies and locations in relation to Function. *Plant Physiology*, *176*, 1751–1763.
17. Tooulakou, G., Giannopoulos, A., Nikolopoulos, D., Bresta, P., Dotsika, E., Orkoula, M. G., Kontoyannis, C. G., Fasseas, C., Liakopoulos, G., Klapa, M. I., & Karabourniotis, G. (2016). Alarm Photosynthesis: Calcium oxalate crystals as an internal CO_2 source in Plants. *Plant Physiology*, *171*, 2577–2585.
18. Gómez-Espinoza, O., González-Ramírez, D., Bresta, P., Karabourniotis, G., & Bravo, L. A. (2020). Decomposition of calcium oxalate crystals in *Colobanthus quitensis* under CO_2 limiting conditions. *Plants*, *9*, 1307.

How to cite this article: Ensikat, H.-J., Malekhosseini, M., Rust, J., & Weigend, M. (2023). Visualisation of calcium oxalate crystal macropatterns in plant leaves using an improved fast preparation method. *Journal of Microscopy*, *290,* 168–177. https://doi.org/10.1111/jmi.13187

Appendix A1

Fossil leaves examined under LM and fossils with better preservation and higher possibility of cast occurrences were selected and borrowed. Here collections from young to old geological times are mentioned.

Fossil collection 1, Late Pliocene, Willershausen (3.6 to 2.6 Ma), Geowissenschaftliches Museum des Zentrums für Geowissenschaften, University of Göttingen, Germany

58 out of 200 examined fossil leaves (under LM) from different species borrowed from the Geowissenschaftliches Museum des Zentrums für Geowissenschaften, University of Göttingen, Germany. All of the fossil leaves belong to the Willerhausen lagerstätte. The sediments and the fossil fauna of the Willershausen site indicates that it was a steep-sided lake in severely distorted layers of the Middle Buntsandstein. The lake basin had a diameter of 150 to 200 m and its outline roughly coincided with that of the later clay pit. Deposits from the former cliffs and a sandy shelf are preserved at the edges. Within a few decametres going down the basin, these sediments change to a light gray tone, then to the finely lamellar black tone of the center of the basin. Subaquatic landslides have been developed on the slopes, which locally switch into fully sheared sediment. The sequence is generally transgressive, the facies of the dark clays was spreading over the marginal sands over time. The basin deepened and widened during sedimentation. A hard, carbonate bank can be traced laterally through all facies of the basin filling as an isochronous conductive horizon. The coarse-clastic sediments near the shore are only cemented by calcite, banded marl with fine-clastic, mostly graded inclusions was deposited on the slopes, and finally fine-laminated dolomitic marl prevailed in the middle of the basin. Almost all of the 50,000 fossils found in the Willershausen clay pit over the past 80 years derived from this one bank. The carbonate bank appears to have formed during a brief period of exceptional hydrographic conditions. The annual stratification in the center of the

basin is very regular at around 1 mm/year. The bench here is 30 cm thick; that means: it was deposited within 300 years. The carbonate here is an extremely fine-grained proto-dolomite (disordered dolomite) with the composition $Mg_{45}Ca_{55}C_{03}$ (Meischner and Paul, 1977; Paul and Meischner, 1991; Meischner and Paul 1982; Kolibáč et al., 2016; Meischner, 2000).

Table A1.1. List of investigated fossil samples with granular structures from the Upper Pliocene of Willerhausen, collection of the Geowissenschaftliches Museum des Zentrums für Geowissenschaften, University of Göttingen, Germany.

Nr.	Species/ Object	Object Number	Time
1	Ulmacea, *Zelkova ungeri*	GZG.W.3458	Upper pliocene
2	Cf. *Salix*	GZG.W.22424	Upper pliocene
3	Cf.*Toona*	GZG.W.21614	Upper pliocene
4	*Acer cappcadocicum*	GZG.W.16391	Upper pliocene
5	*Sorbus*, *Crataegus*	GZG.W.4455	Upper pliocene
6	Magnoliacea (*Liriodendron*), Lauraceae (*Sassafras*+ *Persea*)	GZG.W.17528	Upper Pliocene
7	Betulaceae	GZG.W.2472	Upper Pliocene
8	Hamamelidaceae, *Parrotia*	GZG.W.21247	Upper Pliocene
9	*Quercus roburoides*	GZG.W.16889	Upper Pliocene
10	*Quercus iberica*	GZG.W.14131	Upper Pliocene
11	*Fagus* sp.	GZG.W.4304	Upper Pliocene
12	*Quercus*	GZG.W.16121	Upper Pliocene
13	*Quercus*	GZG.W.12583	Upper Pliocene
14	Juglandaceae	GZG.W.13656	Upper Pliocene
15	Cf.*Magnolia*	GZG.W.2553	Upper Pliocene
16	*Zelkowa ungeri*	GZG.W.14935	Upper Pliocene
17	Saxifragaceae	GZG.W.16782	Upper Pliocene
18	Cf.*Equisetum*	GZG.W.16794	Upper Pliocene

19	Plantae	GZG.W.23663a	Upper Pliocene
20	*Malus pulcherrima*	GZG.W.18136	Upper Pliocene
21	*Ulmus*	GZG.W.6842	Upper Pliocene
22	Rhamnacerae/*Rhamnus saxatilis*	GZG.W.9701	Upper Pliocene
23	Juglandaceae, *Carya*	GZG.W.17510	Upper Pliocene
24	*Quercus*	GZG.W.2214	Upper Pliocene
25	Vitaceae *Vitis*	GZG.W.2214	Upper Pliocene
26	*Fagus*	GZG.W.5706a	Upper Pliocene
27	Cf. *Morus*, Moraceae (Magnoliopsida)	GZG.W.60/59b	Upper Pliocene
28	Magnoliacea (*Liriodendron*), Lauraceae (*Sassafras* + *Persea*)	GZG.W.8518a	Upper Pliocene
29	*Fagus*	GZG.W.5421	Upper Pliocene
30	*Fagus*	GZG.W.5349	Upper Pliocene

Fossil collection 2a, Miocene (13 Ma), Naturkundemuseum Stuttgart, Germany

More than 60 pieces of fossil leaves have been examined under the LM and 19 fossil leaves from the Naturkundemuseum Stuttgart, Germany were borrowed. All of the specimens belong to the Miocene and 3 other pieces belong to the Pliocene of Willershausen. Details about Willershausen have already been mentioned in collection 1 before. The main part of the fossils were collected from the Randecker Maar, Germany. It is the best evidence of Swabian volcanism with a diameter of approx. 1.2 kilometers. It is the largest crater in the Urach-Kirchheimer volcanic area. Due to the water impermeability of the basalt tuff in the volcanic vent, there was a maar lake at the end of the volcanic activity around 17-20 million years ago. The Randecker Maar is a wellknown fossil Lagerstätte at the northern margin of the Swabian Alb, with exceptionally well-preserved fossils from the former lake environment and the surrounding area. As such, it offers a unique window into the time frame of the Mid-Miocene

Climatic Optimum, which was the last period with remarkably thermophilous plants and animals in Central Europe (Early/Middle Miocene, Mammal Neogene Zone MN5). Based on the palaeoecological analysis of 363 plant and animal taxa as well as on the geological background, the palaeoenvironment and the habitats of the Randeck Maar can be characterized as follows: (1) Profundal and pelagic environments with a low species diversity and laminated sediments, among others the so called dysodil. (2) The littoral with a narrow reed belt with insects and freshwater limpets living on the exposed stems. Short termed mass occurrences of some insects, amphibians and fish also existed. (3) The crater wall and the surrounding plateau was characterized by sub humid sclerophyllous to mixed mesophytic forests. Fossils of the Randecker Maar also provide good palaeoclimatic proxies (Rasser et al., 2013; Böttcher, 2013).

Table A1.2. List of investigated fossil samples with granular structures from the Naturkundemuseum Stuttgart, Germany.

Nr.	Species/ Object	Object Number	Site	Time
1	*Acer* spec Oehningen	S19 L6	Oehningen	Miocene
2	*Sapindus falcifolius*	S19 L11	Oehningen	Miocene
3	*Salix* cf. *grandifolia* a-c	S16 L3	Willerhausen	Pliocene
4	?	P2146/30 -L17	Randecker Maar(seehuber)	Early/Middle Miocene
5	*Acer trilobatum* Oehningen	P626-S19L3	Oehningen	Miocene
6	*Cinnamomum* ?	S14 L13	Randecker Maar	Early/Middle Miocene
7	?	P1993/114 S16 L12	Willerhausen	Pliocen
8	?	MN 5 Kauf 2004L13	Randecker Maar	Miocene
9	*Ficus truncata*	Coll Hermann 1947	Randecker Maar	Miocene
10	*Koelreuteria macroptera*	P 1224/513	Randecker Maar	Miocene
11	*Acer trilobatum*	Coll Bruckmann, S19 L5	Oehningen	Miocene

12	*Berchemia parvifolia*	P 1224/543	Randecker Maar	Miocene
13	?	P 2146/32 L17	Randecker Maar	Miocene
14	*Celtis begonioides*	Seemann 15 ?	Randecker Maar	Miocene
15	*Sterculia laurina*	Coll Ludwig 15?	Randecker Maar	Miocene
16	*Cedrelospermum boreale*	?	Rott	Oligocene
17	*Salix*	P 1993/7	Willerhausen	Pliocene
18	?	S16 R13	Indet Enspel	Miocene
19	*Cinnamomophyllum*	?	Rott	Oligocene

Fossil collection 2b, Prague, (Natural History Museum in the National Museum), lower Miocene (23-16 Ma)

The fossil collection from Prague, Natural History Museum, showed well preservation from the upper view but close examination with the SEM showed that in the sediment are plenty of diatoms, which actually penetrated the casts of CaOx, so that an identification of them was impossible.

Bílina site

The fossil flora of the Most Basin exposed in the Bílina Mine is the richest of this age in Europe (Kvaček, 2006). Most of the deposits are from the middle part of the Lower Miocene (Lower Burdigalian, Eggenburgian, Lower Orleanian). In general, the flora of the Most Formation was dominated at the beginning by deciduous broad-leaved elements including beech. Two depositional centres, termed the Žatec and Bílina deltas, were the two main sources of plant fossils, and are lateral equivalents of the brown coal deposits. The flora of the Bílina delta is similar. The sediment of the Most Formation is unusually rich in aquatic plants (*Salvinia, Stratiotes* etc.). However, there are also numerous woody elements as *Juglans, Carya serrifolia, C. denticulate, Comptonia difformis, Podocarpium podocarpum, Celtis japeti, Fraxinus bilinica, Koelreuteria reticulata, Acer angustilobum, Nyssa bilinica, Salix haidingeri, Craigia bronnii, Alnus gaudinii, Mahonia bilinica*.

Table A1.3. List of investigated fossil samples with granular structures from the Lower Miocene of Bilina in the Natural History Museum, Prague.

Species/ Object	Object Number	Collection /site	Time
Acer tricuspidatum	G 11620a-c	Natural History Museum, Prague	Lower Miocene
Salix varians	G 11627	Natural History Museum, Prague	Lower Miocene
Tillia brabenecii	G11628	Natural History Museum, Prague	Lower Miocene
Salix varians	G11623	Natural History Museum, Prague	Lower Miocene
Celtis ?	G 11629	Natural History Museum, Prague	Lower Miocene
Quercus rhenana	G 11625	Natural History Museum, Prague	Lower Miocene
Podocarpidium podocarpum	G13622	Natural History Museum, Prague	Lower Miocene
Myrica integerrima	G11626b	Natural History Museum, Prague	Lower Miocene
Salix heidingeri (2 pieces)	G 11633/ 32	Natural History Museum, Prague	Lower Miocene
Vitis strica	G 11634	Natural History Museum, Prague	Lower Miocene
Alnus (Bechlejovice)	G11624	Natural History Museum, Prague	Lower Miocene

Fossil collection. 3, Rott, Oligocene (34 Ma), Goldfuß Museum, Institute of Geosciences, University of Bonn, Germany

In the current study, 1,120 fossil leaf specimens of the Oligocene Rott fossil site were examined with a stereomicroscope. All samples are from the collection of the late Heinrich Winterscheid, which is kept in the Goldfuß Museum in the Institute of Geosciences, University of Bonn, Germany. The taxonomic assignments of the fossils derive from the works of H. Weyland between 1934 and 1948. The Rott fossil locality, lying between the town of Hennef and the Pleisbach River in the northern Siebengebirge close to the city of Bonn, is known for its abundance of exceptionally well-preserved fossil plants and animals (Koenigswald, 1996). Due to early mining activities, its stratigraphy is well-known (e.g., Kaiser, 1897), and the fossiliferous layers were already discovered in several mines by the 19th century. 200 plant taxa and 35 vertebrate taxa, as well as over 600 insect taxa have already been described

(numerous works of Statz in the years 1930–1952), although most of these descriptions are in need of revision, being nearly 150 to 70 years old (Fikáček et al. 2010).

Table A1.4. List of investigated fossil samples with granular structures from the Oligocene of Rott in the Goldfuß-Museum, Institute of Geosciences, University of Bonn, Germany.

Nr.	Species/ Object	Object Number	Collection /site	Time
1	*Carya serrifolia* (Göpp.) Kräusel	Ro-1.1	Goldfuß-Museum	Oligocene
2	*Sideroxylon salicites* (C.O. Weber) Weyland	Ro-2.1	Goldfuß-Museum	Oligocene
3	*Acer tricuspidatum* Bronn	Ro-3.1	Goldfuß-Museum	Oligocene
4	*Acer* sp. 3	Ro-5.1	Goldfuß-Museum	Oligocene
5	*Ailanthus confucii* Unger	Ro-7.1	Goldfuß-Museum	Oligocene
6	*Nymphaea arethusae* Brongniart	Ro13.1	Goldfuß-Museum	Oligocene
7	Magnoliopsida div. fam. gen. et sp. indet. – spinae	Ro16.1	Goldfuß-Museum	Oligocene
8	*Engelhardia macroptera* (Brongniart) Unger	Ro-20.1	Goldfuß-Museum	Oligocene
9	*Juglans acuminata* Al. Braun ex Unger	Ro-34.1	Goldfuß-Museum	Oligocene
10	*Magnolia burseracea* (Menzel) Mai	Ro-37.1	Goldfuß-Museum	Oligocene
11	*Zelkova zelkovaefolia* (Unger) Bůžek & Kotlaba in Kotlaba	Ro-38.1	Goldfuß-Museum	Oligocene
12	*Tremophyllum tenerrimum* (Weber) Rüffle	Ro-39.1	Goldfuß-Museum	Oligocene
13	*Nyssa ornithobroma* Unger	Ro-40.2	Goldfuß-Museum	Oligocene
14	*Carpinus grandis* Unger emend. Heer	Ro-41.19	Goldfuß-Museum	Oligocene
15	*Engelhardia orsbergensis* (Wess. & Web.) Jähn. et al.	Ro-47.6	Goldfuß-Museum	Oligocene

16	*Myrica ettingshausenii* (Wessel) Knobloch & Kvaček	Ro-48.1	Goldfuß-Museum	Oligocene
17	*Daphnogene cinnamomifolia* f. *cinnamomifolia* f. *lanceolata*	Ro-53.1	Goldfuß-Museum	Oligocene
18	*Zizyphus zizyphoides* (Unger) Weyland	Ro-58.1	Goldfuß-Museum	Oligocene
19	Fabales fam. gen. et sp. indet. – forma 2	Ro-59.1	Goldfuß-Museum	Oligocene
20	*Quercus neriifolia* Al. Braun in Unger	Ro-90.1	Goldfuß-Museum	Oligocene

Fossil collection. 4, Middle Eocene (44,3 Ma), Eckfeld Maar, Museum of Natural History, Mainz, Germany

19 Pieces of leaf fossils borowed from the Museum of Natural History, Mainz, Germany (NHMMZ). All of the fossils have been collected from the fossil lagerstätte of the Eckfeld Maar. The Eckfeld lagerstätte is a deposit of a maar lake, which was formed during the Middle Eocene (Lutz et al. 2010). Its basin was initially formed by volcanic explosions, resulting in deep depressions on top of diatremes that was soon occupied by a lake. Following early stages with succeeding volcanoclastic and predominantly siliciclastic sedimentation, the lake became meromictic and the finely laminated bituminous claystone ("oilshale") was formed in the quiet anoxic bottom layer of the lake. The oil shale contains bio-markers and lithified bacteria, algae, a great diversity of diverse terrestrial flora and fauna representing an ecosystem towards the end of the Middle Eocene (Wappler & Engel, 2003; Wappler & Andersen, 2004; Wappler & Heiss, 2006). Fossil leaves belonging to the Eckfeld lagerstätte were kept in Glycerin. All the fossils are embedded in fine sediment, but the upper side of the leaves were too dark for an examination.The LM showed a layer of pyrite covering the cuticle. To examine the leaves we dried them and with a very fine brush tried to remove the contamination and prepare them for an examination under the LM.

Table A1.5. List of investigated fossil samples with granular structures from the Eckfeld Maar, Museum of Natural History, Mainz, Germany.

AKRONYM	Object Number	INVNR_A	INVNR_Z	Time
NHMMZ	PB_2003	148	LS	early middle Eocene
NHMMZ	PB_2003	163	LS	early middle Eocene
NHMMZ	PB_2003	304	LS	early middle Eocene
NHMMZ	PB_2003	452	LS	early middle Eocene
NHMMZ	PB_2003	488	LS	early middle Eocene
NHMMZ	PB_2003	491	LS	early middle Eocene
NHMMZ	PB_2003	493	LS	early middle Eocene
NHMMZ	PB_2003	494	LS	early middle Eocene
NHMMZ	PB_2003	496	LS	early middle Eocene
NHMMZ	PB_2003	498	LS	early middle Eocene
NHMMZ	PB_2003	499	LS	early middle Eocene
NHMMZ	PB_2003	500	LS	early middle Eocene
NHMMZ	PB_2003	501	LS	early middle Eocene
NHMMZ	PB_2003	502	LS	early middle Eocene
NHMMZ	PB_2003	503	LS	early middle Eocene
NHMMZ	PB_2003	509	LS	early middle Eocene
NHMMZ	PB_2003	715	LS	early middle Eocene
NHMMZ	PB_2021	2	LS	early middle Eocene
NHMMZ	PB_2021	3	LS	early middle Eocene
NHMMZ	PB_2021	4	LS	early middle Eocene
NHMMZ	PB_2021	5	LS	early middle Eocene
NHMMZ	PB_2021	6	LS	early middle Eocene
NHMMZ	PB_2021	7	LS	early middle Eocene
NHMMZ	PB_2021	8	LS	early middle Eocene
NHMMZ	PB_2021	9	LS	early middle Eocene

Other sites and fossil samples from the collection in the Museum of Natural History, Berlin

In the Museum of Natural History Berlin a collection of 100 pieces of fossil leaves of gymnosperms from different sites and times were examined with a LM and 30 pieces have been borrowed for further examinations. The results are accessible in the Gymnosperm chapter.

Fossil collection 5, Jurassic

Table A1.6. List of investigated fossil samples from Jurassic

Nr.	Species/ Object	Object Number	Collection /site	Time
1	*Ginkgo digitata*	MB.Pb. 2000/0852	Yoksire? Whitby	Jurassic
2	*Baiera canaliculata*	MB.Pb. 2000/0858	Cayton Bay b. Scarborough, Yokshire	Jurassic
3	*Ginkgoites* sp.	MB.Pb. 2013/1497	Scalby Ness, Scarborough, Yorkshire	Jurassic
4	*Ginkgo huttoni*	MB.Pb. 2013/1492	Scarborough, Yokshire	Jurassic

Fossil collection 6, Triassic

Table A1.7. List of investigated fossil samples from Triassic

Nr.	Species/ Object	Object Number	Collection	Time
1	*Otozamites* (Bennettitales)		GoldFuß Museum	Triassic
2	*Autunia conferta* (*Callipteris conferta*)		GoldFuß Museum	Triassic
3	*Ginkgo adiantoides*		Museum für Naturkunde Berlin	Triassic
4	*Clathtopteris rosseritii*	MB.Pb.2022/0049	Museum für Naturkunde Berlin	Triassic
5	*Ginkgo digitata*	MB.Pb.2000/0852	Yoksire? Whitby	Triassic

Fossil collection 7, Permian

Table A1.8. List of investigated fossil samples from Permian

Nr.	Species/ Object	Object Number	Collection	Time
1	*Glossopteris* sp.	Dunedoo, Australia	Goldfuß-Museum	Permian
2	*Sphenobaiera digitate*	MB.Pb.2022/0050	Museum für Naturkunde Berlin	Permian
3	*Sphenobaiera digitata*	MB.Pb.2022/0052	Museum für Naturkunde Berlin	Permian
4	*Sphenobaiera digitata*	MB.Pb.2022/0051	Museum für Naturkunde Berlin	Permian
5	*Sphenobaiera digitata*	MB.Pb.2022/0053	Museum für Naturkunde Berlin	Permian

Fossil collection 8, Carboniferous

Table A1.9. List of investigated fossil samples from Carboniferous

Nr.	Species/ Object	Object Number	Site /collection	Time
1	*Paripteris gigantea*	_____	Upper Silesia, Poland, (Col. Andrzej Gorski, 2022)	Carboniferous
2	*Ginkgophytopsis delvali*	_____	Upper Silesia, Poland (Col. Andrzej Gorski, 2021)	Carboniferous

Fossil collection 9, Devonian

Table A1.10. List of investigated fossil samples from DevonianNr

.	Species/ Object	Object Number	Site /collection	Time
1	*Archaeopteris roemeriana*	_____	Goldfuß-Muum	Devonian
2	*Cyclostigma kiltorkense*	_____	Goldfuß-Museum	Devonian

Appendix. 2

Fresh leaves

A2.1. All of the fresh leaves were collected in the Botanical Garden, University of Bonn.

Species/ Object	Collection	Species/ Object	Collection
Hedera helix	BG	*Sequoia sempervirens*	BG
Conocarpus erectus	BG	*Pinus mugo*	BG
Nannorrhops ritchieana	BG	*Welwitschia mirabilis*	BG
Parrotia persica	BG	*Fagus sylvatica*	BG
Araucaria araucana	BG	*Quercus variabilis*	BG
Carpinus kawakamii	BG	*Encephalartos lehmannii*	BG
Malus domesticus	BG	*Ginkgo biloba*	
Quercus robur	BG	*Acer griseum*	
Carya ovata	BG	*Acer pelmatum*	
Camellia japonica l	BG		
Carpinus kawakamii	BG		
Agarista populifolia	BG		
Cycas diannanensis	BG		
C. szechuanensis	BG		
C. rumpii	BG		

Appendix 3. Challenges for the identification of CaOx casts in fossil leaves

1. Lack of cuticles and parenchymal layers in fossil leaves (e.g: Rott) Fine and clayey sediments of the Oligocene Rott Lagerstätte made it an unique site for well-preserved fossils. Since the identification of CaOx traces depends on the presence of at least residual parenchyma and cuticle, their lack made a diagnosis difficult.

2.Contamination of the cuticle (e.g:Eckfeld, Willershausen)All of the fossil leaves from the Eocene Eckfeld Lagerstätte were covered with iron oxide crystals, which led to an obstacle for the investigation of the fossils. Figure A.1 shows that the surface of the fossil leaves is coated with iron oxide which made the identification of the casts and specially casts of individual crystals difficult.

Furthermore, the surface of leaves in the Pliocene of Willershausen is coverd with plenty of tiny crystals, which was a big obstacle in detecting the imprint of individual crystals in the parenchymal residue in fossils leaves, such as *Acer* sp.

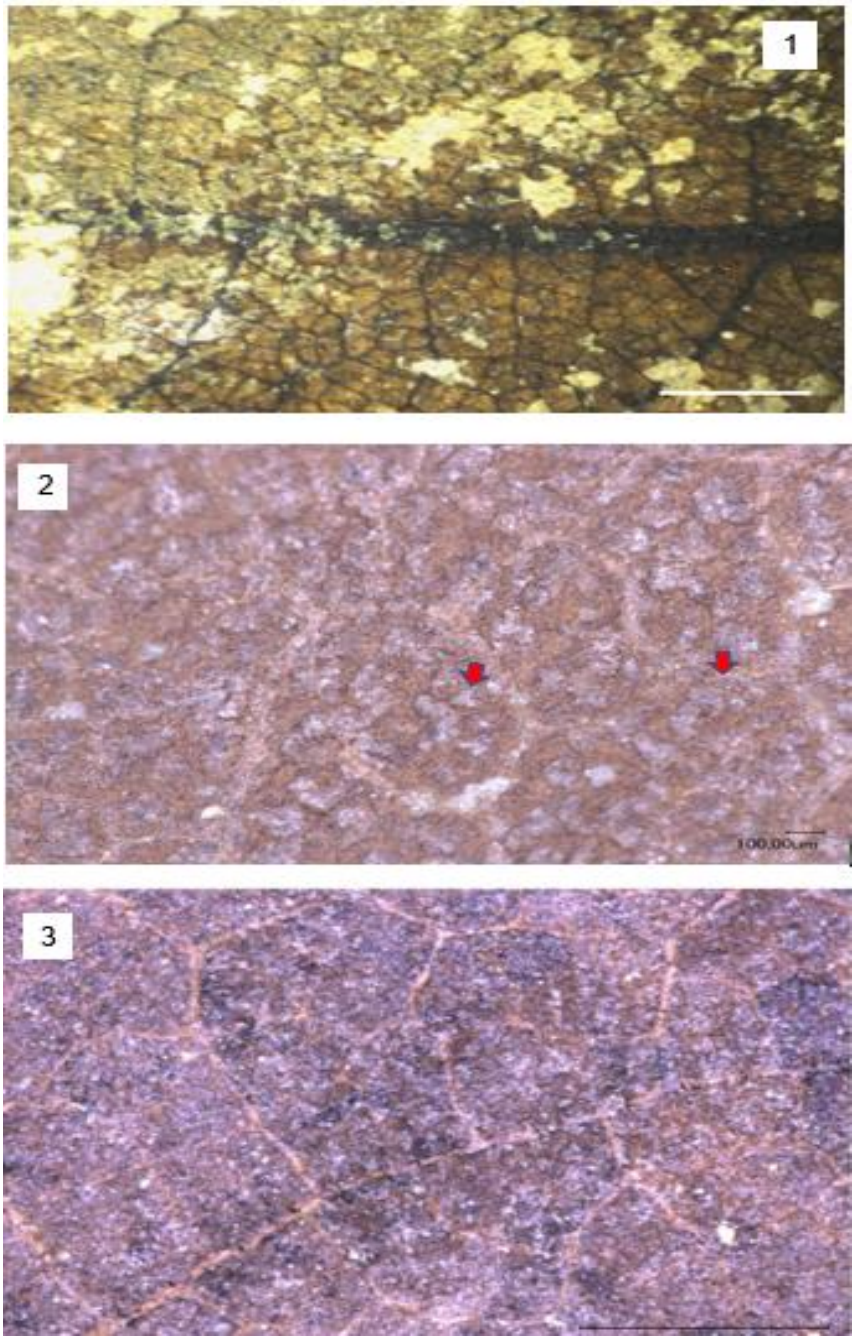

FIGURE A3.1 View of different contaminations on fossil leaves. 1 Iron oxide on Eckfeld fossils. A. 2 and A.3 plenty of tiny crystals (light pink color, marked with a red arrow) covering fossil leaves and in many cases penetrating the cell walls. For this reason, the identification of the CaOx traces was difficult.

3. Type of the sediments surrounding the fossil leavesComparison of the same genera (e.g: *Celtis*) from different sites and fossilization conditions caused to the completely different results. In the Eocene Bilina site almost all of the sediments consists mainly of diatoms (almost flake shaped) and diatoms were the main barrier to identification of the cystoliths. while in fossil leaf from the Randecker Maar cystoliths in *Celtis* were identified even with LM. Under the LM diatoms looked like casts or granules of CaOx, while a more detailed examination with the SEM showed that they are tests of diatoms (**Figure A.2**).

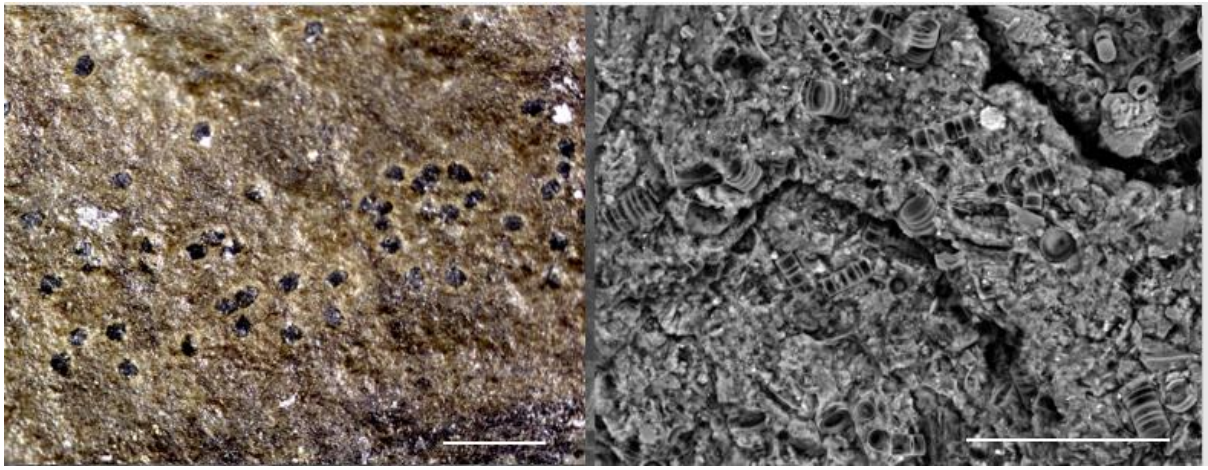

FIGURE A3.2. Comparision of the preservation of CaOx traces in *Celtis* from different sites. Left side *Celtis* from the Miocene Randecker Maar. Right side *Celtis* from the Eocene of Bilina,. Scale bare: left= 40µm, right=200µm.

4.Not systematically identified fossils (e.g. Eckfeld, Rott)

Almost all of the leaf fossils which were borrowed from the NHMMZ were systematically not identified. Although some of the casts were identified under and in the fossil leaves which were refilled with pyrite, no more details concerning their systematic identification resulted from the investigations. Additional examinations of more fossil leaves from the Eckfeld site and a comparison of them with fresh leaves could result in finding a distribution trend of CaOx. In the Oligocene Rott site many of the fossil leaves have been identified just as a Magnoliopsida which can be due to a lack of the cuticle as mentioned above. It is difficult to follow a

systematic pathway in the group of the Magnoliopsida to describe the evolutionary pattern of CaOx in comparison with extant leaves.

5. Missing knowledge concerning the chemical process of fossilization

Analysis by EDX in fresh leaf samples clearly shows the presence of calcium oxalate as seen in Figure A.3, while in the fossil samples, as already mentioned in the results and the discussion, these crystals no longer exist and have been removed from the idioblasts during the fossilization process. They have undergone massive chemical changes during this process. Therefore, only the observation of refilled casts with other elements instead of Ca is possible, e.g. with C as seen in Figure A.3, 3.4.

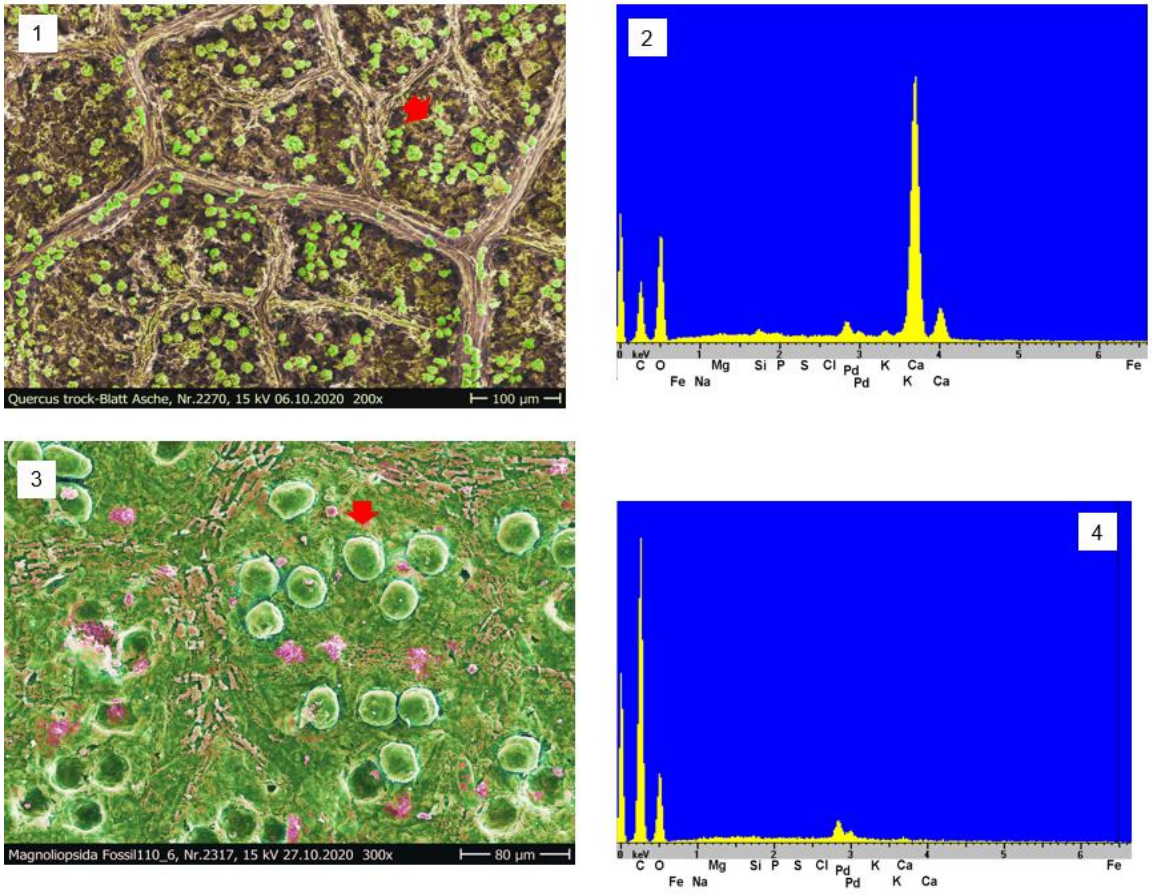

Figure A3.3. Comparision of chemical components in fresh and fossil leaves. A.1. Druses in *Quercus* showed Ca and O in an EDX analysis (A.2). A.3. Granules that refiled the empty casts are made of carbon (A.4).